



FEDERAL UNIVERSITY OF SANTA CATARINA  
CAMPUS FLORIANÓPOLIS  
GRADUATE PROGRAM IN CIVIL ENGINEERING - PPGEC

Alfredo Cali

**Structural identification for heritage buildings:  
an HBIM-based approach applied to cultural masonry structures**

Florianópolis - SC  
2020

Alfredo Cali

**Structural identification for heritage buildings:  
an HBIM-based approach applied to cultural masonry structures**

Supervisor: Prof.<sup>a</sup> Poliana Dias de Moraes, Dr.  
Federal University of Santa Catarina, Brazil  
Co-supervisor: Prof.<sup>a</sup>. Ângela do Valle, Dr.  
Federal University of Santa Catarina, Brazil  
Co-supervisor: Prof. Carmelo Gentile, Dr.  
Polytechnic University of Milan, Italy

Florianópolis SC

2020

Ficha de identificação da obra elaborada pelo autor,  
através do Programa de Geração Automática da Biblioteca Universitária da UFSC.

Calì, Alfredo

Structural identification for heritage buildings : an  
HBIM-based approach applied to cultural masonry structures  
/ Alfredo Calì ; orientadora, Poliana Dias De Moraes,  
coorientadora, Ângela do Valle, coorientador, Carmelo  
Gentile, 2020.

273 p.

Tese (doutorado) - Universidade Federal de Santa  
Catarina, Centro Tecnológico, Programa de Pós-Graduação em  
Engenharia Civil, Florianópolis, 2020.

Inclui referências.

1. Engenharia Civil. 2. H-BIM. 3. Structural analysis  
of heritage building. 4. Vibration-based model updating.  
5. Finite element model updating. I. Dias De Moraes,  
Poliana. II. do Valle, Ângela. III. Gentile, Carmelo IV.  
Universidade Federal de Santa Catarina. Programa de Pós  
Graduação em Engenharia Civil. V. Título.

Alfredo Cali

**Structural identification for heritage buildings: an HBIM-based approach applied to cultural masonry structures**

The present work at the doctoral level was evaluated and approved by an examining board composed of the following members:

Prof. Paulo Barbosa Lourenço, Dr.  
University of Minho, Portugal

Prof. Arivaldo Leão de Amorim, Dr.  
Federal University of Bahia, Brazil

Prof. Wellison José de Santana Gomes, Dr.  
Federal University of Santa Catarina, Brazil

Prof. Roberto Caldas de Andrade Pinto, Ph.D.  
Federal University of Santa Catarina, Brazil

Certified that this is an **original** and **final version** of the conclusion work that was deemed appropriate for the title of doctor in Civil Engineering

---

Coordinator of the graduate program

---

Prof<sup>a</sup>. Poliana Dias de Moraes, Dra.  
Supervisor

Florianópolis, 2020



This work is dedicated to my family, who always has faith in me for each choice with much love and passion.

## ACKNOWLEDGEMENTS

The author would like to acknowledge the advisors Prof. Poliana and Prof. Angela, who accompanied him over the years, suggesting the most appropriate ways to achieve goals and guiding him in the process of investigation and research. The author thanks the advisor Prof. Carmelo Gentile - Department of Architecture, Built Environment and Construction Engineering of the *Politecnico di Milano* - who provided insight and expertise that greatly assisted the proposed research. They helped in the academic development of research, both in content and in expression and presentation. Another thank goes to Prof. Rafael A.R. Higashi, Prof. Wellison José de Santana Gomes, and Prof. Leandro F. Fadel Miguel, who offered their help in evaluating some parameters related to the case study. Furthermore, Prof. A.R. Higashi helped - together with Matheus Klein Flach - in the research regarding the experimental soil tests. Special thanks to Prof. Mário Oliveira Mendonça, who helped the author in the revision and elaboration of the research project presented in the mid-term examination, *Qualificação*. A special thank goes to colleagues of the GIEM research group, and, to Auro, who helped to improve the quality of the research and to face bureaucratic issues. Special acknowledgement to colleagues Giacomo Zonno, Paolo Borlenghi, Antonello Ruccolo, Gabriele Marrongelli, and Gessica Sferrazza Papa, who assisted the author professionally and personally during the research period at the Politecnico di Milano. Finally, the author thanks family, parents, sister and grandma, who supported and accompanied him in every stage of life and every choice.

This project has been funded with the support of the European Commission. This publication reflects the view only of the author, and the Commission cannot be held responsible for any use which may be made of the information contained therein - ELARCH program (Project Reference number 552129-EM-1-2014-1-IT-ERA MUNDUS-EMA21). The research was financed in part by the *Coordenação de Aperfeiçoamento de Pessoal de Nível Superior* - Brazil (CAPES) - Finance Code 001. Furthermore, research on the case study of *Galleria degli Antichi* has been founded with the support of Department of Architecture, Built Environment and Construction Engineering (DABC) of the *Politecnico di Milano*, with the supervision of Professor Carmelo Gentile - "DYNAMIC CHARACTERISATION, MODELLING AND SAFETY ASSESSMENT OF STRUCTURES. HISTORICAL BUILDINGS AND BRIDGES. 2019\_ASSEgni\_DABC\_48" from 01/09/2019 to 31/08/2020.

La conoscenza è il primo stadio della conservazione.

Knowledge is the first stage of conservation.

O conhecimento é a primeira etapa da conservação.

*Almagro et al. (1999) in Verso la 'Carta del rilievo architettonico'*

## RESUMO

A avaliação estrutural de edifícios históricos é uma atividade multidisciplinar desafiadora que envolve diferentes tarefas, como pesquisa histórica e documental, levantamento geométrico, inspeção direta, complementada por testes experimentais, e análise numérica. O diagnóstico do estado de construção das estruturas do patrimônio cultural deve resultar de uma investigação experimental que deve ser não destrutiva (END), na medida do possível. A maioria dos procedimentos de END pode fornecer apenas resultados essencialmente qualitativos. O analista é solicitado a selecionar os ensaios necessários e a interpretar os resultados obtidos. A avaliação estrutural envolve a coleta de dados de uma ampla variedade de fontes e o subsequente processo de seleção. Um alto nível de informação é necessário para simular com precisão o comportamento global do edifício histórico. As informações adquiridas para a avaliação estrutural podem ser armazenadas em um banco de dados para simplificar as análises de pesquisa, prevenindo uma possível perda de informações. Incertezas críticas relacionadas a geometrias e propriedades dos materiais precisam ser minuciosamente investigadas para a obtenção de modelos numéricos confiáveis. Para simular o comportamento estrutural global de um edifício histórico, pode se aplicar uma investigação dinâmica estrutural. Em condições operacionais, é possível obter informações quantitativas globais, como frequências ressonantes e modos vibracionais. Essas informações são representativas da condição estrutural e contribuem notavelmente para o percurso do conhecimento do edifício, reduzindo a incerteza do problema. A proposta da tese foi desenvolver uma metodologia para avaliação estrutural de edifícios do patrimônio cultural, que parte de uma pesquisa histórica e arquitetônica registradas por meio do *Historical Building Information Modelling* (H-BIM) e complementada pelo levantamento dinâmico. A identificação estrutural baseada em análise modal operacional contribui para o aumento do conhecimento sobre o comportamento estrutural do edifício de patrimônio histórico e a subsequente atualização dos parâmetros do modelo de elementos finitos para uma aprimorada representação numérica. A validação da metodologia é feita através de dois estudos de caso de edifícios de patrimônio histórico. O primeiro estudo de caso é a *Galleria degli Antichi*, na cidade de Sabbioneta (Itália). Este edifício monumental, construído no século XVI, pertence à lista de Patrimônio Mundial da UNESCO desde 2008. O segundo estudo de caso é o Quartel da Tropa, edifício do século XVIII, que é um dos principais edifícios da Fortaleza de Santa Cruz, localizado na Ilha Anhatomirim, município de Governador Celso Ramos, Estado de Santa Catarina, Brasil. A avaliação das informações, coletadas pela pesquisa histórica e arquitetônica, o H-BIM e os testes dinâmicos, permitiram a validação da metodologia, reduzindo as principais incertezas quanto à definição de modelos numéricos e à avaliação do estado de preservação da estrutura do edifício, de maneira totalmente não destrutiva. A compreensão do comportamento estrutural da estrutura foi aprimorada pela avaliação do modelo numérico atualizado, aumentando o nível de conhecimento ao respeito dos edifícios patrimoniais analisados. Assim, foi desenvolvida uma metodologia para identificação estrutural de edifícios do patrimônio cultural, que otimiza a gestão de informações através do H-BIM favorecendo a colaboração multidisciplinar necessária para projeto e ações de intervenção em patrimônio.

**Palavras-chave:** H-BIM. *Structural analysis of heritage building. Vibration-based model updating. Finite element model updating.*

## RESUMO EXPANDIDO

### Introdução

Na área de investigação de edifícios de patrimônio histórico, o processo de avaliação do comportamento estrutural global é uma abordagem fundamental para entender as principais características da construção. A criação de um modelo tridimensional interpretativo permite a avaliação do comportamento estrutural global. O nível de confiabilidade desse modelo interpretativo está fortemente relacionado ao nível de detalhes das informações contidas no mesmo modelo.

Além disso, o conhecimento de uma construção histórica envolve compreender quais modificações levaram o projeto inicial ao seu estado atual, e o modo como o fizeram. A análise histórico-crítica durante a pesquisa documental ajuda a compreender a evolução construtiva e os motivos das modificações no ciclo de vida da construção. Por tanto, a análise histórica visa ao entendimento da evolução construtiva, os fenômenos de dano e degradação, e as transformações que podem ter produzido mudanças no comportamento estático estrutural.

Nesse sentido, a pesquisa histórica torna-se uma investigação crítica e base de um conhecimento direcionado à interpretação do comportamento estrutural global. Essa interpretação representa um desafio que requer levantamentos, testes e análises *in-situ* ou em laboratório que podem ser trabalhosos e caros. De fato, o uso sistemático de ensaios não destrutivos é essencial para avaliar os fatores característicos de um edifício. Geralmente, o número de testes que podem ser realizados em uma construção histórica é muito limitado e não permite um tratamento estatístico dos resultados. No entanto, a interpretação dos resultados deve ser rastreada até um julgamento sintético, no qual o uso de poucos dados experimentais pode ser significativo.

Na área de edifícios patrimoniais a falta de informações implica um baixo nível de detalhes, nível este que pode ser aumentado com um melhor conhecimento da construção gerenciada através do *Building Information Modeling* (BIM). Nos últimos anos, o BIM tem sido utilizado nos processos de restauração de edifícios históricos com o nome *Historic Building Information Modeling* (H-BIM). Isto deve-se principalmente ao seu excelente desempenho durante as fases de definição e descrição da evolução construtiva do edifício, da manutenção de seus elementos e avaliação estrutural. Além disso, a interoperabilidade do software BIM disponível permite exportar o modelo estrutural para um software de computação com base no método de elementos finitos (FEM). Dessa forma, uma modelagem mais precisa é possível através de métodos de análise estrutural mais apropriados, como análises modais e dinâmicas. No entanto, o estado da arte da literatura H-BIM confirmou que há ainda necessidade de pesquisas no campo científico da avaliação estrutural do patrimônio histórico.

Dois edifícios históricos são selecionados como estudos de caso para aplicar a metodologia proposta: a *Galleria Degli Antichi*, Sabbioneta, na Itália e o Quartel da Tropa, Ilha Anhatomirim, Estado de Santa Catarina, no Brasil. O primeiro edifício patrimonial foi construído no século XVI e foi incluído na lista de Patrimônio Mundial da UNESCO em 2008. O segundo foi construído no século XVIII e é o maior entre as fortificações brasileiras - é um dos principais edifícios da Fortaleza de Santa Cruz, localizada na Ilha Anhatomirim, no município de Governador Celso Ramos, Estado de Santa Catarina, República Federal do Brasil. Uma extensa campanha de investigação foi realizada através de uma comparação dos documentos de arquivo e inspeções diretas. Os resultados da pesquisa de tais casos de estudo permitem sugerir como aumentar o nível de conhecimento de edifícios históricos envolvendo o fluxo de trabalho H-BIM proposto.

## **Objetivos**

O objetivo geral da pesquisa proposta é desenvolver e validar uma metodologia que permita aumentar o nível de conhecimento dos edifícios de patrimônio histórico. No fluxo de trabalho H-BIM proposto, são implementadas algumas fases da pesquisa consideradas adequadas para os edifícios históricos, ou seja, testes não destrutivos, análise de sensibilidade nas incertezas geométricas e mecânicas, e análise estrutural para avaliação do comportamento global do edifício. Nessas fases, o autor busca aprimorar a metodologia proposta para o conhecimento dos edifícios patrimoniais.

Os objetivos específicos da pesquisa proposta são retomados da seguinte forma: (a) desenvolvimento e validação de uma metodologia orientada ao H-BIM, com o objetivo de aumentar sistematicamente o nível de conhecimento; (b) analisar as incertezas de tal metodologia, com foco na redução das incertezas geométricas e mecânicas dos edifícios de patrimônio histórico; (c) a compreensão do comportamento estrutural geral do patrimônio através da análise modal do modelo numérico; (d) a proposição de uma abordagem sistemática para o projeto da investigação experimental, com base na avaliação da análise estrutural; (e) o aumento do conhecimento dos edifícios de patrimônio históricos, através da investigação experimental do comportamento estrutural, permitindo a identificação estrutural baseada em análise modal operacional; (f) o aprimoramento da representação numérica do comportamento estrutural do patrimônio, através do ajuste do modelo FE

## **Metodologia**

A metodologia proposta visa melhorar o entendimento de edifícios de patrimônio histórico através da identificação estrutural com base no H-BIM. A metodologia proposta pode ser retomada nas seguintes etapas: (a) aquisição de informações; (b) criação do modelo H-BIM; (c) gerenciamento e atualização de informações através do H-BIM; (d) análise linear preliminar no software FEM; (e) validação dos resultados através de testes dinâmicos de AVT; (f) atualização de dados nos modelos FEM e H-BIM. A metodologia permite o processo de atualização contínua dos modelos HBIM e FEM com as informações adquiridas na investigação. Além disso, a pesquisa analisa o desempenho do H-BIM para a avaliação estrutural global, desde a investigação multidisciplinar até a análise estrutural de edifícios históricos.

## **Resultados e Discussão**

A investigação proposta permite incrementar o nível de conhecimento de um edifício de patrimônio histórico através da sua identificação estrutural. Os ensaios experimentais, as documentações técnicas e a comparação dos documentos de arquivos históricos permitem definir um modelo H-BIM através do qual o profissional pode ter acesso imediato às informações requeridas. Esse mesmo modelo representa a base que permite as análises preliminares realizadas no software FEM. Através da metodologia proposta, as análises de sensibilidade - tanto da *Galleria degli Antichi*, como do Quartel da Tropa – proporcionaram um melhor entendimento das influências dos parâmetros físico e mecânicos no desempenho estrutural de edifícios de patrimônio histórico.

Fundamental etapa na avaliação desse desempenho foi a análise histórico-crítica das evoluções construtivas, aprofundada no caso do Quartel da Tropa. Conforme às análises propostas, a configuração de construção atual – ao contrário daquela com que foi inicialmente projetada – tem um comportamento estrutural assimétrico. Em termos de tensão e deslocamento, uma das partes do edifício sofre as maiores tensões e deslocamentos fora do plano. De fato, nesses pontos, algumas manifestações patológicas foram observadas.

Por outro lado, através das análises de sensibilidade foi possível entender quais parâmetros influenciam principalmente o comportamento estrutural dos edifícios patrimoniais. As

incertezas geométricas foram reduzidas e foi possível delimitar a variação dos parâmetros físicos e mecânicos da estrutura avaliada. Além disso, as análises preliminares foram utilizadas para uma melhor concepção do ensaio AVT no estudo de caso da *Galleria degli Antichi*. Isso permitiu avaliar as etapas parciais da metodologia proposta. Como resultado, cada modo vibracional experimental correspondeu a um modo numérico.

A qualidade das correspondências foi avaliada através de dois fatores: a discrepância das frequências de ressonância e o *Modal Assurance Criterion* (MAC), que permitiu a avaliação da correspondência entre formas dos modos vibracionais experimentais e numéricos. O uso do parâmetro MAC contribuiu para a redução de custos e de tempo durante a fase de investigação experimental e de análise dos resultados, já que foi possível realizar uma descrição adequada do comportamento estrutural utilizando um número menor de acelerômetros, e a identificação da correspondência dos modos numéricos foi automatizada. A média das discrepâncias obtida nessa avaliação foi de 7,31%. Por outro lado, o MAC médio foi de 0.919, que descreve uma correspondência adequada.

Esses resultados parciais demonstram como a metodologia proposta resulta ser consistente com os resultados experimentais. Porém, as etapas sucessivas da metodologia proposta mostram que através do *Model Updating* é possível obter resultados. Como resultado dessa etapa, a média das discrepâncias das frequências foi reduzida a 3,34%, com um MAC médio de 0,946. Através da interoperabilidade dos softwares utilizados, conseguiu-se a atualização dos modelos H-BIM e FEM, assim como proposto nos objetivos iniciais. Dessa forma, os resultados obtidos em uma plataforma foram introduzidos na outra, proporcionando uma atualização contínua dos modelos utilizado na pesquisa.

### **Considerações Finais**

Na área de investigação de edifícios de patrimônio histórico, o processo de avaliação do comportamento estrutural global é uma abordagem fundamental para entender as principais características da construção. A falta de informações implica um baixo nível de detalhes, que pode ser aumentado com um melhor conhecimento da construção gerenciada por meio da plataforma de H-BIM. A metodologia proposta permite o processo de atualização contínua entre modelos HBIM e FEM com as informações adquiridas na investigação. Dessa forma, uma modelagem mais precisa é possível através de métodos de análise estrutural mais apropriados, como análises modais e dinâmicas. O uso do ensaio não destrutivo de AVT durante o processo de conhecimento dos edifícios de patrimônio permitiu a validação da própria metodologia, o aumento do conhecimento do comportamento estrutural da construção do patrimônio e a utilização dos resultados experimentais para o processo de atualização dos modelos FEM e HBIM. Além disso, a pesquisa demonstrou um bom desempenho do H-BIM no incremento do nível de conhecimento de edifícios de patrimônio histórico e na identificação estrutural dos edifícios de patrimônio histórico, desde a investigação multidisciplinar até a análise estrutural.

**Palavras-chave:** *H-BIM. Structural analysis of masonry heritage building. Vibration-based model updating. Finite element model updating.*

## ABSTRACT

The structural assessment of heritage buildings is a challenging multidisciplinary activity involving different tasks, *e.g.* historical and documentary research, geometric survey, direct inspection supplemented by experimental tests, numerical analysis. Moreover, the diagnosis of the as-built state of the cultural heritage structures should result from an experimental *in-situ* investigation that must be a non-destructive test (NDT) as far as possible, still giving consistent information. However, most of the NDTs provide results which are essentially qualitative. The designer is asked to select the necessary tests and to interpret the obtained results. Therefore, structural assessment involves the collection of data from a wide range of sources and the subsequent selection process. The information acquired for the structural evaluation can be stored in a database to simplify the research analysis, preventing a possible loss of information. Hence, a high level of information is required to accurately simulate the global behaviour of the heritage building. However, such input data are not easily available. Critical uncertainties related to geometries and material properties must be sufficiently investigated to obtain reliable numerical models. Furthermore, dynamic investigation in operational conditions provides global quantitative information, *i.e.* resonant frequencies, mode shapes. Such information is representative of the structural condition and remarkably contribute to the path to knowledge of the building, reducing the uncertainty of the problem. In this research, the author develops a methodology involving historical and architectural research complemented by H-BIM and dynamic survey for the structural assessment of cultural heritage buildings. A three-dimensional informative model is created through the Heritage Building Information Model (H-BIM). Moreover, vibration-based structural identification through operational modal analysis allows increasing the knowledge of the heritage building structural behaviour and the subsequent Finite Element model tuning for an improved numerical representation of the structural behaviour of the heritage building. The development and validation of the methodology are proposed through two heritage building case studies. The first is the *Galleria degli Antichi* in the historic town of Sabbioneta (Italy). This monumental building, built in the 16<sup>th</sup>-century, belongs to the UNESCO World Heritage list since 2008. The second is the *Quartel da Tropa*, which is the largest among Brazilian military fortifications of the 18<sup>th</sup>-century. It is one of the main buildings of the Fortress of Santa Cruz, located on Anhatomirim Island, municipality of Governador Celso Ramos, State of Santa Catarina, Brazil. The information collected by historical and architectural investigations, H-BIM and dynamic tests allowed validating the methodology, reducing the main uncertainties associated with the numerical models and assessing the structural state of preservation of the building, in a fully non-destructive way. Moreover, the understanding of the overall structural behaviour was improved by the evaluation of the updated numerical model, increasing the level of knowledge of the analysed heritage buildings. Thus, a methodology was developed for the structural identification of cultural heritage buildings, which optimizes information management through H-BIM, improving the multidisciplinary collaboration necessary for heritage projects and intervention actions.

**Keywords:** H-BIM. Structural analysis of heritage building. Vibration-based structural identification. Finite element model updating.



## LIST OF FIGURES

Figure 1 - Example of the stonework section. ....	57
Figure 2 - Qualitative behaviour of multiple-leaf stone masonry: surveys ( <i>Rilievo</i> ) and mechanic models ( <i>Modello Meccanico</i> ). ....	58
Figure 3 - Deformation and failure of a two-leaf wall (a), diatons and their influence on the stability of the wall (b). ....	58
Figure 4 - Example of masonry catalogues: interlocking elements (a, <i>conci di legamento</i> ), good (b, <i>buon ingranamento</i> ) and weak (c, <i>ingranamento insufficiente</i> ) interlocking. ....	59
Figure 5 - Comparison between CAD and BIM project development process. ....	63
Figure 6 - Part of a dataset for the image overlapping (a). General view of TLS survey (b) and comparison between TLS (c) and SfM developed with Photoscan (d) and Recap (e). Point cloud density visualization in TLS (f), Photoscan and ReCap clouds (higher density area in red). ..	66
Figure 7 - Capillary rise of the water: (a) thermographic camera, (b) photographic camera and previous superposition images (c). ....	69
Figure 8 - Endangered fresco by an earthquake: picture and thermographic detection of delaminations and structural cracks. ....	69
Figure 9. Plan of the Cathedral of Noto (Italy) with the tested piers (a), the geometry of the pier P1E and localisation of the sonic tests P1 (b), distribution of the velocity in the vertical of the testes piers and walls (c). Detail of the distribution in the horizontal plane of pier P1 (d, e). .	71
Figure 10 - Horizontal tomographies of the temple of S. Nicolò l'Arena (Italy): the pillar 2 from top to bottom, respectively at 8.9, 7.6, 4.9, 3.8, 1.8 m (a-e), pillar 6 and 10 at 5.8 m (f, g). ....	72
Figure 11 - Phases of the flat-jack test: the initial distances $d_i$ decrease after the mortar removal, the pressure $p_f$ is increased trough flat jack since the initial distance ( $d_i$ ) is reached. ....	73
Figure 12 - Different flat-jack configurations: rectangular flat-jack used after manual material removal or stitch drilling (a and b); circular (c), and semi-circular (d) flat-jack after saw cutting. ....	74
Figure 13 - Comparison of the stress-strain behaviour of two walls with different textures. ..	75
Figure 14 - Ambient vibration tests: (a) schematic of the layout of the sensors; (b-e) selected modes of vibration identified from operational modal analysis (SSI-Cov). ....	78
Figure 15 - Particle-size limits according to several current classification schemes. ....	80
Figure 16 - Particle-size distribution curves for several soil materials. ....	81
Figure 17 - Mohr diagram and failure envelopes. ....	82

Figure 18 - Direct shear test equipment.....	83
Figure 19 - Components of manually operated borehole shear test device.....	84
Figure 20 - Layout of the seismometers installed in the Cathedral of Milan (a): identified modes (b), the variation of frequencies and temperature in time (c), and frequency variation with outdoor temperature (d).....	86
Figure 21 - ICOMOS methodology.....	89
Figure 22 - Finalization of the experimental survey to the structural analysis.....	90
Figure 23 - Dynamic-based assessment of a structure. ....	92
Figure 24 - Vibration-based validation of the Finite Element Model of a historic building....	93
Figure 25 - Modelling strategies for masonry structures: detailed micro-modelling (a), simplified micro-modelling (b), and macro-modelling (c).....	105
Figure 26 - Examples of structural component models for: (a) wall with openings; (b) lumped parameters; (c) beam elements; and (d) macro- elements (rigid or deformable). ....	106
Figure 27 - Schematization of wall models in AndilWall (a), Tremuri (b), and 3DMacro (c). ....	107
Figure 28 - Seismic Assessment by Equivalent Frame Modelling of Palacio Pereira (a), Santiago de Chile: SAM method (b), geometrical and analytical representation (c and d). ....	107
Figure 29 - General three-dimensional body with a generic 8-node three-dimensional element. ....	109
Figure 30 - Nodal point and element equilibrium in a FEA.....	116
Figure 31 - Process of model calibration.....	124
Figure 32 - Graphic plot representation (a), examples of 2D (b) and 3D (c) MAC.....	127
Figure 33 - Simulation workflow applied to the SS. Nome di Maria church at Poggio Rusco, in Mantua (Italy) from the Revit® model to analytic model for structural analysis (SAP2000) (a) and 3D building site layout (b). ....	136
Figure 34 - Pattern book details of architectural components, parametric definition and three-dimensional representation. ....	139
Figure 35 - 3D Modelling of decays with a graphic explanation of the data (through labels), associated with the adaptive component, such as the nature of the decay and the interventions required for cleaning.....	140
Figure 36 - LOD as the relation between the level of detail and level of information.....	140
Figure 37 - Cloud-to-BIM-to-FEM methodology applied to Castel Masegra, Sondrio (Italy): point cloud acquisition/registration (a), creation of the BIM from point clouds by preserving geometric complexity (b), generation of the Finite Element model with tetrahedral meshes (c),	

structural analysis with the new model (d). The case study is Castel Masegra, a castle in Sondrio (Italy). .....	143
Figure 38 - The structural model definition from H-BIM to FEM.....	150
Figure 39 - BIM and FEM software in the interoperability process; structural (a) and analytical (b) H-BIM model with loss of information in the integration through the IFC format (a), contrary to the direct integration (b).....	152
Figure 40 - Workflow of the H-BIM-based structural identification for cultural heritage. ...	164
Figure 41 - Historical (a) and current (c) map of Sabbioneta (a), an aerial photograph of Sabbioneta (b) and built environment of <i>Galleria degli Antichi</i> (d). .....	165
Figure 42 - Hypotheses of the configuration of the ideal city of Sabbioneta (a) and built environment of <i>Piazza delle Armi</i> (b).....	166
Figure 43 - Geometric generative procedure of the <i>Galleria degli Antichi</i> .....	168
Figure 44 - Historical (1920s) (a) and current (b) photos of <i>Piazza D'Armi</i> , <i>Galleria degli Antichi</i> and <i>Palazzo Giardino</i> ; Historical (c and d) and current (e, f and g) of the construction and flying passage from <i>Palazzo Giardino</i> (f). .....	169
Figure 45 - Historical images of <i>Galleria degli Antichi</i> (a and c), modifications of the windows surrounding the aedicule from the door (c) to windows (d). Visual inspection of the material decay in the external (b, e, f) and internal (g and h) elements. ....	170
Figure 46 - As-built state after the 2012 earthquake (a, b, c, e) on the structural elements carried out timber joist of lacunar ceiling (a, b), timber roof truss (c, d). Restoration works with steel reinforcement steel tie-rod in masonry walls (f) and modification in the roof extrados (d). .	172
Figure 47 - Structural intervention after the 2012 earthquake: tie-rods on the top of the façades (a), steel profiles where the timber tie beam are introduced (b) and tie rods on the extrados of the coffered wooden floor (b) and (c).....	172
Figure 48 - As-built state: change in colour of the columns (a, b), configuration of the lacunar wooden ceiling (c, d) and connection with the masonry walls (e). .....	173
Figure 49 - Three-dimensional model obtained from the point cloud (a) and geometrical survey of the <i>Galleria degli Antichi</i> : west façade (b), plan (c) and longitudinal section (d).....	175
Figure 50 - Geometric surveys (a and d): a material survey (b) and material decay survey (c). .....	175
Figure 51 - Structural survey of the out of plumb (in red) of <i>Galleria degli Antichi</i> (a) and (b) and crack pattern on the west façade (c).....	176
Figure 52 - H-BIM model: 3D view, longitudinal and transversal sections. ....	177

Figure 53 - Structural Intervention after the 2012 earthquake at the extrados of the coffered-ceiling level and in the wooden structure roof described in the H-BIM model. ....	178
Figure 54 - Maximum Mises stresses (a) and maximum out-of-plane displacements (b) in the model with mesh size 1.00 m. ....	182
Figure 55 - Exponential increase of degrees of freedom with the element size. ....	183
Figure 56 - Average ( $Q_1$ ) and weighted ( $Q_2$ ) quality mesh according to the mesh size variation. ....	184
Figure 57- Maximum Mises stresses (MPa) (a) and total displacements (mm) (b). ....	185
Figure 58 - Main vibration modes in the transversal ( $TR_{01}$ ) and longitudinal ( $LT_{01}$ ) directions: frequencies $f$ and relative participation mass $RM_Y$ and $RM_X$ . ....	187
Figure 59 - Representative transversal vibration modes selected from the modal analysis. ...	188
Figure 60 - Configurations of the two setups of the accelerometers in the ambient vibration test: piezoelectric accelerometer in uniaxial or bi-axial configuration (d) and (e) connected to a power unit/amplifier (d), whom signal is received from a data acquisition system (c) and elaborated in the acquisition computer Panasonic Toughbook CF-F9 (b). ....	189
Figure 61 - First singular value line (SVD) obtained from the operation modal analysis. ....	191
Figure 62 - Experimental modal shapes. ....	191
Figure 63- Modal Assurance Criterion obtained in Artemis <sup>®</sup> . ....	192
Figure 64 - Modal assurance criterion of the experimental modes. ....	193
Figure 65 - Comparison between experimental and numerical modes, in terms of frequency and modal shapes. ....	194
Figure 66 - Sensitivity coefficients according to the variation of the weight of the three masonry levels. ....	197
Figure 67 - Sensitivity coefficients according to the variation of Young Modulus of the three masonry levels. ....	198
Figure 68 - Sensitivity coefficient of the selected parameters: $E$ , $E_v$ , $E_c$ , $w$ , $w_v$ , $w_c$ , $t_v$ , $t_c$ . ....	202
Figure 69 - MAC-based semi-automatic selection of numerical modes of the updated model. ....	203
Figure 70 - Comparison of numerical and experimental modes for the Base model. ....	204
Figure 71 - Comparison of numerical and experimental modes for the Updated model. ....	205
Figure 72 - Frequency-Modal Assurance Criterion (FMAC) of base and updated models. ...	206
Figure 73 - Loss of the information in the FEM-to-BIM direct integration for a new H-BIM project. ....	208

Figure 74 - Overall view (a) and north-facing orthophoto (b) of the fortress of Anhatomirim Island, Santa Catarina, Brazil. ....	211
Figure 75 - As-designed representation of the <i>Quartel da Tropa</i> : a) north-east façade, b) ground floor plan, c) second-floor plan and d) mezzanine floor plan. ....	213
Figure 76 - <i>Quartel das Tropas</i> in the 1970s structural interventions (a, b, c, and d). Lateral partially buried façades in three sides of the construction (b, c, e and f). ....	214
Figure 77 - <i>Quartel da Tropa</i> (a) in the ‘as-built’ configuration after the 1970s restorations (b, c, d, e) where the simple trussed roof structure (b) was replaced with a collar tie beam (e) and concrete beams (d) were introduced on the masonry arches (c) and (g); three sides of the construction are partially buried (f). ....	215
Figure 78 - Stratigraphy of a masonry wall and transversal connection with the retaining wall. ....	218
Figure 79 - Stratigraphy of second-level masonry walls (a, b), presence of voids due to the pre-existing chimney. Mortar in good condition in arches (c) and columns (d), while bricks in an advanced state of degradation.....	219
Figure 80 - Current state of the wooden slab elements (a, b), supports of the wooden slab (c) and the wooden tie-beams of the roof (d).....	220
Figure 81 - Section of the <i>Quartel da Tropa</i> , with identification of the structural elements of the roof after the intervention of 1970.....	221
Figure 82 - Advanced degradation of floor joists caused by fungi (a), moisture stains on roof rafters (b) and floor (c). Termite degradation in wooden joists (d) and roof tie-beams (e). ..	222
Figure 83 - Constructive evolution in the H-BIM: ‘as-designed’ project (a), the introduction of the central masonry element (b), the introduction of the buttresses (c), ‘as-built’ project (d) and ground-level plan according to the constructive evolution (e). ....	225
Figure 84 - Evolution of the mesh quality dimensionless parameters $Q_1$ e $Q_2$ of the Coons mesh method according to the element size.....	228
Figure 85 - Definition of axes and control-points in the Finite Element model in the north-east façade.....	230
Figure 86 - Evolution of the most representative transversal) and longitudinal mode according to the constructive phases: ‘as-designed’ project (a), the introduction of the central masonry element (b), the introduction of the buttresses (c), ‘as-built’ project (d).....	232

Figure 87 - Out-of-plane top displacement (cm) of the north-east façade according to the constructive evolution: ‘as-designed’ project (a), the introduction of the central masonry element (b), the introduction of the buttresses (c), ‘as-built’ project (d).....	233
Figure 88 - Base compressive stress (MPa) in the control points of the north-east façade according to the constructive evolution.....	234
Figure 89 - Stress distribution in the ‘as-built’ configuration (a); damage in the column of the north-east façade (b). .....	235
Figure 90 - First vibrational modes in transversal ( $\delta_1$ ) (a) and longitudinal ( $\delta_2$ ) (b) directions. Top out-of-plane displacements $\delta_3$ between axes 6 <sup>th</sup> and 7 <sup>th</sup> and $\delta_4$ between axes 4 <sup>th</sup> and 5 <sup>th</sup> (c). Mises stresses at the base of the column $\delta_5$ and the springing line of arch $\delta_6$ in the 4 <sup>th</sup> axis (d). .....	239
Figure 91 - Sensitivity coefficients of structural responses according to the aleatory and epistemic parameters. ....	241
Figure 92 - Damages in the column of the 4th axis of the structure (a, b), connection between column and buttresses (c) and connection of the central slope-shaped masonry with the main façade (d). .....	242
Figure 93 - Experimental test set-up: accelerometer configuration for the modal parameter assessment and the health monitoring, and other non-destructive or minor destructive tests. ....	244

## LIST OF CHARTS

Chart 1 - Comparison of TLS and SfM methods and instruments. ....	65
Chart 2 - Masonry Compressive Mechanical Properties (literature results). ....	76
Chart 3 - Masonry Shear Strength Parameters in literature results. ....	76
Chart 4 - Knowledge levels and corresponding methods of analysis. ....	95
Chart 5 - Recommended minimum requirements for different levels of inspection and testing. .....	95
Chart 6 - Reference values of the mechanical parameters of the masonry and average specific weight for different types of masonry. ....	98
Chart 7 - Maximum corrective coefficients to be applied to the reference values of the mechanical parameters of the masonry (Table C8.5.II of NTC18). ....	99
Chart 8 - Reference experimental test method on the mechanical properties of masonry. ....	100
Chart 9 - The definition of the level of the depth of research on diverse aspects of knowledge and relative partial confidence factors $F_{ck}$ . ....	102
Chart 10 - Generalized stress-strain matrices for isotropic materials. ....	110
Chart 11 - Definition of the level of development (LOD). ....	141

## LIST OF TABLES

Table 1 - Mechanical parameters of the masonry wall ( $E_m, w_m$ ) and vaults ( $E_v, w_v$ ).....	180
Table 2 - Mechanical parameters of the steel and wooden elements. ....	180
Table 3 - Influence of the element size in the transversal and longitudinal vibration modes ( $Y, X$ ), maximum compressive strength ( $\sigma$ ), out-of-plane displacement ( $\delta$ ), degree of freedom (DOF), and variation $\Delta$ DOF. ....	181
Table 4 - Vibration modes in the range of 0-10 Hz. ....	186
Table 5 - Influence of springs in the dynamic behaviour of the structure. ....	187
Table 6 - Vibration modes obtained from the Frequency Domain Decomposition. ....	191
Table 7 - Modal assurance criterion and comparison between experimental (EXP) and numerical (FEM) modes. ....	194
Table 8 - Definition of parameter values of Sensitivity Analysis: lower and upper bounds..	196
Table 9 - Sensitivity coefficient for each assessed parameter. ....	197
Table 10 - Selected parameters to be updated. ....	199
Table 11 - MAC values of numerical modes compared to the experimental data. ....	200
Table 12 - Frequencies of the $2N+1$ analyses, with $N = 7$ number of the parameters. ....	200
Table 13 - Sensitivity coefficients of the selected parameters: $E, E_v, E_c, w, w_v, w_c, t_v, t_c$ .....	201
Table 14 - Optimized parameters obtained from the DR algorithm.....	202
Table 15 – Numerical comparison by modal assurance criterion and frequency discrepancy between the base model ( $MAC_{BM}, DF_{BM}$ ) and the updated model ( $MAC_{UM}, DF_{UM}$ ).....	206
Table 16 - Characteristics of the physical and mechanical parameters of the soil.....	223
Table 17 - Characteristics of the physical and mechanical parameters. ....	227
Table 18 - Modal parameters according to the construction phases.....	231
Table 19 - Deterministic and aleatory parameters of the proposed Sensitivity Analysis.....	237
Table 20 - Response variations $\delta_i$ according to the sensitivity analysis of the aleatory and epistemic parameters. ....	240
Table 21 - Response variation coefficients $\Delta'_k$ according to the sensitivity analysis of the aleatory parameters.....	241



## LIST OF ABBREVIATIONS AND ACRONYMS

ABNT - *Associação Brasileira de Normas Técnicas*

AEC - Architecture, Engineering and Construction

AIA - American Institute of Architects

AR - Aspect Ratio

AVT - Ambient Vibration Test

BIM - Building Information Modelling

CAD - Computer-Aided Design

CBIC - *Câmara Brasileira da Indústria de Construção*

CNR - National Research Council

DOF - Degree of Freedom

DR - Douglas and Reid method

DT - Destructive test

EC - Eurocode

*E.G. - Exemplii gratia*

*ETC. - Et cetera*

HBIM - Historic Building Information Modelling

ICOMOS - International Council on Monuments and Sites

IAI - International Alliance for Interoperability

IE - Inverse Eigensensitivity

*I.E. - Id est*

IFC - Industry Foundation Class

ISCARSAH - International Scientific Committee on the Analysis and Restoration of Structures of Architectural Heritage

FEA - Finite Element Analysis

FC - Confidence Factors

FDD - Frequency Domain Decomposition

FEM - Finite Element Modelling

FM - Facility Management

FMAC - Frequency Modal Assurance Criterion

GIEM - *Grupo Interdisciplinar de Estudos da Madeira*

IRT - Infrared Thermography

KL - Knowledge level

LAMGEO - *Laboratório de Mapeamento Geotécnico*

LOD - Level of development

MAC - Modal Assurance Criterion

MDT - Minor Destructive Test

MT - Modelling Tolerance

OMA - Operational Modal Analysis

NDT - Non-Destructive Test

NTC - *Norme Tecniche per le Costruzioni*

PP - Peak Piking

SA - Sensitivity Analysis

SAM - Simplified Analysis Method

SHM - Structural Health Monitoring

SSI - Stochastic Subspace Identification

SVD - Single Value Decomposition

UNESCO - United Nations Educational, Scientific and Cultural Organization

## LIST OF SYMBOLS

$\alpha_i$  - Mesh quality of each element

$\bar{a}$  - Central value of the ground peak accelerations leading to the referred limit state

$a_k$  - Ground peak acceleration leading to the limit state adopting the aleatory parameter  $k$

$a_{k,min}$  - Ground peak accelerations leading to the referred limit state adopting minimum values of the aleatory parameter  $k$

$a_{k,max}$  - Ground peak accelerations leading to the referred limit state adopting maximum values of the aleatory parameter  $k$

$B^{(m)}$  - Strain-displacement matrix.

$[C]$  - Stress-strain material matrix

$C$  - Cohesion of soil

$C^{(m)}$  - Elasticity matrix of element  $m$

$CMX$  - Cumulative participating mass of the vibration mode in the X direction

$CMY$  - Cumulative participating mass of the vibration mode in the Y direction

$CMZ$  - Cumulative participating mass of the vibration mode in the Z direction

$DF$  - Frequency discrepancy

$\delta\sigma_m$  - Increment of stress

$\delta\varepsilon_m$  - Increment of strain

$\Delta'_k$  -

$\varepsilon$  - Strain vector

$\bar{\varepsilon}$  - Virtual strains corresponding to virtual displacements  $\bar{U}$

$\varepsilon_h$  - Horizontal strain

$\varepsilon_m$  - Masonry actual strain

$\varepsilon_v$  - Vertical strain

$e$  - Error of the solution

$E$  - Elastic Modulus of Young

$\Phi$  - Friction angle of the soil

$f^B$  - Vector of body forces

$f^f$  - Surface forces per unit surface

$f_i^{FEM}$  - Frequency considered as base value compared to the variation  $\partial f_i^{FEM}$  for each variation

$\partial X_k$

$f_m$  - Average compressive strength of masonry  
 $f_{v0}$  - Average shear strength of masonry  
 $F$  - Failure force of Mohr-Coulomb  
 $F_c$  - Confidence factor  
 $F_{ck}$  - Partial confidence factor concerning the level of knowledge  $k$   
 $\{\psi_{cr}^*\}^T$  - the transpose of the modal vector for reference  $c$  and mode  $r$   $\{\psi_{cr}\}$   
 $\{\psi_{dr}^*\}$  - Complex conjugate of modal vector for reference  $d$  and mode  $r$ ,  $\{\psi_{dr}\}$ .  
 $\{\psi_r\}^T$  - Transpose of modal vector for mode  $r$   
 $\{\psi_s\}$  - Modal vector for  $s$ -th mode,  $\{\psi_r\}^T$  is the transpose of modal vector for mode  $r$   
 $G$  - Elastic Shear Modulus  
 $G(f)$  - SVD of the spectral matrix at each frequency  
 $h$  - Height of the element  
 $H$  - Matrix computed either using the Moore-Penrose pseudo-inverse ( $H=S^T(SS^T)^{-1}$ ) or following the Bayesian estimation theory  
 $H^{(m)}$  - Displacement interpolation matrix  
 $i$  - Unit imaginary number  
 $J$  - Radiant emittance of the Stefan-Boltzmann equation  
 $K_a$  - Ratio of the bearing areas between the flat jack in contact with the masonry and the slot  
 $K_m$  - Calibration factor  
 $K$  - Stiffness matrix  
 $K^{(m)}$  - Stiffness matrix of element  $m$   
 $M$  - Mass matrix  
 $N$  - Normal force of Mohr-Coulomb  
 $p$  - Pressure of the flat-jack  
 $\text{®}$  - Registered trademark symbol  
 $R_B$  - Body force vector  $RC$   
 $R_C$  - Vector of the concentrated nodal loads  
 $R_C^i$  - Concentrated nodal loads  
 $R_e$  - Vector associated with the reference response test data  
 $R_I$  - Vector of the element initial stresses  
 $RMX$  - Relative participating mass of the vibration mode in the X direction  
 $RMY$  - Relative participating mass of the vibration mode in the Y direction  
 $RMZ$  - Relative participating mass of the vibration mode in the Z direction  
 $R_s$  - Vector of the surface forces

$R(X_0)$  - Vector containing the responses from the model corresponding to the starting choice  $X_0$  of the updating parameters  
 $s$  - Side of the element  
 $S$  - Sensitivity matrix with terms  $\partial R_i / \partial X_k$   
 $s_{i,k}$  - Sensitivity coefficient  
 $S_u$  - Boundary area related to a body  
 $S_f$  - Surface where forces act  
 $S_y(j\omega_i)$  - Spectrum around an eigenfrequency  $\omega_i$   
 $k_B$  - Stefan-Boltzmann constant  
 $\sigma_m$  - Compressive stress in the masonry  
 $\Sigma$  - Diagonal matrix containing the real positive singular values  
 $Q_1$  - Average quality of each mesh element  
 $Q_2$  - Weighted quality of each mesh element  
 $\tau$  - Stress vector  
 $\tau^{(m)}$  - Given element initial stresses  
 $\tau_0$  - Average shear strength of the masonry  
 $T$  - Absolute temperature ( $^{\circ}\text{K}$ )  
 $u$  - Exact solution  
 $u_h$  - Numerical solution  
 $U$  - Vector of displacement of the generic body  
 $U^{\text{Su}}$  - Vector of prescribed displacements  
 $\widehat{U}$  - Vector of the global displacement components  
 $\dot{u}$  - Vector of the first derivative of the displacement  $u$   
 $\ddot{u}$  - Vector of the second derivative of the displacement  $u$   
 $\{v_i\}$  - Vector of the  $i$ -th mode shape  
 $\nu$  - Poisson's ratio  
 $X$  - Frequency of the first longitudinal mode  
 $X_k$  - Value of  $k$ -th parameter to be identified in the Sensitivity Analysis  
 $Y$  - Frequency of the first transversal mode  
 $w$  - Average specific weight of the masonry  
 $\omega$  - Resonant frequency

## SUMMARY

<b>1</b>	<b>INTRODUCTION .....</b>	<b>47</b>
<b>2</b>	<b>STATE OF THE ART .....</b>	<b>53</b>
2.1	STRUCTURAL ASSESSMENT OF HERITAGE BUILDINGS .....	53
<b>2.1.1</b>	<b>Investigation procedures for the diagnosis of heritage buildings.....</b>	<b>54</b>
<b>2.1.2</b>	<b>Experimental tests for the structural assessment .....</b>	<b>55</b>
2.1.2.1	<i>Visual inspection.....</i>	56
2.1.2.2	<i>Geometric survey.....</i>	59
2.1.2.2.1	Computer-Aided Design.....	60
2.1.2.2.2	Building Information Modelling .....	61
2.1.2.2.3	Laser scanning and photogrammetry.....	64
2.1.2.3	<i>Infrared thermography .....</i>	<i>67</i>
2.1.2.4	<i>The sonic pulse velocity test .....</i>	<i>69</i>
2.1.2.5	<i>Flat jack test .....</i>	<i>73</i>
2.1.2.6	<i>Ambient vibration test.....</i>	<i>76</i>
2.1.2.7	<i>Soil experimental tests for engineering purpose .....</i>	<i>79</i>
<b>2.1.3</b>	<b>Structural health monitoring.....</b>	<b>85</b>
<b>2.1.4</b>	<b>Existing methodologies for the structural assessment of heritage buildings .</b>	<b>88</b>
2.1.4.1	<i>ICOMOS recommendation .....</i>	<i>88</i>
2.1.4.2	<i>The Diagnosis Research Project .....</i>	<i>90</i>
2.1.4.3	<i>Vibration-based structural identification for health monitoring.....</i>	<i>91</i>
2.1.4.4	<i>The level of knowledge as a methodology for heritage buildings .....</i>	<i>93</i>
2.1.4.4.1	European Standard EN 1998-3:2005: Design of structures for earthquake resistance: Part 3: Assessment and retrofitting of buildings.....	94
2.1.4.4.2	Italian standards: NTC 08 and further updating standards.....	96
2.1.4.4.3	Italian Guidelines for evaluation and mitigation of seismic risk to Cultural Heritage	

<b>2.1.5</b>	<b>Partial conclusions</b> .....	<b>103</b>
2.2	VIBRATION-BASED STRUCTURAL IDENTIFICATION.....	104
<b>2.2.1</b>	<b>Types of approach to structural identification</b> .....	<b>104</b>
<b>2.2.2</b>	<b>Structural assessment through Finite Element Analysis</b> .....	<b>108</b>
2.2.2.1	<i>The general problem of structural analysis</i> .....	108
2.2.2.2	<i>Equilibrium of the body through Finite Element Analysis</i> .....	111
2.2.2.3	<i>Mesh element: type, definition and quality</i> .....	115
2.2.2.4	<i>Self-weight analysis</i> .....	118
2.2.2.5	<i>Modal analysis</i> .....	119
<b>2.2.3</b>	<b>Operational modal analysis</b> .....	<b>121</b>
2.2.3.1	<i>Peak Picking</i> .....	122
2.2.3.2	<i>Frequency Domain Decomposition</i> .....	123
2.2.3.3	<i>Stochastic Subsystem Identification</i> .....	124
2.2.3.4	<i>Modal assurance criterion</i> .....	125
<b>2.2.4</b>	<b>Sensitivity analysis for the structural parameter assessment</b> .....	<b>128</b>
<b>2.2.5</b>	<b>Model Updating for the structural identification</b> .....	<b>130</b>
2.2.5.1	<i>The Inverse Eigen-Sensitivity method</i> .....	131
2.2.5.2	<i>Douglas and Reid method</i> .....	131
<b>2.2.6</b>	<b>Partial conclusions</b> .....	<b>133</b>
2.3	BUILDING INFORMATION MODELLING FOR CULTURAL HERITAGE	133
<b>2.3.1</b>	<b>Knowledge management in BIM</b> .....	<b>134</b>
2.3.1.1	<i>The dimensions of Building Information Modelling</i> .....	136
2.3.1.2	<i>Level of development of Building Information Modelling</i> .....	138
2.3.1.3	<i>Interoperability in BIM</i> .....	141
<b>2.3.2</b>	<b>Historic Building Information Modelling for the structural analysis</b> .....	<b>143</b>
<b>2.3.3</b>	<b>Partial conclusions</b> .....	<b>145</b>

<b>3</b>	<b>HBIM-BASED STRUCTURAL IDENTIFICATION FOR CULTURAL HERITAGE.....</b>	<b>147</b>
3.1	ARCHITECTURAL INVESTIGATION .....	148
3.1.1	<b>Historical and documentary research.....</b>	<b>148</b>
3.1.2	<b>Information acquisition.....</b>	<b>149</b>
3.1.3	<b>Historic Building Information Modelling and information management....</b>	<b>150</b>
3.2	PRELIMINARY STRUCTURAL GLOBAL ASSESSMENT .....	151
3.2.1	<b>FEM model.....</b>	<b>151</b>
3.2.2	<b>Preliminary linear elastic analysis .....</b>	<b>152</b>
3.2.3	<b>Modal analysis for the design of ambient vibration tests.....</b>	<b>154</b>
3.2.4	<b>AVT and OMA for the structural identification .....</b>	<b>154</b>
3.2.4.1	<i>Ambient vibration test.....</i>	<i>155</i>
3.2.4.2	<i>Representation of the setups in the H-BIM model.....</i>	<i>155</i>
3.2.4.3	<i>Operational modal analysis.....</i>	<i>155</i>
3.2.4.4	<i>MAC-based semi-automatic procedure .....</i>	<i>156</i>
3.3	MODEL UPDATING FOR THE STRUCTURAL IDENTIFICATION.....	157
3.3.1	<b>Sensitivity Analysis for the model uncertainty understanding.....</b>	<b>158</b>
3.3.2	<b>Finite Element model tuning and H-BIM model updating.....</b>	<b>159</b>
3.4	MANAGEMENT FOR THE LEVEL OF KNOWLEDGE INCREASING .....	160
3.4.1	<b>The dimension of the H-BIM oriented methodology.....</b>	<b>161</b>
3.4.2	<b>Level of development of the H-BIM oriented methodology.....</b>	<b>161</b>
3.4.3	<b>Level of knowledge increase .....</b>	<b>162</b>
3.5	WORKFLOW OF THE METHODOLOGY .....	163
<b>4</b>	<b>H-BIM FOR THE GLOBAL STRUCTURAL BEHAVIOUR ASSESSMENT: THE CASE OF <i>GALLERIA DEGLI ANTICHI</i> .....</b>	<b>165</b>
4.1	HISTORIC AND DOCUMENTARY RESEARCH .....	166
4.1.1	<b>Historic background and architectural geometric generation .....</b>	<b>167</b>
4.1.2	<b>Functional evolution and repair intervention .....</b>	<b>169</b>



4.2	INFORMATION ACQUISITION.....	171
4.2.1	<b>Visual inspection .....</b>	<b>171</b>
4.2.2	<b>From image data acquisition to thematical surveys .....</b>	<b>174</b>
4.3	HISTORIC-BUILDING INFORMATION MODELLING .....	176
4.3.1	<b>H-BIM management: dimension and level of development.....</b>	<b>176</b>
4.3.2	<b>The system configuration of the structural model.....</b>	<b>178</b>
4.3.3	<b>Material properties and assumptions .....</b>	<b>180</b>
4.4	FINITE ELEMENT MODEL.....	180
4.4.1	<b>FE model and mesh element definition.....</b>	<b>181</b>
4.4.1	<b>Mesh quality .....</b>	<b>183</b>
4.5	PRELIMINARY STRUCTURAL GLOBAL ASSESSMENT .....	184
4.5.1	<b>Self-weight analysis.....</b>	<b>184</b>
4.5.2	<b>Built Environment evaluation .....</b>	<b>187</b>
4.6	MODAL ANALYSIS FOR THE DESIGN OF AMBIENT VIBRATION TESTS 188	
4.6.1	<b>Understanding of the overall structural behaviour .....</b>	<b>188</b>
4.6.2	<b>Design of the ambient vibration test .....</b>	<b>189</b>
4.7	OPERATIONAL MODAL ANALYSIS.....	190
4.7.1	<b>Ambient vibration test.....</b>	<b>190</b>
4.7.2	<b>Frequency Domain Decomposition .....</b>	<b>190</b>
4.8	THE MAC-BASED SEMI-AUTOMATIC IDENTIFICATION PROCEDURE	192
4.9	PARAMETER EVALUATION OF HISTORICAL CONSTRUCTION THROUGH SENSITIVITY ANALYSIS .....	195
4.9.1	<b>Definition of the uncertainty value range.....</b>	<b>195</b>
4.9.2	<b>Sensitivity analysis.....</b>	<b>196</b>
4.10	FINITE ELEMENT MODEL TUNING .....	198
4.10.1	<b>Selection of the boundary condition range values .....</b>	<b>199</b>

4.10.2	<b>MAC-based semi-automatic identification.....</b>	<b>199</b>
4.10.3	<b>Sensitivity coefficients for the understanding of the model parameters .....</b>	<b>201</b>
4.10.4	<b>FE model updated.....</b>	<b>202</b>
4.11	H-BIM OPTIMAL MODEL.....	207
4.12	PARTIAL CONCLUSION.....	208
<b>5</b>	<b>UNDERSTANDING THE STRUCTURAL BEHAVIOUR OF HISTORICAL BUILDINGS AND THE TEST PLANNING: THE CASES OF THE <i>QUARTEL DA TROPA</i></b>	<b>211</b>
5.1	MAIN HYPOTHESES OF THE RESEARCH CASE STUDY.....	212
5.2	HISTORIC AND DOCUMENTARY RESEARCH .....	213
<b>5.2.1</b>	<b>Understanding the constructive evolution of the structure .....</b>	<b>213</b>
<b>5.2.2</b>	<b>Historical-critical analysis and survey .....</b>	<b>216</b>
5.3	INFORMATION ACQUISITION.....	217
<b>5.3.1</b>	<b>Visual inspection .....</b>	<b>217</b>
5.3.1.1	<i>Evaluation of the masonry structures .....</i>	<i>217</i>
5.3.1.2	<i>Evaluation of the timber structures .....</i>	<i>219</i>
<b>5.3.1</b>	<b>Wooden characteristic investigation .....</b>	<b>222</b>
<b>5.3.2</b>	<b>Soil characteristic investigation.....</b>	<b>223</b>
5.4	HISTORIC-BUILDING INFORMATION MODELLING .....	223
<b>5.4.1</b>	<b>The system configuration of the structural model.....</b>	<b>224</b>
<b>5.4.2</b>	<b>Material properties and assumptions .....</b>	<b>226</b>
5.5	FINITE ELEMENT MODEL.....	227
<b>5.5.1</b>	<b>Definition and calibration of the mesh.....</b>	<b>227</b>
<b>5.5.2</b>	<b>Definition of loads and boundary conditions .....</b>	<b>229</b>
<b>5.5.3</b>	<b>Preliminary structural global assessment .....</b>	<b>229</b>
<b>5.5.4</b>	<b>Self-weight analysis.....</b>	<b>230</b>
5.5.4.1	<i>Evolution of first vibration modes through the constructive phases .....</i>	<i>230</i>
5.5.4.2	<i>Out-of-plane displacement.....</i>	<i>232</i>

5.5.4.3	<i>Base compressive stress</i> .....	234
5.6	TEST PLANNING HISTORICAL CONSTRUCTION: FROM THE SENSITIVITY ANALYSIS TO THE PARAMETER UNDERSTANDING .....	236
<b>5.6.1</b>	<b>Application of Sensitivity Analysis to historical construction test planning</b>	<b>236</b>
5.6.1.1	<i>Definition of the uncertainty value range</i> .....	237
5.6.1.2	<i>Control point selection</i> .....	238
5.6.1.3	<i>Response variation of the aleatory and epistemic parameters</i> .....	240
<b>5.6.2</b>	<b>Cognitive evaluation for the <i>in-situ</i> test planning design</b> .....	<b>242</b>
<b>5.6.3</b>	<b>Improvement assessment</b> .....	<b>245</b>
5.7	PARTIAL CONCLUSION.....	246
<b>6</b>	<b>GENERAL CONCLUSIONS</b> .....	<b>249</b>
	<b>REFERENCES</b> .....	<b>253</b>
	<b>APPENDIX A - Increasing the level of development of the H-BIM models</b>	<b>273</b>
	<b>APPENDIX B - Soil characteristic investigation</b> .....	<b>275</b>
	<b>ANNEXE A - Photogrammetric Survey of <i>Galleria degli Antichi</i></b> .....	<b>278</b>
	<b>ANNEXE B - Evaluation of the wooden structures of <i>Quartel da Tropa</i> of the Fortress of the Island of Anhatomirim</b> .....	<b>281</b>



## 1 INTRODUCTION

In the research field of heritage buildings, the process of evaluation of the global structural behaviour is a fundamental approach to understand the critical characteristics of the construction. The creation of a three-dimensional interpretive model - consistent with the real behaviour of the structure - allows the global structural behaviour assessment (DIRECTIVE OF THE PRIME MINISTER, 2007; M. IOANNIDES; E. FIN; R. BRUMANA; P. PATIAS; A. DOULAMIS; J. MARTINS MANOLIS WALLACE, 2018; VAN BALEN, K.; VANDESANDE, 2017). The level of reliability of this interpretive model is strongly related to the level of development of the model itself (BIAGINI *et al.*, 2016) and the available data (DIRECTIVE OF THE PRIME MINISTER, 2007; M. IOANNIDES; E. FIN; R. BRUMANA; P. PATIAS; A. DOULAMIS; J. MARTINS MANOLIS WALLACE, 2018; VAN BALEN, K.; VANDESANDE, 2017). Hence, the data relating to cultural heritage buildings concerns multidisciplinary fields of research, *e.g.* historical, architectural, engineering, economic and social issues (DIRECTIVE OF THE PRIME MINISTER, 2007). Consequently, the interpretive model requires an information database suitable for the complete understanding of the analysed structure. Such a model is useful to the analyst for the diagnosis of the structure and the decision-making phases.

The investigation procedure for the diagnosis of heritage building requires a process involving historical research, geometric survey, direct inspection supplemented by experimental tests (BINDA; ROBERTI; ABBANEO, 1994). Furthermore, the historical research of heritage constructions is also related to understanding how and which modifications led the ‘as-designed’ project to its ‘as-built’ state. The historical-critical analysis during the documental research helps to understand the ‘as-built’ configuration and the reason for the constructive modifications during the building life-cycle (MAGENES; MENON, 2009). The historical analysis helps the understanding of the constructive evolution, the damage and degradation decay, the transformations that may have produced changes in the static structural behaviour. In this sense, the historical investigation becomes a crucial source of documentation and knowledge aimed at the interpretation of global structural behaviour (INFRASTRUTTURE; TRASPORTI, 2018).

The understanding of the structural behaviour requires a considerable amount of information about the structure, *e.g.* geometries, mechanical properties, loads, boundary conditions (BINDA; SAISI; TIRABOSCHI, 2000). Such information is acquired through

extensive investigation procedures relying on experimental data. Indeed, the systematic use of non-destructive (NDT) or minor destructive (MDT) tests is essential to evaluate those specific factors within the building (BINDA; SAISI, 2001). Such investigation represents a challenge that requires surveys, *in-situ* or laboratory tests and analysis that can be laborious and expensive (GENTILE; SAISI; CABBOI, 2015; ORENI *et al.*, 2017). A primary investigation is a visual inspection, which is the first direct approach to the as-built assessment. Other type tests commonly used in this field are the computer-aided procedure for the geometrical survey, infrared thermography, sonic pulse velocity, flat-jack (BINDA; SAISI; TIRABOSCHI, 2000). However, the number of tests performed on a historical construction is minimal, and offer partial insights on the material parameter characteristic evaluated on local specimens (BINDA; ROBERTI; ABBANEO, 1994). Such tests usually do not allow a statistical treatment of the results (CNR, 2014). Hence, the interpretation of the results must lead to a synthetic judgment, in which the use of only one experimental data can be significant (CNR, 2014).

Limited resources have been usually allocated to the diagnosis of the mechanical behaviour of cultural heritage, which includes non-destructive *in-situ* testing, laboratory testing, and the development of reliable numerical tools (LOURENÇO, 2002). The path to knowledge of historical structures is characterized by issues related to geometric and data missing, complexity and cost of the assessment of the mechanical properties of the used materials (BINDA *et al.*, 2004; LOURENÇO, 2002; ROCA *et al.*, 2010). Information about the structural elements is difficult to be investigated due to the large variability of mechanical properties caused by the craft and the use of natural materials and the occurrence of significant changes in the core and constitution of structural elements, associated with long construction periods. Lack of knowledge of the construction sequence is common, which makes the understanding of the global structural behaviour difficult, and, consequently, the evaluation of possible damage to the structure (LOURENÇO, 2002). Moreover, standards are not easily applicable to such type of buildings, and specific guidelines to the application of the national codes must be consulted (DIRECTIVE OF THE PRIME MINISTER, 2007).

Such a lack of information implies a low level of development of models for the heritage building projects, which can be improved by a better knowledge of the construction managed through the Building Information Modelling (BIM). In recent years, the BIM process has been used in the restoration projects of historical buildings with the name of Historic-Building Information Modelling (H-BIM) (ANTONOPOULOU; BRYAN, 2017). Such a process showed to fit with the phases of the description of the constructive building evolution,

the maintenance of its elements and its structural assessment. Furthermore, the interoperability of the available BIM software allows exporting the structural model to computing software based on the Finite Element Method (FEM). Such interoperability permits more precise modelling and provides more appropriate methods of analysis, *e.g.* modal and dynamic analyses (ANTONOPOULOU; BRYAN, 2017). However, interoperability between different object is not a trivial issue, and special attention is required (BARAZZETTI *et al.*, 2015a). Such an approach enhances the structural analysis considering the overall H-BIM modelled to improve the knowledge and the preservation process (BRUMANA *et al.*, 2018a).

In the BIM environment, data and information are connected to three-dimensional objects, using sets of parameters. In this way, the BIM technology combines the advantages of 3D geometric digital representation with a detailed understanding of how the building is constructed and what its performance is (ANTONOPOULOU; BRYAN, 2017). In literature, BIM was deeply investigated as a methodology for the information management in the development and construction of projects (EASTMAN, CHUCK; TEICHOLZ, PAUL; SACKS, RAFAEL; LISTON, 2011). The BIM models can be used for various applications: evaluation of design options, error detection, estimation and reduction cost, construction simulation, energy modelling, project management, economic management of resources and assets (EASTMAN, CHUCK; TEICHOLZ, PAUL; SACKS, RAFAEL; LISTON, 2011).

Regarding the application of BIM to the heritage field (H-BIM), the literature showed extensively the application of such methodology for the geometric representation, enhanced by laser scanning and photogrammetry tools (ANTONOPOULOU; BRYAN, 2017; MURPHY; MCGOVERN; PAVIA, 2009; ORENI *et al.*, 2014). However, the state of the art of the H-BIM literature confirmed that there is still a need for research in the scientific field of heritage structural assessment (BRUNO; DE FINO; FATIGUSO, 2018; POCOBELLI *et al.*, 2018). Indeed, a lack of knowledge in such field includes the improvements offered by H-BIM for the evaluation of health and safety status of the structures through BIM-to-FEM approaches, and the understanding of the dynamic behaviour of the cultural heritage, *i.e.* frequencies and modal shapes assessment (BRUNO; DE FINO; FATIGUSO, 2018).

The proposed research aims to develop and validate a methodology to increase the understanding of the structural behaviour of heritage buildings, the H-BIM based structural identification of heritage building. Such a methodology is proposed to organize different existing procedures systematically, focusing on the preservation of historical constructions. The systematization of the collected information through the proposition of a novel workflow

addresses to reduce the uncertainties of the investigations for a better decision-making phase both for the investigation procedures for the diagnosis of heritage buildings both for the planning of the preservation programs. The specific aims of the thesis are resumed as follow:

- a) the development and validation of an H-BIM- oriented methodology aimed to increase the knowledge systematically;
- b) the evaluation of the uncertainties of structural assessment, focusing on the reduction of the geometrical and mechanical uncertainties of heritage buildings;
- c) the understanding of the overall structural behaviour of the heritage building through FE modal analysis;
- d) the proposition of a systematic approach for the design of the experimental test investigation, based on the structural analysis assessment;
- e) the increase of knowledge of the heritage buildings, through the experimental investigation of the as-built structural behaviour allowing the vibration-based structural identification;
- f) the improvement of the numerical representation of the heritage building structural behaviour, through FE model tuning.

This thesis is composed of 6 chapters. In the first introductory chapter, the main topics of the research were explained together with the main theoretical bases, the case studies, and the main aims of the research. In the second chapter, the state of the art is investigated to understand the current state of the proposed field research. It is focused on the main topics of a structural assessment of heritage building, historical building information modelling, non-destructive tests, and vibration-based structural identification. In the third chapter, the methodology is described in its three parts, *i.e.* architectural investigation, preliminary structural global assessment, and model updating. In the fourth and fifth chapters, the case studies are presented to apply and validate the proposed methodology. Finally, the sixth chapter is used to summarize the research process and draw conclusions of the proposed work.

Two heritage buildings are selected as case studies to apply the proposed multidisciplinary workflow: The *Galleria Degli Antichi* building, Sabbioneta, Italy and the *Quartel da Tropa*, Anhatomirim Island, State of Santa Catarina, Brazil. The first heritage building built in the 16<sup>th</sup>-century belongs to the UNESCO World Heritage list since 2008. The second, built in the 18<sup>th</sup>-century, is the largest among Brazilian fortifications. It is one of the main buildings of the Fortress of Santa Cruz, located on Anhatomirim Island, municipality of Governador Celso Ramos, State of Santa Catarina, Brazil. The results of the research of such



case studies allow suggesting how to systematically increase the level of knowledge of heritage buildings involving the proposed H-BIM methodology.



## 2 STATE OF THE ART

In this chapter, the state of the art of the field research of H-BIM-based structural identification for cultural heritage is investigated to understand the current knowledge in such a topic. The main topics are the structural assessment of heritage buildings, the vibration-based structural identification of heritage buildings and the historic building information modelling. At the end of each section, a partial conclusion is proposed. It is useful to understand the strengths and weaknesses of each topic, including the possible lack of research to be investigated in the proposed thesis.

### 2.1 STRUCTURAL ASSESSMENT OF HERITAGE BUILDINGS

The first section of Chapter 2 is focused on the topic of the structural assessment of heritage buildings. Main issues are presented through the investigation procedures for the diagnosis of this kind of structures. Then a brief overview of the structural problem is given. Moreover, some of the experimental tests are approached to the general understanding of the topic. Furthermore, Structural Health Monitoring (SHM) is presented as a comprehensive approach to the damage identification problem. Finally, some existing methodologies are presented as proven approaches to the structural assessment of heritage buildings.

Conservation of heritage buildings requires an in-depth knowledge of structures and materials, their characteristics, the state of damage and its causes (BINDA; SAISI, 2009a). The prevention and rehabilitation decision-making phases rely on the diagnosis of the state of damage of the building. The diagnosis and structural identification of the heritage building should result from an experimental *in-situ* and laboratory investigation. It must be non-destructive as far as possible and give information with good precision (BINDA; SAISI; TIRABOSCHI, 2000).

Some reviews of the NDTs for historic constructions can be found in the literature in Binda, Saisi, Tiraboschi (2000), Breyse, (2012), Dwivedi, Vishwakarma, Soni (2018), Hussain, Akhtar (2017), and McCann and Forde (2001). Due to the importance of the NDTs in the assessment of heritage buildings, many application were also found in the scientific literature (BINDA *et al.*, 2004, 2008; BINDA; SAISI, 2001, 2009b; CASARIN; MODENA, 2008; GONÇALVES; TRINCA; PELLEGRINO CERRI, 2011; LOURENÇO *et al.*, 2016; MIRANDA, L.; CANTINI, L.; GUEDES, J.; BINDA, L.; COSTA, 2013). Most of the ND

procedure can give only qualitative results; therefore, the designer is asked to interpret the results and use them at least as comparative values between different parts of the same masonry structures (BINDA; SAISI, 2009a).

A comprehensive understanding of the global structural behaviour is fundamental in the knowledge path of cultural heritage buildings (DIRECTIVE OF THE PRIME MINISTER, 2007; LOURENÇO, 2014). The structural analysis of historic structures is a complex task that poses several challenges to the analyst, *e.g.* historical and documentary research, geometric survey, direct inspection supplemented by experimental tests, time-consuming numerical analysis (LOURENÇO, 2002; ROCA, 2004). Such tasks involve the collection of data from a wide range of sources and the subsequent merging process.

The proposed literature research underlines the significance of accurate planning of such activities to get reliable information about the structural characteristics supporting structural Modelling (BINDA; SAISI; TIRABOSCHI, 2000). Such challenges are investigated in the following subsections.

### **2.1.1 Investigation procedures for the diagnosis of heritage buildings**

The investigation procedure for the diagnosis of heritage building requires a process involving historical research, geometric survey, and direct inspection supplemented by experimental tests. Indeed, the diagnosis of the current state of the Cultural Heritage structures should result from an experimental *in-situ* investigation that must be a non-destructive test as far as possible and give information with good precision (BINDA; SAISI; TIRABOSCHI, 2000).

In general, such an investigation can be performed on different materials, *i.e.* metals, plastics, ceramics, composites, types of cement, and coatings. It aims at the identification of cracks, internal voids, surface cavities, delamination, incomplete defective welds and any type of flaw which would lead to premature failure (DWIVEDI; VISHWAKARMA; SONI, 2018).

However, as analysed in the research of Lourenço (2002), limited resources have been allocated to the diagnosis of the mechanical behaviour of cultural heritage, which includes non-destructive *in-situ* testing, laboratory testing, and development of reliable numerical tools (LOURENÇO, 2002). In Lourenço (2002), the difficulties of knowledge are mainly related to the analysis of historical structures:

- a) geometric and data missing;

- b) information about the inner core of the structural elements;
- c) difficulty and cost of characterization of the mechanical properties of the used materials;
- d) the large variability of mechanical properties caused by the craft and the use of natural materials;
- e) the occurrence of significant changes in the core and constitution of structural elements, associated with long construction periods;
- f) the lack of knowledge of the construction sequence;
- g) unaware of the existence of damage to the structure;
- h) regulations and codes are not applicable.

A wide variety of non-destructive techniques or methods exists in literature and reviews of the NDTs for general engineering purpose. Reviews of the structural assessment of heritage buildings can be found regarding the diagnosis of historic masonry structures (BINDA; SAISI, 2009a; BINDA; SAISI; TIRABOSCHI, 2000; CARVALHO *et al.*, 2014; LIVINGSTON, 1999; LOURENÇO, 2002; MAGENES; PENNA, 2009; ROCA *et al.*, 2010), concrete structures (BREYSSE, 2012; HUSSAIN; AKHTAR, 2017; MCCANN; FORDE, 2001), and the reduction and mitigation of seismic hazard for heritage buildings (DIRECTIVE OF THE PRIME MINISTER, 2007; FERRITO; MILOSEVIC; BENTO, 2016; LAGOMARSINO *et al.*, 2011; LOURENÇO *et al.*, 2011; MAGENES; PENNA, 2009).

### **2.1.2 Experimental tests for the structural assessment**

Conservation of heritage buildings requires an in-depth knowledge of structures and materials, their characteristics, the state of damage and its causes (BINDA; SAISI, 2009a). The decision-making phases regarding prevention and rehabilitation can be accomplished if a diagnosis of the state of building damage has been formulated. The diagnosis and the structural identification of the heritage building should result from an experimental *in-situ* and laboratory investigation (BINDA; ROBERTI; ABBANEO, 1994).

Non-destructive tests have full application in the structural assessment. They are considered as crucial in heritage building researches (BINDA *et al.*, 2004, 2008; BINDA; SAISI, 2001, 2009b; CASARIN; MODENA, 2008; GONÇALVES; TRINCA; PELLEGRINO CERRI, 2011; LOURENÇO *et al.*, 2016; MIRANDA, L.; CANTINI, L.; GUEDES, J.; BINDA, L.; COSTA, 2013). However, most of the ND procedure can give only qualitative results;

therefore, the designer is asked to interpret the results and use them, at least, as comparative values between different parts of the same masonry structures (BINDA; SAISI, 2009a). Even if such type of structure is common both in Europe and Brazil, few Brazilian research studies on such a type of structures were found. They show significant variability in the results, meaning that research on masonry structures is required to enhanced the knowledge of such a type of constructions (ARASH, 2012; CARVALHO *et al.*, 2014). Some of the experimental tests for the structural assessment are presented in the following subsections.

### 2.1.2.1 Visual inspection

The first non-destructive test is the *in-situ* visual inspection, which can also suggest the type of problems to be solved and the type of techniques to be applied (BINDA; SAISI, 2009b). Indeed, engineers or architects may be able to establish the possible causes of structural damage. Hence, analysts must identify which NDT methods could be most suitable for any further investigation (UMAR; HANAFI; LATIP, 2015).

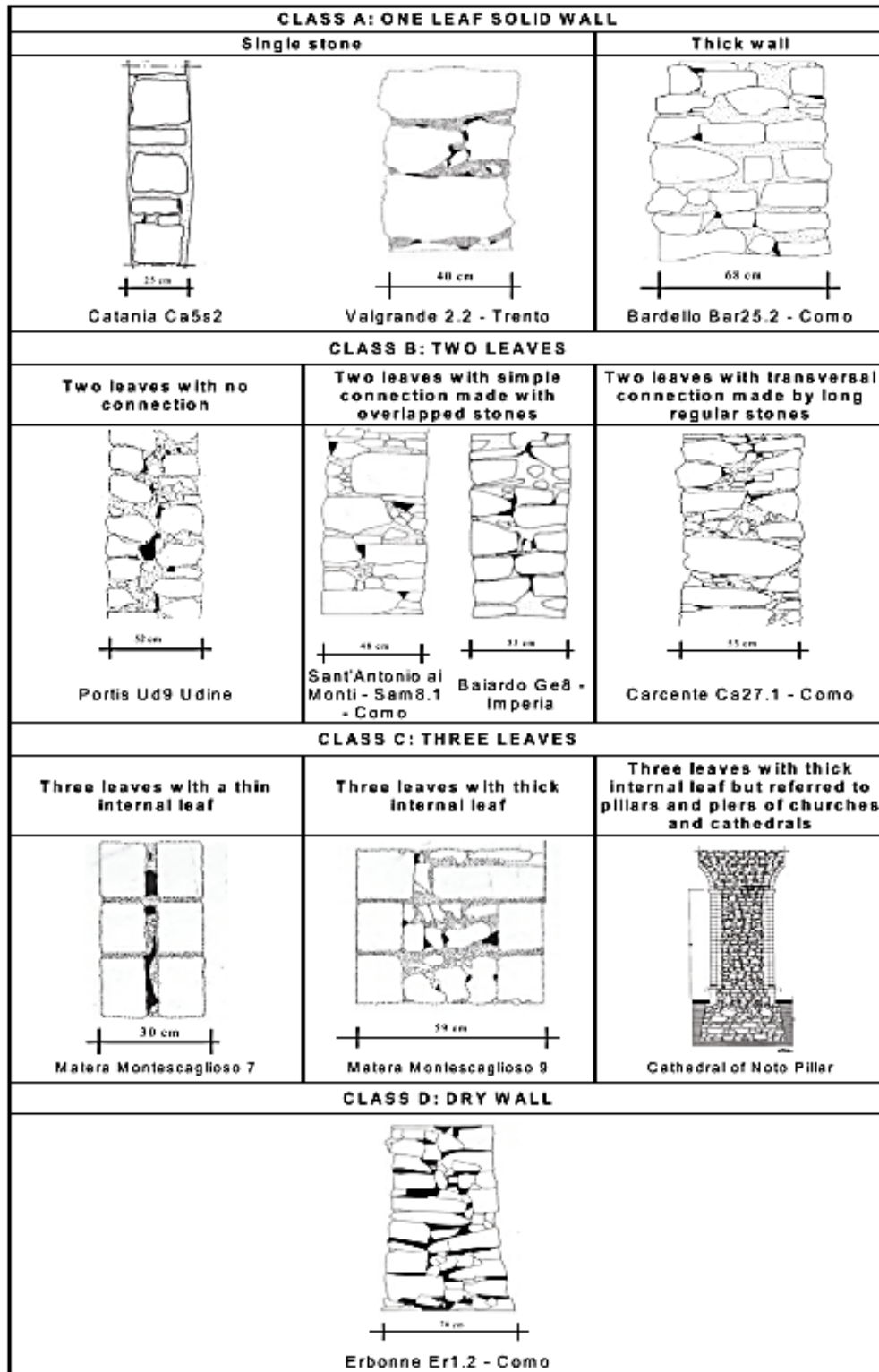
Giuffrè (1991) - *apud* Binda and Saisi (2005) - proposes the visual inspection as a first evaluation of the mechanical behaviour of a stone wall, looking for the presence of particular characteristics which permits the wall to be considered as built according to ‘the rule of art’ (Figure 1). According to such a rule - formulated in 19<sup>th</sup>-century, even if it was already known previously - the layout of the stones has to be analysed since they are aimed to guarantee a good response of the wall toward external actions (BINDA; SAISI, 2005; BINDA; SAISI; TIRABOSCHI, 2000).

The presence of some other characteristics, such as the connection elements, called diatons, can also be a discriminating parameter for the evaluation of mechanical behaviour of walls (figures 1 to 4) (BINDA; SAISI; TIRABOSCHI, 2000; GIUFFRÈ, 1991, 1993; GIUFFRÈ; CAROCCI, 1999). Such an investigation could allow defining if a masonry wall built according to these rules had a predictable monolithic behaviour (Figure 2). Such behaviour means that wall reaches the collapse - for instance, under seismic loads - through the formation of cylindrical springs whereas the portions of the wall maintain a ‘rigid body’ behaviour (BINDA; SAISI; TIRABOSCHI, 2000; GIUFFRÈ, 1991, 1993).

With a similar approach, the Italian Standard Circolare 617/09 introduced a mechanical parameter estimation based on a systematic visual inspection of the masonry structures. Such an approach is utilized for the preliminary assumption of the mechanical

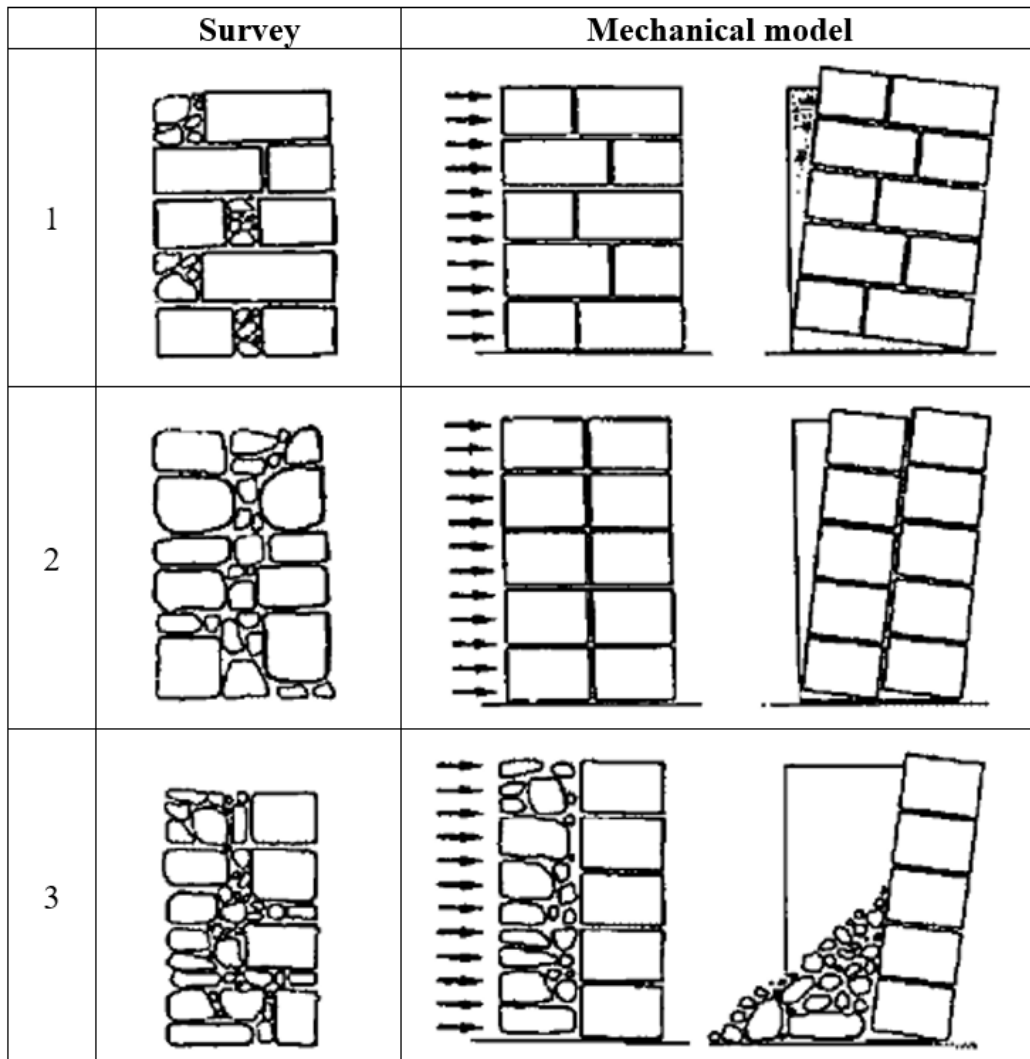
parameters of masonry structures in lack of experimental tests (CS.LL.PP., 2009), and it will be presented in Subsection 2.1.4.4.2 of this thesis.

Figure 1 - Example of the stonework section.



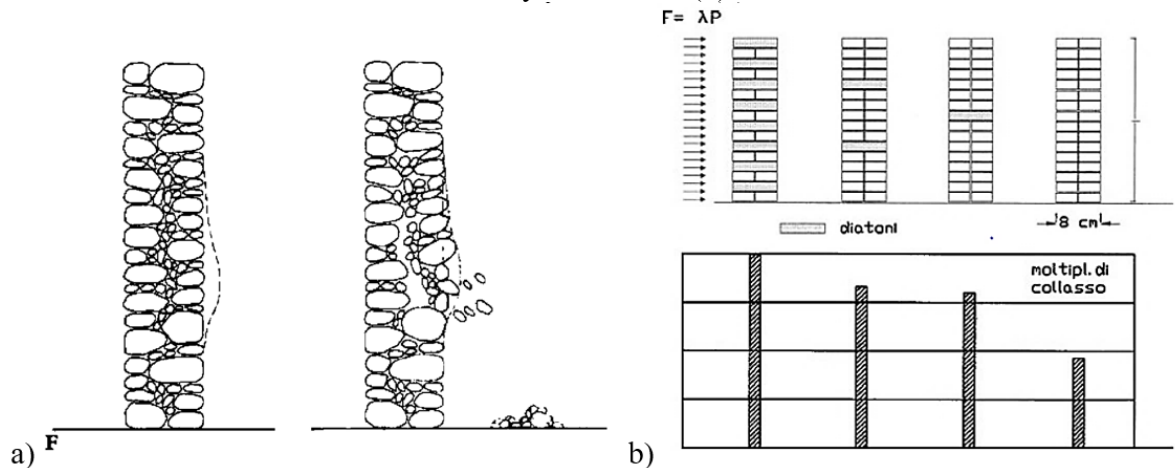
Source: Binda and Saisi (2009).

Figure 2 - Qualitative behaviour of multiple-leaf stone masonry: surveys (*Rilievo*) and mechanic models (*Modello Meccanico*).



Source: Giuffrè and Carrocci (1999) *apud* Binda and Saisi (2005), modified by the author

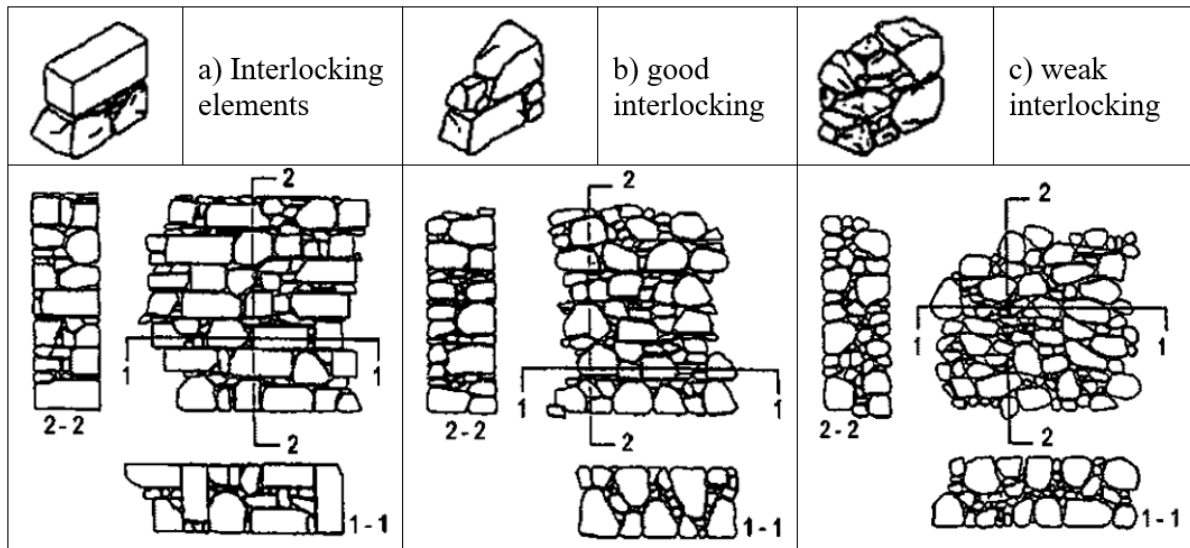
Figure 3 - Deformation and failure of a two-leaf wall (a), diatons and their influence on the stability of the wall (b).



Source: Giuffrè (1990) *apud* Binda and Saisi (2005).



Figure 4 - Example of masonry catalogues: interlocking elements (a, *conci di legamento*), good (b, *buon ingranamento*) and weak (c, *ingranamento insufficiente*) interlocking.



Source: Giuffrè (1990) *apud* Binda and Saisi (2005), modified by the author.

In general, visual inspection is used as an evaluation of the state of conservation of structural elements. Moreover, visual inspection carried out together with other NDT shows to be very useful in different applications, *i.e.* masonry failure mechanism assessment (BINDA; SAISI, 2005; GIUFFRÈ, 1991), wooden species assessment for timber element (BRANCO *et al.*, 2015; TEREZO, 2005). Indeed, a detailed visual inspection - aimed to the detection of visible mechanical damages, fissures, material decay, moisture stains, *etc.* - is essential for the further steps of geometric assessment of the structure (BRANCO *et al.*, 2015).

#### 2.1.2.2 Geometric survey

The geometrical survey of the building is essential for the assessment of cultural heritage. It and has to be carried out accurately using simple or more sophisticated techniques (*e.g.* photogrammetry, laser scanning) according to the type of geometry or the available budget (BINDA; SAISI, 2009b). The crack pattern should be classified and accurately documented by photos and reported on the geometrical survey (BINDA; SAISI, 2009b). The definition of the structural model can be carried out not only based on the geometrical survey but also of the crack pattern. As an example, the crack pattern survey can be helpful in seismic areas where it is essential to predict from known damages the kinematic mechanisms of collapse, which can

occur during an earthquake (BINDA; SAISI, 2009b). Following subsections will focus on the researches founded in last decades regarding computer-aided geometric survey techniques.

#### 2.1.2.2.1 Computer-Aided Design

In the last decades, the development in Information Technology (IT) has taken place affecting both the architectural representation (POCOBELLI *et al.*, 2018) and the structural mechanic analysis, *e.g.* FE analysis (COONS, 1967; HO-LE, 1988; LAWSON, 1977). At the end of the last century, Computer-Aided Design (CAD) allowed the professionals to draw their projects described by lines, arcs, and dimensions (MURPHY, 2012). However, these objects are only graphic entities, but they did not have intelligence (IBRAHIM; KRAWCZYK; SCHIPPOREIT, 2003). Indeed, they were not parametric until feature-based CAD was introduced. A review of feature-based design can be found in Shahin (2008).

Parametric CAD differs from generic 3D CAD, as parameters are assigned to an object. Standard 3D CAD is usually an object-oriented programme. The objects - used to create the lines, arcs, and dimensions - define architectural elements, but they are not parametric (MURPHY, 2012). While a 3D CAD model allows creating three-dimensional objects, plans and sections, it is still formed by purely geometrical elements. Instead, a smart model has all its elements linked to a database containing all the related metadata (POCOBELLI *et al.*, 2018).

Furthermore, feature-based CAD can refer to geometry, specification of materials *etc.*, in addition to function which describes the objects role (*e.g.* wall, door, window) and performance (VAN LEEUWEN; WAGTER, 1997; VAN LEEUWEN; WAGTER; OXMAN, 1995). Such types of software allow the modification and variation of such parameters by the user, the incorporation of object features (such as openings in elements) and interactions between elements within a spatial environment (VAN LEEUWEN; WAGTER, 1997; VAN LEEUWEN; WAGTER; OXMAN, 1995).

Parametric Modelling introduces the concept of variables for the representation of geometry, shape, surface texture or feature which improve the object's real-world depiction (SHAH; MÄNTYLÄ, 1995). As an evolution of such concepts, Building Information Modelling was implemented as a process, rather than technology (POCOBELLI *et al.*, 2018), and it will be presented in the next subsection.

#### 2.1.2.2.2 Building Information Modelling

Modern software allows the creation of interactive database collectors for the elaboration of architectural projects, including structural characteristics. Such software is based on the Building Information Modelling (BIM) method, which describes collaborative processes for the production and the management of structured electronic information (ANTONOPOULOU; BRYAN, 2017). BIM has its origins in modelling applications used in parametric objects for mechanical system designs in the 1980s (ANTONOPOULOU; BRYAN, 2017).

In the BIM environment, data and information are attached to three-dimensional objects, using sets of parameters. In this way, the BIM technology combines the advantages of 3D geometric digital representation with a detailed understanding of how the building is constructed and what its performance is (ANTONOPOULOU; BRYAN, 2017). The BIM represents a method for the information management in the development and construction of projects (EASTMAN, CHUCK; TEICHOLZ, PAUL; SACKS, RAFAEL; LISTON, 2011). The BIM models can be used for various applications: evaluation of design options, error detection, estimation and reduction cost, construction simulation, energy modelling, project management, economic management of resources and assets (EASTMAN, CHUCK; TEICHOLZ, PAUL; SACKS, RAFAEL; LISTON, 2011).

The BIM process is mainly used for new building rather than for existing building since existing buildings have many constraints to respect, *e.g.* the will to preserve the correspondence between the parametric model and the existing structure (DORE; MURPHY, 2012). Indeed, BIM has been used for the past 20 years in the Architecture, Engineering and Construction (AEC) industry, especially in the design and management of new buildings, construction and infrastructure (ANTONOPOULOU; BRYAN, 2017).

Furthermore, the concept of the BIM project needs a change of approach from the professionals, which are mainly used to work with CAD tools (MURPHY, 2012). Besides, BIM offers a solid structure for collaborative multidisciplinary processes of information production and exchange. Such a process is based on the creation of a reliable and shared knowledge track that can be used for communication, planning, consultation, and decision making.

The largest software companies have robust BIM software that comes with online help and training communities (MURPHY, 2012). The leading BIM software platforms are Autodesk Revit® (AUTODESK, 2011), GraphiSoft ArchiCAD (GRAPHISOFT, 2011) and

Bentley Architecture (BENTLEY, 2011). Most of the large companies that make CAD software also have a BIM product. Indeed, choosing the program in the same family of products is suggested to improving the conversion process and to ensure compatibility between programs, (VAN WAGENEN, 2012), since the interoperability process is not ‘error-free’ (DEL GIUDICE; OSELLO, 2013). However, for the professional applications, it is costly to move from CAD to BIM, *i.e.* software licenses are expensive and must be upgraded every few years (MURPHY, 2012).

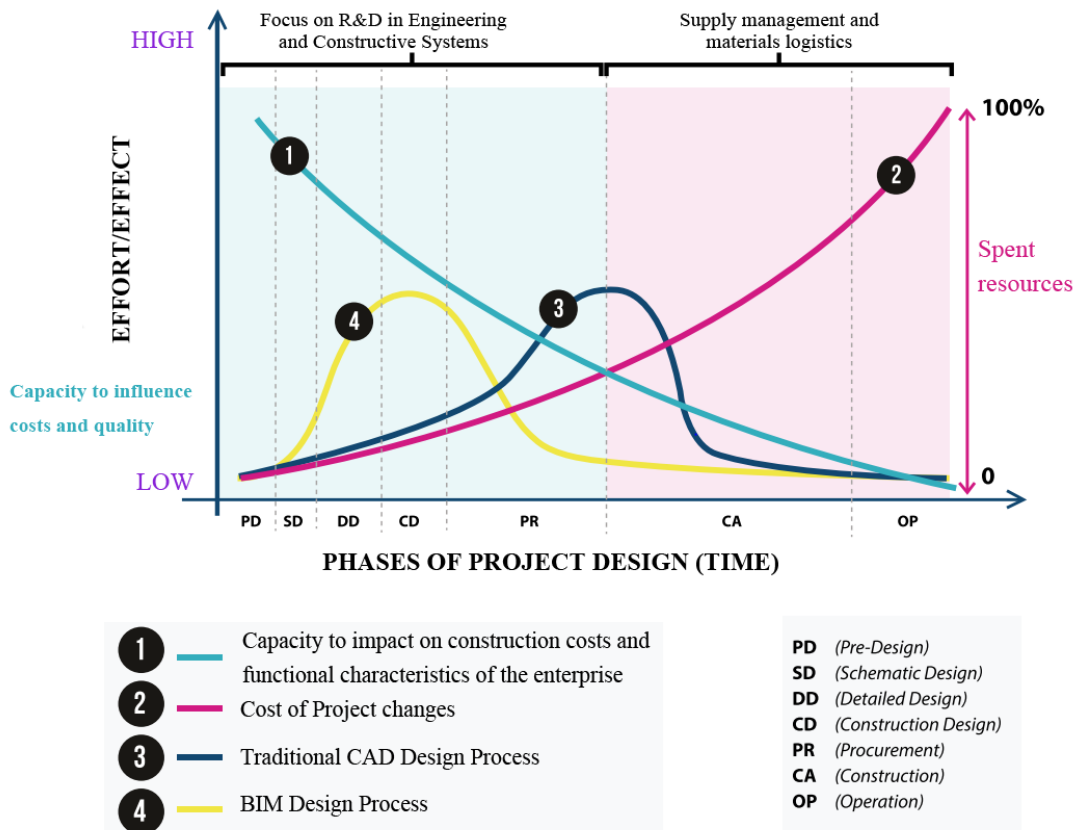
An in-depth overview of the BIM software can be found in Lopez *et al.* (2018), and it is presented as follow:

- a) ArchiCAD (Graphisoft) allows users to work with objects and model them with parametric data; the use of the open-source scripting language Geometric Description Language (GDL) aims at the creation of the object and the storage of these objects in the program’s internal libraries, thus permitting them to be reused or modified in the future; such software can import and export DWG, DXF, and SketchUp files; it also provides interoperability with other BIM platforms through the use of Industry Foundation Classes (IFC);
- b) Tekla Structures is used for the detailed design, cutting, manufacturing, and assembly of all types of structures for construction; high complexity 3D models are created and managed in real-time; this software is an open solution that can import models from other BIM applications using IFC; it also supports DWG, CFI, DGN, DXF, CIS/2, DTSV, and SDNF files;
- c) Bentley System is subdivided into several modules; the platform is used to address all AEC industry aspects; it consists of a set of applications and services based on open-platform, providing solutions for the entire infrastructure life-cycle; it can link IFC, DWG, DGN, DXf, and PDF files; it can open and manipulate point cloud files;
- d) Revit® Autodesk: This is an efficient BIM platform to accurately model regular and irregular surfaces, as well as geometric anomalies of the different elements; the software has a changing parametric behaviour that helps to construct and change elements into a 3D model quickly; moreover, this platform generates construction documents with a high level of quality and flexibility; the Revit® platform provides interoperability between different software applications through the use of IFC files; moreover, it can link DWG,

DGN, DXF, Sat, and SKP files, and it is also a useful tool to open and manipulate point clouds that are stored in TXT, RCP, or RCS formats; moreover, the Revit® platform allows for users to add new functions or add-ins from the application programming interface (API), programming languages that could be used to create add-ins written in C ++, C # and Python; Autodesk offers a free student version for three years (LÓPEZ *et al.*, 2018).

Furthermore, the advantages of BIM-oriented projects are analysed in terms of time and effort, from the initial design to the management and maintenance (Figure 5) (CBIC, 2016). In the initial phases, the BIM process requires more significant effort than other processes, from the professional point of view, with the highest amount of information necessary for the development of the model (CBIC, 2016). In the subsequent phases, once the model is defined in its parts, the BIM methodology will guarantee more significant effect/benefit in terms of time and effort (CBIC, 2016). The usefulness of adopting the BIM method has been deeply analysed over the years (EASTMAN, CHUCK; TEICHOLZ, PAUL; SACKS, RAFAEL; LISTON, 2011).

Figure 5 - Comparison between CAD and BIM project development process.



Source: *Câmara Brasileira da Indústria de Construção* (2016) modified by the author.

In general, the benefits of implementing BIM in construction projects include (ANTONOPOULOU; BRYAN, 2017):

- a) efficient collaboration within a multidisciplinary project team;
- b) improving design and construction coordination;
- c) better construction planning, including the possibility of prefabricating design elements;
- d) cost planning, cost reduction during construction (reduction of delays on site, retrieval, information requests) and operation (continuous information delivery for management of delivery facilities);
- e) improved performance regarding the standard implementation.

Furthermore, BIM differentiates itself as an object intelligent architectural CAD tool rather than a drafting tool and represents building elements and components as information-rich parametric objects to create or to represent an entire building (ANTONOPOULOU; BRYAN, 2017). BIM uses building semantics to include physical elements such as walls and floors, and conceptual elements, such as spaces and openings (BOEYKENS; SANTANA QUINTERO; NEUCKERMANS, 2008). In addition to 3D visualisation, BIM can automate the production of digital documentation, *e.g.* 3D model, photo rendering, orthographic projections cut sections, details and schedules (MURPHY, 2012).

Many types of research were presented in this section to approach the BIM topic. Most of them focus on the challenge for a high-quality geometrical description of the ‘as-built’ configuration of the heritage building. In such researches, the information of the geometry is acquired through laser scanning and photogrammetry. The majority of current software - platforms for creating engineering drawings from laser scan surveys - functions by mapping vectors on to the point cloud or textured point cloud (MURPHY, 2012). Such tools are presented in the following subsection.

#### 2.1.2.2.3 Laser scanning and photogrammetry

In the field of cultural heritage, digital recording of construction sites using laser scanning and photogrammetry become a topic of great interest (CHIABRANDO; LO TURCO; SANTAGATI, 2017). As referred in the research of Chiarabondo, Lo Turco, Santagati (2017), digital photogrammetry free, low cost and open source contributes to the widespread use of Image-based 3D modelling techniques, especially in the field of Cultural Heritage.

The 3D Laser scanning technologies have been introduced in the field of surveying and can acquire 3D information about physical objects of various shapes and sizes in a cost and time-effective way (ARAYICI; TAH, 2007). While laser scanning based on the triangulation principle and high degrees of precision have been widely used since the 80s, time of flight instruments has only been developed for metric survey applications in this decade (BORNAZ; RINAUDO, 2004).

Time of flight 3D laser scanners utilize a laser beam to survey the subjects. Such a procedure allows calculating the time of flight required for the laser beam to travel from the terrestrial laser scanner (TLS) to the target and back to the instrument (VAIOPOULOS; GEORGOPOULOS; LOZIOS, 2012). Since such instrument allows recording millions of points in a few minutes, laser scanning is widely used in the field of architectural, archaeological and environmental surveying (VALANIS; TSAKIRI, 2004).

However, researches show that TLS can be costly, not sufficiently dense, or not easy to access (CHIABRANDO; SPANÒ, 2013; GRUSSENMEYER *et al.*, 2008; INZERILLO *et al.*, 2016; KADOBAYASHI *et al.*, 2004; LICHTI *et al.*, 2002; REMONDINO *et al.*, 2014; RONCELLA; RE; FORLANI, 2012). Moreover, another drawback of laser scanners is that colour images of an object cannot be obtained or, if it is possible, the quality of the colour images is worse than that of the photographs (KADOBAYASHI *et al.*, 2004).

Chart 1 - Comparison of TLS and SfM methods and instruments.

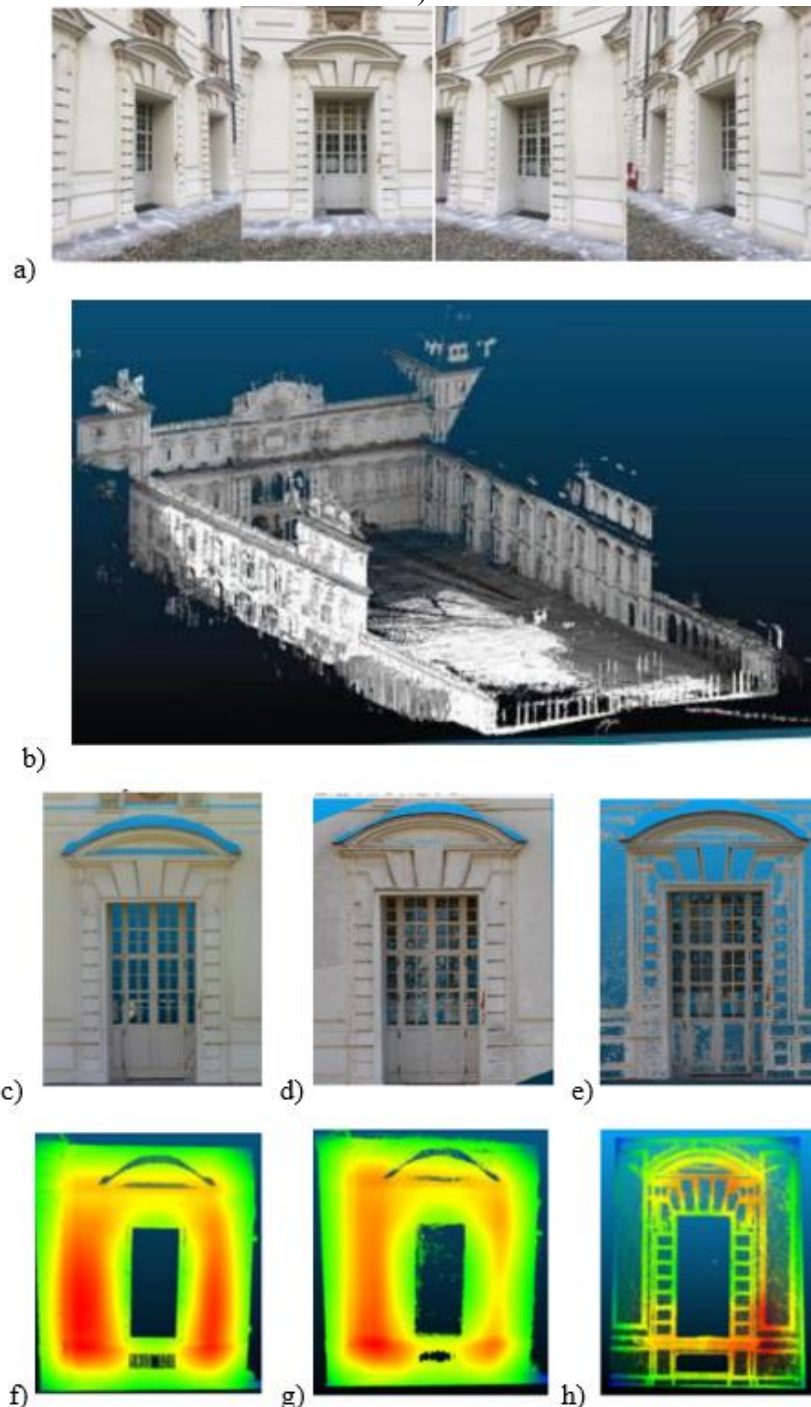
	<b>TLS</b>	<b>SfM (Photoscan)</b>	<b>SfM (ReCap)</b>
Cost (instrument)	---	- (Reflex camera) + (mirror less camera)	- (Reflex camera) + (mirror less camera)
Cost (software)	+	++	+++
Time for data acquisition	+++	+	+
Time for data processing	++	-	++
Easy to use	+++	+	++
Density	+++	++	+
Accuracy	+++	++	++

Source: Chiabrando, Lo Turco, Santagati (2017).

Furthermore, the field of digital recording of cultural heritage has changed thanks to the spread of imaged-bases 3D modelling techniques, *i.e.* digital photogrammetry free, low cost and open-source packages (CHIABRANDO; LO TURCO; SANTAGATI, 2017). As an example, the results of the research of Chiabrando, Lo Turco and Santagati (2017) are given in Figure 6. The authors used both TLS (Terrestrial Laser Scanner) surveying and

photogrammetric SfM (Structure from Motion) based techniques for 3D data acquisition. Such research was carried out to compare the techniques, both in terms of accuracy, density and file size (Chart 1 and Figure 6) (CHIABRANDO; LO TURCO; SANTAGATI, 2017).

Figure 6 - Part of a dataset for the image overlapping (a). General view of TLS survey (b) and comparison between TLS (c) and SfM developed with Photoscan (d) and Recap (e). Point cloud density visualization in TLS (f), Photoscan and ReCap clouds (higher density area in red).



Source: Chiabrando, Lo Turco, Santagati (2017) modified by the author.



Nowadays, laser scanning technology is integrated with 3D photogrammetric orthoimages. It allows to accurately identify the surface profile and thickness (BRUMANA *et al.*, 2018b). Furthermore, Computer Vision algorithms allow extracting 3D point clouds using the photogrammetric workflow in a more automatic way (REMONDINO *et al.*, 2014).

The easy use of those new generations of software improves the programs that allow extracting 3D point clouds (CHIABRANDO; LO TURCO; SANTAGATI, 2017). 3D points clouds models help to obtain the 2D and 3D generation geometry, with their spatial and radiometric data, including temporal information of the progressive survey. Such a procedure guarantees the appropriateness of geometrical accuracy, and to obtain all correlate information, to complete the semantic definition (QUATTRINI *et al.*, 2015).

### 2.1.2.3 Infrared thermography

Infrared thermography (IRT) is a non-destructive technique that allows measuring remotely - *i.e.* at a distance and without contact - the energy that is naturally emitted from a body in the infrared field (between 1 and 20  $\mu\text{m}$ ) (DANESE *et al.*, 2010). IRT has been successfully applied since '60 in many fields for several purposes. It was mainly applied to map the surface temperature to control buildings, as well as humans or animals body, electrical appliances, engines, electronics, and corrosion (GRINZATO, 2012). Due to the advantages that it offers in several applications, IRT is extensively applied to the investigation of cultural heritage (MERCURI *et al.*, 2011). Some examples are the preliminary assessments for the conservation interventions, the efficiency assessment after the cleaning of architectural surfaces, the consolidation interventions, and the restoration of masonries by repair mortars or the monitoring of plastered mosaic surfaces (AVDELIDIS; MOROPOULOU, 2004).

The theoretical bases of IRT are related to the idealization of the black body model of Stefan-Boltzmann (Equation 1), which affirms that the intensity and the spectrum of that energy are functions only of the temperature of the body that emits this energy (STEFAN, 1879 *apud* DANESE *et al.* (2010) and De LIMA AND SANTOS (1995).

$$J = k_B \cdot T^4, \tag{1}$$

where  $J$  is the radiant emittance, that is the radiation emitted per unit of surface ( $\text{W}/\text{m}^2$ ),  $k_B$  is Stefan-Boltzmann constant ( $5.67 \times 10^{-8} \text{ W}/\text{m}^2 \text{ K}^4$ ), and  $T$  is the absolute temperature ( $^\circ\text{K}$ ).

Indeed, thermal parameters like the specific heat and the thermal diffusivity are affected by the deterioration processes (MERCURI *et al.*, 2011). For real objects, such parameters are also a function of surface characteristics of the material, according to the grey body mode. IRT measures the emittance of the analysed object, *i.e.* grey bodies, through the radiation measured with the thermal camera, which allows determining the temperature of the body and its characteristics (DANESE *et al.*, 2010). Proper use of IRT on historic buildings is for materials whose temperature is above 40 °F (5 °C) (ROSINA; ROBISON, 2012). IRT renders the image of the analysed object in colours or greyscale, concerning the temperature scale (figures 7 and 8) (AVDELIDIS; MOROPOULOU, 2004).

Two main IRT methods are available, and they are defined as active and passive. The difference between the two methods is in the source that creates the process of heat transfer. While in active thermography, the source is artificial, in passive thermography, it is natural (DANESE *et al.*, 2010). Some of the analysed researches are carried out by applying the active method where the thermal stimulation of the sample is required (AVDELIDIS; MOROPOULOU, 2004; MERCURI *et al.*, 2011). However, for heritage applications, a passive method is preferred because of the non-invasiveness (AVDELIDIS; MOROPOULOU, 2004; DANESE *et al.*, 2010; LERMA *et al.*, 2014; LUDWIG *et al.*, 2013, 2004; MERCURI *et al.*, 2011; MOROPOULOU *et al.*, 2013; ROSINA; ROBISON, 2012).

As previously mentioned, the main IRT advantage is the capability of inspecting large surfaces without any contact or damage (GRINZATO, 2012). Due to the different thermal diffusion that each material layer renders, IRT can detect the different sub-surfaces on the plastered surfaces, *e.g.* painting, mosaics, *etc.* (AVDELIDIS; MOROPOULOU, 2004). Some applications of IRT to the diagnosis of heritage building are the monitor of the moisture of structures (Figure 7) (LUDWIG *et al.*, 2004), crack detection and fresco detachment sizing (Figure 8) (GRINZATO, 2012; GRINZATO *et al.*, 2002). Moreover, other examples are classification and visualization of the building materials below the finishing layer (GRINZATO *et al.*, 2002), quantitative evaluation of the material decay through the construction of the spatio-temporal dataset comparing images of the same elements over with the time (DANESE *et al.*, 2010). However, most IRT instruments have a high sensitivity threshold and can detect only high amounts of the emitted radiation, *i.e.* the higher the temperature, therefore, the higher the accuracy of the measurement (ROSINA; ROBISON, 2012).

Figure 7 - Capillary rise of the water: (a) thermographic camera, (b) photographic camera and previous superposition images (c).



Source: Lerma *et al.* (2014).

Figure 8 - Endangered fresco by an earthquake: picture and thermographic detection of delaminations and structural cracks.



Source: Grinzato (2012).

#### 2.1.2.4 The sonic pulse velocity test

The sonic pulse velocity test is based on the generation of elastic waves by sonic impulses at a specific point of the structure. Waves can be generated by different sources, *e.g.* by an instrumental hammer (MIRANDA, L.; CANTINI, L.; GUEDES, J.; BINDA, L.; COSTA, 2013), or by ultrasound equipment (BRANCO *et al.*, 2015; GONÇALVES; TRINCA; PELLEGRINO CERRI, 2011; GORNIK; MATOS, 2000; TEREZO, 2005), where the travel time is measured employing accelerometers. Moreover, other parameters can be calculated, *e.g.* such as amplitude and frequencies of waves (BINDA; SAISI; TIRABOSCHI, 2001).

In general, sonic tests allow obtaining qualitative information on the morphology, consistency and state of the analysed element, since the velocity of wave propagation is

influenced by the composition of the medium, the presence of inhomogeneities, voids, and deteriorated areas (CASARIN; MODENA, 2008; MAIERHOFE *et al.*, 2005). The velocity of an elastic wave passing through a solid material is theoretically proportional to the density, dynamic modulus and Poisson's ratio of the material (BINDA; SAISI; TIRABOSCHI, 2001). For example, researchers have applied ultrasonic methods for the assessment the compressive strength of concrete (UMAR; HANAFI; LATIP, 2015) or the species identification of wood, through the evaluation of density, elastic constants, moisture content (BRANCO *et al.*, 2015; GONÇALVES; TRINCA; PELLEGRINO CERRI, 2011; GORNIK; MATOS, 2000; TEREZO, 2005).

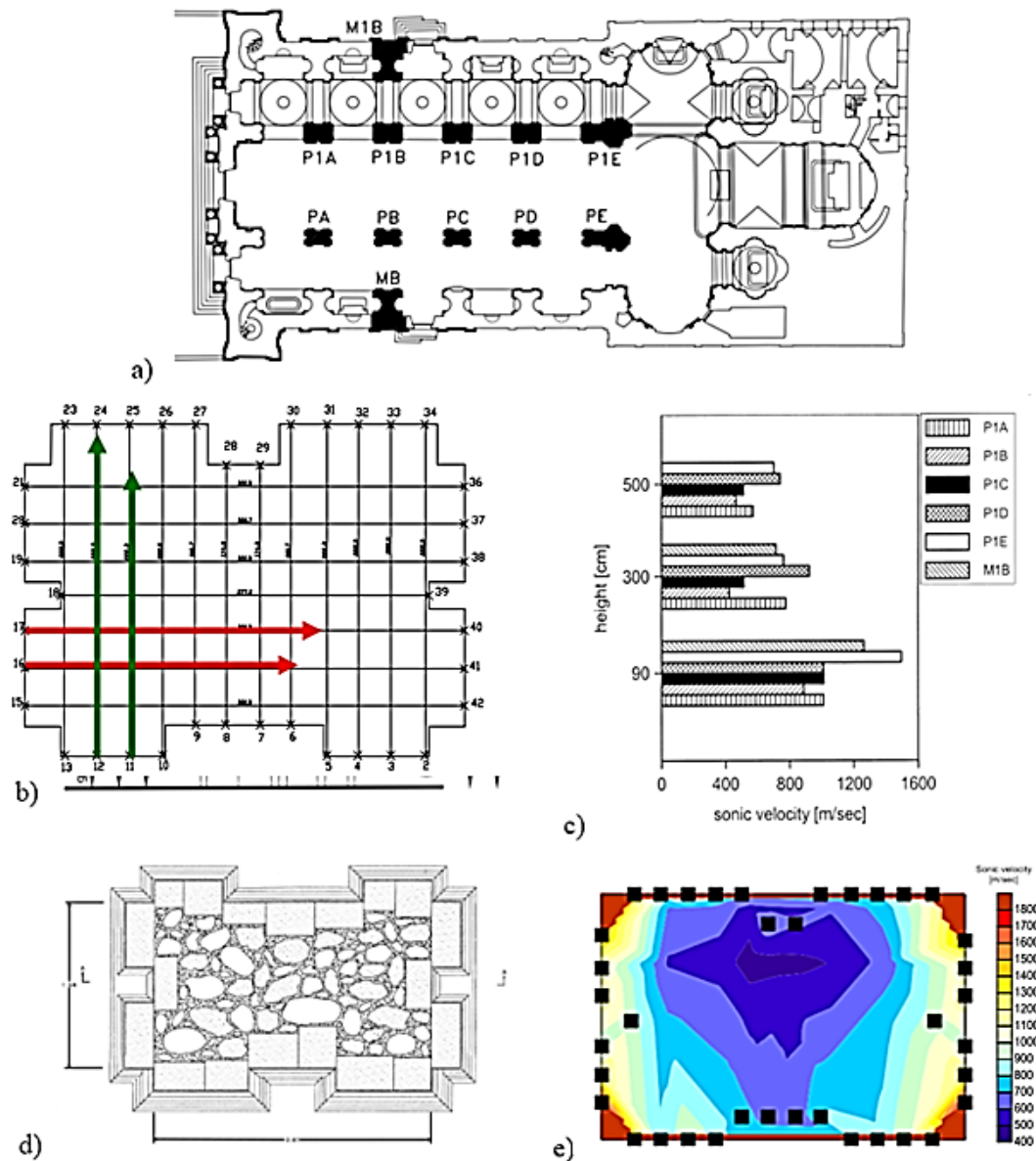
Due to its non-invasiveness, the sonic test is one of the most widely used for masonry heritage building (BINDA; SAISI; TIRABOSCHI, 2001). Masonry can be a very inhomogeneous material, and only global variations of velocities can be indicative. Furthermore, the sonic test is suitable for rubble masonry structures (Figure 9.d), since the high attenuation caused by joints, voids and inhomogeneities do not allow the use ultrasonic (BINDA; SAISI; TIRABOSCHI, 2001). The use of sonic tests for the evaluation of masonry heritage building is carried out to qualify masonry through the morphology of the wall section (BINDA; SAISI; TIRABOSCHI, 2001). Moreover, it allows detecting the presence of voids and flaws, finding crack and damage patterns, controlling the effectiveness of repair by injection technique, and detecting when the physical characteristics of materials have changed (Figure 10) (BINDA; SAISI; TIRABOSCHI, 2001).

Tests can be carried out on the same side of the structural element or through its section. Moreover, sonic tomographies can be performed in the thickness of the element (BINDA; SAISI, 2009b; SCHULLER *et al.*, 1997; VALLE; ZANZI, 1998). In such a case, the measures of sonic pulse velocity are combined along different wave's paths on a cross-section of masonry, as a result of a series of single direct emissions between pairs of point (Figure 9.b) (MAIERHOFE *et al.*, 2005; ZANZI *et al.*, 2001). Such data is subsequently processed to define mean values of velocity on each portion of the wall section itself (BINDA; SAISI; ZANZI, 2003; KAK; SLANEY; WANG, 2002).

As a result, velocity and attenuation maps are generated from algorithms of tomographic imaging, which main principles can be found in Kak, Slaney, Wang (2002). The attenuation distribution is related to the non-elastic behaviour of the material, *e.g.* the presence of damage, cracks, hidden conditions and morphology of structural elements (Figure 10) (BINDA; SAISI; ZANZI, 2003).

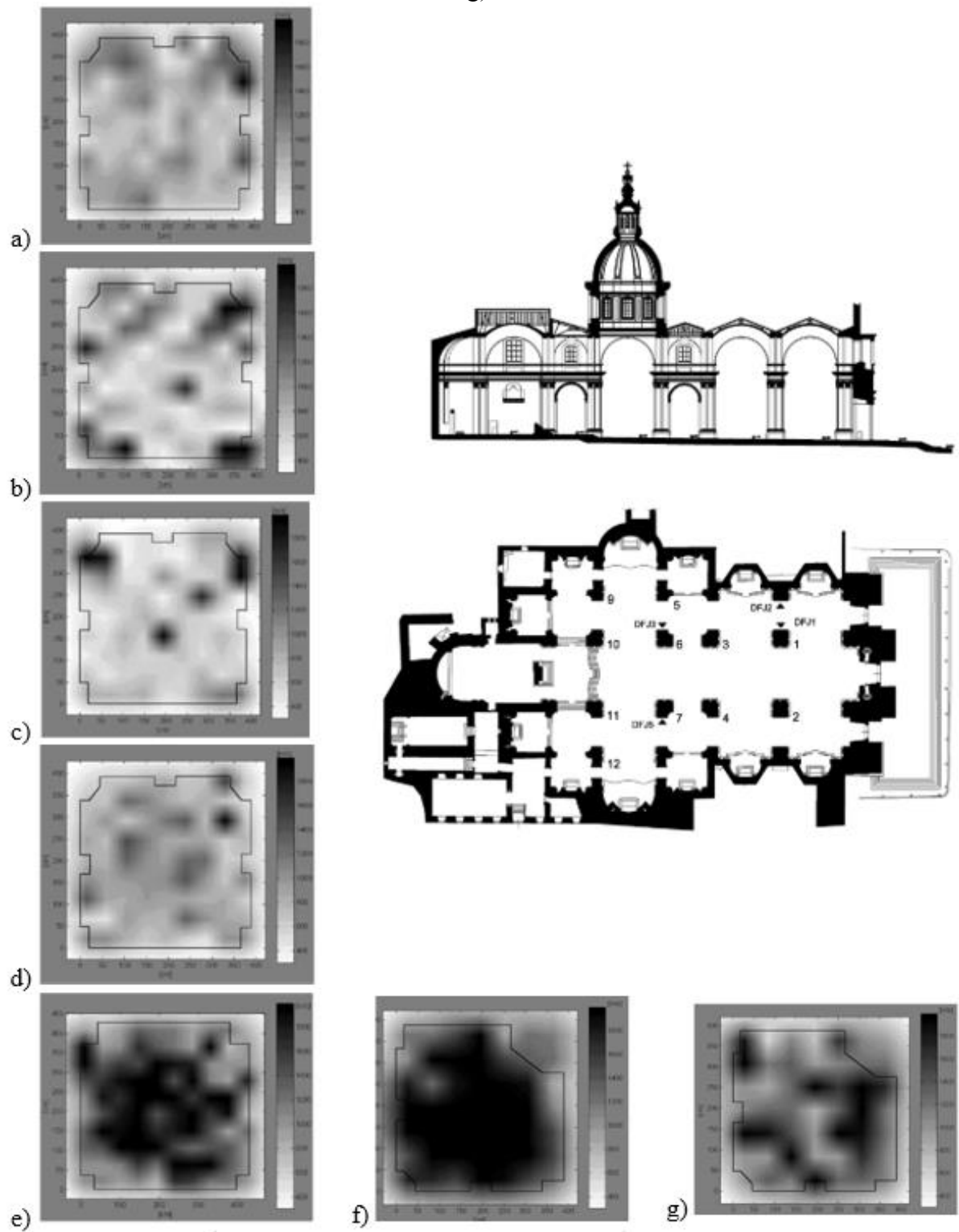
However, Binda, Saisi and Zanzi (2003) analysed how a good understanding of tomographic survey is required. Indeed, the design of the test and the required results are influenced by the measurement locations, *i.e.* the angular distribution of the observations and their spatial sampling, and the physical limits related to the wavelength (BINDA; SAISI; ZANZI, 2003). Furthermore, the sonic test is usually carried out systematically in different parts of the buildings and together with other types of non-destructive tests because results are related to local investigations and give qualitative information.

Figure 9. Plan of the Cathedral of Noto (Italy) with the tested piers (a), the geometry of the pier P1E and localisation of the sonic tests P1 (b), distribution of the velocity in the vertical of the testes piers and walls (c). Detail of the distribution in the horizontal plane of pier P1 (d, e).



Source: Binda, Saisi and Tiraboschi (2001) modified by the author.

Figure 10 - Horizontal tomographies of the temple of S. Nicolò 1'Arena (Italy): the pillar 2 from top to bottom, respectively at 8.9, 7.6, 4.9, 3.8, 1.8 m (a-e), pillar 6 and 10 at 5.8 m (f, g).



Source: Binda, Saisi and Zanzi (2003) modified by the author.

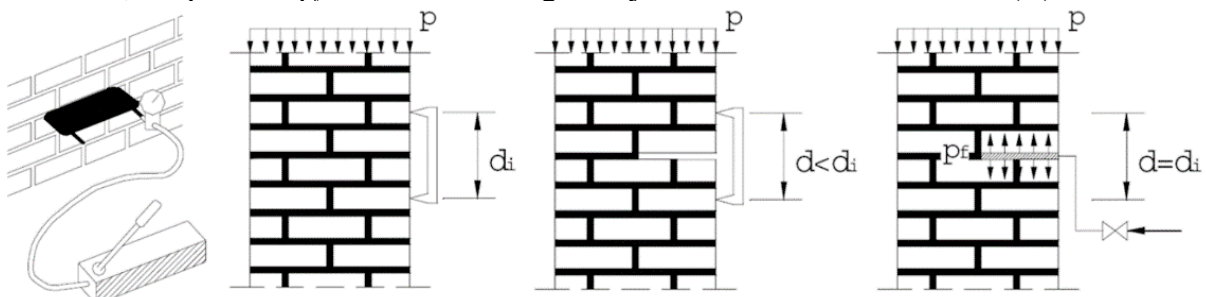
### 2.1.2.5 Flat jack test

Flat-jack is an *in-situ* test that was introduced for the analysis of the field of rock mechanics and successively adapted by researcher Paolo Rossi for the use with masonry in the 1980s (GREGORCZYK; LOURENÇO, 2000). Since flat-jack test requires the removal of a portion of mortar from the bed joint, it is considered non-destructive (or minor-destructive) because the damage is temporary and easily repaired after testing (GREGORCZYK; LOURENÇO, 2000).

Standards for masonry evaluation were developed by the American Society for Testing and Materials International (ASTM) and The International Union of Laboratories and Experts in Construction Materials, Systems and Structures (RILEM): on “*In-situ* Compressive Stress Within Solid Unit Masonry Estimated Using Flat-jack measurements” (ASTM C 1106-91), “*In-situ* Measurement of Masonry Deformability Properties Using the Flatjack Method” (ASTM C 1197-91), “*In-situ* stress tests on masonry based on the flat jack” (RILEM LUM.D.2, 1990) and “*In-situ* strength/elasticity tests on masonry based on the flat-jack” (RILEM LUM.D.3, 1990).

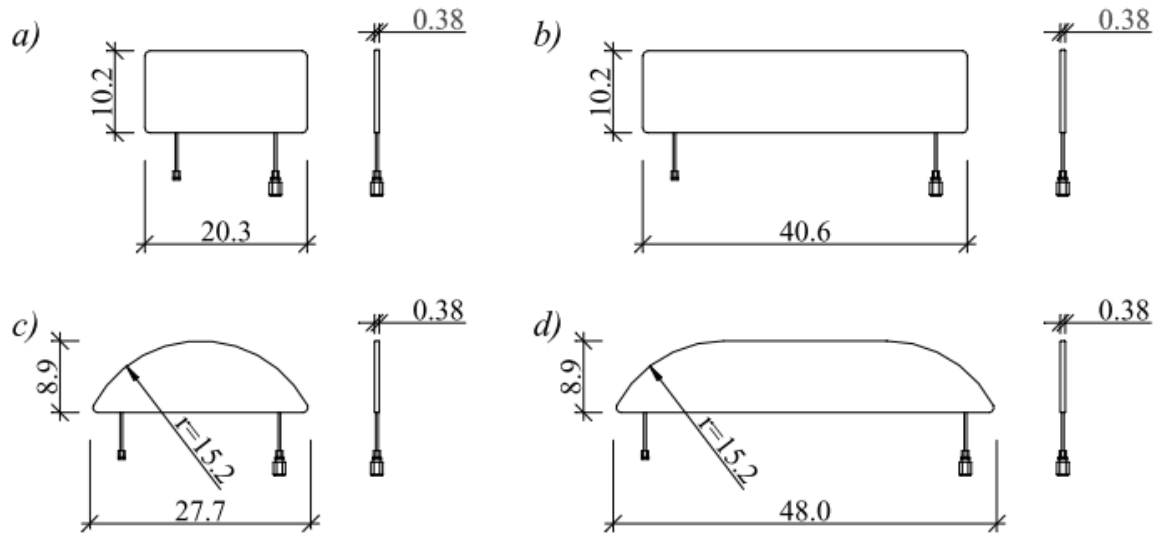
The method is based on stress release caused by a perpendicular cut of the wall surface (SOVEJA; OLTEANU, 2016). The general procedure of this test consists of restoring the vertical displacement caused by a horizontal cut made in a loaded masonry (Figure 11). The flat-jack device is used to restore the displacement (Figure 12). Oil is pumped in the jack until the distance is restored to the initial situation. The distance between several points fixed across the slot is measured before and after cutting (Figure 13).

Figure 11 - Phases of the flat-jack test: the initial distances  $d_i$  decrease after the mortar removal, the pressure  $p_f$  is increased trough flat jack since the initial distance ( $d_i$ ) is reached.



Source: Grecchi (2012).

Figure 12 - Different flat-jack configurations: rectangular flat-jack used after manual material removal or stitch drilling (a and b); circular (c), and semi-circular (d) flat-jack after saw cutting.



Source: Gregorczyk and Lourenço (2000).

Hence, the objective of the flat-jack test is to obtain the local state of stress in compression of a masonry element, loaded by vertical stress. The single flat-jack test allows to estimate the compressive strength through the applied pressure (CARPINTERI; INVERNIZZI; LACIDOGNA, 2009; SIMÕES *et al.*, 2012):

$$\sigma_m = pK_mK_a, \quad (2)$$

where  $\sigma_m$  is the compressive stress in the masonry,  $p$  is the flat-jack pressure,  $K_m$  is the calibration factor, which is a laboratory calibration (PARIVALLAL *et al.*, 2011). Moreover,  $K_a$  is the ratio of the bearing area of the jack, which is in contact with the masonry to the bearing area of the slot (CARPINTERI; INVERNIZZI; LACIDOGNA, 2009).

The double flat-jack method allows determining the deformation properties of unreinforced masonry (equations 3 to 5) (ASTM, 1991). The test is usually carried out after the single flat-jack test, where a second flat-jack is placed parallelly to the first one, one above the other (Figure 13) (CARPINTERI; INVERNIZZI; LACIDOGNA, 2009). By gradually increasing the flat-jack pressure, compressive stress is induced on the masonry in between. The stress-strain relation can be obtained measuring the deformation of the masonry, and the compressive strength can be obtained, if the test is continued to local failure (CARPINTERI;



INVERNIZZI; LACIDOGNA, 2009). However, this may also cause damage to the masonry in the area adjacent to the flat-jacks failure (CARPINTERI; INVERNIZZI; LACIDOGNA, 2009).

The Poisson ratio  $\nu$  can be estimated as the ratio between the experimental horizontal and vertical strains (Equation 5) (SIMÕES *et al.*, 2012). The tangent and secant stiffness modulus can be obtained as follows:

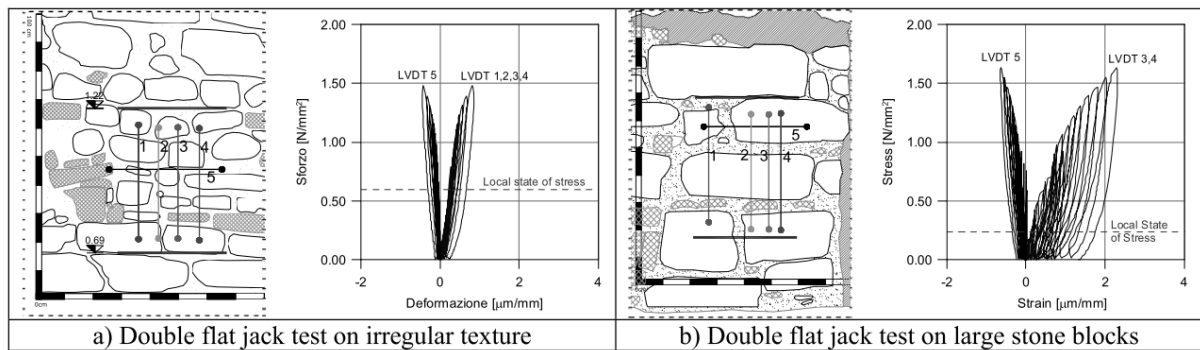
$$E_m = \frac{\delta\sigma_m}{\delta\varepsilon_m}, \quad (3)$$

$$E_s = \frac{\sigma_m}{\varepsilon_m}, \quad (4)$$

$$\nu = \frac{\varepsilon_h}{\varepsilon_v}, \quad (5)$$

where  $\delta\sigma_m$  is the increment stress,  $\delta\varepsilon_m$  is the increment of strain, while  $\sigma_m$  and  $\varepsilon_m$  are the actual stress and strain, respectively, while  $\varepsilon_h$  and  $\varepsilon_v$  are the horizontal and vertical strains.

Figure 13 - Comparison of the stress-strain behaviour of two walls with different textures.



Source: Binda *et al.* (2008).

In Simões *et al.* (2012), a method to the shear strength assessment is proposed based on the procedure suggested by Calì (2009). Such a procedure consists in the creation of two vertical cuts and the application of a horizontal force. Further explanations can be found in Simões *et al.* (2012a and 2012b) and Calì (2009). In this subsection, the results of Simões (2012a) are presented in charts 2 and 3, where experimental results are compared to scientific literature and standards.

Chart 2 - Masonry Compressive Mechanical Properties (literature results).

Type of Test		Maximum Compressive Stress (MPa)*	Young's Modulus E (MPa)	
Vicente (2008)	Double Flat-Jack Test on limestone rubble masonry and air lime mortar ( <i>in-situ</i> )	0.76	144 - 2670	Secant between 30% and 60% of the maximum stress
Pagaimo (2004)	Double Flat-Jack Test on limestone rubble masonry and clay air lime mortar ( <i>in-situ</i> )	0.93 - 1.05	210 - 380	Secant between 30% and 60% of the maximum stress
Roque (2002)	Double Flat-Jack Tests on 'xisto' rubble masonry and clay mortar ( <i>in-situ</i> )	0.60 - 0.80	800 - 1200	Secant between 30% and 60% of the maximum stress
OPCM 3274 (2003)	Table 11.D.1 - Irregular stone masonry (pebbles, erratic and irregular stone)	0.60 - 0.90	690 - 1050	-
	Table 11.D.1 - Uncut stone masonry with facing walls of limited thickness and infill core	1.10 - 1.55	1020 - 1440	-
*For double flat jacks tests the 'Maximum Compressive Stress' values correspond to the maximum stresses applied during the test, which may not be the masonry compressive strength. The values from OPCM 33274 are indicative values for the masonry compressive strength.				

Source: Simões *et al.* (2012).

Chart 3 - Masonry Shear Strength Parameters in literature results.

Type of test		Cohesion $\tau_0$ (MPa)	Coefficient of friction $\mu$
Milošević <i>et al.</i> (2011)	Triplet Tests on limestone rubble masonry and air lime mortar specimens	0.0815	0.558
	Diagonal Compression Tests on limestone rubble masonry and air lime mortar specimens	0.024	
OPCM 3274 (2003)	Table 11.D.1 - Irregular stone masonry (pebbles, erratic and irregular stone)	0.020 - 0.032	
	Table 11.D.1 - Uncut stone masonry with facing walls of limited thickness and infill core	0.035 - 0.051	0.40 (Characteristic value)

Source: Simões *et al.* (2012).

#### 2.1.2.6 Ambient vibration test

The ambient vibrations Test (AVT) is a fully non-destructive technique, which is suitable for the experimental investigation of heritage buildings (GENTILE; SAISI, 2013). AVT has become the primary experimental method available for assessing the dynamic behaviour of full-scale structures, and it has demonstrated to be especially suitable for flexible

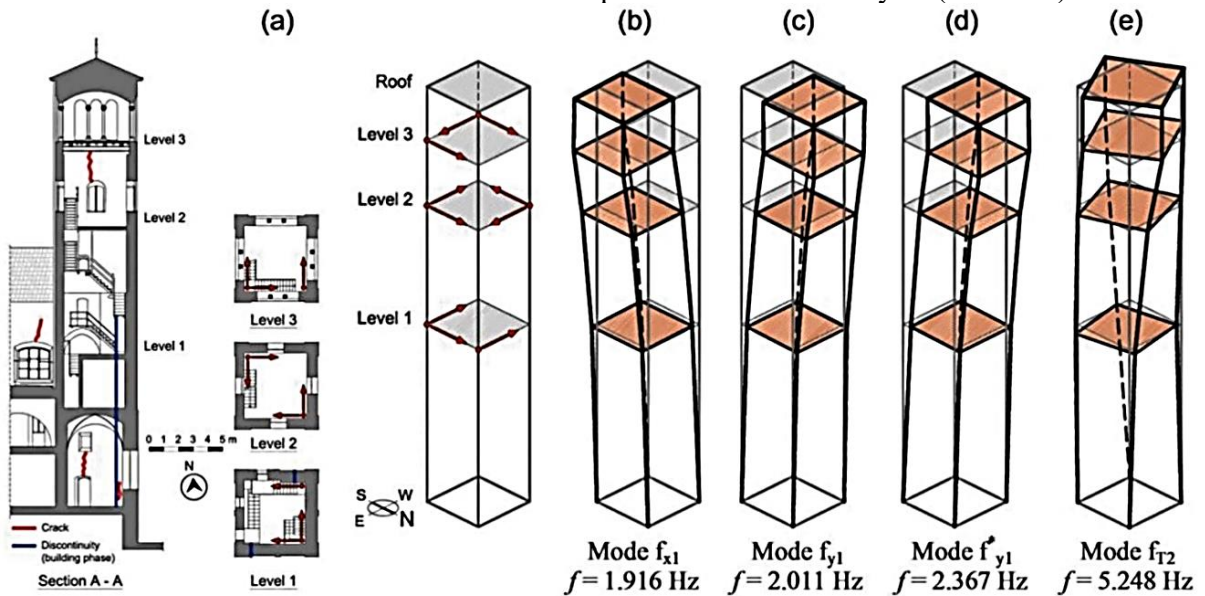
systems (GENTILE; SAISI, 2007). Examples of AVT applications are related to suspension bridges (ABDEL-GHAFFAR, 1978; ABDEL-GHAFFAR; SCANLAN, 1985; BROWNJOHN; DUMANOGLU; SEVERN, 1992), cable-stayed bridged (BROWNJOHN; XIA, 2000; GENTILE; MARTINEZ Y CABRERA, 1997, 2004; RAMOS *et al.*, 2010; WILSON; LIU, 1991) and high-rise buildings (BROWNJOHN, 2003).

AVT is carried out using a data acquisition system of piezoelectric accelerometers, each one connected to a power unit/amplifier, providing the constant current needed to power accelerometer's internal amplifier, signal amplification, and selective filtering. These sensors allow for recording acceleration or velocity responses. The tests involve the definition of different set-ups aiming at reducing the number of sensors to be used to cover the required selected measurement points (GENTILE; SAISI, 2007; GENTILE; SAISI; CABBOI, 2015). It means that some sensors are held stationary as reference transducers in different setups. Signals converted to digital form are stored in ASCII form (American Standard Code for Information Interchange) on the hard disk of the data acquisition computer (GENTILE; SAISI, 2007). The experimental results obtained from the AVT are elaborated through operational modal analysis (OMA) to understand the dynamic behaviour of the structure.

In the case of heritage buildings, AVT is performed by measuring the response of the structure in operational conditions, which usually has a low ambient excitation. Such an issue is overcome thanks to the highly sensitive and relatively inexpensive accelerometers available in the market (GENTILE; SAISI, 2007). Such instrumentation allows obtaining dynamic information of the construction such as frequencies and modal shapes. Indeed, it has been known for several decades that the frequencies and mode shapes obtained from environment tests are generally in good agreement with the results of forced vibration tests (BINDA; SAISI; TIRABOSCHI, 2000).

The modal frequencies are parameters representative of the global behaviour of the system, while the modal shapes allow detection of the local performance (BINDA; SAISI; TIRABOSCHI, 2000). Hence, ambient vibration tests aim to obtain the dynamic identification of the considered structure (Figure 14). In such a test, the data acquisition system and the piezoelectric accelerometers allow acceleration or velocity responses to be recorded (GENTILE; SAISI, 2007). Location, number, and type of equipment are defined according to the research proposals and the available accelerometer sensors. Modal parameters are calculated from the experimental results through the operational modal analysis is explained in Subsection 2.2.3.

Figure 14 - Ambient vibration tests: (a) schematic of the layout of the sensors; (b-e) selected modes of vibration identified from operational modal analysis (SSI-Cov).



Source: Gentile, Ruccolo, and Saisi (2019) modified by the author.

The use of AVT for Cultural Heritage is emerging as a subject of great importance, although a limited number of complete investigations are reported in the literature (GENTILE; SAISI; CABBOI, 2015). They are mainly related to historic towers or minarets (BENNATI; NARDINI; SALVATORE, 2005; GENTILE; SAISI, 2007, 2013; IVORRA; PALLARÉS, 2006; PEÑA *et al.*, 2010; RAMOS *et al.*, 2010), churches (CASARIN; MODENA, 2008; DE MATTEIS; MAZZOLANI, 2010; RAMOS *et al.*, 2010) and monuments (ARAS *et al.*, 2011; JAISHI *et al.*, 2003; PAU; VESTRONI, 2008). The procedure of identification of the structural response of a building through AVT and OMA is called vibration-based structural identification. More information about such a procedure is given in Section 2.2 of this thesis.

### 2.1.2.7 *Soil experimental tests for engineering purpose*

The knowledge of geotechnical characteristics of the soil is fundamental to carry out structural analysis in engineering research. It also allows understanding the occurrence of physical phenomena, the material behaviours, the interaction soil-structure, the foundation modelling, and the damage assessment due to the differential soil displacements, earth pressure on the structure (DIRECTIVE OF THE PRIME MINISTER, 2007; SAKAMOTO; OLIVEIRA, 2015a). A brief resume of the experimental tests for the assessment of the main characteristics of soil is presented the following subsections.

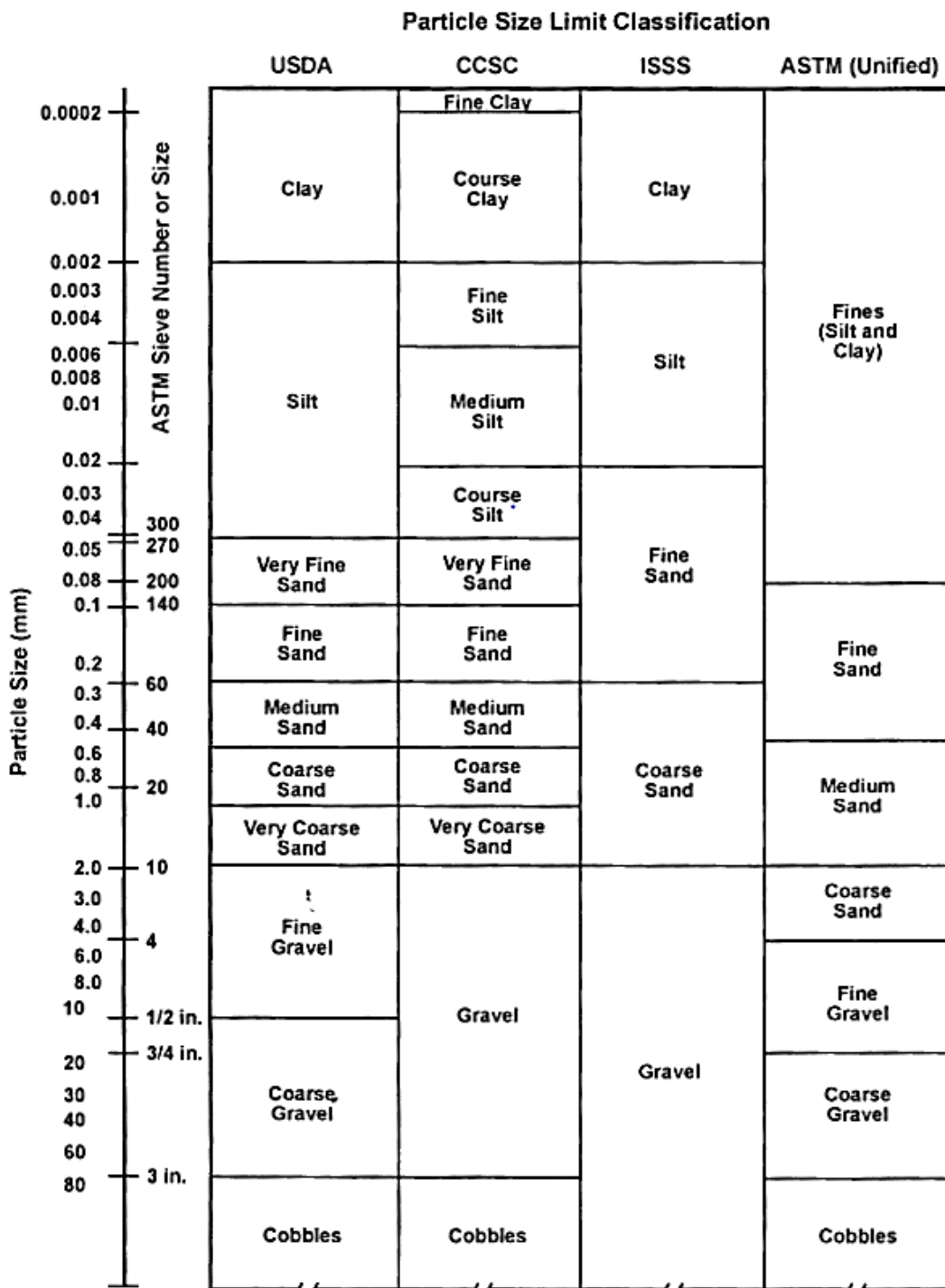
#### 2.1.2.7.1 Particle size analysis

Preliminary understanding of the geotechnical characteristic is carried out through the analysis of the soil texture by particle-size analysis (PSA) (GEE; OR, 2002). It is a measurement of the size distribution of individual particles in a soil sample (Figure 15). The objective of the test is to determine the mass percentage of individual size particle ranges found in the soil (CEN, 2007). According to Glendon and Or (2002), particle-size distribution curves are used extensively by geologists in geomorphological studies. It aims at the evaluation of sedimentation and alluvial processes (GEE; OR, 2002). Such authors compare some national standards defining the relation between particle size limit classification and particle size according to the following standards: USDA, U.S. Department of Agriculture (UNITED STATES. SCIENCE; EDUCATION ADMINISTRATION, 1975), CSSC, Canada Soil Survey Committee (MCKEAGUE, J.A.; STOBBE, 1978), ISSS, International Soil Sci. Soc. (YONG; WARKENTIN, 1966), ASTM - American Society for Testing and Materials (ASTM, D-2487, 2000).

Furthermore, PSA is commonly used also by civil engineers to evaluate materials used for foundation, road fills, and other construction purposes (GEE; OR, 2002). PSA results are usually presented in a cumulative particle-size distribution curve (figures 15 and 16) (GEE; OR, 2002) according to the National Standards used in the experimental test definition (Figure 15) (ABNT, 1984; ASTM, 2000; CEN, 2007; MCKEAGUE, J.A.; STOBBE, 1978; UNITED STATES. SCIENCE; EDUCATION ADMINISTRATION, 1975; YONG; WARKENTIN, 1966).

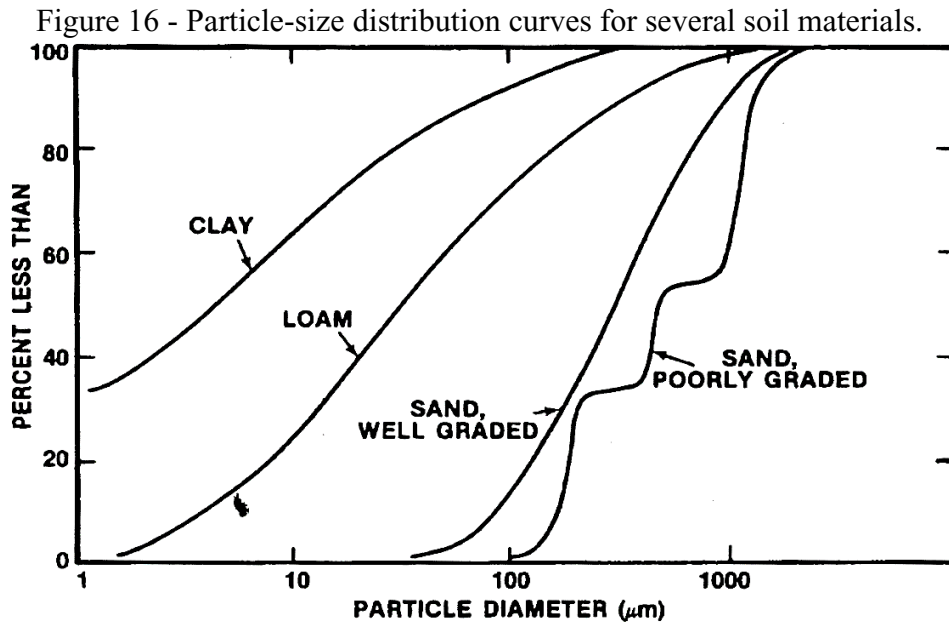
Moreover, soil strength characteristic is one of the leading mechanical properties of soil. Its accurate determination is the key to the analysis of slope and stability of foundation and calculation of soil pressure (YUAN *et al.*, 2013). The most commonly used strength failure criterion for soils is known as the Mohr-Coulomb criterion (AUGARDE, 2012; COULOMB, 1776; LABUZ; ZANG, 2012; MOHR, 1900).

Figure 15 - Particle-size limits according to several current classification schemes.



Source: Gee and Or (2002).

Several types of research can be found dealing with the soil resistance assessment, through the definition of two parameters, cohesion ( $C$ ) and angle of internal friction ( $\Phi$ ) (EL-EMAM, 2011; FEDA, 1984; HANNA; AL-ROMHEIN, 2008; LABUZ; ZANG, 2012; MESRI; HAYAT, 1993; PRADEL, 1994; YUAN et al., 2013). Mohr-Coulomb relation usually appears for the two-dimensional case (Figure 17), describing the stress state at failure (AUGARDE, 2012).



Source: Gee and Or (2002).

In the research of Augarde (2012), such a failure criterion is defined as a mathematical representation of the simple model of friction (Equation 12):

$$F = N \tan \phi, \quad (6)$$

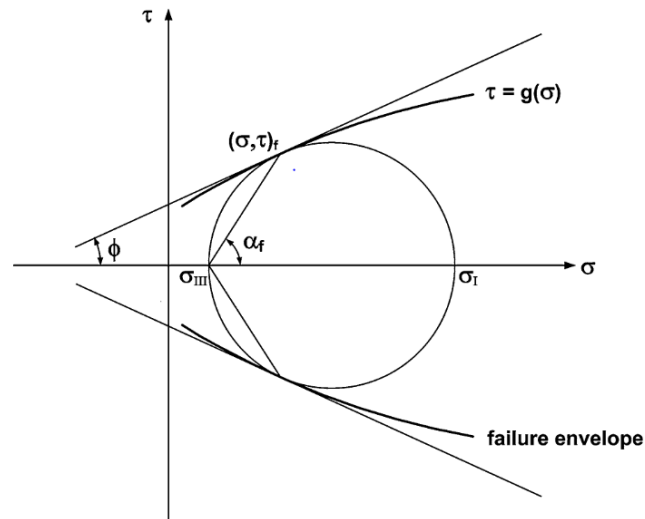
where  $\phi$  is the friction angle of the soil. Extensive research on the Mohr-Coulomb failure criterion is presented in Labuz and Zang (2012), where the authors explain the Mohr-Coulomb criterion failure (Equation 13), proposed in the investigations of retaining walls:

$$\tau_{MC} = c + \sigma \tan \phi. \quad (7)$$

The Mohr-Coulomb criterion contains two material constants cohesion and internal friction (Figure 17), while other criteria, *e.g.* Tresca criterion and Von Mises, propose one material constant (LABUZ; ZANG, 2012; MATSUOKA; NAKAI, 1985; NADAI, 1950).

Cohesion, which is independent of applied stresses, represents the force between soil particles, to hinder the relative sliding between them, while the internal friction angle represents the frictional characteristics between the particles (LABUZ; ZANG, 2012; SAKAMOTO; OLIVEIRA, 2015b).

Figure 17 - Mohr diagram and failure envelopes.



Source: Labuz and Zang (2012).

Soil parameters - required for the soil modelling for the civil engineering purpose - can be obtained from the execution of *in-situ* and laboratory tests. Some of these tests will be briefly approached in the following subsections.

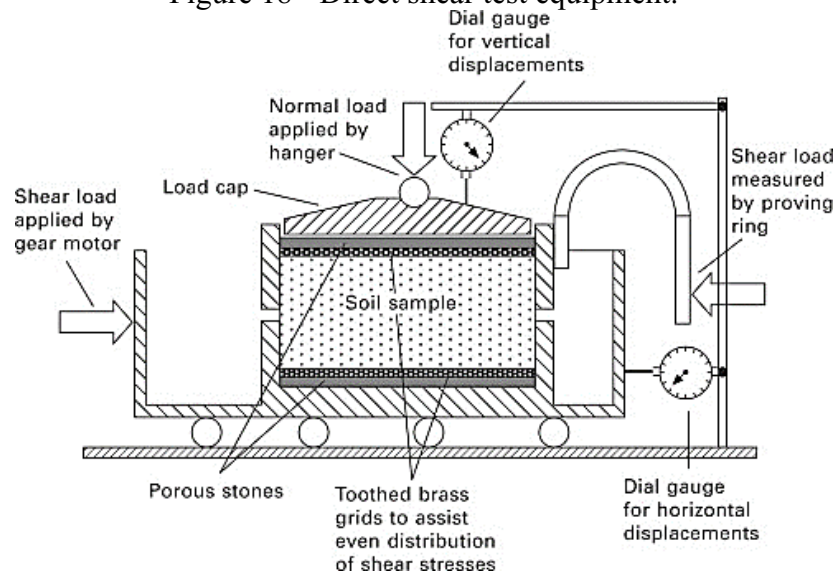
#### 2.1.2.7.2 Direct shear test

The direct shear test is based on the Mohr-Coulomb failure criterion (COULOMB, 1776; LABUZ; ZANG, 2012; MOHR, 1900). The soil is placed into a small open chamber in the device, and a vertical load is applied, while the base of the device is slowly displaced horizontally (Figure 18). The horizontal load and displacement are measured (AUGARDE, 2012). According to the results obtained varying the vertical loads for each test, a failure envelope is defined, and the values of angle of internal friction ( $\Phi$ ) and cohesion ( $C$ ) are obtained (AUGARDE, 2012; YUAN *et al.*, 2013). Such a test has been used due to its low cost, smooth operation and the broad scope of application. However, some shortcomings are found in the analysed literature (SAKAMOTO; OLIVEIRA, 2015b; YUAN *et al.*, 2013). As affirmed in Yuan *et al.* (2013), the test is not capable of preserving the moisture of specimens. It has a



low measurement precision and uneven distribution of inner stress and strains in specimens during the shear (YUAN *et al.*, 2013).

Figure 18 - Direct shear test equipment.



#### 2.1.2.7.3 Triaxial test

In the triaxial test, a cylindrical soil sample, surrounded by an impermeable membrane, is placed in a water-filled chamber (AUGARDE, 2012; LABUZ; ZANG, 2012; MESRI; HAYAT, 1993). The sample is loaded vertically while the constant pressure of the water is applied in the other directions. As affirmed in Augarde (2012), triaxial testing is a more difficult test, but it provides more information and control than the direct shear test. It also does not force the sample to yield across a predefined plane, as happens in the direct shear test (AUGARDE, 2012). Furthermore, drained and undrained tests are possible as the sample ends are supported on discs, which can be porous and linked to a drainage system (AUGARDE, 2012). Additional sensors can be implemented to monitor water pressures, determining effective stresses or stress paths (AUGARDE, 2012).

#### 2.1.2.7.4 Borehole shear test

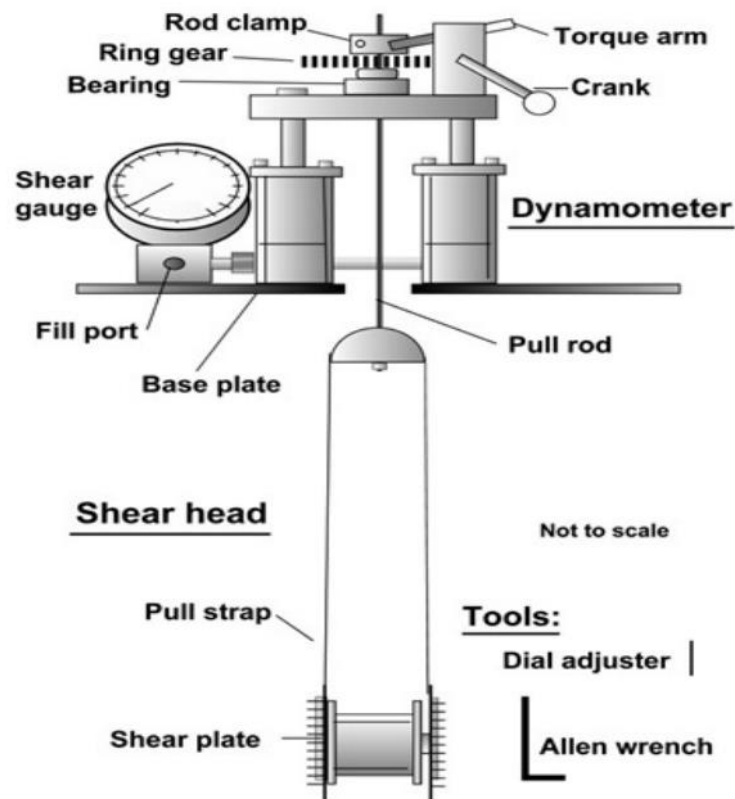
The Borehole Shear Test (BST) equipment was created at Iowa State University by Dr Richard Handy and his associates (HANDY; FOX, 1967). It is an *in-situ* test aimed at the

estimation of resistance parameters of the drained soil. The test can determine the drained friction angle and cohesion of almost any soil type by essentially performing a direct shear test (BECHTUM, 2012).

In Bechtum (2012), an extensive review of such method is proposed. The author affirms that the borehole shear test has the advantage of measuring shear strength parameters directly in situ without the need for laboratory testing or empirical correlations, soil disturbance is minimized since the soil being tested is not removed from the ground.

The BST apparatus functions by lowering an expandable shear head into a prepared borehole. Subsequently, normal stress is applied to the soil by the shear head, and time (typically 5 to 15 minutes) is allowed for any excess pore water pressure caused by the application of the normal stress to dissipate (BECHTUM, 2012; HANDY, 2002; HANDY; FOX, 1967). After sufficient consolidation time has elapsed, an upward force is applied to the shear head by a hand-crank, and the shear strength (peak shear stress) is measured using a shear gauge and dynamometer (Figure 19) (BECHTUM, 2012; HANDY, 2002; HANDY; FOX, 1967).

Figure 19 - Components of manually operated borehole shear test device.



Source: Handy (2002).

### 2.1.3 Structural health monitoring

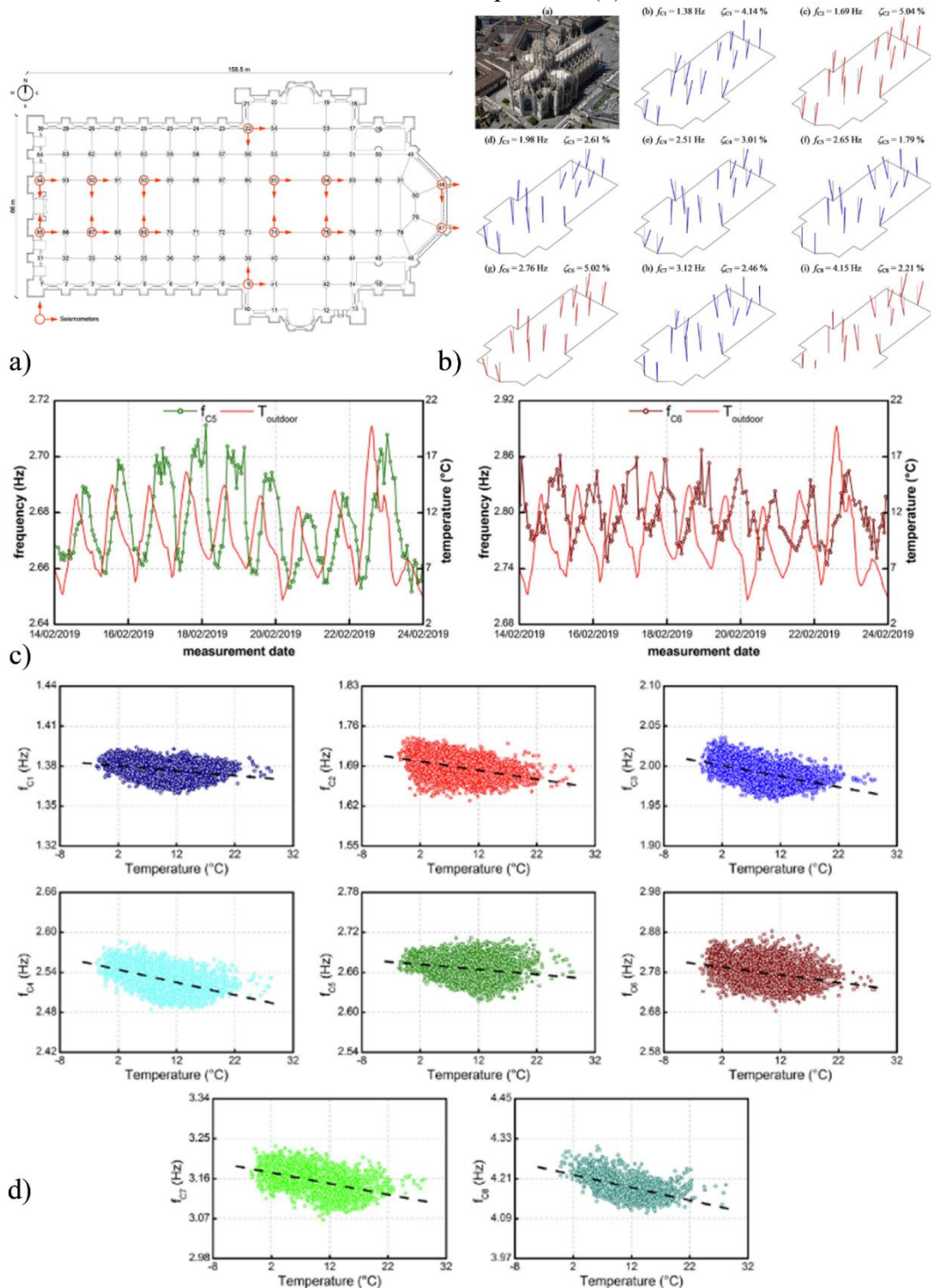
Structural health monitoring (SHM) is defined as the process of implementing a damage identification strategy, initially developed for aerospace, civil and mechanical engineering infrastructure (FARRAR; WORDEN, 2007). In research of Farrar and Worden (2007), a comprehensive approach to SHM is presented. In such a research, the damage is defined as “changes to the material or geometric properties of these systems, including changes to the boundary conditions and system connectivity, which adversely affect the system's performance” (FARRAR; WORDEN, 2007). Moreover, the damage identification in a structural and mechanical system is related to the comparison between two different states of the system (FARRAR; WORDEN, 2007). The first one is assumed to represent the initial or the undamaged state. While the second is the structure analysed - over the time using periodically-spaced measurements - for the extraction of damage-sensitive features and the statistical analysis of the measurements to determine the current state of system health (FARRAR; WORDEN, 2007).

SHM is usually carried out in conjunction with non-destructive evaluation, together with condition monitoring, statistical process control and damage prognosis (FARRAR; WORDEN, 2007). SHM is a fundamental tool for detecting damage in early stages in civil engineering structures (AGUILAR *et al.*, 2019) since it can provide useful, real-time information on the condition of buildings (ZONNO *et al.*, 2018). In the heritage field, SHM has increasingly become of interest to improve the knowledge of existing structural systems and their seismic performance (ZONNO *et al.*, 2018).

The literature reports several applications of SHM of heritage buildings which were mainly aimed at assessing the structural performance and tracking its evolution in time through a vibration-based approach (ELYAMANI *et al.*, 2017). Such a vibrations-based damage assessment was initially developed for bridge structures and buildings since the early 1980s (FARRAR; WORDEN, 2007). Modal properties, such as frequencies, modal shapes, damping, and dynamic stiffness matrix, are obtained with AVT and used to identify damage (Figure 20) (PEETERS; MAECK; DE ROECK, 2004). Such dynamical properties damping are functions of the mass and stiffness distribution of the structure (AGUILAR *et al.*, 2019). Moreover, environmental and operational condition variability presents significant challenges to the monitoring applications, mainly bridge application (FARRAR; WORDEN, 2007). However,

the idea to perform cost-effective vibration-based Structural Health Monitoring (SHM) of the historic structure has been taking shape recently. (CABBOI; GENTILE; SAISI, 2017).

Figure 20 - Layout of the seismometers installed in the Cathedral of Milan (a): identified modes (b), the variation of frequencies and temperature in time (c), and frequency variation with outdoor temperature (d).



Source: Gentile, Rucolo and Canali (2019) modified by the author.

The possibility to use a limited number of sensors and automated OMA in the SHM of historical construction leads to the choice of resonant frequencies as characteristic features of the structural condition (SAISI; GENTILE; GUIDOBALDI, 2015). However, resonant frequencies are also affected by external sources (Figure 20), *e.g.* temperature and humidity, other than structural changes in a way that is likely more significant than variations induced by small damage (SAISI; GENTILE; GUIDOBALDI, 2015).

The selection of sensor placement plays a significant role in the structural health monitoring (LENTICCHIA; CERAVOLO; ANTONACI, 2018). Indeed, some techniques of optimal sensor placement could assure a reliable positioning of the sensor for the SHM (LENTICCHIA; CERAVOLO; ANTONACI, 2018). However, such a topic is not extensively investigated in cultural heritage, showing a lack of knowledge in such a field.

The challenging problem of the removal of the effects of unmeasured environmental factors from identified resonant frequencies is still an open issue, even if some novelty methodologies can be found in the literature. They are applied to churches (GENTILE; RUCCOLO; CANALI, 2019; RAMOS *et al.*, 2010, 2013; SANCIBRIAN *et al.*, 2017), towers (FOTI *et al.*, 2012; GENTILE; SAISI; CABBOI, 2015), buildings (PAU; VESTRONI, 2008; ZONNO *et al.*, 2019a) and bridges (ARAS *et al.*, 2011; BRENCICH; SABIA, 2008; PAU; VESTRONI, 2008; RAMOS; AGUILAR; LOURENÇO, 2011).

The correct interpretation of vibration-based SHM results leads to the understanding of the current status of the analysed systems, as well as the detection of issues related to materials ageing and degradation (NEU *et al.*, 2017). However, in vibration-based SHM, continuous observation of modal parameters is another challenging task due to the large amount of data generated. Indeed, automatic data processing capabilities are essential to achieve the monitoring objectives (RAINIERI; FABBROCINO, 2015).

Nowadays, vibration-based SHM is finding an increased relevance in the structural health assessment of cultural heritage constructions, due to its non-destructive nature and the capability of classifying structural behaviour in real-time (ZONNO *et al.*, 2019a).

The studies made by Ramos *et al.* (2006), Oyarzovera *et al.* (2014) and Masciotta *et al.* (2014) in stone masonry historical structures show that vibration-based damage detection is possible. Indeed, modal parameters of such building types are sensitive to damage (ZONNO *et al.*, 2019a). Recent studies regarding the long-term structural response of historical adobe constructions indicate that the modal parameters are much affected by environmental

conditions, which makes more difficult the possibility of accurate detection of changes associated to structural damage (ZONNO *et al.*, 2019a).

#### **2.1.4 Existing methodologies for the structural assessment of heritage buildings**

In this subsection, examples of existing methodologies for the structural assessment of heritage buildings are presented. In the first subsection, the International Council on Monuments and Sites (ICOMOS) recommendations are presented, which can be considered as the theoretical base of a methodology aimed at the investigation of cultural heritage buildings. Subsequently, the Diagnosis Research Project of Binda, Roberti and Abbaneo (1994) and the Vibration-based structural identification for Structural Health Monitoring of Gentile and Saisi (2007) are presented to approach the challenging issue of a comprehensive methodology for the structural assessment. In the last subsection, the idea of the level of knowledge through the European and Italian Standards. They can be considered as methodologies since systematic workflows of investigation are described.

##### *2.1.4.1 ICOMOS recommendation*

The International Council on Monuments and Sites proposed a general multidisciplinary methodology to approach the research field of the structural analysis of historical construction (Figure 21) (ISCARSAH, 2003). The scientific method used in these phases is to blend hypotheses deriving from the structural model, experimental results obtained from the historical-critical analysis, inspection of as-built conditions, and monitoring of the structure (LOURENÇO, 2014). Such a conservation methodology for historical constructions proposed by the International Council on Monuments and Sites is summarized as follow:

- a) data acquisition, through the historical survey, the geometrical survey of the structure, the *in-situ* investigation campaign together with laboratory experiments and structure monitoring;
- b) structural behaviour, through a structural schematic understanding, creation of a model, definition of the characteristics of the materials and actions in the structure;
- c) diagnostic and safety plan, through historical-critical, qualitative, quantitative and experimental analysis;

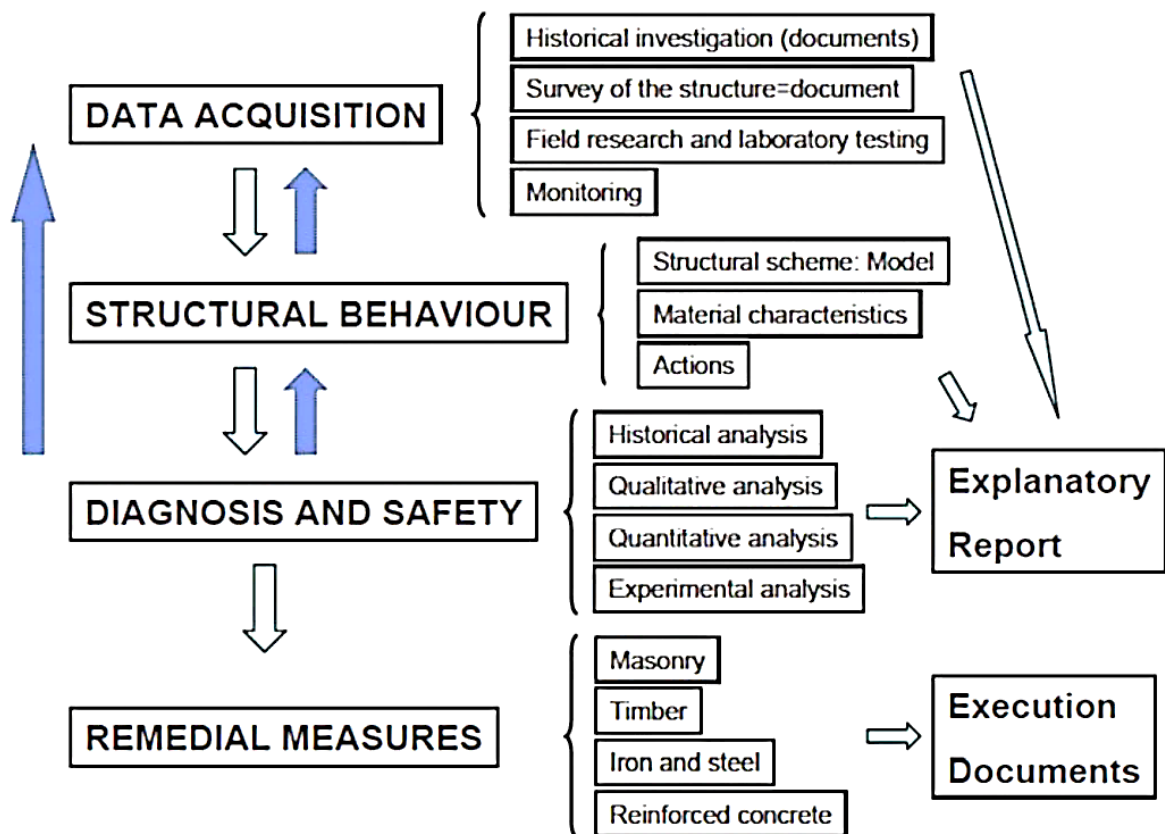
- d) proposals for restoration work involving masonry structures, wood, iron and steel, and reinforced concrete.

In a similar approach, a brief set of activities aiming at the historical building structural assessment based on ICOMOS Recommendation is presented in the research of Roca (2004) (ROCA, 2004):

- the inspection and characterization of the as-built state of the construction, based both on visual recognizance and profound observation employing (preferably) non-destructive techniques;
- the historical research carried out from the available historical documentation;
- the monitoring of the building using different types of sensors;
- the structural modelling and analysis of the building.

It must be remarked that ICOMOS recommendations represent nowadays a crucial methodology on which almost every other novel methodology relies (BINDA; SAISI; TIRABOSCHI, 2000; GENTILE; SAISI, 2007; LOURENÇO, 2002; ROCA, 2004).

Figure 21 - ICOMOS methodology.

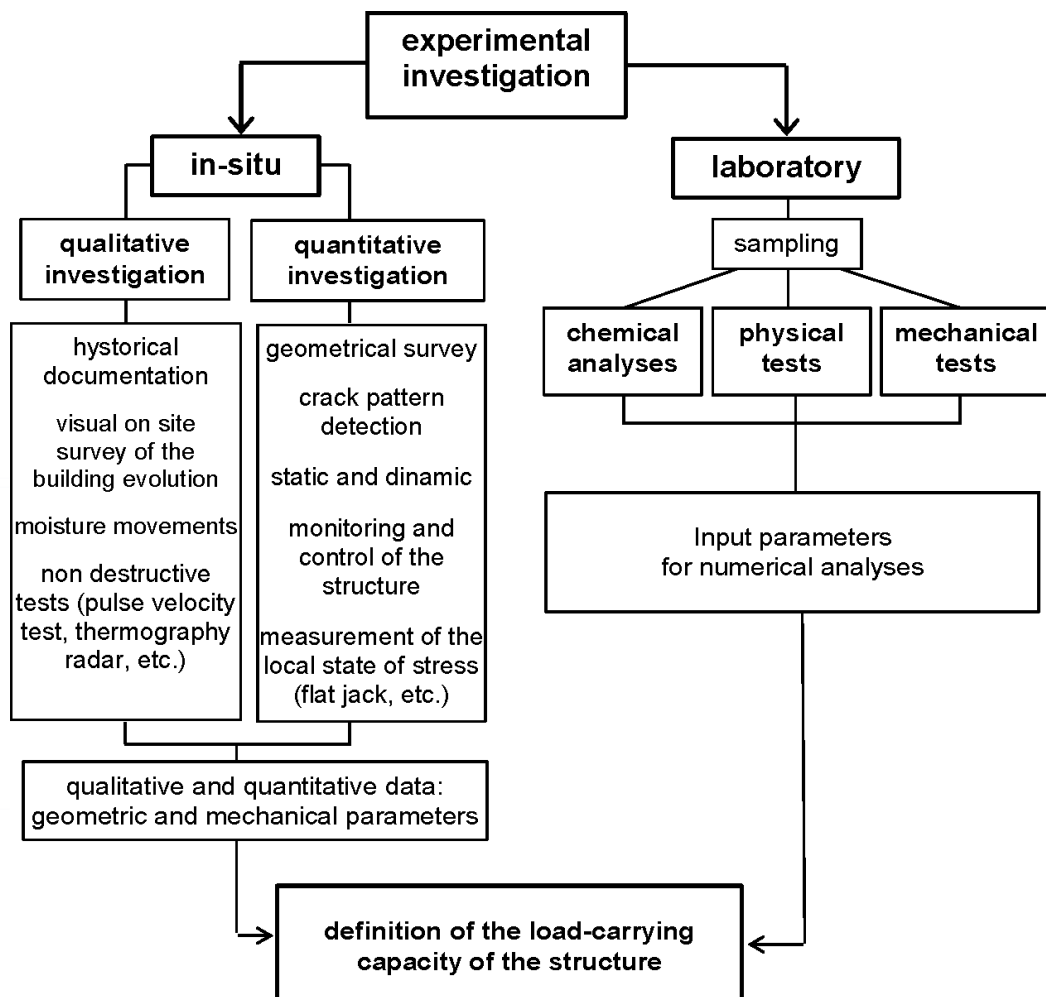


Source: Lourenço (2014).

### 2.1.4.2 The Diagnosis Research Project

Another methodology on the structural assessment of heritage structures was proposed in The Diagnosis Research Project by Binda, Roberti and Abbaneo (1994). Herein, the authors affirm that the Friuli (1976) and Irpinia (1981) earthquakes, and subsequent experiences, have underscored the need for adequate damage assessment before seismic rehabilitation (BINDA; ROBERTI; ABBANEO, 1994). The authors also notice that assessment can be enhanced by preventive studies carried out by those in charge of hazard mitigation, *e.g.* architects, engineers, researchers (BINDA; ROBERTI; ABBANEO, 1994). They propose a research procedure that must be defined so that findings can be used for further phases of damage assessment and as input data for the structural analysis and control models (BINDA; ROBERTI; ABBANEO, 1994) (Figure 22).

Figure 22 - Finalization of the experimental survey to the structural analysis.



Source: Binda, Roberti, Abbaneo (1994).



In such research, the authors focus on the responsibilities of who is responsible for the diagnosis (BINDA; ROBERTI; ABBANEO, 1994). Even if the member of the design team needs for consulting experts in the field, he must:

- a) set up the *in-situ* and laboratory survey project;
- b) regularly oversee the survey;
- c) understand their use as input data for structural analysis;
- d) choose appropriate models for the structural analysis;
- e) arrive at diagnosis at the end of the study.

Binda, Roberti and Abbaneo (1994) also affirm that an appropriate and rational use of structural analysis helps to define the state of danger, forecasting the future behaviour of the structure. However, when the structure is complex, often linear elastic models are easily usable, since nonlinear models or limit state design models are challenging to apply, also because the needed constitutive laws for the material are seldom available (BINDA; ROBERTI; ABBANEO, 1994). Such a methodology was developed along with the time, and it was implemented in many further types of research (BINDA et al., 2004; BINDA; SAISI, 2001, 2005).

#### 2.1.4.3 *Vibration-based structural identification for health monitoring*

The Vibration-based structural identification of masonry towers for health monitoring methodology is mainly proposed for condition monitoring (Figure 23). It involves three main steps:

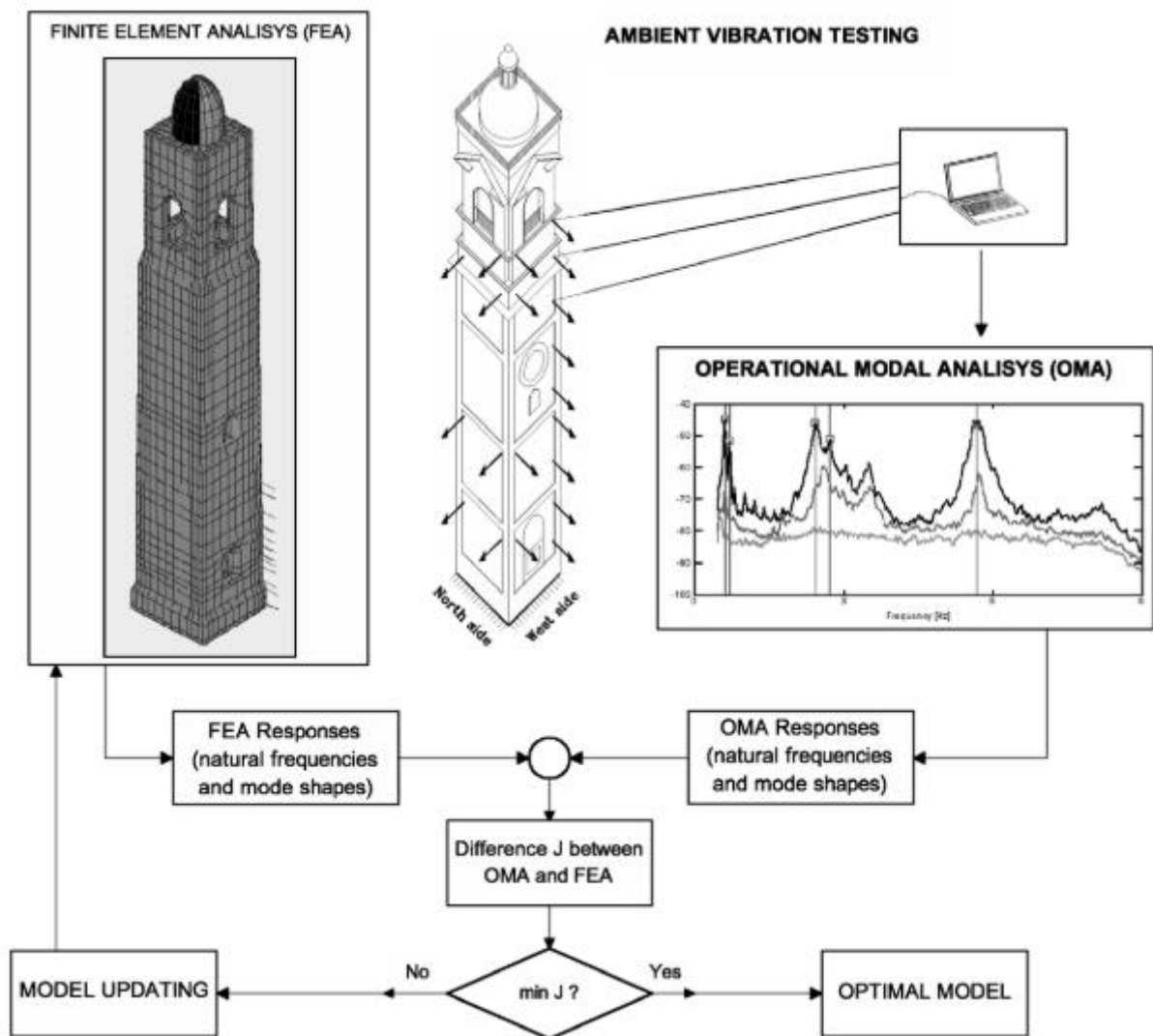
- a) automated modal identification from continuously collected data;
- b) development of predictive models through Principal Component Analysis (PCA) (BELLINO *et al.*, 2010; MAGALHÃES; CUNHA; CAETANO, 2012) and removal of environmental effects from identified resonant frequencies, to estimate cleaned observations for damage detection;
- c) damage assessment through continuous updating of some structural parameters of the baseline Finite Element model from cleaned observations.

Main tasks of such a procedure are the development of a FE model, sensitivity analysis and preliminary identification of the uncertain structural parameters of the model by minimising the difference between experimental and numerical modal features. The application of FE model updating for SHM of masonry towers is developed in a complementary rational

methodology, developed for the calibration of the numerical model of historic masonry towers (Figure 24), and presented in Gentile, Saisi, Cabboi (2015). Such a procedure is based on:

- historical and documentary research and *in-situ* geometric survey;
- evaluation of the overall state of preservation by accurate visual inspection;
- performing non-destructive tests or minor destructive tests *in-situ* and laboratory tests.

Figure 23 - Dynamic-based assessment of a structure.

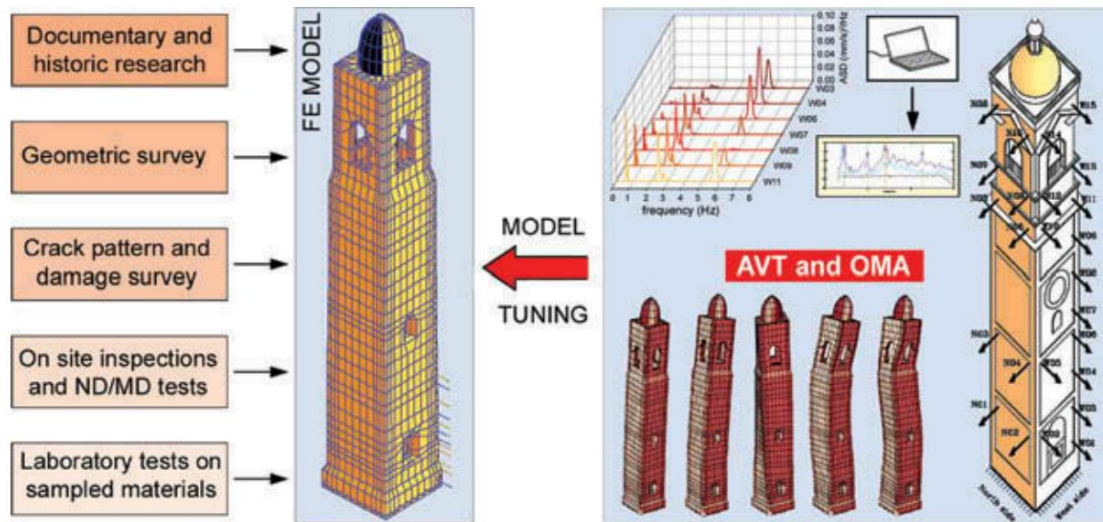


Source: Gentile and Saisi (2007).

As conclusions, Gentile, Saisi, Cabboi (2015) affirm that a rational methodology - developed for the calibration of the numerical model of historic masonry towers - relies on the development of a FE model. Such a model should accurately represent the dynamic behaviour

of the structure, *i.e.* natural frequencies and mode shapes. Such parameters are measured through ambient vibration tests to identify the uncertain parameters of the model.

Figure 24 - Vibration-based validation of the Finite Element Model of a historic building.



Source: Gentile, Saisi and Cabboi (2015).

Although the ambient vibrations that existed during the tests were low, AVT and OMA have proved to be useful tools for identifying the dynamic characteristics of fundamental vibration modes (GENTILE; SAISI; CABBOI, 2015). The authors suggest that such methodology - involving systematic manual tuning and sensitivity analysis - seemed appropriate (although slightly time-consuming) to simultaneously handle the uncertainties of historical construction and the possible ill-conditioning of the inverse problem (GENTILE; SAISI; CABBOI, 2015).

The application of such a procedure provided a linear elastic model of the tower, representing an excellent approximation of the structure in its as-built state. Further explanation of the procedure of vibration-base structural identification is given in Section 2.2 of the current thesis.

#### 2.1.4.4 *The level of knowledge as a methodology for heritage buildings*

In Italy - but generally in Europe (EC8, 1998-3) - during the last decades, the topics of the inspection, diagnosis, and assessment of historical constructions and monuments were deeply analysed. Indeed, the problem of the security of the existing buildings was explored,

both for the high vulnerability, *e.g.* regarding the seismic behaviour, both for the historical, architectonic and environmental value of most of the existing heritage building (NTC 08, Chapter 8).

Aiming at the choice of the suitable type of analysis, the European Standard (EUROCODE 8, 2005) and the Italian National Standards (CS.LL.PP., 2009; INFRASTRUTTURE; TRASPORTI, 2018) introduced the fundamental problem of the knowledge of the structure. Such definitions introduced the concepts of different knowledge levels and consequent confidence factors for the structural assessment (MAGENES; PENNA, 2009).

More information concerning building knowledge issues are given in Binda and Saisi (2009) and Magenes and Penna (2009). Such information will be presented in the following subsections. Moreover, a comparison between different type of confidence factors and its definition according to the knowledge level can be found in Cattari *et al.* (2015) and Magenes and Penna (2009). A detailed definition of the level of knowledge can be found in Section 3.3 of the Eurocode 8 - Part 3 and Section C8A.1.B.3 of the *Circolare* 617/2009, respectively.

#### 2.1.4.4.1 European Standard EN 1998-3:2005: Design of structures for earthquake resistance: Part 3: Assessment and retrofitting of buildings

The European Standard EN 1998-3:2005 (EC8 - Part 3) defines three knowledge levels (KL), each based on the quality and quantity of the information acquired on the existing building (section 3.3, page 18 of EC8 - Part 3). It suggests how structural evaluation based on a state of limited knowledge shall be performed through linear analysis method, either static or dynamic, and the relevant partial safety factor for the material properties shall be appropriately defined. Such European Standard describes each level of knowledge according to three aspects, *i.e.* geometry, details and materials (Chart 4). The classification of the levels of inspection and testing (limited, extended and comprehensive) is related to the percentage of checked structural elements. Such classification depends on the number of material samples per floor that must be taken for testing (Chart 5).

Defining the knowledge level (KL) and the confidence factor (CF), in the Eurocode 8, 1998-3, the application of the CF values for the verifications of limit states is suggested. CF is used in the capacity member calculations, where the mean values of the material properties are divided by the selected CF. Such a factor is also used as a multiplier of the mechanical

properties of the ductile components when the strength is used to determine the actions affecting brittle components or mechanisms (PINTO, 2011). Such additional partial material factor, CF, is appropriate to cover the more significant uncertainties on existing structures, due to lack of knowledge. Furthermore, in the CF, the variability of the results due to epistemic uncertainties is not considered, *i.e.* they cannot be reduced by additional tests and inspections (PINTO, 2011). Indeed, in many cases, type and number of inspections are limited. Hence a measure of epistemic uncertainty is usually present and must be carefully considered (PINTO, 2011).

Chart 4 - Knowledge levels and corresponding methods of analysis.

	<b>KL1 - Limited knowledge</b>	<b>KL2 - Normal knowledge</b>	<b>KL3 - Full knowledge</b>
geometry	From original construction drawings with sample visual survey or the <b>full</b> survey		
details	Simulated design following the relevant practice and from <b>limited in-situ</b> inspection	From incomplete original detailed construction drawings with limited <i>in-situ</i> inspection or <b>extended in-situ</b> inspection	From original detailed construction drawings with limited <i>in-situ</i> inspection or <b>comprehensive in-situ</b> inspection
materials	Default values following standards of the time of construction and from <b>limited in-situ</b> testing	From original design specification with limited <i>in-situ</i> testing or from <b>extended in-situ</b> testing	From original test reports with limited <i>in-situ</i> or from <b>comprehensive in-situ</b> testing
structural model	local verification of <b>element capacity</b> and set up a <b>linear</b> structural analysis model	local verification of <b>element capacity</b> and set up a <b>linear</b> or <b>non-linear</b> structural analysis model	
structural evaluation	<b>linear</b> analysis methods, either <b>static</b> or <b>dynamic</b>	either <b>linear</b> or <b>non-linear</b> analysis methods, either <b>static</b> or <b>dynamic</b>	
CF	1.35	1.20	1.00

Source: Pinto and Franchin (2011) modified by the authors.

Chart 5 - Recommended minimum requirements for different levels of inspection and testing.

	<b>Inspection of details</b>	<b>Testing of materials</b>
	For each type of primary element (beam, column, wall)	
Level of inspection and testing	Percentage of elements that are checked for details	Material sample per floor
Limited	20	1
Extended	50	2
Comprehensive	80	3

Source: Table 3.2 of Eurocode 8 - Part 3 (EN 1998-3:2005).

The use of partial factor approach is also suggested in EC 0 where partial factor  $\gamma_F$ ,  $\gamma_M$ ,  $\gamma_G$ ,  $\gamma_{Rd}$  and  $\gamma_{Sd}$  also account for model uncertainties and dimensional variations, amplifying the load actions (STANDARD, 2010). Moreover, EC8 introduce the partial factor  $\gamma_{Rd}$  as the model uncertainty factor on the design value of resistance in the estimation of capacity design action effects, which also accounts for various sources of overstrength. It varies from 1.00 to 1.20, and

it is used to amplify the loads acting on the structures. Such partial factors can vary according to the understanding of the related uncertainties and can be reduced through the level of knowledge increase.

#### 2.1.4.4.2 Italian standards: NTC 08 and further updating standards

Regarding the Italian Standards, the Eurocode 8 was implemented in the so-called NTC08, which application has also been defined in Circolare 617/09. Such standard was recently updated in the *Decreto del Ministero delle Infrastrutture e dei Trasporti*, 17 January 2018 *Aggiornamento delle «Norme tecniche per le costruzioni»* (INFRASTRUTTURE; TRASPORTI, 2018). In the Italian National Standards, a procedure for existing buildings is defined. It is based on historical-critical analysis, a geometrical survey with construction details, mechanical characterization of materials, the definition of the level of knowledge and confidence factor, and loads (CS.LL.PP., 2009; INFRASTRUTTURE; TRASPORTI, 2018).

Both European and Italian standards pose the inspection and diagnosis as the first step for rehabilitation or conservation of existing buildings. However, Italian national standards analyse the problem of the impossibility to have the same concepts and procedure to all types of structures, *e.g.* masonry, reinforced concrete (r.c.) and steel structures (MAGENES; PENNA, 2009). The so-called NTC08 (and further modifications of *Circolare 617/09 and NTC 2018*) suggests different procedures and different type of construction details, dividing the intervention by the type of material of the building structure, *e.g.* masonry buildings, reinforced concrete, steel buildings and timber buildings. For the masonry buildings, the details that must be analysed are:

- a) quality of the connection between vertical walls;
- b) quality of the connection between the walls and horizontal structures and possible presence of beams or other connecting devices;
- c) the existence of structurally efficient lintels above the openings;
- d) the presence of elements structurally efficient able to eliminate the stresses that may be present;
- e) the presence of elements, including non-structural, high vulnerability;
- f) type of masonry.

For the reinforced concrete buildings, instead, some other aspects must be considered:

- a) identification of the structural construction and verification of compliance with the regularity criteria (indicated in Section 7.2.2 of the NTC08); this is obtained based on the original drawings of the project appropriately verified with investigations *in-situ*, or with a new survey;
- b) identification of the foundation structures;
- c) identification of the categories of soil as specified in Section 3.2.2 of the NTC08;
- d) information on the geometric dimensions of the structural elements, the quantities of steel reinforcement, the mechanical properties of materials, connections;
- e) information on possible local defects of materials;
- f) information on possible defects in construction details;
- g) information on the rules used in the original design;
- h) description of the class of use, the category and the nominal life according to Section 2.4 of the NTC08;
- i) evaluation of variable loads, depending on the intended use;
- j) information on the nature and intensity of any damage incurred previously and repair information made.

For timber buildings, the possible variability of the material, especially in the historical building, is recognised. For these reasons, the investigation of individual elements is suggested. Moreover, concerning the levels of knowledge that it is intended to achieve, the investigation aims at the assessment of biotic and abiotic degradation, where possible. The inspection of the conditions of the end sections of the element is suggested when in contact with other material.

The definition of the knowledge level - in Italian “*livelli di conoscenza*” (LC) - is similar to Eurocode 8 (Chart 4). As was previously mentioned, specifications regarding each type of material are given, *i.e.* masonry, reinforced concrete and steel, and timber structures (section C8.5.4). Regarding the mechanic characterization of the material properties, *in-situ* and laboratory tests are suggested for each material-type structure. As an example, for masonry structures, referential values of the mechanical parameters are given (Chart 6). Such parameters are defined as follow:

- a)  $f_m$ , the average compressive strength of masonry;
- b)  $\tau_0$ , the average shear strength of the masonry;
- c)  $f_{v0}$ , the average shear strength of masonry;

- d)  $E$ , the average value of the modulus Young modulus of elasticity;
- e)  $G$ , the average value of the shear modulus of elasticity;
- f)  $w$ , the average specific weight of the masonry.

Chart 6 - Reference values of the mechanical parameters of the masonry and average specific weight for different types of masonry.

Masonry typology	Category	$f$	$\tau_0$	$f_{v0}$	$E$	$G$	$w$ (kN/m <sup>3</sup> )
		min-max	min-max	min-max	min-max	min-max	
Irregular stone masonry (pebbles, erratic, irregular stones)	I	1.0 2.0	0.018 0.032	-	690 1050	230 350	19
Uncut stone masonry with facing walls of limited thickness and infill core	II	2.0	0.035 0.051	-	1020- 1440	340 480	20
Cut stone with good bonding	III	2.6 3.8	0.056 0.074	-	1500 1980	500 660	21
Uncut soft stone masonry (tuff, limestone, etc.)	IV	1.4 2.2	0.028 0.042	-	900 1260	300 420	13 16
Cut soft stone masonry (tuff, limestone, etc.)	V	2.0 3.2	0.04 0.08	0.18 0.28	2400 3300	800 1100	
Dressed rectangular (ashlar) stone masonry	VI	5.8 8.2	0.09 0.12	0.18 0.28	2400 3300	800 1100	22
Solid brick masonry with lime mortar	VII	2.6 4.3	0.05 0.13	0.13 0.27	1200 1800	400 600	18
Hollow brick masonry with cementitious mortar	VIII	5.0 8.0	0.08 0.17	0.20 0.36	3500 5600	875 1400	15

Source: Magenes and Penna (2009) modified by the author.

The reference values of the mechanical parameters of the masonry can be modified by a corrective coefficient (BOSCHI; GALANO; VIGNOLI, 2019) according to the insight of the visual inspection, *i.e.* good mortar quality, thin joints, stringcourses, *etc.* (Chart 7). Indeed, visual inspection is considered as an *in-situ* investigation that plays a crucial role in all the level of knowledge defined in the Italian Standard. Regarding the quantification of material parameters, in the category 'limited *in-situ* testing' - which defines the minimum knowledge level - the development of one test per floor at least is recommended as a reference (MAGENES; PENNA, 2009).

In the NTC 2018, the previous reference values for each level of knowledge (LC) are defined, the minimum resistance value must be used for LC1, and mean value for LC1 and LC2



(CS.LL.PP., 2018). In the case of LC3, reference values are modified according to the results obtained from *in-situ* and laboratory test (section C8.5.4.1 of NTC 2018). A relation between the parameter and the experimental test is given in Table C.8.5.III of NTC 2018.

Chart 7 - Maximum corrective coefficients to be applied to the reference values of the mechanical parameters of the masonry (Table C8.5.II of NTC18).

Masonry typology category	As-built state			Intervention of Consolidation			
	Good mortar	String-courses	Transversal connections	Injections	Reinforced plaster mortar	Reinforce pointing - transversal connections	Maximum coefficient
I	1.5	1.3	1.5	2	2.5	1.6	3.5
II	1.4	1.2	1.5	1.7	2.0	1.5	3.0
III	1.3	1.1	1.3	1.5	1.5	1.4	2.4
IV	1.5	1.2	1.3	1.4	1.7	1.1	2.0
V	1.6	-	1.2	1.2	1.5	1.2	1.8
VI	1.2	-	1.2	1.2	1.2	-	1.4
VII	1.2	-	1.3	1.2	1.5	1.2	1.8
VIII	1.2	-	-	-	1.3	-	1.3

Source: Magenes and Penna (2009) modified by the author.

Furthermore, in the National Standard, the investigation plan is defined. It must be appropriately calibrated according to the preliminary analysis and concerning the level of knowledge to be reached. Moreover, regarding the dynamic investigation, all modes with significant participating mass must be considered, *i.e.* when participating mass is greater than 5%. For the global structural behaviour assessment, a total participating mass greater than 85% must be reached. Usually, a minimum number of investigations and testing is prescribed in addition to a list of advisable tests to be adopted (Chart 8). The use of the double flat-jack test or tests for the mortar characterization is required to reach KL2, while the diagonal compression test or the combined shear-compressive one is necessary to reach KL3 (CATTARI *et al.*, 2015). However, such tests are minor destructive and destructive, and special care for the heritage buildings must be given.

A common approach for the mechanical properties of masonry is given in Cattari *et al.* (2015), and defined as follow: in case of KL1, based on default values, following standards in force at the time of construction or as derived from literature; in case of KL2 and KL3, also by taking into account the support of experimental test results. Furthermore, the experimental investigation must be oriented to the knowledge of the structural elements, both concerning their stress and their role for the safety of the structure, analysing the homogeneity of the results

of the preliminary tests and their agreement with the original documents (MINISTERO DELLE INFRASTRUTTURE E DEI TRASPORTI, 2019).

Chart 8 - Reference experimental test method on the mechanical properties of masonry.

Experimental test type	Structural parameter
A direct test of compressive strength on the masonry wall	E
	f
Double flat jack	E
	f
Test of compressive and shear strength on an isolated panel - Sheppard type	G
	$\tau_0, f_{v0}$
Diagonal compressive strength test	G
	$\tau_0$
Direct shear test on mortar joint	$f_{v0}$
Laboratory test on each masonry component (brick, mortar, <i>etc.</i> )	$f_b, f_m, f_g$

Source: NTC 2018 modified by the author.

#### 2.1.4.4.3 Italian Guidelines for evaluation and mitigation of seismic risk to Cultural Heritage

The previous European and Italian standards - together with the methodologies previously presented (see Subsection 2.1.2.10) - can be considered as the basis for the approach proposed in “Guidelines for the assessment and mitigation of the seismic risk of cultural heritage” (DIRECTIVE OF THE PRIME MINISTER, 2007). The Italian Guidelines contains the alignment of the Directive of the President of the Council of Ministers for the assessment and reduction of seismic risk of the cultural heritage of 12 October 2007 to the Technical Standards for Construction 2008 (NTC08, 2008). However, such guidelines could be adopted even where the seismic hazard is minimum in the structural assessment of heritage building, extending the field of its application in Nation where the seismic hazard is neglected. The main aspects of this document are the analysis of the territorial contexts surrounding the construction, its location concerning certain risk areas and the initial survey of the building, with the identification of elements that may affect the level of risk (DIRECTIVE OF THE PRIME MINISTER, 2007). Such a path to knowledge is related to the following activities:

- a) general description of the heritage building;
- b) identification of the building, its location concerning certain risk areas, and its relationship with the built context;

- c) investigation of the functional characteristics of the building and its possible evolutions during the lifecycle;
- d) geometric survey of the building in its current state with a complete volumetric description of the structure, including damages and pathology phenomena;
- e) historical analysis of earthquakes and subsequent interventions on the building, *i.e.* the identification of the evolution of the construction, as a sequence of processing steps for the construction, since the original configuration to the as-built configuration;
- f) a survey of construction materials and conservation states, aiming at the identification of the structural and non-structural elements, with attention to the construction techniques, *e.g.* the construction details, the connections between the elements, *etc.*;
- g) identification of materials, including physical and mechanical properties;
- h) knowledge of the terrain and foundation structures.

The use of non-destructive tests is recommended in such a methodology (DIRECTIVE OF THE PRIME MINISTER, 2007). Structural health monitoring is here considered highly desirable for the knowledge of historic heritage buildings. As explained in Subsection 2.1.3, SHM is based on a periodic control of the building, representing the primary technique for wise conservation, as it allows scheduling maintenance and acting punctually in the intervention procedure, in case of structural damage (DIRECTIVE OF THE PRIME MINISTER, 2007). In the Italian Guidelines, concepts related to the knowledge levels of heritage buildings are defined in the confidence factors (Chart 9). Once the constructions have been identified in relation to the depth of the geometric survey, the material, and constructive surveys, and the mechanical research regarding the terrain and foundation, the designer assigns a confidence factor  $F_c$  ranging from 1 to 1.35 (DIRECTIVE OF THE PRIME MINISTER, 2007). This parameter (Equation 14) grades the reliability of the structural analysis model and the evaluation of the seismic safety index:

$$F_c = 1 + \sum_{k=1}^4 F_{ck}, \quad (8)$$

where  $F_c$  is the confidence factor and  $F_{ck}$  the partial confidence factor defined in Chart 9.

Chart 9 - The definition of the level of the depth of research on diverse aspects of knowledge and relative partial confidence factors  $F_{ck}$ .

<b>Geometric survey</b>	<b>Material and construction survey</b>	<b>Mechanical properties of the materials</b>	<b>Terrain and foundations</b>
The Geometric survey has been completed	Limited survey of materials and constructive elements	Mechanical parameters deduced from available data	Limited survey of terrain and foundations, in the absence of geological data or availability of information about the foundation
$F_{C1} = 0.05$	$F_{C2} = 0.12$	$F_{C3} = 0.12$	$F_{C4} = 0.06$
The geometric survey has been completed along with the graphic rendering of cracking and deformities	Extensive survey of materials and constructive elements	Limited research of mechanical parameters of materials	Geological data and Information regarding the foundation structures is available, limited research on terrain and foundation
	$F_{C2} = 0.06$	$F_{C3} = 0.06$	$F_{C4} = 0.03$
	Exhaustive survey of materials and constructive elements	Extensive research of mechanical parameters of materials	Extensive or exhaustive research on the terrain and foundations
$F_{C1} = 0$	$F_{C2} = 0$	$F_{C3} = 0$	$F_{C4} = 0$

Source: Italian Guidelines for evaluation and mitigation of seismic risk to Cultural Heritage (2007).

The confidence factor is applied differently depending on the model for evaluating seismic safety:

- a) models which consider the deformability and the resistance of the materials and structural elements;
- b) models which consider the balance limits of the various elements of the structure, considering the masonry materials as stiff and non-resistance to traction.

In the first case, the confidence factor is applied to the properties of the materials. It reduces both the plastic model as well as the resistance. In the second case, regarding rigid blocks, in which the resistance of the materials is not taken into consideration, the confidence factor is applied directly to the structural capacity (DIRECTIVE OF THE PRIME MINISTER, 2007).

The use of the partial factor is a common approach to the level of uncertainty (level of knowledge) in the European and Italian Standards. As an example, in the recent "Italian Guidelines for the classification and risk management safety assessment and monitoring of

existing bridges” (2020), the progressive deepening of the investigations is defined as capable to ensure the development of structural models characterized by increasing accuracy. Therefore, such knowledge increase allows for the execution of more reliable and better representative safety assessments of the structural behaviour of the building (CS.LL.PP., 2020). Consequently, it allows the use of confidence factors and partial factors gradually smaller, when appropriately motivated (CS.LL.PP., 2020).

### 2.1.5 Partial conclusions

The analysed methodologies on the structural assessment of heritage buildings are mainly focused on the seismic response assessment or the historic masonry structure conservation. However, they propose general concepts and approaches that can be considered as valid bases for general-type of heritage buildings. They should be adopted even where the seismic hazard is minimum or neglected in the structural assessment of heritage building, *e.g.* in Nation where the seismic hazard is minimal and usually neglected in the professional field. Analysed methodologies allow concluding the following considerations:

- a) the knowledge of the building is deeply related to the information acquired; hence, a high level of information improves the reliability of the structural analysis model, which is fundamental to the path to knowledge of heritage buildings;
- b) in-depth investigation on the main model uncertainties - *e.g.* the geometrical and the mechanical properties- should be included in the heritage building methodologies
- c) cultural heritage characteristics can affect the choice of a specific type of software to be used; main characteristics are the geometrical typology of the structure, the material properties and the constructive details, the static, dynamic or kinematic approach analysis, the benefit-effect in terms of time and costs efforts between the architectural and the structural modelling, the ability to easily access texts, spreadsheets and image data coordination of multidisciplinary types of professionals.
- d) the development of a methodology collecting such aspects for the problem of the global structural understanding will improve the scientific knowledge about cultural heritage structures.

## 2.2 VIBRATION-BASED STRUCTURAL IDENTIFICATION

Vibration-based structural identification is presented in this section. Such methodology involves structural assessment of the construction based on dynamic investigations (GENTILE; SAISI, 2007; GENTILE; SAISI; CABBOI, 2015; RAMOS; AGUILAR; LOURENÇO, 2011). Such a procedure is commonly used to investigate structures like bridges, cable-stayed bridges, high-rise buildings (GENTILE; SAISI, 2007).

In the last decades, applications were carried out in heritage structure, *i.e.* churches, towers and minarets, through AVT experimental investigation (see Subsection 2.1.2.6). In such a procedure, AVT can be considered a reliable non-destructive procedure to verify the structural behaviour and integrity of a building (BINDA; SAISI, 2009a). Indeed, due to the highly sensitive and relatively inexpensive accelerometers available in the market, AVT showed the ability to measure the structural response even in operational conditions, which generally has a low ambient excitation.

Once the experimental data are acquired from AVT, the OMA offers different approaches to obtain modal parameters, each one with a different level of complexity, related to the required information. They will be briefly approached in the following subsections. Frequencies and modal shapes have a crucial role in the vibration-based structural identification method. Thus, an OMA procedure mainly aimed at the comparison of experimental and numerical parameters should be adopted.

Consequently, numerical parameters should be tuned to better fit experimental results. Regarding such a model updating process, the comparison between the Inverse Eigen-Sensitivity (IE) method and the Douglas and Reid (DR) method (1982) was carried out in the research of Gentile and Saisi (2007). The DR seemed to be particularly fitted since the identification procedure was based on the minimization of the frequency discrepancies. Main steps of the procedure of vibration-based structural identification will be briefly presented in the following subsections.

### 2.2.1 Types of approach to structural identification

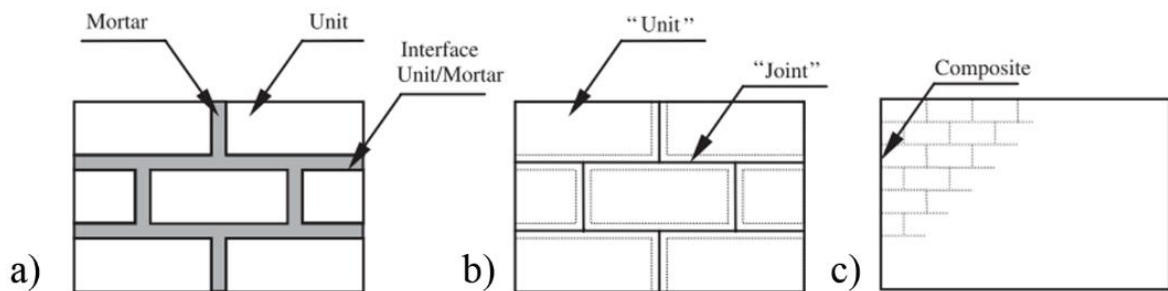
Engineering structures present several typologies with different behaviour for which many modelling approaches have been adopted (MARQUES, 2014). In general, two different main scales have been applied to the structural identification, namely the micro-modelling and

macro-modelling approaches (LOURENÇO, 2002). Such approaches depend on the level of accuracy and simplicity desired (LOURENÇO, 2002). In the case of masonry buildings, for example, micro-modelling can be applied at two different levels of detail. In Lourenço (2002), the differences between such approaches are given:

- a) detailed micro-modelling, where units and mortar are represented by continuum elements and the unit-mortar interfaces is represented by discontinuum elements (Figure 25.a);
- b) simplified micro-modelling, where expanded units are represented by continuum elements and the behaviour of the mortar joints and the unit-mortar interface is lumped in discontinuum elements (Figure 25.b);
- c) macro-modelling, where units, mortar and unit-mortar interface are simplified in a homogeneous continuum (Figure 25.c).

Each type of modelling strategy has a different application field. While micro-modelling allows understanding local behaviour, macro-modelling is useful to model the overall structure for global assessment (LOURENÇO, 2002). The type of problem to be solved will define which of the modelling strategy fit better.

Figure 25 - Modelling strategies for masonry structures: detailed micro-modelling (a), simplified micro-modelling (b), and macro-modelling (c).



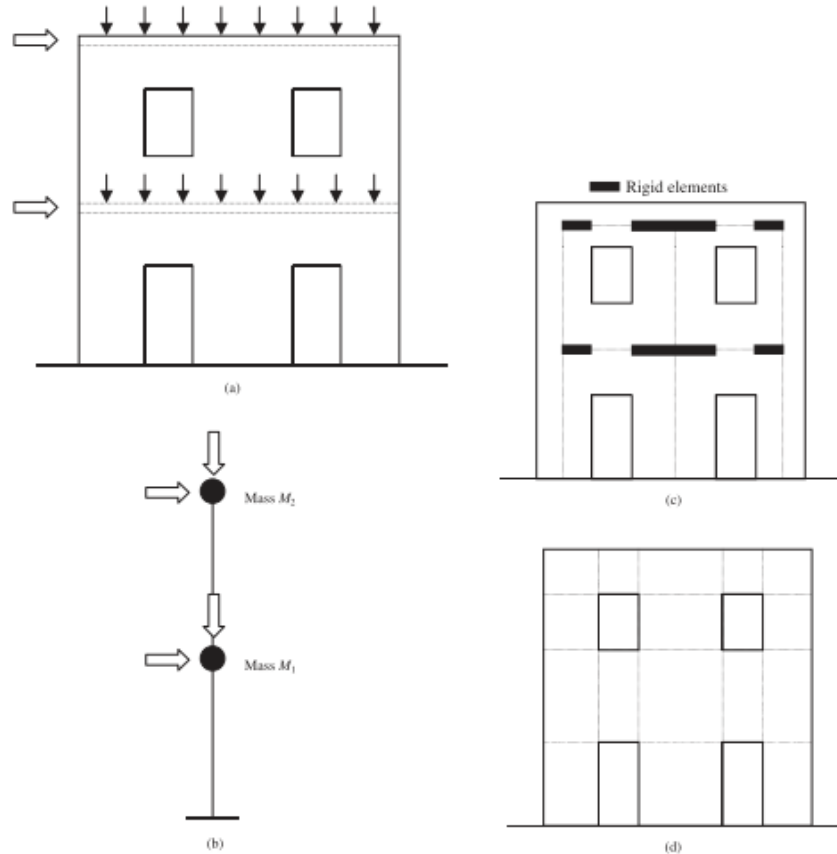
Source: Lourenço (2002).

Moreover, the simplest approach to the structural analysis of complex buildings is carried out using structural component models (MARQUES, 2014), *e.g.* truss, beam panel, plate or shell elements to represent columns, piers, arches and vaults. In such cases, homogenous material behaviour is assumed (LOURENÇO, 2002). The use of structural component models was introduced by Tomažević (1978) and applied mainly to perform seismic assessment (MARQUES, 2014).

In Figure 26, some example of modelling of a wall are given, *i.e.* lumped mass approach, a beam approach and a panel macro-model (LOURENÇO, 2002). The lumped mass

approach (mass-spring-dashpot model) is a model with a rough representation of the geometry, with floor levels and lumped parameters as structural components (LOURENÇO, 2002).

Figure 26 - Examples of structural component models for: (a) wall with openings; (b) lumped parameters; (c) beam elements; and (d) macro- elements (rigid or deformable).



Source: Lourenço (2002).

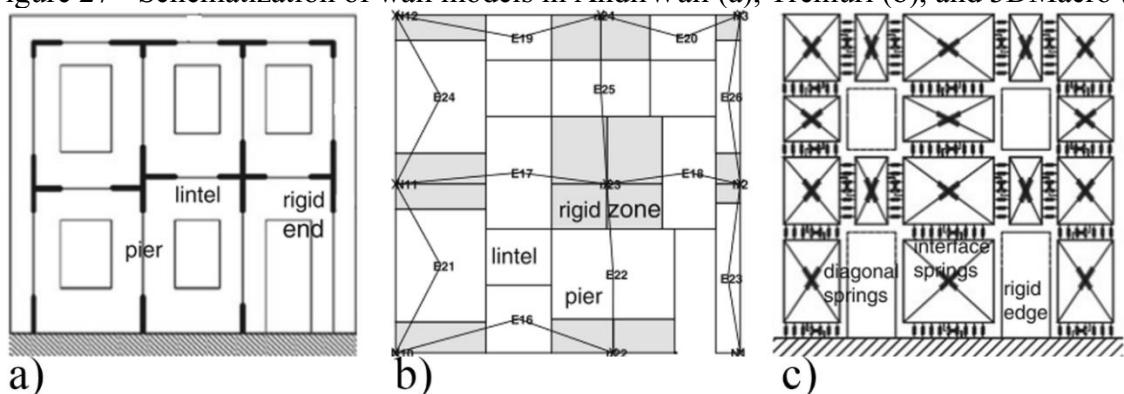
The model represented in Figure 26.c is defined by rigid and deformable beam elements, with an increased geometry accuracy. The primary assumption of such a frame modelling is that deformable beams are defined in the lintels and piers while their connection is assumed as rigid beams (CALÌ, 2015). Moreover, an approach with an improved geometry description is shown in Figure 26.d. Geometry is defined by rigid or deformable panel macro-elements as structural components (LOURENÇO, 2002).

Some software has been developed according to macro-modelling for assessing the seismic safety of unreinforced masonry buildings (Figure 27) (MARQUES, 2014). Marques and Lourenço (2011) benchmarked the ANDILWall/SAM II (CALLIARI *et al.*, 2010; MAGENES, 2000), the TreMuri (LAGOMARSINO *et al.*, 2009), and the 3DMacro (SISMICA, 2013) software codes, providing their main formulations. AndilWall (SAM-method) and



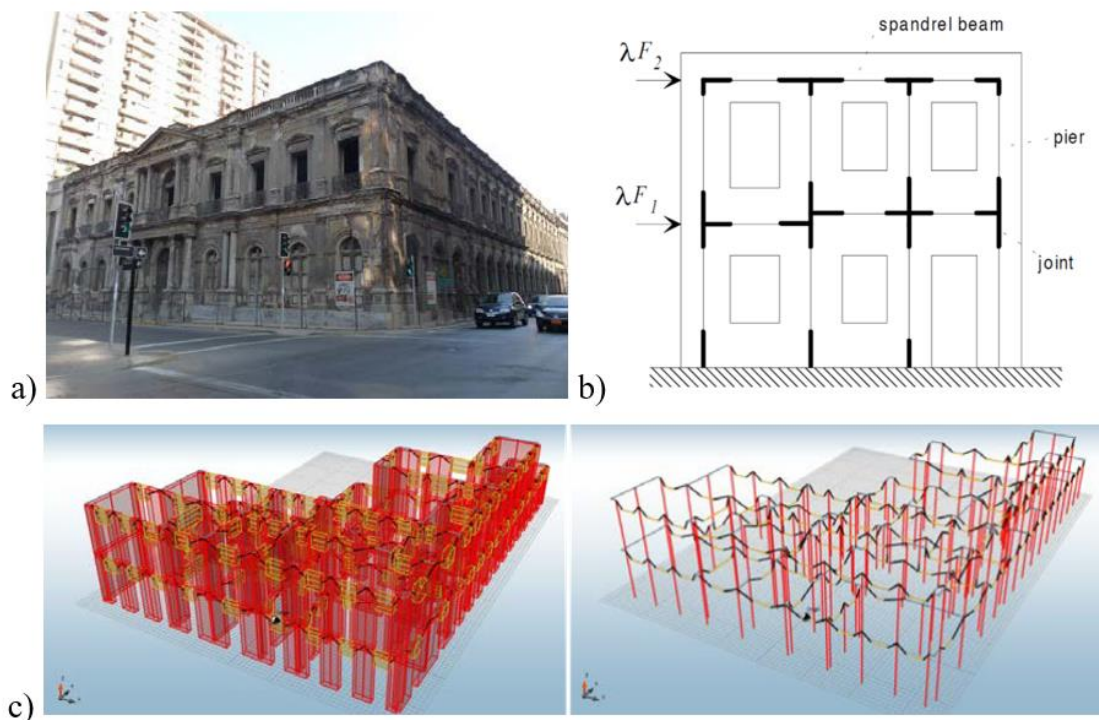
TreMuri are based on frame-type modelling by using one-dimensional macroelements. In contrast, the 3DMacro is based on a discretization with two-dimensional discrete elements (MARQUES, 2014). Such a method allows for the seismic assessment through performance-based approaches, *i.e.*, procedures for nonlinear static (pushover) analysis, according to Eurocodes (CEN, 2004). Moreover, such software in the last years improved the interoperability with CAD and BIM software due to the increasing understanding of the potentiality of such tools in the geometrical accuracy.

Figure 27 - Schematization of wall models in AndilWall (a), Tremuri (b), and 3DMacro (c).



Source: Marques (2014).

Figure 28 - Seismic Assessment by Equivalent Frame Modelling of Palacio Pereira (a), Santiago de Chile: SAM method (b), geometrical and analytical representation (c and d).



Source: the author, Master thesis (2015).

However, complex geometries of historic structures - in terms of structural component models - leads to the use of Finite Element models (LOURENÇO, 2002). For these reasons, the proposed bibliography review focuses on the crucial role of the dynamic behaviour of the constructions, through the numerical and experimental approaches (output-only), based on FEM and OMA, respectively. An extensive review of such approaches can be found in Lourenço (2002) and Marques (2014). Further information can be found in the author master SAHC thesis, since AndilWall - Simplified Analysis of Masonry buildings (SAM) method - was used to the seismic assessment of Palacio Pereira in Chile (CALÌ, 2015, 2016).

## 2.2.2 Structural assessment through Finite Element Analysis

In the structural assessment of historical constructions, linear analysis is always performed, before the application of more sophisticated approaches (ROCA *et al.*, 2010). It allows for an overall understanding of the structural behaviour, the range values, the distributions of the loads, the mesh definition, and calibration (ROCA *et al.*, 2010). The main theory of such an approach is presented in the following subsections.

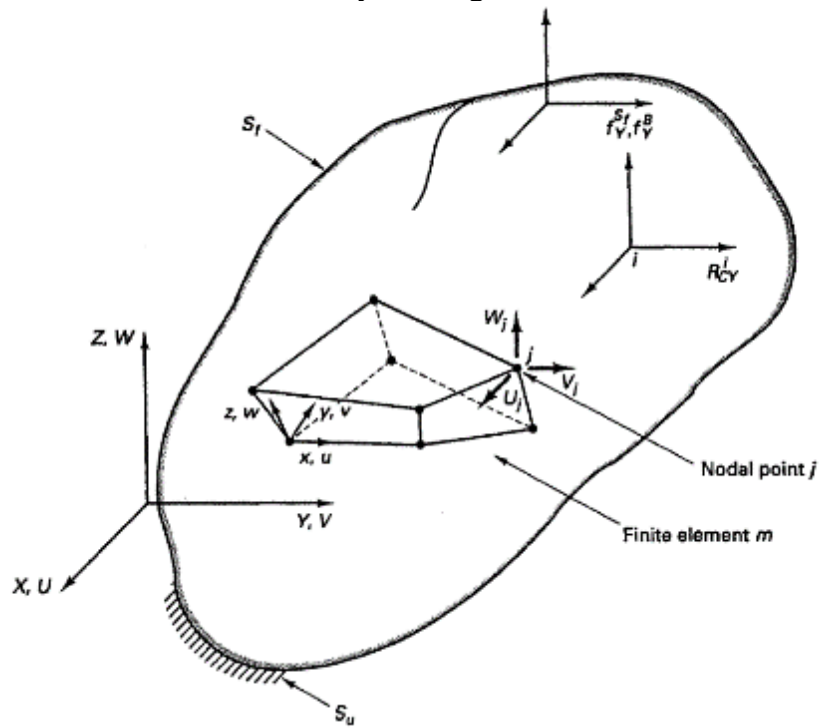
### 2.2.2.1 The general problem of structural analysis

In this subsection, the general elasticity problem, *i.e.* the definition of the equation of the equilibrium of a general three-dimensional body. Different authors have dealt with this topic (BATHE, 2006; BESSELING, 1974; BODIG; JAYNE, 1982; DEL PIERO, 1989; HO-LE, 1988; HOSFORD, 2010; LOURENÇO, 2002; MELI; PEÑA, 2004; PIERRON; GREDIAC, 2012; ROCA *et al.*, 2010; ZIENKIEWICZ, O. C., TAYLOR, 2000). A brief overview of the problems is presented hereinafter.

According to Bathe (2006), the body is considered in a fixed stationary coordinate system  $X, Y, Z$ . Such body is supported on the area  $S_u$  and characterized by a prescribed displacements  $U^{Su}$ , body forces  $f^B$ , surface forces per unit surface  $f^{Sf}$  acting on the area  $S_f$ , and concentrated nodal loads  $R_C^i$  (Figure 29), which are defined in the Equation 9:

$$f^B = \begin{bmatrix} f_x^B \\ f_y^B \\ f_z^B \end{bmatrix}; \quad f^{Sf} = \begin{bmatrix} f_x^{Sf} \\ f_y^{Sf} \\ f_z^{Sf} \end{bmatrix}; \quad R_C^i = \begin{bmatrix} R_{CX}^i \\ R_{CY}^i \\ R_{CZ}^i \end{bmatrix}. \quad (9)$$

Figure 29 - General three-dimensional body with a generic 8-node three-dimensional element.



Source: Bathe (2006).

The displacement  $U$  of the body from the unloaded configuration is measured in the coordinate system  $X, Y, Z$  and defined as follow (Equation 10):

$$U(X, Y, Z) = \begin{bmatrix} U \\ V \\ W \end{bmatrix}, \quad (10)$$

where  $U=U_{S_u}$  on the surface  $S_u$ . Consequently, strains (equations 11 and 12) and stresses (equations 13 and 14) corresponding to  $U$  and  $\varepsilon$  are:

$$\varepsilon^T = [\varepsilon_{xx} \quad \varepsilon_{yy} \quad \varepsilon_{zz} \quad \gamma_{xy} \quad \gamma_{yz} \quad \gamma_{xz}], \quad (11)$$

$$\begin{aligned} \varepsilon_{xx} &= \frac{\partial U}{\partial X}, & \varepsilon_{yy} &= \frac{\partial V}{\partial Y}, & \varepsilon_{zz} &= \frac{\partial W}{\partial Z}, \\ \gamma_{xy} &= \frac{\partial U}{\partial Y} + \frac{\partial V}{\partial X}, & \gamma_{yz} &= \frac{\partial V}{\partial Z} + \frac{\partial W}{\partial Y}, & \gamma_{xz} &= \frac{\partial W}{\partial X} + \frac{\partial U}{\partial Z}, \end{aligned} \quad (12)$$

$$\tau^T = [\tau_{xx} \quad \tau_{yy} \quad \tau_{zz} \quad \tau_{xy} \quad \tau_{yz} \quad \tau_{xz}], \quad (13)$$

$$\tau = C\varepsilon + \tau', \quad (14)$$

where  $C$  is the stress-strain material matrix and the vector  $\tau'$  denotes given initial stresses (Chart 10) (BATHE, 2006).

Chart 10 - Generalized stress-strain matrices for isotropic materials.

Problem	Material matrix $C$
Bar	$E$
Beam	$EI$
Plane stress	$\frac{E}{1-\nu} \begin{bmatrix} 1 & \nu & 0 \\ \nu & 1 & 0 \\ 0 & 0 & \frac{1-\nu}{2} \end{bmatrix}$
Plane strain	$\frac{E(1-\nu)}{(1+\nu)(1-2\nu)} \begin{bmatrix} 1 & \frac{\nu}{1-\nu} & 0 \\ \frac{\nu}{1-\nu} & 1 & 0 \\ 0 & 0 & \frac{1-2\nu}{2(1-\nu)} \end{bmatrix}$
Axisymmetric	$\frac{E(1-\nu)}{(1+\nu)(1-2\nu)} \begin{bmatrix} 1 & \frac{\nu}{1-\nu} & 0 & \frac{\nu}{1-\nu} \\ \frac{\nu}{1-\nu} & 1 & 0 & \frac{\nu}{1-\nu} \\ 0 & 0 & \frac{1-2\nu}{2(1-\nu)} & 0 \\ \frac{\nu}{1-\nu} & \frac{\nu}{1-\nu} & 0 & 1 \end{bmatrix}$
Three-dimensional	$\frac{E(1-\nu)}{(1+\nu)(1-2\nu)} \begin{bmatrix} 1 & \frac{\nu}{1-\nu} & \frac{\nu}{1-\nu} & 0 & 0 & 0 \\ \frac{\nu}{1-\nu} & 1 & \frac{\nu}{1-\nu} & 0 & 0 & 0 \\ \frac{\nu}{1-\nu} & \frac{\nu}{1-\nu} & 1 & 0 & 0 & 0 \\ 0 & 0 & 0 & \frac{1-2\nu}{2(1-\nu)} & 0 & 0 \\ 0 & 0 & 0 & 0 & \frac{1-2\nu}{2(1-\nu)} & 0 \\ 0 & 0 & 0 & 0 & 0 & \frac{1-2\nu}{2(1-\nu)} \end{bmatrix}$
Plate bending	$\frac{Eh^3}{12(1-\nu^2)} \begin{bmatrix} 1 & \nu & 0 \\ \nu & 1 & 0 \\ 0 & 0 & \frac{1-\nu}{2} \end{bmatrix}$

Notation:  $E$ =Young's modulus,  $\nu$ =Poisson's ratio,  $h$ = thickness of the plate,  $I$ =moment of inertia

Source: Bathe (2006).

Moreover, Bathe (2006) explains as the analysis problem is the calculation of displacements  $U$  of the body (Chart 10). Such displacements are related to  $\varepsilon$  and stress  $\tau$ , given the initial system previously described, *i.e.* geometry, applied loads  $f^f, f^B, R^i_C, i=1, 2, \dots, n$ , support conditions on  $S_u$ , material stress-strain law, and the initial stresses in the body (Figure 29).

A necessary condition for the linearity of a structural problem is that characteristics of the system are satisfied at the same time the following hypotheses, in terms of materials, geometry and boundary conditions (DEL PIERO, 1989; ROCA *et al.*, 2010): geometric linearity is assumed for structural behaviour; linear elastic materials is supposed; constraints of the structure are considered bilateral; not depending on the entity of the acting loads. Infinitesimal displacements (Equation 4) allow supposing that the equilibrium of the body is solved for its unloaded configuration (BATHE, 2006).

Bathe (2006) affirms that closed-form analytical solutions are possible only when relatively simple geometries are considered. For more complex systems, approximate procedures of the solution must be employed, *e.g.* Finite Element Analysis (FEA) (BATHE, 2006; ZIENKIEWICZ, O. C., TAYLOR, 2000). The governing differential equations of equilibrium should be defined to calculate the response of the body. They have to be solved considering the boundary conditions. Such a procedure will be approached in the following section. Besides, the resolution of the structural analysis requires a considerable amount of information about the structure (Chart 10), as geometries, mechanical properties, loads, boundary conditions (BINDA; SAISI; TIRABOSCHI, 2000). Such information is acquired through extensive investigation procedures relying on experimental data.

#### 2.2.2.2 *Equilibrium of the body through Finite Element Analysis*

The Finite Element Method is a numerical tool, which is widely used in the field of mechanics of structures (PIERRON; GREDIAC, 2012). FEM is a procedure for obtaining numerical approximations to the solution of boundary value problems presented in the previous subsections.

The basis of such a procedure is the principle of virtual work (BATHE, 2006). It states that the equilibrium of the body (Figure 29) requires that for any compatible virtual displacements imposed on the body in its state of equilibrium, the total internal virtual work is equal to the total external virtual work (BATHE, 2006) (Equation 15):

$$\int_V \bar{\varepsilon}^T \tau dV = \int_V \bar{U}^T f^B dV + \int_{S_f} \bar{U}^{Sf^T} f^{Sf} dS + \sum_i \bar{U}^i R_C^i, \quad (15)$$

where  $\bar{\varepsilon}$  are the virtual strains corresponding to virtual displacements  $\bar{U}$  (the overbar denotes virtual quantities), while  $\tau, f^B, f^{Sf}$ , and  $R_C^i$  are stresses in equilibrium with applied loads. Bathe (2006) also emphasizes that:

- a) stresses  $\tau$  are assumed to be known quantities and are the unique stresses that correctly balance the applied loads;
- b) the virtual strains  $\bar{\varepsilon}$  are calculated by differentiations given in Equation 4 from the assumed virtual displacements  $\bar{U}$ , which represents a continuous virtual displacement field;
- c)  $\bar{U}$  equal to zero at the points and surfaces and corresponding to the components of displacements that are prescribed at those points and surfaces on  $S_u$ ; also, the components in  $\bar{U}_{Sf}$  simply the virtual displacements  $\bar{U}$  evaluated on the surface  $S_f$ ;
- d) all integrations are performed over the original volume and surface of the body, unaffected by the imposed virtual displacements.

In the FE analysis, the body is approximated as an assemblage of discrete Finite Elements. Such elements are interconnected at the nodal point on the element boundaries, deriving the governing FE equations for the general three-dimensional body. The following equations 16 to 18 define the displacements, strain and stresses of element  $m$  (BATHE, 2006):

$$u^{(m)}(x, y, z) = H^{(m)}(x, y, z) \hat{U}, \quad (16)$$

$$\varepsilon^{(m)}(x, y, z) = B^{(m)}(x, y, z) \hat{U}, \quad (17)$$

$$\tau^m(x, y, z) = C^{(m)} \varepsilon^m + \tau', \quad (18)$$

where  $H^{(m)}$  is the displacement interpolation matrix, and  $\hat{U}$  is a vector of the global displacement components at all nodal point and  $B^{(m)}$  is the strain-displacement matrix. The rows of  $B^{(m)}$  are

obtained by appropriately differentiating and combining rows of the matrix  $H^{(m)}$ ,  $C^{(m)}$  is the elasticity matrix of element  $m$  and  $\tau'^{(m)}$  are the given element initial stresses (BATHE, 2006).

The displacement interpolation matrix  $H_{(m)}$  depends on the element geometry, the number of element nodes/degrees of freedom, and convergence requirements. Furthermore, the material law specified in  $C^{(m)}$  for each element can be that for an isotropic or an anisotropic material and can vary from element to element (BATHE, 2006). All nodal point displacements are listed in vector  $\widehat{U}$ . However, for a given element, only the displacements at the nodes of the elements affect the displacement and strain distributions within the element - according to equations 19-21. Consequently, an independent coordinate system is properly defined (BATHE, 2006):

$$K U = R, \quad (19)$$

$$K = \sum_m \int_{V^{(m)}} B^{(m)T} C^{(m)} B^{(m)} dV^{(m)} = K^{(m)}, \quad (20)$$

$$R = R_B + R_S - R_I + R_C, \quad (21)$$

where  $R_B$  body force vector,  $R_S$  surfaces forces,  $R_I$  element initial stresses  $R_C$  nodal concentrated loads. Such vectors are defined as follow (equations 22 to 24):

$$R_B = \sum_m \int_{V^{(m)}} H^{(m)T} f^{B^{(m)}} dV^{(m)} = R_B^{(m)}, \quad (22)$$

$$R_S = \sum_m \int_{S_1^{(m)}, \dots, S_q^{(m)}} H^{S^{(m)T}} f^{S^{(m)}} dS^{(m)} = R_S^{(m)}, \quad (23)$$

$$R_I = \sum_m \int_{V^{(m)}} B^{(m)T} \tau^{I^{(m)}} dV^{(m)} = R_I^{(m)}. \quad (24)$$

Up to now, the equilibrium equation problem was presented from a static point of view, *i.e.* the relations of forces, loads, stress and strain do not vary in time. However, measured dynamic responses of structures is time depending and show that energy is dissipated during vibration, which in vibration analysis is usually taken account of by introducing velocity-dependent damping forces (BATHE, 2006). In this case, the vectors  $f^{B^{(m)}}$  do not include inertia

and time-depending parameters, which are considered in the following equations 25, 26, and 27:

$$M\ddot{U} + C\dot{U} + K U = R , \quad (25)$$

where  $M$  and  $C$  are the mass and damping matrix, respectively. Such matrixes are defined as follow:

$$M = \sum_m \int_{V^{(m)}} \rho^{(m)} H^{(m)T} H^{(m)} dV^{(m)} = M^{(m)} , \quad (26)$$

$$C = \sum_m \int_{V^{(m)}} k^{(m)} H^{(m)T} H^{(m)} dV^{(m)} = C^{(m)} , \quad (27)$$

where  $k^{(m)}$  is the damping property of element  $m$ .

Bathe in his work (2006) affirms how it is difficult, if not impossible, to determine the damping parameters for general Finite Element since damping properties are frequency dependent. For this reason, the matrix  $C$  - which also depends on the system nonlinearities - is in general not assembled from element damping matrices but is obtained using the mass matrix and stiffness matrix of the complete element assemblage together with experimental results on the amount of damping (BATHE, 2006). In general, the above equations can be non-linear, *i.e.* stiffness matrices are dependent on non-linear material properties or large deformation field (ZIENKIEWICZ, O. C., TAYLOR, 2000). Furthermore, all the matrices approached in Equation 25 are usually defined as symmetric. However, some cases involving nonlinearity and non-symmetric matrices are discussed in Chapter 6 of Bathe (2006) and Chapter 2 (Volume 3) of Zienkiewicz and Taylor (2000).

The process, suggested for the Finite Element Analysis, is here summarized (BATHE, 2006):

- a) the structure or continuum is idealized as an assemblage of discrete elements connected at nodes of the elements;
- b) the externally applied forces (body forces, surface tractions, initial stresses, concentrated loads, inertia and damping forces, and reactions) are lumped to these nodes using the virtual work principle to obtain equivalent externally applied nodal point forces;



- c) the equivalent externally applied nodal point forces are equilibrated by the element nodal point forces that are equivalent to the internal element stresses,  $\sum F^{(m)} = R$ ;
- d) compatibility and the stress-strain material relationship are satisfied precisely; however, instead of equilibrium on the differential level, the global equilibrium for the complete structure, at the nodes, and of each element  $m$  under its nodal point forces  $F^{(m)}$  is satisfied.

### 2.2.2.3 Mesh element: type, definition and quality

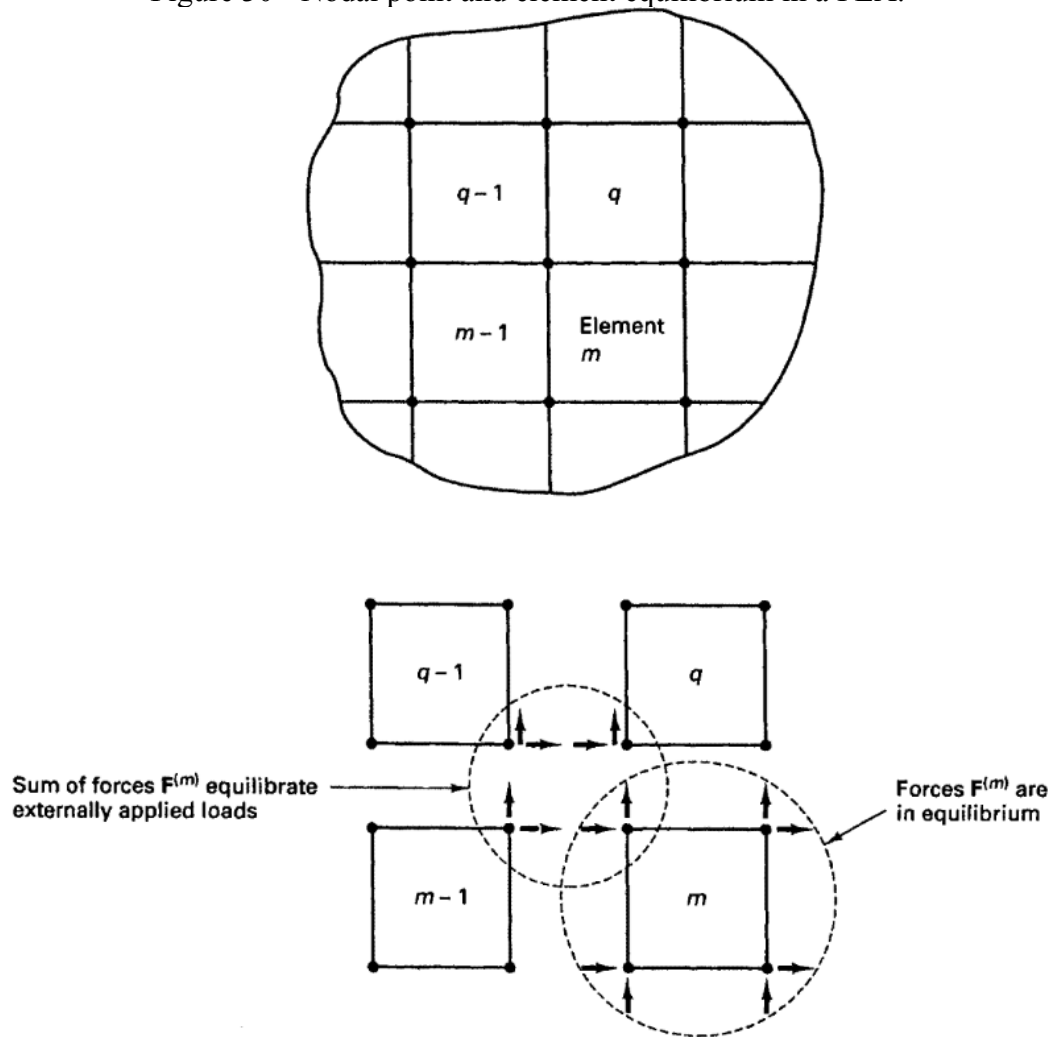
In the previous subsection, the general problem of the equilibrium was presented. In this subsection, the topic of mesh element is approached. The choice of element and the construction of the corresponding entries in  $H^{(m)}$  (Equation 16) constitute the necessary steps of a Finite Element solution (BATHE, 2006).

Once the Finite Element assemblage (also called Finite Element mesh) is defined, the solution of the equilibrium problem is defined as nodal point equilibrium and element equilibrium (Figure 30). At any node, the sum of the element nodal point forces is in equilibrium with the externally applied nodal loads (Figure 30), *i.e.* body forces, surface tractions, initial stresses, concentrated loads, inertia and damping forces, and reactions (BATHE, 2006). Each element  $m$  is in equilibrium under its forces  $F^{(m)}$ , according to the following Equation 28:

$$\sum_m F^{(m)} = K U. \quad (28)$$

Finite Element method has been used as a powerful and versatile analysis tool over with the time (HO-LE, 1988), where the selection of the element type characterize the obtained solution, such a procedure is known as the mesh generation. Such an issue can be very time-consuming so that leading software offers to the user the possibility to use a few types of the mesh element type. Some formulation on surface definition and mesh generation is offered by Coons (1967) and Katili (1993). Furthermore, a comparison between several types of mesh is presented in Ho-Le (1999) and Katili, Batoz, Jauhari (2018). Ho-Le (1999) explains as many mesh generators produce a mesh of triangles by first creating a node mesh, from which triangles are derived (HO-LE, 1988).

Figure 30 - Nodal point and element equilibrium in a FEA.



Source: Bathe (2006).

Previous researches shown as the problem of the quality of the elements is an essential issue in the process of the mesh generation, *i.e.* it has to be considered for a better approximation of the real body into a Finite Element mesh (HO-LE, 1988; KOLCUN, 1999). An exhaustive review regarding the element mesh quality is presented by Kolcun (1999). He affirms that the mesh generation is a part of pre-processing for any type of numerical analysis, and the quality of the mesh influences the solution. He also suggests how to design a suitable FEM mesh, the assessment of the discretization error of the solution is required (Equation 29) (KOLCUN, 1999):

$$e = \|u - u_h\|, \quad (29)$$

where  $u$  is the exact solution and  $u_h$  is a numerical one.

A procedure for the selection of the mesh size and mesh smoothening can be found in the research of Provatidis and Kanarachos (2000). Since the quality mesh is essential in the Finite Element Analysis, many types of research focus on such parameter (BARAZZETTI *et al.*, 2015a; CARVALHO *et al.*, 2014; CRESPI *et al.*, 2015; HO-LE, 1988). According to Barazzetti *et al.* (2015), the quality mesh was evaluated in the final mesh model, through the percentage of deformed elements. The aspect ratio ( $AR$ ) can be estimated as the ratio between height ( $h$ ) and side ( $s$ ) of the single elements. The research considers 2% as a reasonable threshold, in which most of the element have a 0.65 value, which was considered as a good compromise (BARAZZETTI *et al.*, 2015a). A similar approach can be found in FEM software like Abaqus/CAE software (SIMULIA, 2007), which allows the user to set the values of threshold aspect ratio and provide the percentage of the elements with good quality. Other software introduces some parameter to the mesh quality assessment. For example, in Robot<sup>®</sup> (AUTODESK, 2015b) two dimensionless parameters are provided to evaluate the global mesh quality coefficient. In the first parameter  $Q_1$ , the quality of each mesh element (triangles, quadrilaterals) is averaged (AUTODESK, 2015b). In the second parameter,  $Q_2$ , the weighted quality of each mesh element - weighted by the area of elements (triangles, quadrilaterals) - is averaged (AUTODESK, 2015b).

$$Q_1 = \frac{1}{n} \sum_{k=1}^n \alpha_i, \quad (30)$$

$$Q_2 = \frac{1}{\Omega} \sum_{k=1}^n \Omega_i \alpha_i, \quad (31)$$

$$\alpha(ABC) = 2\sqrt{3} \frac{\overline{CA} \times \overline{CB} \cdot \vec{n}}{\|CA\|^2 + \|AB\|^2 + \|BC\|^2}, \quad (32)$$

where  $\alpha_i$  is the mesh quality of each element calculated according to the Equation 32,  $\Omega_i$  the area of the  $i$ -th element and  $\Omega$  the total area of the mesh elements,  $\Omega_i$  the area of each  $i$ -element,  $n$  number of mesh element, and  $\vec{n}$  is the norm between the two vectors. Any quadrilateral  $ABCD$  is divided into four overlapped triangles ( $ABC$ ,  $ACD$ ,  $ABD$ , and  $BCD$ ). Calculation of  $\alpha_i$  coefficients is done for each triangle:  $\{\alpha_1, \alpha_2, \alpha_3, \alpha_4\} = \{\alpha(ABC), \alpha(ACD), \alpha(ABD), \alpha(BCD)\}$ . Once these coefficients are calculated, the quality coefficient is calculated (Autodesk, 2015b).

Once the geometry of the analysed body is discretized through the mesh, the issue of the material characterization needs further investigation. Such investigation procedures for the assessment of such characteristics was presented in Subsection 2.1.1. Once such information is acquired structural analysis is carried out, focusing on the diagnosis of heritage buildings. Such topics are presented in the following subsections.

#### 2.2.2.4 *Self-weight analysis*

In the heritage analysis field, linear elastic analysis is commonly used as an auxiliary tool assisting in the diagnosis of large structures (ROCA *et al.*, 2010). While its application to heritage buildings is widely used, it does not consider the non-linear response and other essential features of real structural behaviour. Due to the high level of uncertainties about the non-linear properties of the materials, linear elastic analysis is usually chosen as a qualitative approach to the structural behaviour assessment (ROCA *et al.*, 2010). Such an approach leads to suppose the following hypotheses: mechanical behaviour of materials is linearly elastic, displacements of the structure in the deformed configuration are small, and the structural constraints are bilateral and do not depend on the entity of the acting load (DEL PIERO, 1989; ROCA *et al.*, 2010).

The linear elastic analysis allows increasing the understanding of the structural behaviour of the considered building through the resolution of the linear equation system (DEL PIERO, 1989). As resumed in Churilov *et al.* (2016), many parameters influence the stiffness and mass properties involved in the stiffness  $K$  and mass  $M$  matrixes of a structure (Equation 33) (CHURILOV; MILKOVA; DUMOVA-JOVANOSKA, 2016). Some of them are Young's modulus of elasticity, unit weight, the geometry of the building, cross-section of the walls, element current state and continuity (with or without cracks), connections of walls to floors and roof, the type of foundations, the type and property of the foundation soil, *etc.* (CHURILOV; MILKOVA; DUMOVA-JOVANOSKA, 2016).

The knowledge of geotechnical characteristics of the soil is fundamental to carry out structural analysis in engineering researches or to understand the occurrence of physical phenomena, enabling the simulation of the material behaviour (DIRECTIVE OF THE PRIME MINISTER, 2007; SAKAMOTO; OLIVEIRA, 2015a). Frequently, research studies about the dynamic response of heritage buildings by FE perform a perfect fixed constraint at the foundation base (ACITO *et al.*, 2014; GENTILE; SAISI, 2007; LOURENÇO, 2002; MILANI;

VALENTE, 2015; ROCA *et al.*, 2010). Such approximation is correct if the foundation soil has the elastic feature of a compact rock. Otherwise, it can lead to an inaccurate estimation of the crack pattern (CASOLO; DIANA; UVA, 2017). For these reasons, researches aimed to the definition of detailed numerical modelling of the structure - *e.g.* in the crack pattern definition or non-linear analysis - should implement sophisticated models (CASOLO; DIANA; UVA, 2017). Such models should be endowed with a suitable geometric detail with a sufficiently refined constitutive model for both the material (KOUROUSSIS; VERLINDEN; CONTI, 2011; KUHLEMEYER; LYSMER, 1973) and the foundation soil (BURMAN; MAITY; SREEDEEP, 2010; CAMATA *et al.*, 2008). However, such a detailed approach is challenging to manage within a single, complete model, which is why the simplification of the foundation soil is commonly adopted in the literature (CASOLO; DIANA; UVA, 2017).

#### 2.2.2.5 Modal analysis

Regarding the modal analysis, frequency, modal shapes and damping ratio, which characterize each vibration mode, are usually selected as qualitative characteristics describing the overall structural dynamic behaviour of the structure (GENTILE; SAISI, 2007). However, the structural analysis of heritage buildings, even when all the collected information is accurately represented, continues to involve significant uncertainties, *i.e.* the geometries, material properties and their distribution, the boundary conditions. Indeed, such aspects are fundamental for historic buildings, which usually are characterized by different constructive phases (BARAZZETTI *et al.*, 2015a; CALÌ *et al.*, 2019). A suitable approach for the uncertainties understanding should be provided for the structural parameter assessment of heritage buildings (GENTILE; SAISI, 2007).

As already mentioned in subsections 2.2.2.1 and 2.2.2.2, non-linearities of the structural system influence the damping matrix  $[C]$  (Equation 25). In a Finite Element model, the damping matrix  $[C]$  cannot be obtained from element damping matrices, such as the mass and stiffness matrices of the element assemblage (BATHE, 2006). Moreover, relating to the mode superposition analysis for the numerical solution of the Finite Element model, equilibrium equations usually involve only the stiffness and mass matrices  $[K]$  and  $[M]$ , neglecting the damping matrix  $C$  (BATHE, 2006). For these reasons, in the process of structural identification, the comparison between the numerical model and the experimental data is carried out through the evaluation of the stiffness and mass matrix, in linear elastic fields (GENTILE;

SAISI; CABBOI, 2015; RAMOS *et al.*, 2010; SANCIBRIAN *et al.*, 2017; STANDOLI *et al.*, 2020). Neglecting damping or forcing terms, the dynamic problem of Equation 25 is defined as follow (ZIENKIEWICZ, O. C., TAYLOR, 2000):

$$M \ddot{u} + Ku = 0. \quad (33)$$

A general solution of such an equation can be expressed shown in Equation 36, which represents a general linear eigenvalue or characteristic value problem, and for a non-zero solution, the determinant of the above coefficient matrix must be zero:

$$|-\omega_i^2 M + K|=0, \quad (34)$$

where  $n$  value of  $\omega^2$  if matrices  $K$  and  $M$  are  $n \times n$ , symmetric positive definite. While the solution of Equation 37 cannot determine the actual values of  $u$ ,  $n$  vectors of virtual displacements  $\bar{u}_j$  can be found, giving the proportions for the various terms (ZIENKIEWICZ, O. C., TAYLOR, 2000). Such entities are the eigenvectors, which are also called normal modes of the structure, and they are usually normalized as follow:

$$\bar{u}_j^T M \bar{u}_j = 1, \text{ with } j = 1, 2, \dots, n. \quad (35)$$

At this stage, it is useful to note the property of modal orthogonality that:

$$\bar{u}_i^T M \bar{u}_j = 0, \text{ when } i \neq j, \quad (36)$$

$$\bar{u}_i^T M \bar{u}_j = 1, \text{ when } i = j. \quad (37)$$

The condition of the orthogonality for matrix  $M$  is extensively given in chapter 17.4 of Zienkiewicz and Taylor (2000). Such a condition leads to the orthogonality of the vectors with  $K$ :

$$\bar{u}_i^T K \bar{u}_i = \omega^2. \quad (38)$$

Such modal analysis allows for the obtention of the numerical model and further comparison with experimental results, aiming at the model updating. Experimental modal parameters are obtained from OMA, which results are elaborated through AVT. Operational modal analysis techniques are briefly presented in the following subsections.

### 2.2.3 Operational modal analysis

Operational modal analysis of historic structures and monuments is a rather recent topic, and the number of complete investigations reported in the literature is growing in the last years (FOTI *et al.*, 2012; GENTILE; SAISI; CABBOI, 2015; RAMOS *et al.*, 2010; RAMOS; AGUILAR; LOURENÇO, 2011; UBERTINI *et al.*, 2017). A large number of output-only modal identification techniques are available in the literature (BRINCKER; ZHANG, 2009; GADE *et al.*, 2005; JACOBSEN; ANDERSEN; BRINCKER, 2006; PEETERS; ROECK, 2001). Such output-only methods - developed in the frequency or time domain - are the Peak picking (PP), the Frequency Domain Decomposition (FDD) and the Stochastic Subspace Identification (SSI). They will be presented in the following subsections.

While the SSI method identifies a stochastic state-space model from output-only data in the time domain (PEETERS; ROECK, 2001), the PP and FDD are procedures that evaluate the spectral matrix in the frequency domain (BRINCKER; ZHANG; ANDERSEN, 2000; GENTILE; SAISI; CABBOI, 2015):

$$G(f) = E_v[A(f)A^H(f)], \quad (39)$$

where  $A(f)$  is the vector of the acceleration responses in the frequency domain,  $A^H$  is the complex conjugate transpose matrix, and  $E_v$  is the vector of the expected values. The diagonal values terms of the matrix  $G(f)$  are (real-valued) autospectral densities (ASD), while the other terms are (complex) cross-spectral densities (CSD) (GENTILE; SAISI, 2007):

$$G_{pp}(f) = E_v[A_p(f) A_p^*(f)], \quad (40)$$

$$G_{pq}(f) = E_v[A_p(f) A_q^*(f)], \quad (41)$$

$$G_{pq}(f) = E_v[A_p(f) A_q^*(f)], \quad (42)$$

where the symbol  $*$  means complex conjugate. Further explanation of ASD and CSD can be found in Gentile and Saisi (2007).

The PP method is probably the most widely used method for ambient vibration measurement evaluation in civil engineering because of its simplicity (BENDAT; PIERSOL, 1993; JAISHI *et al.*, 2003; PEETERS; ROECK, 2001). The FDD is a rather simple procedure that represents an extension of the PP, where modes can be estimated from the spectral densities calculated, in the condition of a white noise input, and a lightly damped structure (GADE *et al.*, 2005). Differently from the SSI, the techniques of PP and FDD are non-parametric, where the modal parameters are directly estimated from signal processing calculations (GADE *et al.*, 2005). The methods mentioned above are briefly presented in the next subsections.

### 2.2.3.1 Peak Picking

The Peak Picking (PP) is an output-only method where the natural frequencies are obtained from the observation of the peaks on the graph of the average normalized power spectral densities for all measure channels simplicity (JAISHI *et al.*, 2003). The primary conditions of such a method are low damping and well-separated eigenfrequencies. Hence the spectrum around an eigenfrequency  $w_i$  can be approximated by:

$$S_y(jw_i) \approx \alpha_i \{v_i\} \{v_i^H\}, \quad (43)$$

where  $\alpha_i$  is a scalar factor depending on the damping ratio, the eigenfrequency, the modal participation factor, and the input covariance matrix, while  $\{v_i\}$  is the  $i$ -th mode shape (PEETERS; ROECK, 2001). According to Equation 42, each row or column of the spectral matrix at an eigenfrequency can be considered as an estimation of the mode shape at that frequency (PEETERS; ROECK, 2001). Furthermore, the square-root of the diagonal terms of the spectral matrix at a resonant frequency can be considered as an estimation of the mode shape at that frequency (GENTILE; SAISI, 2007). Drawbacks of the PP method are due to the difficulties in identifying closely spaced modes and damping ratio (GENTILE; SAISI, 2007).



### 2.2.3.2 Frequency Domain Decomposition

The Frequency-Domain Decomposition (FDD) is a non-parametric technique, where very accurate results are provided for natural frequencies and mode shapes (GADE *et al.*, 2005). The disadvantages are that no damping is obtained or estimated, and the frequency resolution depends on the measurement concerning the Noise Bandwidth of the band-pass filters FFT line spacing (GADE *et al.*, 2005). FDD technique allows the estimation of the spectral matrix, and the Singular Value Decomposition (SVD) at each frequency. An extensive explanation of this method can be found in Brincker and Zhang (2009). The SVD of the spectral matrix at each frequency is given by the following Equation 44:

$$G(f) = U(f)\Sigma(f)U^H(f), \quad (44)$$

where  $\Sigma$  is the diagonal matrix, which contains the real positive singular values, in decreasing order, while  $U$  is the complex matrix containing the singular vectors as a column. The SVD is used for estimating the rank of  $G$  at each frequency. The number of non-zero singular values are equal to the rank; if only one mode is essential at a given frequency  $f_r$  (as it has to be expected for well-separated modes) the spectral matrix approximates a rank-one matrix as (GENTILE; SAISI, 2007):

$$G(f) \cong \sigma_1(f)u_1(f)u_1^H(f). \quad (45)$$

Analysing the SVD curves allows understanding the identification of the resonant frequencies and the estimation of the corresponding mode shape using the information contained in the singular SVD vectors. The comparison between equations 44 and 45 shows that the first singular vector  $u_1(f)$  is an estimation of the mode shape. Since the first singular value  $\sigma_1(f)$  at each frequency represents the strength of the dominating vibration mode at that frequency, the first singular function can be suitably used as a modal indication function (yielding the resonant frequencies as local maxima) (GENTILE; SAISI, 2007).

An extension of FDD was proposed to determine also damping factors, the Enhanced Frequency Domain Decomposition (EFDD) (BRINCKER; ZHANG; ANDERSEN, 2000; COMPAN; PACHÓN; CÁMARA, 2017; FOTI *et al.*, 2012; GADE *et al.*, 2005; JACOBSEN; ANDERSEN; BRINCKER, 2006). It uses a simple linear regression curve fitting techniques,

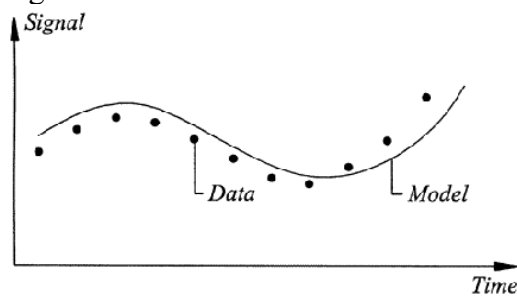
where the averaged frequency and damping values are estimated as well as their standard deviations from all data sets (GADE *et al.*, 2005).

In the research of Gade *et al.* (2005), the authors analyse the disadvantage of EFDD, explaining how the algorithm does not work correctly if no distinguished peak is found in some of the data sets. It is also required to select some modal estimation parameters, like Modal Assurance Criterion (MAC) (see Subsection 2.2.3.4), Rejection Level, maximum and minimum correlation (*i.e.* correlation interval) for each resonance frequency in each dataset. Such a choice may be a very time-consuming procedure when many data sets and/or many modal frequencies are acquired (GADE *et al.*, 2005). However, in the same research, the author considers that both techniques have highly accurate results even for weakly excited modes, closely spaced modes, and a large number of channels and a large amount of data (GADE *et al.*, 2005).

### 2.2.3.3 Stochastic Subsystem Identification

The Stochastic Subspace Identification (SSI) method is based on the discrete-time state-space form of the dynamics of a linear-time-invariant system under unknown excitation (GENTILE; SAISI, 2013; GENTILE; SAISI; CABBOI, 2015; VAN OVERSCHEE; DE MOOR, 1996). In the SSI techniques, a parametric model is fitted directly to the raw times series data (BRINCKER; ZHANG; ANDERSEN, 2000). Such a parametric model is a mathematical model with some parameters that can be adjusted to change the way the model fits the data (Figure 31) (ANDERSEN, 2010). In general, a set of parameters is selected to minimize the deviation between the predicted system response of the model and measured system response (ANDERSEN, 2010). This process is often called model calibration (Figure 31).

Figure 31 - Process of model calibration.



Source: Andersen (2010).

Two general assumptions - made in the output-only modal analysis - are that the underlying physical system behaves linearly and time-invariant (GENTILE; SAISI, 2013;

GENTILE; SAISI; CABBOI, 2015; VAN OVERSCHEE; DE MOOR, 1996). The linearity implies that if an input with an amplitude generates an output with a certain amplitude, then input with twice the amplitude will generate an output with twice the amplitude as well. The time-invariance implies that the underlying physical system does not change in time. The stochastic state-space system is a typical parametric model structure to use in output-only modal analysis of linear and time-invariant physical systems (GENTILE; SAISI; CABBOI, 2015; PEETERS; ROECK, 2001):

$$x_{k+1} = Bx_k + w_k, \quad (46)$$

$$y_k = Cx_k + v_k, \quad (47)$$

where  $x_k$  is the discrete-time state vector,  $w_k$  is the process noise,  $y_k$  is the output vector,  $v_k$  is the measurement noise,  $B$  is the discrete state matrix, and  $C$  is the discrete output matrix. The vector  $x_k$  contains displacements and velocities. It also describes the state of the system at time instant  $t_k = k\Delta t$ .

The matrix  $B$  depends on the mass, stiffness and damping properties of the structure (GENTILE; SAISI, 2013; GENTILE; SAISI; CABBOI, 2015; VAN OVERSCHEE; DE MOOR, 1996). Equation 45 of such model structure is called the state equation. It models the dynamic behaviour of the physical system. In contrast, the Equation 46 is called the observation or output equation, since it controls which part of the dynamic system that can be observed in the output of the model (ANDERSEN, 2010; GENTILE; SAISI; CABBOI, 2015). Different types of SSI-methods are found in literature, and an extensive review can be found in (PEETERS; ROECK, 2001). Each method depends on a range of parameters, where the primary choice is the method itself, *e.g.* Principal Component (PC), Unweighted Principal Component (UPC), Canonical Variate Analysis, (CVA). As affirmed in the research of Gade *et al.* (2005), no proper guidelines seem to exist in the literature for SSI-methods (GADE *et al.*, 2005).

#### 2.2.3.4 Modal assurance criterion

The Modal Assurance Criterion (MAC) is a statistical indicator. It was originated from the need for a quality assurance indicator for experimental modal vectors that are estimated

from measured frequency response functions (ALLEMANG, 2003). The MAC is commonly used to check the orthogonality of the vibration modes.

$$\{\psi_r\}^T [M] \{\psi_s\} = 0, \text{ for } r \neq s, \quad (48)$$

$$\{\psi_r\}^T [M] \{\psi_s\} = M_r, \text{ for } r = s, \quad (49)$$

where  $\{\psi_s\}$  is the modal vector for  $s$ -th mode,  $\{\psi_r\}^T$  is the transpose of modal vector for mode  $r$ ,  $[M]$  is the mass Matrix,  $M_r$  is the mass Matrix relative to the mode  $r$ . Experimentally, the result of zero for the cross-orthogonality calculations ( $r \neq s$ , Equation 52) can rarely be achieved. However, values up to one-tenth of the magnitude of the generalized mass of each mode are considered to be acceptable (ALLEMANG, 2003) (Figure 32).

The modal assurance criterion is defined as a scalar constant relating the degree of consistency (linearity) between one modal and another modal reference vector as follows:

$$MAC_{cdr} = \frac{|\{\psi_{cr}\}^T \{\psi_{dr}^*\}|^2}{\{\psi_{cr}\}^T \{\psi_{cr}^*\} \{\psi_{dr}\}^T \{\psi_{dr}^*\}} = 0, \quad (50)$$

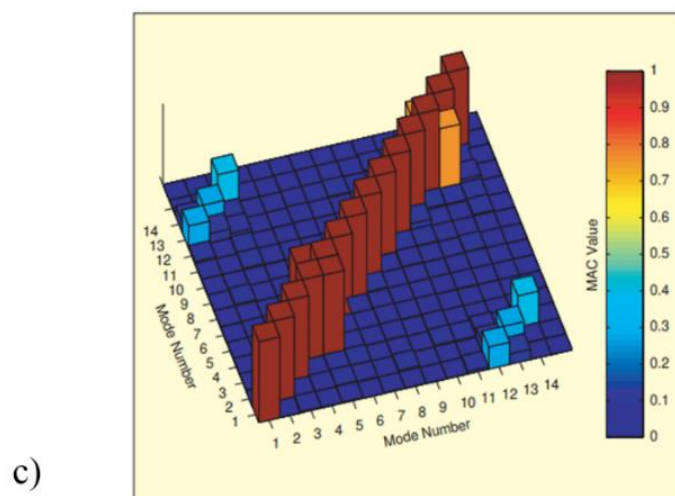
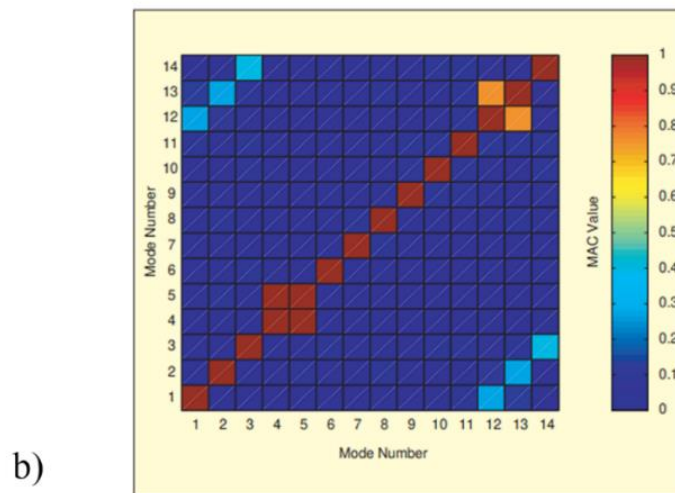
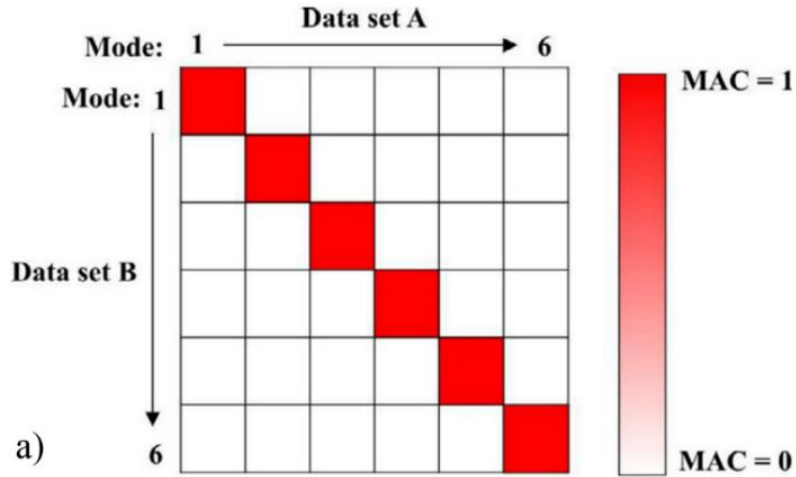
where  $\{\psi_{cr}^*\}^T$  is the transpose of the modal vector for reference  $c$  and mode  $r$   $\{\psi_{cr}\}$  and  $\{\psi_{dr}^*\}$  is the complex conjugate of modal vector for reference  $d$  and mode  $r$ ,  $\{\psi_{dr}\}$ .

Furthermore, Allemang (2003) suggests some of the potential uses of Modal Assurance Criterion reported in the literature:

- a) validation of experimental modal models;
- b) correlation with analytical modal models (mode pairing);
- c) correlation with operating response vectors;
- d) mapping matrix between analytical and experimental modal models;
- e) modal vector error analysis; modal vector averaging; experimental modal vector completion and/or expansion;
- f) weighting for model updating algorithms;
- g) modal vector consistency/stability in modal parameter estimation algorithms;
- h) repeated and pseudo-repeated root detection;
- i) structural fault/damage detection;
- j) quality control evaluations;

k) optimal sensor placement.

Figure 32 - Graphic plot representation (a), examples of 2D (b) and 3D (c) MAC.



Source: Pasto, Blinda and Harčarik (2012) (a) and Allemang (2003) (b and c).

Another extension of the modal assurance criterion is used by the addition of frequency scaling to the MAC. Such an extension offers a means of displaying the mode shape correlation, the degree of spatial aliasing and the frequency comparison in a single plot simultaneously. This extension is known as Frequency Modal Assurance Criterion (FMAC). An extensive explanation of Modal Assurance Criterion meanings and uses is contained in the research of Allemang (2003).

Nowadays, most computer systems routinely utilize colour to present magnitude data like MAC using 2D and 3D plot (Figure 32) (PASTOR; BINDA; HARČARIK, 2012). It is important to remember that MAC is a discrete calculation and what appears as a colour contour plot represents the discrete mode to mode comparison (PASTOR; BINDA; HARČARIK, 2012). Nevertheless, a colour plot does allow for more data to be presented in an understandable form in minimum space (PASTOR; BINDA; HARČARIK, 2012).

#### **2.2.4 Sensitivity analysis for the structural parameter assessment**

Sensitivity analysis is a widespread method used to investigate the influence of parameters within the structural response assessment (ASGARI; OSMAN; ADNAN, 2013; CATTARI *et al.*, 2015; GENTILE; SAISI; CABBOI, 2015; MENDES; LOURENÇO, 2014; SALTELLI, A.; TARANTOLA, S.; CAMPOLONGO F.; RATTO, 2004; ZORDAN; BRISEGHHELLA; LIU, 2014). Two main approaches will be presented in this subsection.

In the first approach, some knowledge elements are introduced as necessary for the sensitivity analysis. They concern the geometry of the structural organism, the construction details and the mechanical properties of materials (CNR, 2014). According to the Italian National Research Council (CNR) (2014), those elements are usually obtained from:

- a) the historical-critical analysis aimed at reconstructing the constructive process and the subsequent modifications and events suffered over time by the building;
- b) documental projects relating to implementation and subsequent modifications;
- c) geometric-structural survey referring the construction, *i.e.* the constructive elements, relationships with any structures in adherence, quality, and state of preservation of materials and building parts;
- d) experimental investigations aimed at completing the information framework related to the mechanical properties of materials.

According to the first approach, the knowledge factors (see Subsection 2.1.4) are distinguished between:

- a) factors that can be considered known in deterministic terms, *i.e.* with a low value of uncertainty, in absolute terms or terms of the relative sensitivity of the response; for these factors, a single value is used for all analyses;
- b) factors affected by the uncertainty of aleatory type, generally associated with the intrinsic variability of characteristics of the structure;
- c) factors affected by epistemic uncertainty, associated with a lack of knowledge of the structure or the mechanical behaviour of its components.

Regarding the epistemic uncertainties, instead, they cannot be modelled as continuous variables. For this reason, according to the Italian National Council of Research, a parameter that allows describing both aleatory and epistemic uncertainties was proposed, and the sensitivity of the selected characteristic on the structural response was analysed (CNR, 2014). This parameter was introduced to carry-out the sensitivity analysis of the structural response - in terms of peak ground acceleration values that lead to the considered limit state - according to the aleatory (54) and epistemic (55) parameters variation (CNR, 2014).

$$\Delta'_k = \frac{a_{k,max} - a_{k,min}}{\bar{a}}, \quad (51)$$

$$\Delta'_j = 2 \frac{|a_1 - a_2|}{a_1 + a_2}, \quad (52)$$

where  $a_{k,max}$  and  $a_{k,min}$  are the ground peak accelerations leading to the referred limit state adopting maximum and minimum values of the aleatory parameters,  $\bar{a}$  is the central value of the ground peak accelerations leading to the referred limit state,  $a_1$  and  $a_2$  are the ground peak accelerations leading to the referred limit state adopting the two alternative epistemic options 1 and 2. In the case of the alternative options,  $m_j$ , are more than two, Equation 55 is generalized as follow (CNR, 2014):

$$\Delta'_j = 2 \frac{\max(a_p) - \min(a_p)}{\max(a_p) + \min(a_p)}, p = 1, m_j, \quad (53)$$

where  $a_p$  is the ground peak accelerations leading to the referred limit state adopting the  $p$ -th alternative option.

The second approach aims at assessing which parameters affect the variation of each vibration mode, and it is useful for the understating of the overall structural behaviour (GENTILE; SAISI, 2007; GENTILE; SAISI; CABBOI, 2015). A sensitivity coefficient  $s_{i,k}$  is selected as an investigation parameter. It is evaluated by a perturbation technique in the normalized form, representing the percentage variation in mode frequency per 100% change in the updating parameter.

$$s_{i,k} = 100 \frac{X_k}{f_i^{FEM}} \frac{\partial f_i^{FEM}}{\partial X_k}; \quad i=1, 2, \dots, M, \quad (54)$$

where  $X_k$  ( $k=1, 2, \dots, N$ ) is the  $k$ -th parameter to be identified,  $f_i^{FEM}$  is the frequency considered as base value compared to the variation  $\partial f_i^{FEM}$  for each variation  $\partial X_k$ . A detailed definition of  $s_{i,k}$  can be found in Gentile and Saisi (2007) and Gentile *et al.* (2015) (GENTILE; SAISI, 2007; GENTILE; SAISI; CABBOI, 2015).

Some differences between the two approaches are that the first allows calculating the sensitivity for epistemic parameters, which do not depend on continuous values but alternatives hypotheses - at least two (Equation 56,  $p = 1, m_j$ ). While the second allows understanding the sensitivity according to the range variation of the parameters to be identified,  $X_k$ , which are continuous values (Equation 57). Such sensitivity analysis is commonly used in the model updating procedure to the understanding of which parameter must be tuned. Such a procedure will be presented in the following subsection.

### 2.2.5 Model Updating for the structural identification

In the procedure of the structural identification, once the results of OMA and numerical modal analysis are obtained, they are compared to understand if the parameters of the Finite Element Model fit with the experimental results. In the case of discrepancy of the results, a process of model updating is carried out to obtain the optimal parameter to be implemented in the Finite Element Model. Such optimal values - updating structural parameters - can be determined to minimize the difference between numerical and experimental natural frequencies. Two different system identification algorithms for the model updating were mainly found in literature: the Inverse Eigen-Sensitivity (IE) method (COLLINS *et al.*, 1974; FOTI *et*



*al.*, 2012; FRISWELL; MOTTERSHEAD, 2013; LIN; LIM; DU, 1995) and the Douglas and Reid (DR) method (1982) (DOUGLAS; REID, 1982; FOTI *et al.*, 2012; GENTILE; SAISI; CABBOI, 2015; ZORDAN; BRISEGHIELLA; LIU, 2014).

#### 2.2.5.1 *The Inverse Eigen-Sensitivity method*

The Inverse Eigen-Sensitivity method is defined as an inverse problem where the change of eigenvalues and eigenvectors are given (LIN; LIM; DU, 1995), obtained from experimental frequencies and modal shapes. Instead, the physical and mechanical parameter needs to be defined. In the IE technique, the relation between the experimental responses and the structural parameters  $X$  of the model is expressed in terms of a Taylor series expansion, limited to the linear terms (GENTILE; SAISI, 2007):

$$R_e = R(X_0) + S(X - X_0), \quad (55)$$

where  $R_e$  is the vector associated with the reference response test data,  $R(X_0)$  is a vector containing the responses from the model corresponding to the starting choice  $X_0$  of the updating parameters, and  $S$  is the sensitivity matrix with terms  $\partial R_i / \partial X_k$  (GENTILE; SAISI, 2007). In the research Gentile and Saisi (2007), the authors explain that Equation 58 is used to derive the following iteration scheme to evaluate  $X$ :

$$X_{n+1} = X_n + H[R_e - R(X)], \quad (56)$$

where the matrix  $H$  is generally computed either using the Moore-Penrose pseudo-inverse ( $H = S^T(SS^T)^{-1}$ ) or following the Bayesian estimation theory (COLLINS *et al.*, 1974; FRISWELL; MOTTERSHEAD, 2013).

#### 2.2.5.2 *Douglas and Reid method*

According to Douglas and Reid method (DOUGLAS; REID, 1982; GENTILE; SAISI; CABBOI, 2015; ZORDAN; BRISEGHIELLA; LIU, 2014), the dependence of the natural frequencies of the model on the unknown structural parameters  $X_k$  ( $k = 1, 2, \dots, N$ ) is approximated around the current values of  $X_k$ , by the following:

$$f_i^*(X_1, X_2, \dots, X_N) = \sum_{k=1}^N [A_{i,k} X_k + B_{i,k} X_k^2] + C_i, \quad (57)$$

where  $f_i^*$  represents the approximation of the  $i$ -th frequency of the FE model. Once the set of approximating functions (Equation 60) is established, the structural parameters of the model are evaluated by a least-square minimization of the difference between each  $f_i^*$  and its experimental counterpart  $f_i^{EXP}$ :

$$J = \sum_{i=1}^M w_i \varepsilon_i^2, \quad (58)$$

$$\varepsilon_i = f_i^{EXP} - f_i^*(X_1, X_2, \dots, X_N), \quad (59)$$

where  $w_i$  is a weight constant and  $M$  is the number of considered modes. However, in Equation 60, a reasonable approximation in a range is presented, around the “base” value of the structural parameters  $X_k^B$ , limited by lower  $X_k^L$  and upper values  $X_k^U$  ( $k = 1, 2, \dots, N$ ). Thus, the coefficients  $A_{ik}$ ,  $B_{ik}$ , and  $C_i$  are dependent on both the base value of the structural parameters and the range in which these parameters can vary. The coefficients,  $A_{ik}$ ,  $B_{ik}$ , and  $C_i$  are evaluated from  $(2N+1)$  Finite Element analyses (DOUGLAS; REID, 1982): the first choice of the parameters corresponds to the base values; then each parameter is varied, one at the time, from the base value to the upper and lower limit, respectively. Furthermore, the quadratic approximation in Equation 60 is as better as the base values are closer to the solution. Hence the accuracy and stability of the optimal estimations should be carefully checked either by the complete correlation with the experimental data or by repeating the procedure with new base values until the required threshold is reached (GENTILE; SAISI; CABBOI, 2015; ZORDAN; BRISEGHHELLA; LIU, 2014).

In the research of Gentile and Saisi (2007), a comparison between Inverse Eigensensitivity (IE) and Douglas and Reid (DR). Results show that the natural frequencies of the DR optimal model are practically equal to the experimental ones, as it has to be expected since the identification procedure was based on the minimization of the frequency discrepancies (GENTILE; SAISI, 2007). Hence, the FE model updating represents an inverse process is investigated to identify or correct the uncertain parameters of FE models, posed as an optimization problem (REN; CHEN, 2010).

### 2.2.6 Partial conclusions

Analysed researches concerning the vibration-based structural identification mainly focus on bridges, cable-stayed bridges and high-rise buildings. However, in the last decades, masonry heritage buildings were also investigated, which are common type in the field of historic construction both in Brazil and in Europe. Moreover, analysed researches allow concluding the following considerations:

- a) increasing the level of knowledge of the structural identification of different types of building can be useful to identify suitable methodologies that accompany the professional during the analysis of a characteristic structure;
- b) methodologies should aim to the understanding of the constructive evolution of a historical building, concerning the evaluation of the physical, mechanical and geometric characteristics of the construction;
- c) the procedure of structural identification from operational modal analysis is essential where a lack of knowledge regards the structural parameters of the heritage construction; consequently, such parameters are obtained from the elaboration of the output-only procedures;
- d) OMA and AVT allow increasing the understanding of the structural behaviour of cultural heritage buildings; hence, numerical models can be tuned to better fit the experimental results; such a path to the knowledge is crucial for the decision-making phase for restoration and rehabilitation proposals of historic buildings.

## 2.3 BUILDING INFORMATION MODELLING FOR CULTURAL HERITAGE

As previously mentioned in Subsection 2.1.2.2.2, BIM method is a widespread practice in the Architecture, Engineering and Construction (AEC) industry management for new buildings (EASTMAN, CHUCK; TEICHOLZ, PAUL; SACKS, RAFAEL; LISTON, 2011). However, finding BIM implementations in the structural assessment of buildings with historical value is less common (VOLK; STENGEL; SCHULTMANN, 2014). Such an issue is mainly due to the initial effort required to digitize acquired data management obtained from a different type of investigations. Indeed, such a data is often incomplete, fragmented and not up-to-date for comprehensive and complete modelling (VOLK; STENGEL; SCHULTMANN, 2014).

Furthermore, in BIM software, some errors are created in the automatic generation of the analytical model from the architectural one. For these reasons, data management and interoperability are the most severe informational challenges (KHADDAJ; SROUR, 2016).

In the field of Building Information Modelling concerning cultural heritage, different terms were founded in the analysed researches, *e.g.* “Historic Building Information Modelling”, ‘Historic-BIM”, “Heritage BIM”, “HBIM”, “BIM for heritage”, and “BIM for historic buildings”, “CHIM” (Cultural Heritage Information Management)(BRUNO; DE FINO; FATIGUSO, 2018). They have been used almost interchangeably (ANTONOPOULOU; BRYAN, 2017). However, to simplify the understanding of the topic, the term Historic Building Information Modelling (H-BIM) will be used in this document. Main topics related to H-BIM will be approached in the following subsection.

### **2.3.1 Knowledge management in BIM**

Nowadays, BIM has evolved significantly in the field of cultural heritage (LÓPEZ *et al.*, 2018), where the knowledge management is fundamental and concerns different levels of the investigation in the conservation process (SIMEONE *et al.*, 2014). The as-built conservation state of analysed buildings can be represented in a virtual environment, including facility management (FM) related to operational maintenance. FM is defined as the organizational function which integrates people, place and process within the built environment to improve the quality of life of people and the productivity of the core business. (ISO 41011:2017, 2017).

Moreover, the heritage sector does not only involve only construction, but also planning, historic asset management, preventative maintenance, documentation, investigation, and research. BIM offers new tools for such sectors in support of all these activities through digital collaboration and efficient information management. Moreover, the 3D (geometry) and 4D (time- based) modelling capabilities of BIM technology can be useful for heritage interpretation, presentation and simulation applications (ANTONOPOULOU; BRYAN, 2017).

In Simeone *et al.* (2014), the main issues of built heritage representation are presented:

- a) difficulty in checking the information stored and finding errors and inconsistencies within the documentation sets;
- b) lack of integration, coherence and coordination among different documentation sets generated by the multidisciplinary heritage process;
- c) poor information management with consequent lack or duplication of data;

- d) difficulty to share knowledge and collaboration between the different users during the investigation and the restoration phases.

The BIM process allows incorporating both qualitative and quantitative information about a built heritage. Physical and functional characteristics, documental data, geometric surveys, can be integrated into the 3D model in a structured and consistent way, which allows for easy information extraction (ANTONOPOULOU; BRYAN, 2017). Such a process is crucial in the decision-making and management of the heritage lifecycle. Simulation of the consequences of a design decision is possible, obtaining the most appropriate and meaningful images to represent the structure. Moreover, communication with other professionals involved in the work is allowed (Figure 33) (BIAGINI *et al.*, 2016).

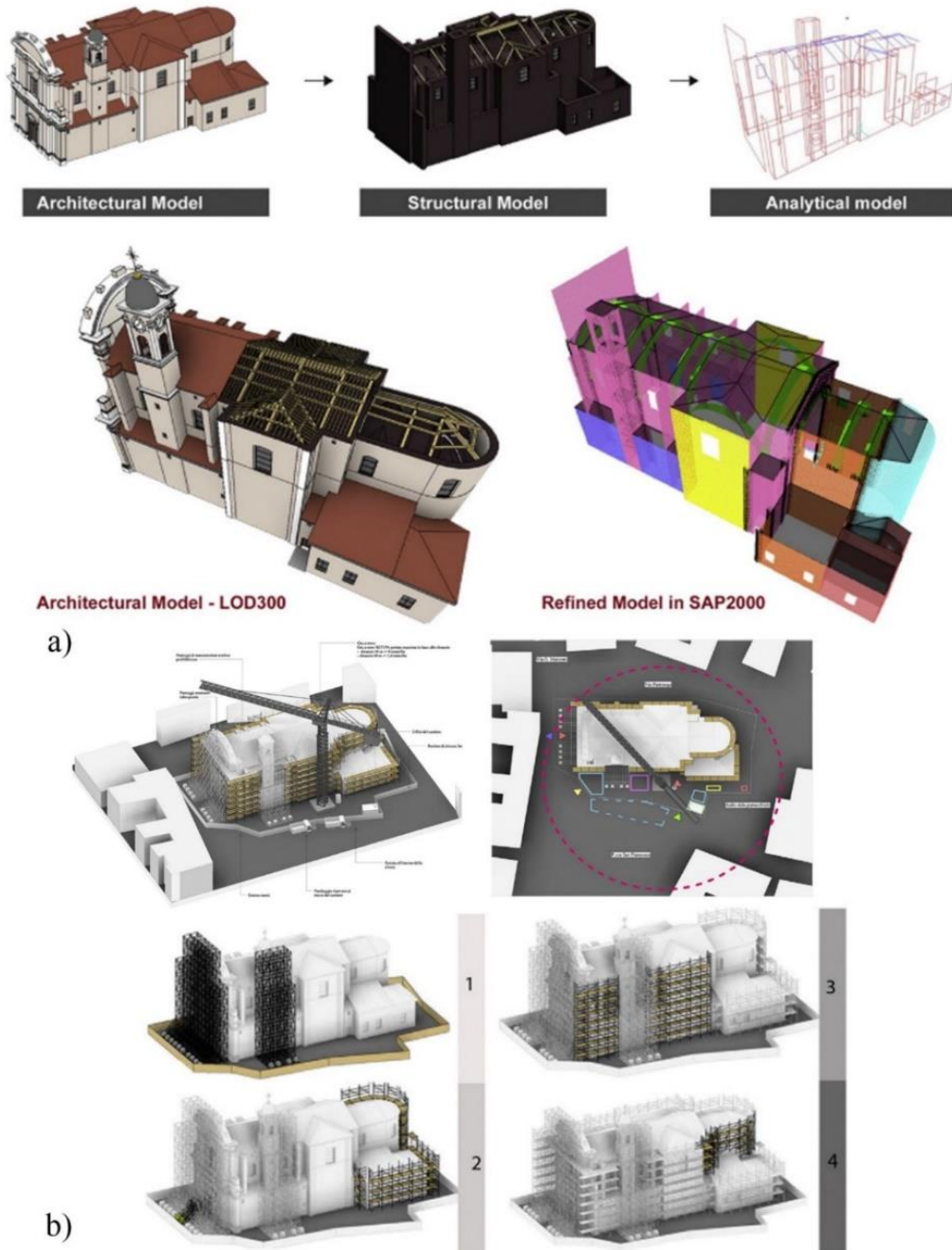
As an example, an innovative H-BIM approach to the construction management of historical building interventions is proposed in Biagini *et al.* (2016) (Figure 33):

- a) parametric modelling of historical buildings, starting with laser scanner survey, LoD (level of development) definition and measurement accuracy, with relation to modelling procedures;
- b) parametric modelling of the site and the several phases of restoration work in a fixed schedule (4D dimension);
- c) 3D graphic representation of safety procedures and related tools.

In Biagini *et al.* (2016), a general model to describe the intervention is defined, including the design, management, and organization of the building site activity, allowing for the simulation of the intervention and executive control during the work. Besides, the management of the digital model differs in each case study, concerning the use of construction, the age, the ownership, *etc.* (BIAGINI *et al.*, 2016; VOLK; STENGEL; SCHULTMANN, 2014). Furthermore, each case study involves a different level of development (LOD) to be achieved.

Provide a level of information suitable for data exchange and sharing among the several specialist software analysis and BIM tools in necessary to limit information loss (BIAGINI *et al.*, 2016). Those aspects are significant for the phase management of time and cost (the so-called fourth and fifth dimension of BIM). Another crucial issue for better management is the interoperability between different software to avoid the data lost (BIAGINI *et al.*, 2016). Such concepts of dimensions of BIM, level of development, and interoperability will be presented in the following subsection.

Figure 33 - Simulation workflow applied to the SS. Nome di Maria church at Poggio Rusco, in Mantua (Italy) from the Revit® model to analytic model for structural analysis (SAP2000) (a) and 3D building site layout (b).



Source: Biagini *et al.* (2016).

### 2.3.1.1 The dimensions of Building Information Modelling

The BIM methodology has several levels of information, known as dimensions. Each model can have different dimensions 4D, 5D, 6D, 7D, up to n-D, depending on the context and the aim of use (VOLK; STENGEL; SCHULTMANN, 2014). BIM technologies allow for the

documentation, generation, importation, or manipulation of three-dimensional models using such parametric information as (LÓPEZ *et al.*, 2018; MASOTTI, 2014; PAUWELS *et al.*, 2008):

- a) 2D Graph - dimension of the planar drawings, where the building plans are graphically represented;
- b) 3D Model - spatial dimension, where it is possible to view objects dynamically. The 3D model can be used in the visualization in perspective, *e.g.* textures and lighting simulations. Each 3D component has attributes and parameterization that characterize them as part of the virtual construction;
- c) 4D Planning - time dimension, defining when each element will be created, stored, prepared, installed, used. It also organizes the layout of the construction site, the maintenance and movement of the teams, the equipment used and other aspects that are chronologically related;
- d) 5D Budget - cost dimension, determining the cost of each part of the work, the allocation of resources and its impact on the budget, the control of work goals according to costs.

Furthermore, two additional dimensions were defined by Calvert (2013):

- a) 6D Sustainability - energy dimension to the model, quantifying and qualifying the energy used in construction, the energy to be consumed in its life cycle and its cost, in parallel to the 5th dimension;
- b) 7D Facility Management - operational dimension, where the user can extract information about the overall operation of the construction lifecycle, *i.e.* maintenance procedures.

The safety dimension (8D) was introduced by Kamardeen (2010), which consists of three main tasks:

- a) hazard profiling of BIM model elements;
- b) providing design suggestions for revising high hazard profiled elements;
- c) proposing on-site risk controls for hazards that are uncontrollable through design revisions.

Hence, the dimension of Building Information Modelling leads to an increase in the level of knowledge. Such a concept is included in the so-called level of development of BIM, presented in the following subsection.

### 2.3.1.2 Level of development of Building Information Modelling

The components of historical construction generally consist of elements which geometries can be affected due to weather or structural deformation. Such aspects are difficult to be accurately represented using parametric BIM objects. Besides, buildings belonging to specific architectural styles can be characterized by organic or complex shapes, which can be difficult or take longer to be modelled using simple solid geometry (Figure 34) (MURPHY; MCGOVERN; PAVIA, 2009). These latter observations have direct implications for Historic-BIM. The modelling process, despite advances in Scan-to-BIM tools and workflows (such as automatic geometry extraction), is still challenging and time-consuming (ANTONOPOULOU; BRYAN, 2017).

The amount of time concerning the effort increases according to the degree of geometric detail in the model (CBIC, 2016). The detailed and accurate representation of the 3D complex geometries generally results in large files, which are more difficult to work (DORE *et al.*, 2015). The restrictions of the BIM software also make it difficult or impossible to use native parametric objects for irregular geometries without limiting the model's functionality (ANTONOPOULOU; BRYAN, 2017).

However, in recent years, different techniques of three-dimensional digital reconstruction have been developed that help to reduce discrepancies between the reality of the building and its digital representation (AIA, 2013). These techniques provide geometric shapes of the current state of construction, from point clouds, obtained employing photogrammetry or laser scanning methods (DORE *et al.*, 2015)

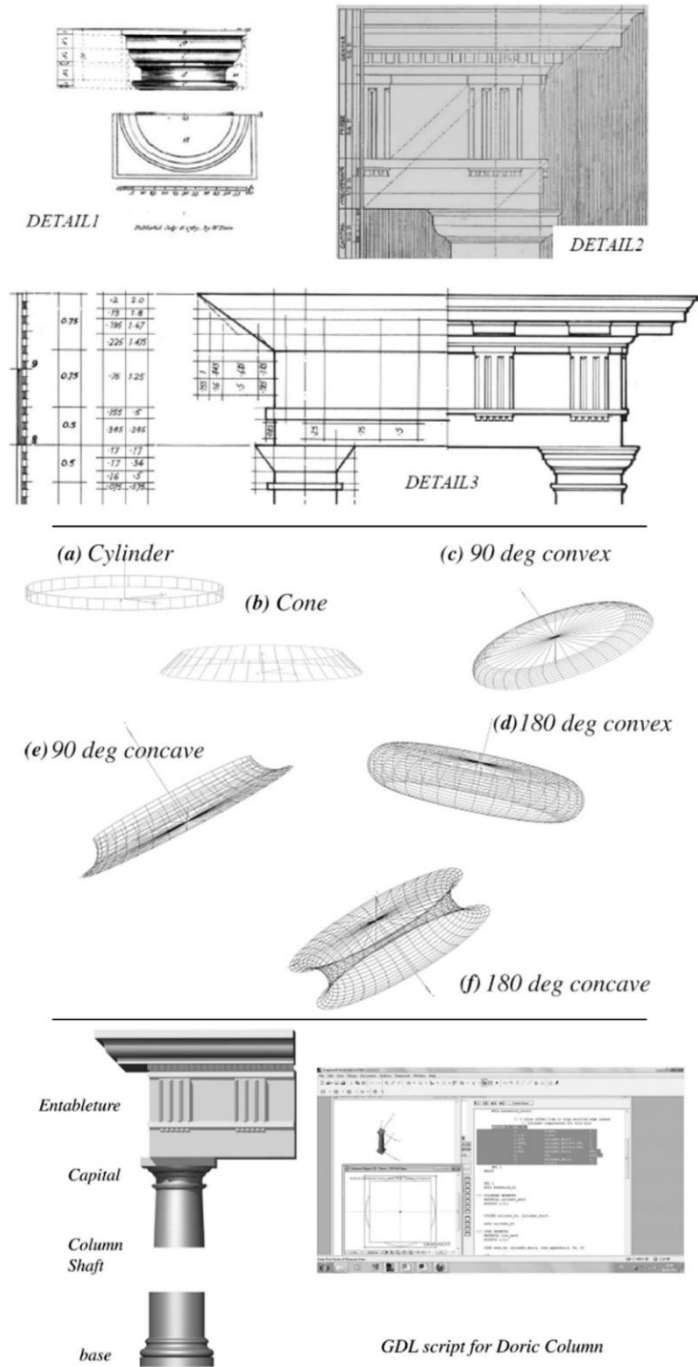
As affirmed by Antonopoulou and Bryan (2017), in the cultural heritage field, two useful tools allow professionals and clients to use H-BIM and accompany them in decision making: Modelling Tolerance and level of development. The modelling tolerance refers to the precision with which the BIM model of the as-built structure is created. Modelling tolerance has to be defined at the beginning of the project and must respect some Scan-to-BIM modelling specifications (ANTONOPOULOU; BRYAN, 2017).

Furthermore, the LOD structure, Level of Development, was developed by the American Institute of Architects ((AIA), 2013) (Chart 11). The level of development (LOD) defines the minimum requirements at the dimensional, spatial, quantitative, qualitative level, among others, that the modelled element must include authorizing the uses related to that same level (COSTA OLIVEIRA, 2016). Each component modelled in BIM, whether architectural or



structural, becomes an object that includes a series of information, eventually useful in the process of knowledge (figures 34 and 35), *e.g.* constructive understanding of the structure, pathologies, degradations and interventions to be made, *etc.* (CHIABRANDO; LO TURCO; SANTAGATI, 2017).

Figure 34 - Pattern book details of architectural components, parametric definition and three-dimensional representation.



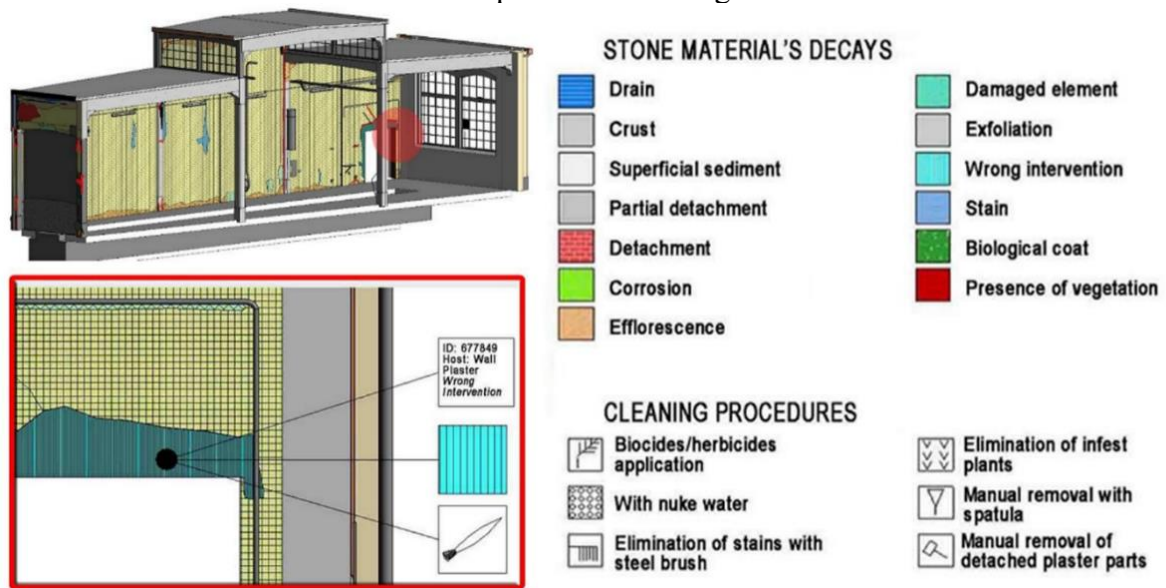
3D Model

Source: Murphy, McGovern, and Pavia (2013).

Although LODs are sometimes interpreted as Levels of Detail, these concepts differ significantly. The level of detail is defined as the precision associated with the modelled element (AIA, 2013), focusing only on geometric issues. On the contrary, the Level of Development (LOD) represents the quantification of the degree of confidence associated, not only with the geometric characteristics and the level of detail of the modelled object but also with the level of information of the object (Figure 36) (COSTA OLIVEIRA, 2016).

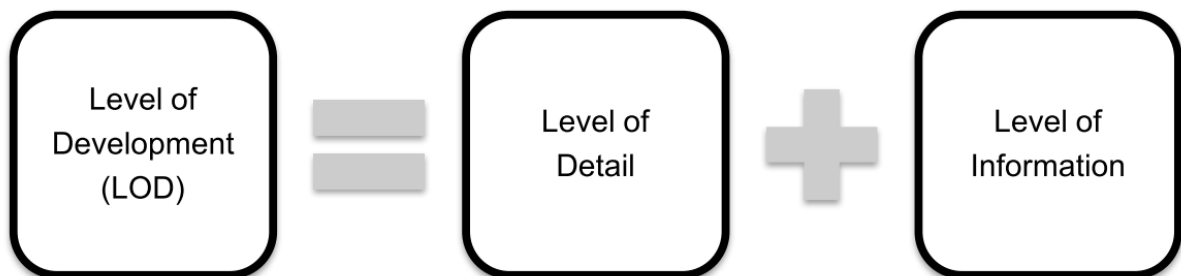
Furthermore, information about materials, quantities (such as the decay extension, expressed in square meters) and photos are added to the BIM model. Therefore, multiple analysis can be done thank to qualitative and quantitative data, increasing the level of information of the 3D model (Figure 35) (LO TURCO; MATTONE; RINAUDO, 2017).

Figure 35 - 3D Modelling of decays with a graphic explanation of the data (through labels), associated with the adaptive component, such as the nature of the decay and the interventions required for cleaning.



Source: Lo Turco, Mattone and Rinaudo (2017) modified by the author.

Figure 36 - LOD as the relation between the level of detail and level of information.



Source: Costa Oliveira (2016).

Chart 11 - Definition of the level of development (LOD).

Level	Definition
LOD 100	The object can be represented graphically in the model employing symbols or other generic representations, but it does not satisfy the requirements that make it into a LOD200. The information related to the object can be obtained through other objects in the model.
LOD 200	the object is represented graphically in the model as a system, object or generic set with approximate quantities, dimensions, shapes, locations and orientations. Non-graphical information may also be associated with the modelled object
LOD 300	the object is represented graphically in the model as a specific system, object or assembly in terms of quantity, dimension, shape, location and orientation. Non-graphical information may also be associated with the modelled object
LOD 400	the object is represented graphically in the model as a specific system, object or assembly in terms of quantity, dimension, shape, location, and orientation with information on details, manufacture, assembly and installation. Non-graphical information may also be associated with the modelled object
LOD 500	the modelled object is a representation verified on the ground in terms of dimension, shape, location, quantity and orientation. Non-graphical information may also be associated with the modelled object

Source: American Institute of Architects, AIA (2013).

### 2.3.1.3 Interoperability in BIM

Interoperability is defined in Eastman *et al.* (2008) as “the ability to exchange data between applications, and for multiple purposes simultaneously contribute to manual work” adding that “at the very least, it eliminates the need for manually copy data previously generated in other applications”. The benefits and challenges posed by Building Information Modelling in documenting the heritage buildings come from the development of the digital support to the needs, compatibility, and interoperability of applied technologies, regarding the available knowledge and skills to use in a wide range of software (STOBER *et al.*, 2018).

The high number of applications and software used in the heritage field leads to the production of different archive formats in which information is contained. It hinders their compatibility and creates the need for interoperability standards. To overcome such an issue, the International Alliance for Interoperability (IAI) developed Industry Foundation Class (IFC) standard. IAI is a global union of industry practitioners, software vendors, and researchers that work to support interoperability throughout the AEC/FM community (ARAYICI; TAH, 2007). The IFCs are defined as a high-level, object-oriented data model for the AEC/FM industry. The IFC standard is an open data exchange format for BIM data, it is a non-proprietary format, and it is supported by most BIM software (ANTONOPOULOU; BRYAN, 2017). According to Froese (2003) IFCs model all types of AEC/FM information such as parts of a building, *e.g.* the

geometry and material properties of building products, project costs, schedules, and organizations. IFC is defined by ISO 16739:2013 Industry Foundation Classes (IFC) for data sharing in the construction and facility management industries. More information is available on the Building SMART website [[buildingsmart.org/](http://buildingsmart.org/)] (ANTONOPOULOU; BRYAN, 2017)

As an example of a methodology involving different software, the researches of Barazzetti et al (2015a and 2015b) are here presented. The case study used to the application of such a workflow was Castel Masegra, a castle in Sondrio (Italy) (Figure 37). The research work was carried out to determine how an accurate H-BIM from laser clouds (Cloud-to-BIM) can be used for Finite Element Model analysis and simulation (BIM-to-FEM). Furthermore, it was developed to check the main difficulties in the analytic description and to evaluate the numerical performances and the required simplifications for numerical computations (BARAZZETTI *et al.*, 2015a).

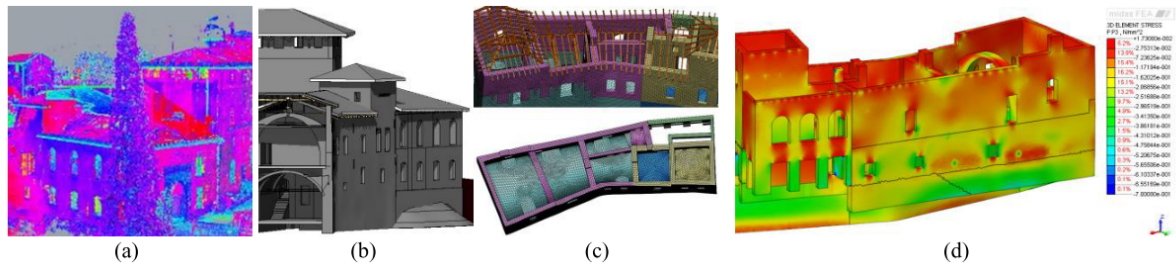
The structural simulation was carried out using the BIM as a starting point for the generation of the mesh for FEA. The work was carried out with Autodesk Revit<sup>®</sup>, for the generation of the BIM. However, in Revit<sup>®</sup> software, the mesh generation is not customizable (AUTODESK INC, 2010). Thus Midas FEA was used for the mesh generation and the structural simulations (BARAZZETTI *et al.*, 2015a). Moreover, the authors developed a set of tools to overcome the several limitations occurred in the H-BIM model in Revit<sup>®</sup> (BARAZZETTI *et al.*, 2015a). Particular attention was paid to the translation of the BIM model into the interoperable format IFC. However, some issues were found:

- a) mesh compatibility: single entities need a perfect node-to- node correspondence to ensure geometric continuity between different objects. This result could be automatically achieved with auto-meshing procedures, but the corresponding faces of two generic elements should be precisely the same (same edges): this is not true in the case of complex BIM composed of multiple connected objects;
- b) local distortions: an ideal mesh must be composed of regular tetrahedral objects. However, the error for the approximation of the solution with an alveolar structure increases with distorted elements. For this reason, very distorted elements should be avoided or at least limited, especially in critical areas;
- c) small elements: elements (that increase the LOD of the BIM) without a direct connection with the load-bearing function should be eliminated to avoid the

- generation of distorted or small Finite Elements, reducing the number of Finite Elements;
- d) small imprecisions: the available Revit® tools sometimes give very small imprecisions in the final mesh. A FEA requires the exact correspondence of the nodes to avoid the generation of thin faces with very distorted “fissure elements”;
  - e) complex architectural objects: this is the case of vaults where the parametric modelling capability leads to inconsistent self-intersection between curved objects (*e.g.* the extrados of a vault modelled from its intrados) (BARAZZETTI *et al.*, 2015a).

As a conclusion, the authors affirm that for future work is mandatory to improve the exchange of information, especially in the case of advanced surfaces. Furthermore, they analysed as such an approach for the structural assessment of cultural heritage is still impossible in a full BIM perspective (BARAZZETTI *et al.*, 2015b)

Figure 37 - Cloud-to-BIM-to-FEM methodology applied to Castel Masegra, Sondrio (Italy): point cloud acquisition/registration (a), creation of the BIM from point clouds by preserving geometric complexity (b), generation of the Finite Element model with tetrahedral meshes (c), structural analysis with the new model (d). The case study is Castel Masegra, a castle in Sondrio (Italy).



Source: Barazzetti *et al.* (2015b).

### 2.3.2 Historic Building Information Modelling for the structural analysis

As mentioned in the previous subsection, thanks to the increasing of BIM interoperability, the same model can be used for many purposes (CRESPI *et al.*, 2015). Such interoperability is fundamental for the exchanging of information between the different professionals involved in a project. As an example, specific BIM tools exist for the structural field. They allow users to perform Finite Element Analysis. However, they can deal only with simple and regular geometric objects (CRESPI *et al.*, 2015). On the contrary, for historical

buildings, this procedure results to be not feasible for many reasons, one of which is the complexity of real geometry (CRESPI *et al.*, 2015; DORE; MURPHY, 2012). However, in the recent scientific literature of heritage buildings, BIM-oriented methodologies have been found in Brumana *et al.* (2018a), Bruno, De Fino and Fatiguso (2018), Lourenço (2004 and 2014), and Pocobelli *et al.* (2018). They integrate multidisciplinary processes of interaction between information, documentation, management, and knowledge of historical buildings (BRUMANA *et al.*, 2018a; BRUNO; DE FINO; FATIGUSO, 2018; LOURENÇO, 2004, 2014; POCOBELLI *et al.*, 2018). Nevertheless, those methodologies do not include structural analysis. Only a combination of those methodologies can lead to a multidisciplinary approach to improve the knowledge path of historical buildings and to increase the Level of Development (LoD), that represents both the level of detail of the geometric definition and the level of information associated with it (COSTA OLIVEIRA, 2016).

Furthermore, despite many BIM types of research being analysed, they are mostly focused on the geometrical description of the 'as-built' configuration of heritage building through laser scanning and photogrammetry or on the organization of the data sources. Few examples of H-BIM in combination with structural FEM analysis were found in Barazzetti *et al.* (2015b), Chi, Wang and Jiao (2015), Dore *et al.* (2015), Murphy (2012), and Oreni *et al.* (2017). However, few cases consider the constructive heritage phases for the structural assessment of the building (BARAZZETTI *et al.*, 2015b; CRESPI *et al.*, 2015). As an example, the research proposed by Dore *et al.* (2015) presented the bases for structural simulations and building conservation analyses. In the previous work, the architectural rules and grammars are exploited to systematically model parts of structures to accelerate and automate parts of the process (DORE *et al.*, 2015). The resulting H-BIM is used to automatically produce conservation documentation and structural analysis of the historical building, as well as their visualization (DORE *et al.*, 2015).

Besides, the transformation of a 3D architectonic model into a Finite Element Model (FEM) with the meshing procedure to get a compatible and regular mesh is not a trivial operation (CRESPI *et al.*, 2015). Moreover, a shape rationalization is required since the initial modelling phases, according to the structural analysis requirements (CRESPI *et al.*, 2015). Indeed, the analyst must be able to distinguish the irregularities and complexities that can influence the mechanical behaviour of an element, such as vaults or irregular walls, from the small irregularities not relevant from a structural point of view (CRESPI *et al.*, 2015).

Some software available on the commercial market allows the integration between FEA and BIM technology. For instance, Robot Structural Analysis<sup>®</sup> ([www.autodesk.com](http://www.autodesk.com)) or 3D FEM professional<sup>®</sup> ([www.sofistik.de](http://www.sofistik.de)) are integrated with Revit<sup>®</sup> and provide advanced structural simulation capabilities for FEA of large and complex structures (BARAZZETTI *et al.*, 2015a). Scia Engineer<sup>®</sup> ([www.nemetschek-scia.com](http://www.nemetschek-scia.com)) enables Revit<sup>®</sup> users to analyse complex and large 3D models. FEM-Design is integrated with Revit Structure<sup>®</sup>, Tekla and ArchiCAD<sup>®</sup> ([www.archicad.com](http://www.archicad.com)). It performs advanced static and dynamic calculations, including earthquake analysis. However, these packages were developed for modern buildings with regular elements, such as straight columns, simple beams and vertical walls (BARAZZETTI *et al.*, 2015a), meaning that the application to the cultural heritage field is still an open issue.

### 2.3.3 Partial conclusions

The use of the BIM method in newly built projects is now a recurring practice in the construction industry. However, finding BIM applications in the structural assessment of heritage buildings is less common than in contemporary ones. In the analysed works, a lack of research in the field of structural assessment and identification of heritage building through the BIM was found. The analysed researches allow concluding the following considerations:

- a) BIM is a suitable paradigm for the path to knowledge, including a collection of historical information, the physical and mechanical characteristics of historical buildings;
- b) BIM also proves to fit with a multidisciplinary field in which information on theoretical hypotheses, experimental tests, and structural analysis must be merged and summarized for the decision-making process;
- c) further research is required to fill the scientific gaps in the integration between BIM with diagnostics, structural analysis and monitoring for structural elements; useful insights can be obtained including dynamic analysis of the modal parameters, *i.e.* frequencies and modal shapes assessment, evaluation of health and safety status of the structures through FEA.
- d) the contribution of the H-BIM model to the whole dynamic behaviour simulation to enhance the preservation requires to be further investigated

- e) the literature review shows a lack of H-BIM researches investigating constructive evolution, which is fundamental for the structural assessment.
- f) in the analysed researches, the FEA is the last step of the H-BIM methodologies aimed at the structural assessment of the heritage building. However, the continuous process of communication and updating between the FEM and the H-BIM models is not investigated; moreover, when the FEM analyses are carried out, the reverse workflow - in which the information acquired in the FEM analysis are exported in the H-BIM model - is not included.



### 3 HBIM-BASED STRUCTURAL IDENTIFICATION FOR CULTURAL HERITAGE

The analysed methodologies on the structural assessment of heritage buildings are mainly focused on the seismic response assessment or the historic masonry structure conservation. Instead, the H-BIM-oriented methodology for the structural identification for masonry cultural heritage - here proposed- is developed for a general-purpose and general-type masonry buildings. Moreover, existing methodologies on similar topics - presented in the literature review - suggest how the knowledge of the building is deeply related to the information acquired. For this reason, in the proposed methodology, the H-BIM is evaluated as a process for the path to knowledge. Furthermore, the H-BIM allows for the creation of a FEM model carried out for the structural analysis.

The proposed methodology aims to increase the level of information, improving the path to knowledge. In this methodology, the investigation of the uncertainties of the structural parameters of heritage buildings is included. Furthermore, the inverse process of structural parameter definitions through experimental results is investigated. Such a process allows identifying and eventually updating the uncertain parameters of FE models. Hence, after the FE model updating through the structural vibration identification, the acquired information is imported in the HBIM software, providing the HBIM database updating. The methodology for the global structural assessment mainly consists of three steps:

- a) architectural investigation;
- b) preliminary global structural assessment;
- c) vibration-based structural identification.

Moreover, two main issues must be remarked, primarily for the development of the proposed methodology, *i.e.* the selection of the cases studies and the type of software to be used. In the heritage field of application, investigating similar case studies is essential to typify a defined group of structures, *e.g.* bridges, churches, towers, minarets. In the proposed methodology here presented, the selection of the case studies was made to investigate a type of building that has not been investigated in the reviewed literature. Such a type of masonry buildings is characterized by a prevalent dimension in the longitudinal direction, meaning that others two dimensions are respectively comparable. Such a methodology could offer insights for future researchers which will develop investigations for the same type of building.

Furthermore, the proposed methodology aims at updating both architectural and structural models using compatible software. Hence, an essential characteristic of the BIM and

FEM software is interoperability because the modifications introduced in one of the two software should be easily exported to the other one (AUTODESK INC, 2010). Such interoperability also allows systematic modification of the FEM model and consequently updating the H-BIM model at a later stage (AUTODESK INC, 2010).

### 3.1 ARCHITECTURAL INVESTIGATION

The phase of architectural investigation for the structural identification of cultural heritage is crucial for the entire methodology because it is the primary source of knowledge that researches have. In the proposed methodology, such a phase is composed of documentary and historical research, information acquisition and creation of the Historic-Building Information Model. Such steps are presented in the following subsections.

#### **3.1.1 Historical and documentary research**

The historical research allows for the building identification, the constructive evolution and the functional use evaluation (ROCA, 2004). It also increases the understanding of how and which modifications led the as-designed project to its as-built state. The historical-critical analysis allows for initial identification of the existing structural system (INFRASTRUTTURA; TRASPORTI, 2018). It is crucial to reconstruct the realization process, and the subsequent modifications suffered during the life-cycle of the heritage building (CALÌ *et al.*, 2019), as well as the events that interested it (INFRASTRUTTURA; TRASPORTI, 2018).

Existing surveys are analysed to understand which level of knowledge was reached in previous studies, collected in archives or digital sources. Such phase is useful to avoid repeating phases of the investigation that have already been done, or critically compare the further results with those obtained by other researchers. Historical and documentary researches provide a huge amount of information that must be interpreted and filtered by the designers, aiming at the implementation of the useful information in the three dimensional model of the proposed H-BIM-oriented methodology.

### 3.1.2 Information acquisition

Once the historical sources are collected, information acquisition relies on the *in-situ* investigation. Such a procedure begins with a visual inspection. Visual inspection is carried out to describe the as-built state of heritage construction. Such an inspection allows the assessment concerning the structural connection of the different elements, *i.e.* type of connection wall-beam and beam-beam that will be modelled in further steps. It also allows resuming the relevant information in the thematic surveys, according to the required research purpose, *i.e.* the surface materials with their decay, the crack pattern and the type connection between the structural elements, *etc.* (BRUMANA *et al.*, 2014). The comparison of the archive documents with the visual inspection improves the knowledge of the current state of the heritage buildings (SAISI; TERENZONI, 2018).

Later on, in case of lack of existing geometrical surveys, photogrammetry and laser scanning reconstructions support the researcher for the description of the as-built buildings (BIAGINI *et al.*, 2016). As a result, a point cloud is obtained and elaborated to extract 2D information by using CAD software or directly imported in BIM software. Such a procedure was already approached in Subsection 2.1.2.2. Such information allows for the generation of geometric and thematic surveys with a high level of accuracy and details. The geometrical and the thematic surveys have primary importance in buildings because they help to resume the investigation carried out in the construction (LOURENÇO, 2014). For example, the material survey is created to describe where precious surfaces, as frescoes and stuccos, are simultaneously present with modern materials; the survey of the decay is addressed to point out the effectiveness of past intervention repairs and the eventual damage produced to the ancient materials (SAISI; TERENZONI, 2018). In the case of geometric and thematical surveys are already available, the researcher must collect, control and select the relevant information.

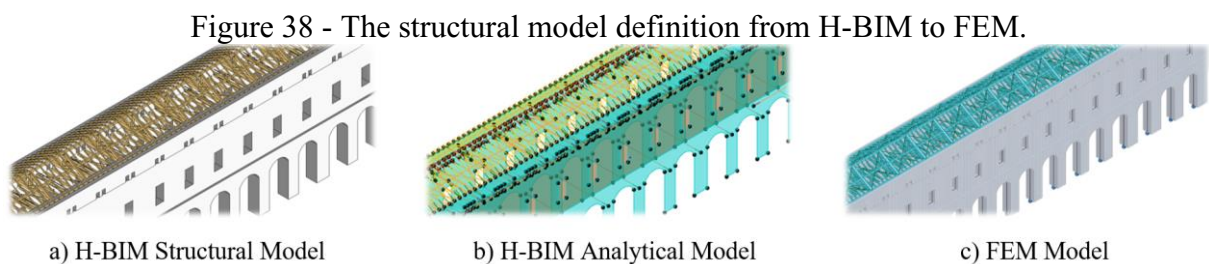
In the case where geometrical and thematical surveys were already available, a critical comparison with the as-built state is carried out. It is developed through a systematic visual inspection. Such a procedure allows for the selection of the required information from the available sources. Such a database is useful to the creation of the H-BIM model as described in the following subsection.

### 3.1.3 Historic Building Information Modelling and information management

The previous steps of historical research, thematic surveys, and *in-situ* investigation allow defining the main characteristic of the heritage building. The selected information is recreated, represented and resumed in the H-BIM model. Models can be obtained from the point clouds or 2D technical drawings. Research for the obtention of point-cloud from laser scanning and photogrammetry, aiming at the creation of geometrical BIM models was extensively investigated in literature (see Subsection 2.1.2.2.3). In the selection of the case studies, the author chose to create the H-BIM model from the 2D files obtained from the elaboration of the point clouds or CAD geometrical surveys. Such an approach allows extending the proposed methodology to the general case where only 2D drawings are available.

In the proposed H-BIM-oriented methodology, a continuous updating process is executed. The created 3D objects (walls, openings, beams, *etc.*) are used as a database for information management. Such intelligent objects contain data about physical and mechanical characteristics of the material, structural connections, boundary conditions and loads. Such data are automatically exported from the BIM to the FEM software, where interoperability is allowed. The intelligent 3D objects are updated each time new information is acquired, without a time-consuming effort during the modification process. Furthermore, each object is defined and dated according to the constructive phase evolution obtained from the historical research.

Once the H-BIM model satisfies the proposed purpose, the structural model is defined from the selection of the structural elements. From the structural model, an analytical model is generated simplifying the structural three-dimensional objects in structural elements like two-dimensional panels, or mono-dimensional columns and beams, according to the selected structural model to be investigated in FEM software (Figure 38).



Source: the author.

## 3.2 PRELIMINARY STRUCTURAL GLOBAL ASSESSMENT

The phase of preliminary structural global assessment aims at the preliminary understanding of the overall behaviour of the structure. It relies on the creation of the FEM model, which allows running preliminary linear elastic analysis. Through such analysis, the design of ambient vibration test is carried out. AVT experimental results are elaborated through operational modal analysis for the obtention of main modal parameters, *i.e.* resonant frequencies and modal shapes. Such steps are presented in the following subsections.

### 3.2.1 FEM model

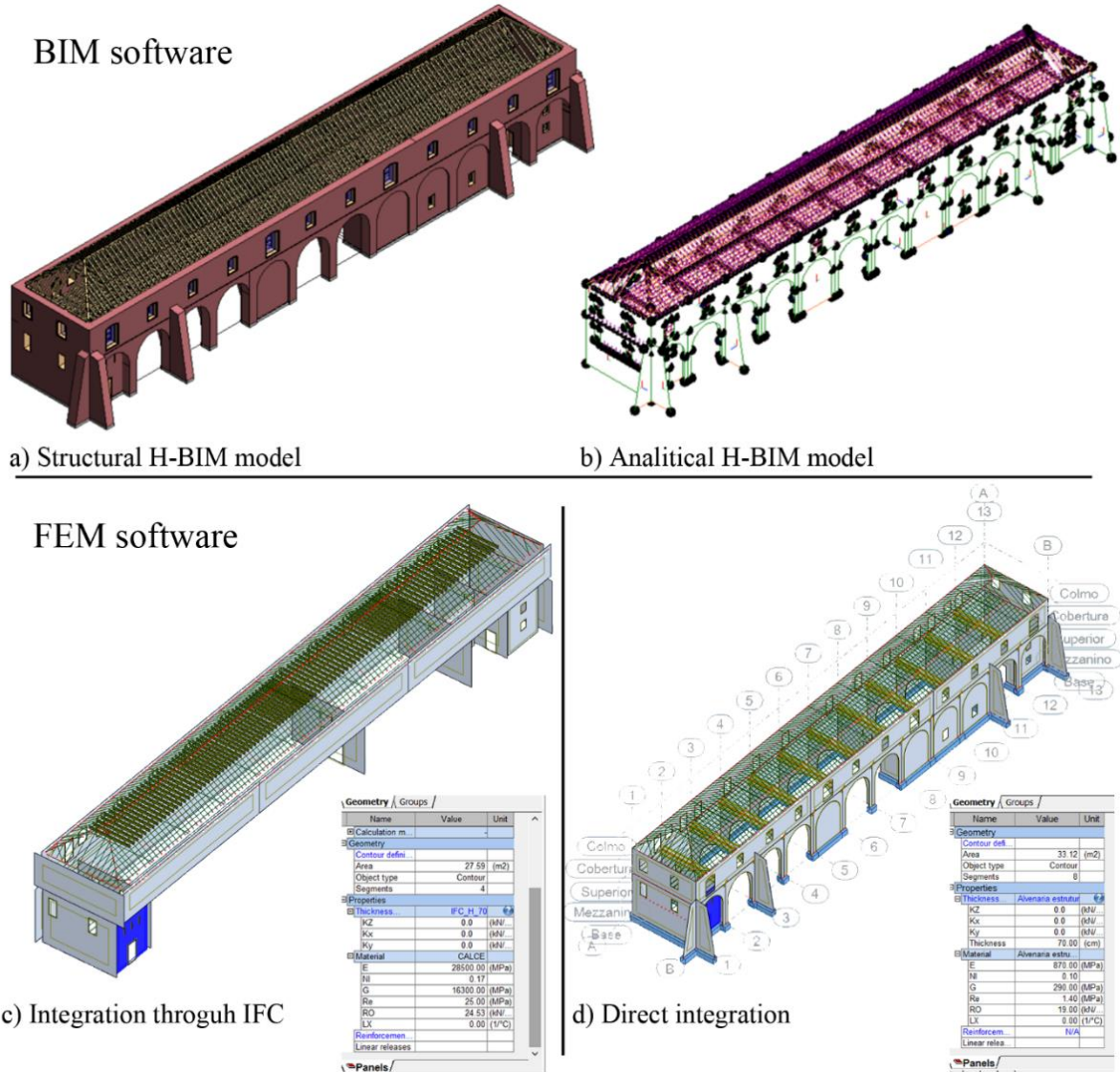
The generation of the Finite Element model is developed in a FEM software. Such workflow allows the user to modify the Finite Elements meshing discretization, that in BIM software is not customizable (AUTODESK INC, 2010). As was explained in Subsection 2.3.1.3, the process of interoperability between BIM and FEM software is not trivial (Figure 39). For this reason, a systematic check of the member elements is required.

Indeed, the generation of the analytical model in BIM software generates some errors due to the non-alignment of the automatic simplification process of the structural elements. Care must be done for the wall and beam elements to assess if they correspond to the required geometrical configuration. Furthermore, geometric and mechanical parameter information - *e.g.* geometrical axes, loads, boundary condition, type of connections - must be controlled. They represent the primary sources of the proposed methodology. Indeed, it is crucial that in the process of compatibility, the objects do not lose any information. For instance, if H-BIM model is exported IFC format - and then imported in the FEM software - information can be lost (Figure 39). Direct integration between H-BIM and FEM software should be preferable.

Once the interoperability issues are overcome, and no information is lost, the process of mesh generation is carried out. Mesh element type should be selected according to the user requirement (see Subsection 2.2.2.3). The type of element, together with the mesh size, influences the FE model representation of the real construction, and the quality mesh should be assessed. In such an analysis, the user must analyse the size and quality of the mesh to obtain a consistent model. However, an excessive refinement of the mesh leads to an exponential increase of the Finite Element nodes. Such an increase - corresponding to the increase of the degree of freedom of the model - causes a computational time-effort for the structural analysis

and large file size. Such issues should be investigated for each FE model before the preliminary linear elastic analysis, which is presented in the following subsection.

Figure 39 - BIM and FEM software in the interoperability process; structural (a) and analytical (b) H-BIM model with loss of information in the integration through the IFC format (a), contrary to the direct integration (b).



Source: the author.

### 3.2.2 Preliminary linear elastic analysis

Once that the H-BIM model is exported in the FEM software, linear static analysis is carried out considering the dead loads. Such an iterative analysis allows understanding the consistency of the model, *i.e.* the hypotheses of continuity of elements and connections. As was explained in the previous subsection, the generation of the analytical model in BIM software

generates some errors. Once such errors are fixed, the linear elastic analysis is used as qualitative tools to understand where stress and strain due to the dead load reach the maximum values.

In the structural assessment of historical constructions, linear analysis is always performed, before the application of more sophisticated approaches. Such analysis allows for the initial phases of definition and calibration of the mesh. Subsequently, self-weight linear elastic analysis allows for the overall understanding of the structural behaviour, the range values, and distributions of the loads and the mesh definition and calibration (ROCA *et al.*, 2010).

The necessary condition for the linearity of a structural problem is that some characteristics of the system satisfy at the same time the following hypotheses, in terms of materials, geometry and boundary conditions. In the proposed methodology, geometric linearity has been assumed for structural behaviour, and linear elastic materials were assumed as well, the constraints of the structure are bilateral and do not depend on the entity of the acting loads (DEL PIERO, 1989; ROCA *et al.*, 2010). Indeed, the field investigated in the proposed methodology is a linear elastic problem for definition, as explained in Subsection 2.2. Moreover, due to the high level of uncertainties about the non-linear properties of the materials, in the proposed research linear elastic analysis is chosen mainly as a qualitative approach to the structural behaviour assessment (ROCA *et al.*, 2010). Such an approach leads to suppose the following hypotheses. Mechanical behaviour of materials is linear-elastic, displacements of the structure in the deformed configuration are small, and the structural constraints are bilateral and do not depend on the entity of the acting load (DEL PIERO, 1989; ROCA *et al.*, 2010).

A fundamental methodology step aimed to understand the behaviour of a historical building is structural analysis in each construction phase (MAGENES; MENON, 2009). Such types of buildings can be briefly described by vertical elements such as walls, arches or pillars, and horizontal elements, slabs, roofs or vaults. The structural behaviour of these constructions is influenced by the type of connections between vertical and horizontal structural elements. The horizontal structural elements are in-plane-stressed, and the stresses are transferred to the foundation through the opposition of the structural walls. The presence of a horizontal element, also referred to as a diaphragm, with good wall-to-wall and wall-to-diaphragm connections, can improve the overall ability to withstand horizontal actions (CATTARI *et al.*, 2015; CNR, 2014; DIRECTIVE OF THE PRIME MINISTER, 2007; LOURENÇO *et al.*, 2011).

### 3.2.3 Modal analysis for the design of ambient vibration tests

Once preliminary analyses prove the consistency of the model, an extensive modal analysis is carried out. The aim of this step is the increase in knowledge about the global structural behaviour in terms of modal parameters. Frequencies, modal shapes, and participating masses percentage are obtained as modal parameters for the description of the structural behaviour (BINDA *et al.*, 2004).

In the proposed methodology, modal analysis allows for the preliminary understanding of the overall structural behaviour. Furthermore, the identification of first-mode mechanisms in each direction is an essential element of the structural assessment procedure of masonry buildings assessment (MAGENES; MENON, 2009). Moreover, modal analysis is here proposed also for the design of the experimental test campaign, and it will be carried out before the experimental tests. Since in the case of heritage buildings non-destructive tests must be preferred to destructive tests (DT), the author chose to carry out ambient vibration tests. Such a test aims at the identification of the leading experimental modes of the construction (CABBOI; GENTILE; SAISI, 2017; GENTILE; SAISI, 2007; GENTILE; SAISI; CABBOI, 2015). Once the Finite Element Analysis is completed, the H-BIM model is updated with the FEM-to-BIM direct integration with the modifications made in the FEM software.

### 3.2.4 AVT and OMA for the structural identification

Ambient vibration tests, together with operational modal analysis provides the dynamic identification of the heritage building. In such a test, the data acquisition system and piezoelectric accelerometers allow acceleration or velocity responses to be recorded (GENTILE; SAISI, 2007). The location, number, and type of accelerometers are defined according to the research proposals. The set-ups and locations where equipment will be installed depend on several factors, *i.e.* spatial configuration, safety access to the instrumentation, maximum displacement points obtained from the preliminary analysis, shapes of the selected modes (GENTILE; SAISI, 2007). The knowledge acquired through the architectural investigation and the preliminary structural analysis help the researchers in the selection of these factors in the process of structural identification through ambient vibration tests.



#### 3.2.4.1 *Ambient vibration test*

The AVTs are carried out using a data acquisition system, piezoelectric accelerometers, each one connected to a power unit/amplifier, providing the constant current needed to power accelerometer's internal amplifier, signal amplification, and selective filtering. These sensors allow for recording acceleration or velocity responses. Since the number of sensors is limited, in the proposed methodology, the tests involve the definition of different setups aiming at reducing the number of sensors to be used to cover the required selected measurement points (GADE *et al.*, 2005; GENTILE; SAISI, 2007; LOURENÇO *et al.*, 2016). It means that some sensors are held stationary as reference transducers in different setups.

#### 3.2.4.2 *Representation of the setups in the H-BIM model*

The configuration of the setups and the connected devices are represented in the H-BIM model. This implementation of the H-BIM model is useful to record and manage the acquired experimental data. Furthermore, the external file data obtained from the AVTs and OMA will be linked to the accelerometers previously modelled in the H-BIM file. The use of the phase filter of the BIM software - which allows the user to group and visualize elements with the same characteristics - is adapted to the experimental tests. Since several AVTs tests can be carried out each one concerning a different setup (GADE *et al.*, 2005; GENTILE; SAISI, 2007; LOURENÇO *et al.*, 2016), an equivalent number of phases is created for each set-up. In each phase, the position of the accelerometers is recorded in the BIM digital elements. Those elements include relevant information such as time and date of the Experimental Tests, type and model of the accelerometers and the data acquisition systems. Such an approach leads to the simplification of data management and representation. The AVTs and OMA output could be readily consulted in the further step of analysis directly from the H-BIM model.

#### 3.2.4.3 *Operational modal analysis*

Operation modal analysis is carried out from ambient vibration data. Such analysis aims to obtain the modal parameter of the cultural heritage, in terms of frequencies and modal shapes. In the proposed research, the chosen output-only procedure is the Frequency Domain Decomposition (FDD), because it is a widespread non-parametric technique and - as shown in

the Subsection 2.2.3.2 - provided very accurate results for natural frequencies and mode shapes (GADE *et al.*, 2005). As explained in the bibliography review (Subsection 2.2.3.2), the frequency-domain decomposition technique allows the estimation of the spectral matrix, and the Singular Value Decomposition (SVD) at each frequency (GENTILE; SAISI, 2007). Analysing the SVD curves allows understanding the identification of the resonant frequencies and the estimation of the corresponding mode shape (GENTILE; SAISI, 2013).

#### 3.2.4.4 MAC-based semi-automatic procedure

In the proposed methodology, Modal Assurance Criterion (MAC) is used for a semi-automatic procedure of comparison between numerical and experimental modes. As previously mentioned in the bibliography review Subsection 2.2.3.4, the statistical indicator MAC is created from the need for a quality assurance indicator for experimental modal vectors estimated from measured frequency response functions (ALLEMANG, 2003). While it is commonly used to check the orthogonality of the vibration modes, in the proposed methodology, it is also used to establish which of the experimental modal shapes correspond to the numerical ones in a semi-automatic procedure. Such a semi-automatic approach overcomes the issue of having a limited number of experimental modes and a broader number of numerical modes. Furthermore, measurement point references in AVT are usually limited, *e.g.* when some parts of the building are restricted (or unsafe) or when limited economic resources are available. Hence, the proposed methodology manages to reduce the effort of the experimental procedures in terms of time and cost. Comparing the experimental and numerical modal shapes with the Modal Assurance Criterion (MAC) (Equation 63) is possible to identify the frequency discrepancy (DF) (Equation 64) between experimental and numerical frequencies (GENTILE; SAISI, 2013; GENTILE; SAISI; CABBOI, 2015; PAU; VESTRONI, 2008):

$$MAC(\psi_i^{EXP}, \psi_j^{FEM}) = \frac{|\{\psi_i^{EXP}\}^T \{\psi_j^{FEM}\}|^2}{(\{\psi_i^{EXP}\}^T \{\psi_i^{EXP}\})(\{\psi_j^{FEM}\}^T \{\psi_j^{FEM}\})} \quad (60),$$

$$DF(f_i) = \frac{f_i^{FEM} - f_i^{EXP}}{f_i^{EXP}} * 100 \quad (61),$$

where  $\psi_i^{EXP}$ ,  $\psi_j^{FEM}$  are the  $i$ -th experimental and the  $j$ -th numerical modal shapes, while  $f_i^{FEM}$  and  $f_i^{EXP}$  are the numerical and experimental frequencies of the  $i$ -th modes, respectively. The MAC value has a range between 0 and 1, and the comparison could be considered satisfied with a MAC value superior to 0.8 (FRAGONARA, 2012) while a MAC value less than 0.40 is considered a poor match (GENTILE; SAISI; CABBOI, 2015).

In the proposed methodology, MAC evaluation in structural identification has a dual function. It allows increasing the level of knowledge of the heritage building identifying vibrational modes representing the structural behaviour. Besides, it is used as validation of the methodology itself, to understand if the proposed methodology leads to consistent results and if a further step of refinement is required. Indeed, the results of the FEM analysis and OMA can converge - in terms of frequency and modal shapes. FEM analysis and OMA can also reach a satisfactory reliability MAC and DF thresholds, according to the requirement of the researcher. On the contrary, if the MAC and DF values are not satisfactory, a further step of Modal updating is required for the structural identification of the heritage building. Such a step is presented in the following subsection.

### 3.3 MODEL UPDATING FOR THE STRUCTURAL IDENTIFICATION

Once the experimental modal parameters are obtained, a comparison with the FE analysis results is carried out. Such a check has two objectives. The first is the validation of the research workflow aiming at assessing if the geometrical, physical and mechanical parameters have been chosen with a reasonable degree of approximation. The second objective is the global assessment of the structure can be carried out through the understanding of the vibration modes. In the case of good correspondence between numerical and experimental results, the supposed structural hypotheses are considered valid for the description of the building and the H-BIM model can be updated according to the FEM model parameters. On the contrary, the model must be tuned to match the experimental results with a process of modal updating.

The parameters obtained in such a tuning procedure are updated both architectural and structural models. The modifications made in the BIM software must be exported in the FEM software, and *vice-versa*. Thus, is the interoperability between all the selected software is a fundamental characteristic of the H-BIM based methodology (AUTODESK INC, 2010). In this perspective of software interoperability, the structural parameters are defined in the BIM software. They are imported, analysed and possibly tuned in the FEM model. Finally, they are

updated in the BIM software. In this further step of the methodology, a sensitivity analysis is carried to understand the influences of the physical and mechanical parameters in the global structural behaviour of the heritage building.

### 3.3.1 Sensitivity Analysis for the model uncertainty understanding

The structural model of a historic structure, even when all the collected information is accurately represented, continues to involve significant uncertainties, *i.e.* the geometries, material properties and their distribution, the boundary conditions. This aspect is especially critical for complex historic buildings evolved in different constructive phases (BARAZZETTI *et al.*, 2015a; GENTILE; SAISI; CABBOI, 2015).

In the proposed methodology, sensitivity analysis (SA) is used to investigate the influence of model parameters within the structural response assessment (ASGARI; OSMAN; ADNAN, 2013). The knowledge elements - necessary for this analysis - concern the geometry of the structural organism, the construction details and the mechanical properties of materials (CNR, 2014). Such parameters must be distinguished as deterministic, aleatory or epistemic. Indeed, those three types of parameters must be analysed differently. Two types of approaches will be carried out to understand the strength and weaknesses of the existing type of sensitivity coefficient selected in literature.

Firstly, the sensitivity coefficient  $s_{i,k}$  is selected as an investigation parameter for the aleatory knowledge elements since it is widely used in literature (Equation 62). It represents the percentage variation in mode frequency per 100% change in updating parameter by a perturbation technique in the normalized form (GENTILE; SAISI, 2007). Secondly, another sensitivity coefficient is used to the evaluation of the epistemic uncertainties since they cannot be modelled as continuous variables. For this reason, an alternative parameter is considered, since it allows describing both aleatory and epistemic uncertainties was selected. The parameter  $\Delta'_k$  - presented in the 2.2.4 - was adapted to the proposed methodology. It is useful to show how the results in the structural response differ to the average model varying aleatory (Equation 63) and epistemic (Equation 63) parameters (ASGARI; OSMAN; ADNAN, 2013; CNR, 2014):

$$\Delta'_k = \frac{R_{k,max} - R_{k,min}}{\bar{R}}, \quad (62)$$

$$\Delta'_j = 2 \frac{\max(R_p) - \min(R_p)}{\max(R_p) + \min(R_p)}, \quad (63)$$

where  $R_{k,max}$  and  $R_{k,min}$  represent the values - in terms of structural response - associated with the parameter  $k$ , varying from its maximum to its minimum values;  $\bar{R}$  is the structural response associated with the average model,  $R_p$  is the structural response associated with the epistemic parameter  $p$ , which is the number of alternative options of the discrete epistemic variable,  $p=1, m_j$ .

The step of the sensitivity analysis (SA) is useful for the understanding of the parameter influences of the FEM model on the structural response of the heritage building. Furthermore, SA is helpful to understand which parameters should be assessed in the experimental investigation design, since a limit number of tests is typically carried out, in terms of costs and parts of the structures. Moreover, SA is also used to select the parameters to be tuned for structural identification.

### 3.3.2 Finite Element model tuning and H-BIM model updating

The Finite Element model tuning is carried out to improve the consistency of the numerical model to the experimental results. In the proposed research, the FE model correspondence between the experimental and numerical behaviour of the heritage building is evaluated through the modal parameter of the frequency and modal shape. The numerical and experimental modal shapes are compared through the MAC value, that in case of similar numerical modal shapes, allows identifying which one must be selected for the model tuning. Besides, the value of the frequency and the discrepancy DF are chosen as parameters, representing the accuracy of the FE model. The method proposed in Douglas and Reid (1982) was selected for the FE model tuning since the identification procedure is based on the minimization of the frequency discrepancies DF.

The selection of the input parameters plays a crucial role in the FE tuning process. Often, experimental results of the physical and mechanical of the analysed structure are not available. In such cases, scientific literature (BINDA *et al.*, 2004; BINDA; SAISI; TIRABOSCHI, 2000; CATTARI *et al.*, 2015; LOURENÇO, 2002) and national standards (ABNT, 2008; ABNT NBR 6118:2003, 2005; ASSOCIAÇÃO BRASILEIRA DE NORMAS

TÉCNICAS - ABNT, 1997; CS.LL.PP., 2009; EUROCODE 8, 2005; NTC08, 2008) provide a reasonable range of value for an initial approximation.

The selected parameters to be updated vary in a range, around the “base” value of the reference model,  $X_k^B$ , limited by lower  $X_k^L$  and upper values  $X_k^U$  ( $k = 1, 2, \dots, N$ ). As already explained, the coefficients  $A_{ik}$ ,  $B_{ik}$ ,  $C_i$  are dependent on both the base value of the structural parameters and the range in which these parameters can vary. The coefficients,  $A_{ik}$ ,  $B_{ik}$ ,  $C_i$ , are evaluated from  $(2N+1)$  Finite Element analyses: the number of the selected parameters  $N$  should be minor to the number of the vibration modes selected for the model tuning (DOUGLAS; REID, 1982; GENTILE; SAISI, 2007; ZORDAN; BRISEGHELLA; LIU, 2014).

Furthermore, the solution is as better as the base values are closer to the solution. Hence the accuracy and stability of the optimal estimations should be carefully checked either by the complete correlation with the experimental data or by repeating the procedure with new base values until the required threshold is reached (GENTILE; SAISI, 2007). The results of the previous methods allow the FE model tuning. Once the parameters obtained by the updating process are implemented in the FEM model, modal analysis is carried out to confirm the prediction of the results of the Douglas and Reid method.

Once the check is evaluated, the information acquired in the FEM model is imported in the H-BIM software, and the optimal H-BIM model is obtained according to the research proposal. Such an H-BIM model could be used as a database for the multidisciplinary professionals, for further phases of more sophisticated structural analysis, and the decision making regarding the heritage building conservation.

### 3.4 MANAGEMENT FOR THE LEVEL OF KNOWLEDGE INCREASING

This section is useful to underline the importance of information management. Indeed, the role of information management is implicit in the BIM platform. However, the concepts here presented are related to each phase of the proposed methodology. Indeed, systematic information management is carried out for each object. When new information is acquired, the analyst must evaluate if it increases the level of information of the H-BIM model. The user must apply the concept of modelling tolerance (MT) (see Subsection 2.3.1.2) since the beginning of the process. MT should be related to the focus of the research, and object details must be analysed - and eventually reduced or neglected - according to the research purpose.

In the proposed research, the structural purpose leads to the simplification of the architectural details, when they are not considered affecting the structural behaviour. Moreover, such a procedure allows reducing the information loss during the data sharing process between BIM and FEM software.

### **3.4.1 The dimension of the H-BIM oriented methodology**

Regarding the dimensions of the BIM, the proposed methodology investigates the spatial (3-D) and time (4-D) information. The historical research and the geometric survey allow representing the spatial configuration of the building both in 3-D and 4-D. As mentioned in Subsection 2.3.1.1, the time dimension (4-D) is usually managed to defining when each element will be created, stored, prepared, installed, used. Such a dimension is also used to organizes the layout of the construction site, the maintenance and movement of the teams. No BIM investigations on the influence of constructive evolution on structural behaviour were found in the literature. For these reasons, the author wants to investigate the time dimension of the structure, but in a novel H-BIM approach. Each objected is related to its constructive phase, along with the time. It is useful for the easy understanding of the evolution phases of the heritage building.

The proposed methodology also allows reducing the time-cost effort in different phases, also increasing the cost/benefit point of view (5-D). Indeed, the application of the methodology allows identifying the structure with only the non-destructive test, the AVT. Furthermore, when other experimental tests are required, in the proposed methodology, the sensitivity analysis approach is provided. It permits the understand which NDT must be done according to the required parameter, avoiding unnecessary investigations.

Furthermore, the safety dimension (8-D) is explored. Indeed, the proposed methodology focus on the structural assessment of the building heritage and its structural identification. Such assessment allows the understanding of the possible hazard of the heritage buildings, aiming to provide suggestions for further safe design (KAMARDEEN, 2010)

### **3.4.2 Level of development of the H-BIM oriented methodology**

The information management carried out according to the proposed methodology allows increasing the level of development (LOD) of the H-BIM model. Indeed, as mentioned

in Subsection 2.3.1.2, the elements are represented graphically as an overall system, in their as-built configuration, representing quantities, dimensions, shapes, location and orientation. Furthermore, not-graphic information (text, images, spreadsheet) are associated with the objects. The minimum LOD reached after the development of the proposed methodology can be considered as LOD 300 (see Chart 11). Furthermore, when technical details, decay survey, and technical reports are implemented and connected to the referring object, the H-BIM model reach the definition of LOD 400. If such an H-BIM model is also modelled with regards to the environmental configuration, *i.e.* buildings in proximity, spatial terrain configuration through contour lines, soil characterization, the LOD 500 could be reached (see Chart 11).

### 3.4.3 Level of knowledge increase

The proposed methodology aims to increase the level of development, which in terms results increasing the level of knowledge. Such an increase is useful to avoid time-consuming analysis without proper knowledge of geometry and the mechanical behaviour of the real structure. Moreover, it allows approaching the dynamic behaviour of the structure before the results of complex dynamic and kinematic analyses. Indeed, such understanding enables the analyst to prioritize those analyses that better fit to the real structural behaviour.

The concept of the level of knowledge one, proposed by European and Italian standards (see Subsection 2.1.4.4), was introduced as crucial aspect able to define design coefficients and assessment strategies (BIONDI, 2008). Indeed, a discrepancy reduction in analysis results and a progressive convergence to the real behaviour are expected, moving from KL1 to KL3. However, such level increase requires time-consuming analysis and extensive (or exhaustive) *in-situ* investigations. The author suggests a procedure for the increase of the level of knowledge, which prioritizes the vibration-based structural identification for the real assessment of the structure, more than costly NDTs systematically repeated in the structure. Such a vibration-based procedure is not mentioned in the standards as a possible NDT for structural parameter assessment.

Subsequently, local NDTs should preferably be carried out to confirm the obtained results from FEM preliminary analysis and OMA, aiming at developing further analysis (*e.g.* non-linear static, dynamic or kinematic analyses). After such further analysis, LV3 level could be reached in a more effective path to knowledge. Such a higher understanding of the structural



behaviour will be useful for risk assessment, hazard mitigation strategies, global seismic assessment or conservation project design.

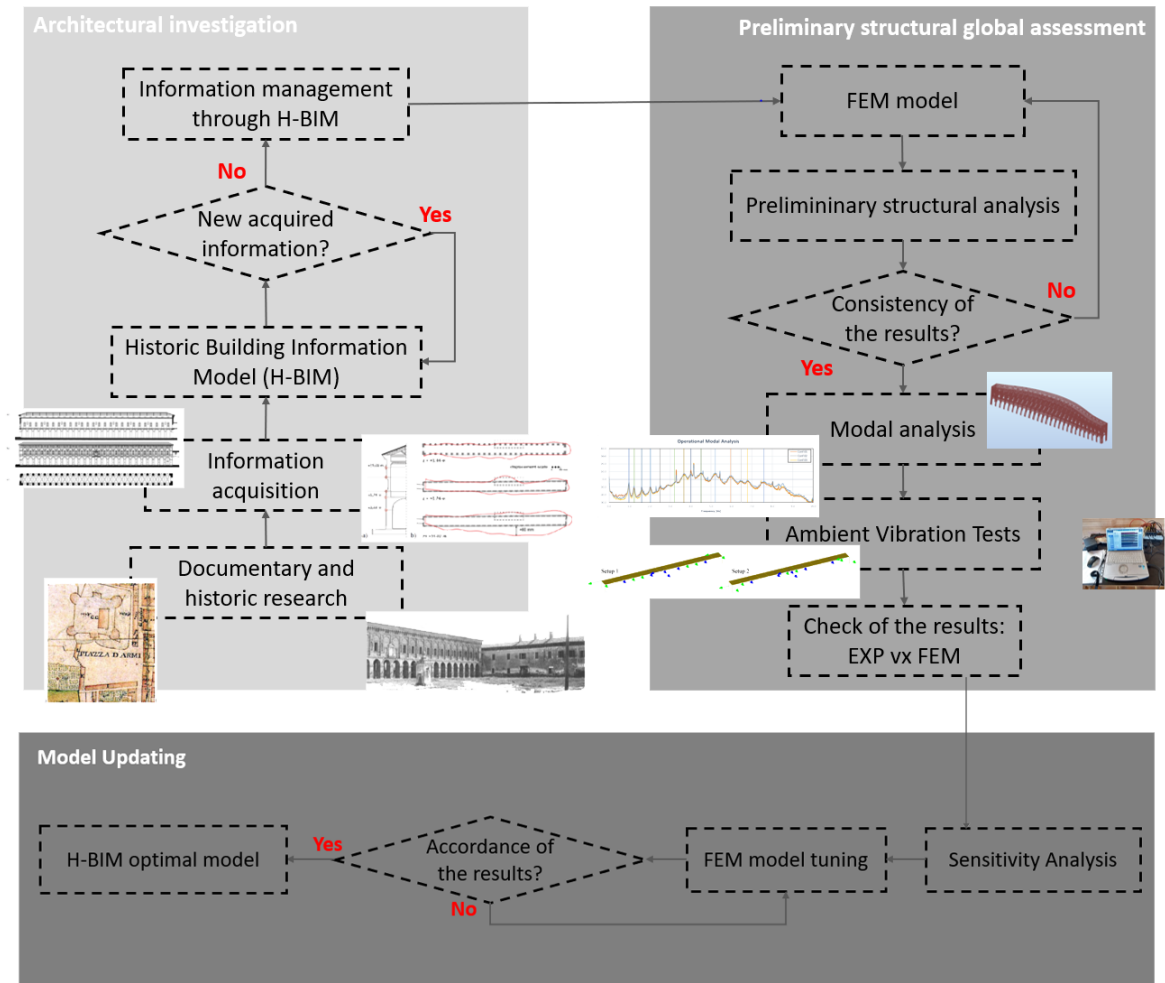
Furthermore, such H-BIM-oriented structural identification can be the base for further investigations, such as Structural Health Monitoring (SHM). SHM indeed requires a reliable referential model - also known as ‘numerical twin’ - to compare with the experimental results recorded in time. Such comparison will allow understanding better the environmental aspect influencing the modal parameters of the structure, *i.e.* natural frequencies, damping ratios, modal shapes. Such understanding is useful for further investigation of the structural system and for predicting and localizing damage (ZONNO *et al.*, 2017).

### 3.5 WORKFLOW OF THE METHODOLOGY

The proposed methodology for the global structural assessment is resumed in this section. Three main phases are architectural investigation, preliminary global structural assessment and vibration-based structural identification through modal updating (Figure 40).

The first step of the proposed methodology begins with the process of information acquisition. Such information is obtained from historical research, on-site investigations, geometrical and thematic surveys (ORENI *et al.*, 2013; QUATTRINI *et al.*, 2015). In the case of heritage buildings, historical research allows for the understanding of the construction life cycle, in terms of constructive phases process, environment evolution, use and re-use of the considered building along with the time, critical events and damage history (CALÌ; DIAS DE MORAES; DO VALLE, 2020). Such information allows the generation of the H-BIM model, from which the Finite Element model is obtained. The preliminary global structural assessment is carried out using FEA. Such an approach helps to design the ambient vibration tests for modal identification of the heritage build. The results of AVTs are used to validate the consistency of the proposed workflow. They also allow the process of modal updating of the structural parameters for the global structural assessment of the historical buildings. As a conclusion of the proposed multidisciplinary approach, the H-BIM model is updated with all the relevant acquired information.

Figure 40 - Workflow of the H-BIM-based structural identification for cultural heritage.

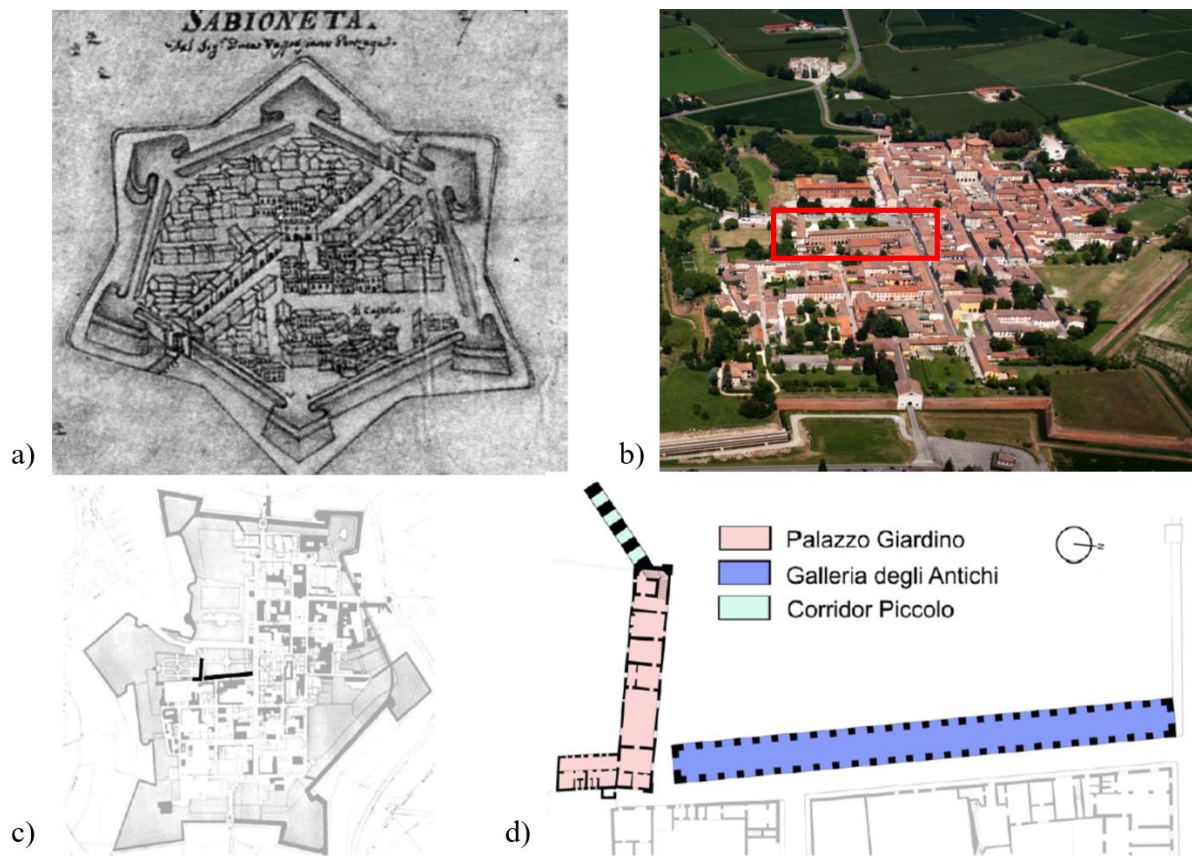


Source: the author.

#### 4 H-BIM FOR THE GLOBAL STRUCTURAL BEHAVIOUR ASSESSMENT: THE CASE OF *GALLERIA DEGLI ANTICHI*

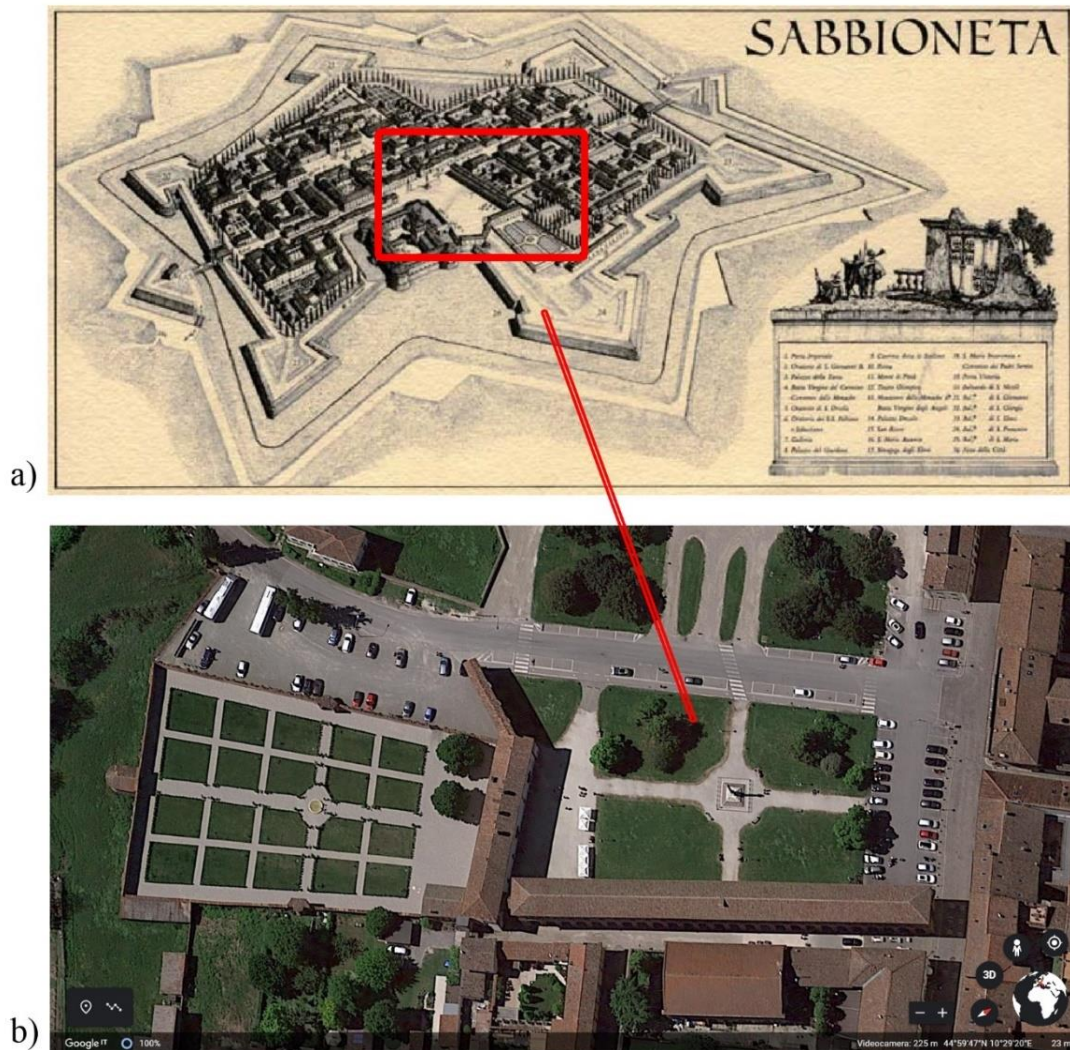
In this chapter, the proposed case study of the *Galleria Degli Antichi* (literally Gallery of the Ancients) is presented. The analysed heritage building - located in Sabbioneta, Italy - was built in the 16<sup>th</sup> century, and it was included in the UNESCO World Heritage list in 2008 (figures 41 and 42). Such an impressive building has the main dimension of almost 100 m. *In-situ* inspection and tests were carried to increase the knowledge of the heritage buildings and its as-built structural behaviour. Such information, together with the evaluation of the existing research and geometrical surveys (DAL BARCO; PEROBELLI; SARTOR, 2016; SAISI; TEREZONI, 2018), allows defining the main characteristics of this heritage built and summarizing them in a Historic-Building Information Model (H-BIM).

Figure 41 - Historical (a) and current (c) map of Sabbioneta (a), an aerial photograph of Sabbioneta (b) and built environment of *Galleria degli Antichi* (d).



Source: Saisi, Terenzoni (2018).

Figure 42 - Hypotheses of the configuration of the ideal city of Sabbioneta (a) and built environment of *Piazza delle Armi* (b).



Source: Confortini (XI century) *apud* Apollonio (2008) and Google Earth (2020) modified by the author.

The main aim of this part of the research is the validation of the proposed methodology. Such methodology allows improving the path to the knowledge of the structural behaviour of the construction. Moreover, the evaluation of the model uncertainties is carried out through the FE analysis and experimental investigation of the as-built structural behaviour. Such experimental investigation also allows improving the consistency of the numerical model for the understanding of the heritage building structural behaviour.

#### 4.1 HISTORIC AND DOCUMENTARY RESEARCH

The proposed methodology - applied to the *Galleria degli Antichi* - begins with the historical-critical analysis of the documental sources (APOLLONIO, 2008; DAL BARCO;

PEROBELLI; SARTOR, 2016; MELLEY; TEDESCHI; VERNIZZI, 2019; SAISI; TERENZONI, 2018). Documentary research was carried out collecting documents aimed at pointing out the evolution of the buildings, the sequence of intervention and functional services (APOLLONIO, 2008; DAL BARCO; PEROBELLI; SARTOR, 2016; MELLEY; TEDESCHI; VERNIZZI, 2019; SAISI; TERENZONI, 2018). Such documents rely on information mainly acquired in the archives of the technical offices of *Soprintendenza* di Brescia, Cremona and Mantua, and national archive of Mantua (Italy) (DAL BARCO; PEROBELLI; SARTOR, 2016). Most of the documentary sources are related to the intervention in the XX century, confirming the typical difficulties of the analysts about historic research.

#### 4.1.1 Historic background and architectural geometric generation

The Gallery was built in Sabbioneta between 1583 and 1584. The city of Sabbioneta is known as an "ideal city" of the Renaissance (Figure 42) since it was built and designed according to humanistic principles (Figure 43) (APOLLONIO, 2008). The *Galleria degli Antichi* was designed to enclose the southern side of the great square *Piazza delle Armi* (figures 41 and 42). It was commissioned by the Duke Vespasiano Gonzaga, and it was designed Giuseppe Dattaro (SAISI; TERENZONI, 2018).

The building had a function of passage, but the project was not completed (DAL BARCO; PEROBELLI; SARTOR, 2016). At present, the only access to the second level is through a flying passage from *Palazzo Giardino* (Figure 44.f). The visitors have to cross all the ground floor of the *Palazzo Giardino*, to reach the east staircase, and to go through the first floor of the palace (SAISI; TERENZONI, 2018).

The construction has a long open arcade on the ground floor with 27 couple of massive squared columns made by brick masonry (Figure 41.d). The façade of the gallery is made by masonry brick (figures 44.a and 44.b). The ground floor is composed of a portico of twenty-six arches, with masonry cross vaults resting on twenty-seven pairs of mighty pillars (Figure 44.e). On the first floor, the building has a long gallery with 26 windows on each side (Figure 44). The gallery walls were frescoed and stuccoed in a very refined way by the most famous painters and craftsman of the time (Figure 44.c) (SAISI; TERENZONI, 2018). Such a gallery is covered by a wooden coffered ceiling with panels richly decorated but apparently in a low state of preservation (figures 44.d and 44.g).



Figure 43 - Geometric generative procedure of the *Galleria degli Antichi*.



Source: Melley, Tedeschi, Vernizzi (2019).

Figure 44 - Historical (1920s) (a) and current (b) photos of *Piazza D'Armi*, *Galleria degli Antichi* and *Palazzo Giardino*; Historical (c and d) and current (e, f and g) of the construction and flying passage from *Palazzo Giardino* (f).



Source: Source: Dal Barco, Perobelli, Sartor (2016). Saisi Terenzoni (2018).

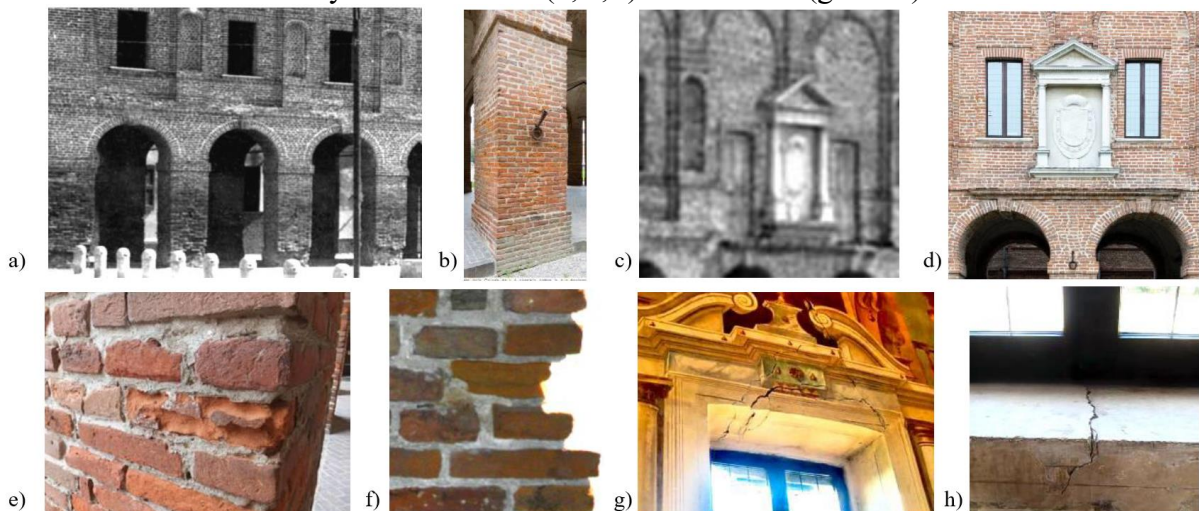
#### 4.1.2 Functional evolution and repair intervention

An essential step of the research is the evaluation of the building evolution, resulting from the different interventions, uses, and owners. Currently, the building houses a museum, but it had different uses during its life-cycle. In 1927 troops billeted in *Palazzo Giardino* as happened in 1806 with the Napoleon Army, as well. In 1928 the building hosted the offices and the meeting rooms of the fascist party (DAL BARCO; PEROBELLI; SARTOR, 2016). In 1947 some halls on the ground floor were used as food shop with a kitchen, and in 1948 an organization involved in social, cultural and free-time activities for the workers rent some rooms (DAL BARCO; PEROBELLI; SARTOR, 2016). In 1975 and 1990, *Palazzo Giardino* and *Galleria degli Antichi* hosted the antique market (figures 41 and 45) (DAL BARCO; PEROBELLI; SARTOR, 2016).

The archive research documents several repair interventions following each intervention of the building systematically. The restorations concerned mainly the surfaces, the frescoes, and the stuccos (SAISI; TERNZONI, 2018). Similarly, other interventions were carried out in 1935, 1953, 1966, 1989, 2001 to repair the effect of the water leakage due to the roof damage. Substantial interventions to the structure were performed in 1952, including the rebuilding of the flyover passage. In 1961, the west staircase of *Palazzo Giardino* was rebuilt (DAL BARCO; PEROBELLI; SARTOR, 2016; SAISI; TERNZONI, 2018). The available historical pictures are of primary importance to recognize such damage, as well as the transformations, occurred to the buildings (figures 44 and 46).

In Figure 45, the transformations of the *Galleria degli Antichi* are documented. In Figure 45.a (datable to late 1920s), the bases of the columns are damaged by the rising damp. They were repaired in 1939, increasing the base dimension (Figure 45.b) (SAISI; TERNZONI, 2018). The columns were repaired several times by local dismantling and reconstruction; these interventions are recognizable by observing the characteristics of the bricks (Figure 45.b). Other changes concern the openings at each side of the aedicule in the west façade, transformed from the former doors (Figure 45.c) into windows (Figure 45.d). At present, steel ties restrain the ground floor vaults. They were probably introduced during the 1950s restoration works. It is not known if there were present before (SAISI; TERNZONI, 2018).

Figure 45 - Historical images of *Galleria degli Antichi* (a and c), modifications of the windows surrounding the aedicule from the door (c) to windows (d). Visual inspection of the material decay in the external (b, e, f) and internal (g and h) elements.



Source: Saisi, Terenzoni (2018).



After the 2012 earthquake, further structural interventions were developed, both in the *Galleria degli Antichi* and in the *Palazzo Giardino*. In this intervention, steel ties were inserted at the vaulted slab and roof levels and anchored to the masonry walls. At the extrados of the coffered wooden ceiling, steel beams were anchored to each masonry pier. Steel beams were connected by a system of diagonal and transversal steel ties (Figure 47). Besides, timber tie-beams were introduced in such an anchoring system (Figure 47.b), probably to resist the axial compressive stresses. Such beams are connected with the steel L-type beams and steel ties (Figure 47). The phases of historic and documentary research allow the understanding of the existing information source. However, they were critically evaluated through the information acquisition phases carried out by the author, which will be presented in the following section.

## 4.2 INFORMATION ACQUISITION

In this section, visual inspection is presented as a crucial source of information acquisition to critically interpret the existing documental sources and to obtain insight on the as-built configuration. Moreover, the process of analysis of the thematic survey is presented in the following subsections.

### 4.2.1 Visual inspection

Visual inspection was carried out by the author comparing the own insights obtained from the direct inspections with previous research and *in-situ* inspection carried out by Dal Barco, Perobelli, Sartor (2016) and Saisi and Lorenzoni (2018). Hence, the as-built state of *Galleria degli Antichi* does not suffer significative modifications since then.

Columns show a modification in colour due to the capillary humidity and the local dismantling and reconstruction. However, no evidence of damage to the mortar joint of the masonry was noticed. The walls of the second floor have little cracks in the lintels and spandrels of the windows (figures 45.g and 45.h). Visual inspection allowed assessing the structural element connections. Columns are estimated to have a fixed constraint to the ground. Furthermore, particular care was given to the assessment of the wooden elements of the lacunar ceiling (Figure 48). It is characterized by transversal timber joist, which insists on longitudinal timber support, in connection with the masonry walls (Figure 48.e). The level above the lacunar ceiling and below the roof is not accessible. Therefore the evaluation of spaces and construction

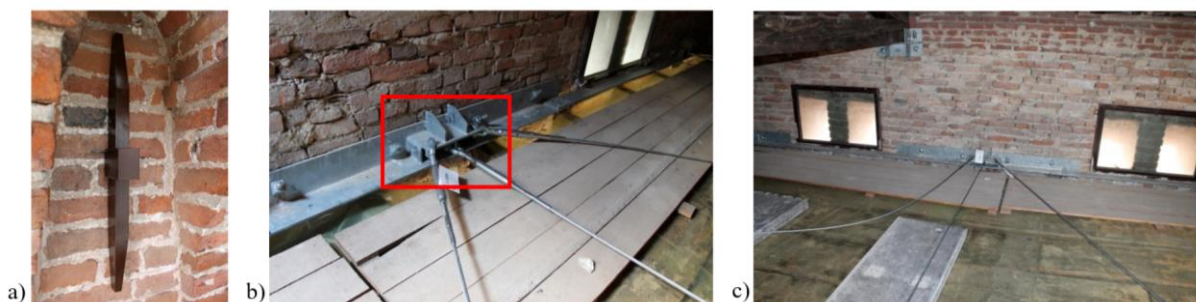
elements was made through the analysis of the restoration intervention carried out by the study of Engineering Studio Amigoni (figures 46 and 47). Technical drawings are available at [http://www.studioamigoni.com/?page\\_id=prodotti&idcontenuto=279&idparent=480&iddetail=512&LID=0](http://www.studioamigoni.com/?page_id=prodotti&idcontenuto=279&idparent=480&iddetail=512&LID=0).

Figure 46 - As-built state after the 2012 earthquake (a, b, c, e) on the structural elements carried out timber joist of lacunar ceiling (a, b), timber roof truss (c, d). Restoration works with steel reinforcement steel tie-rod in masonry walls (f) and modification in the roof extrados (d).



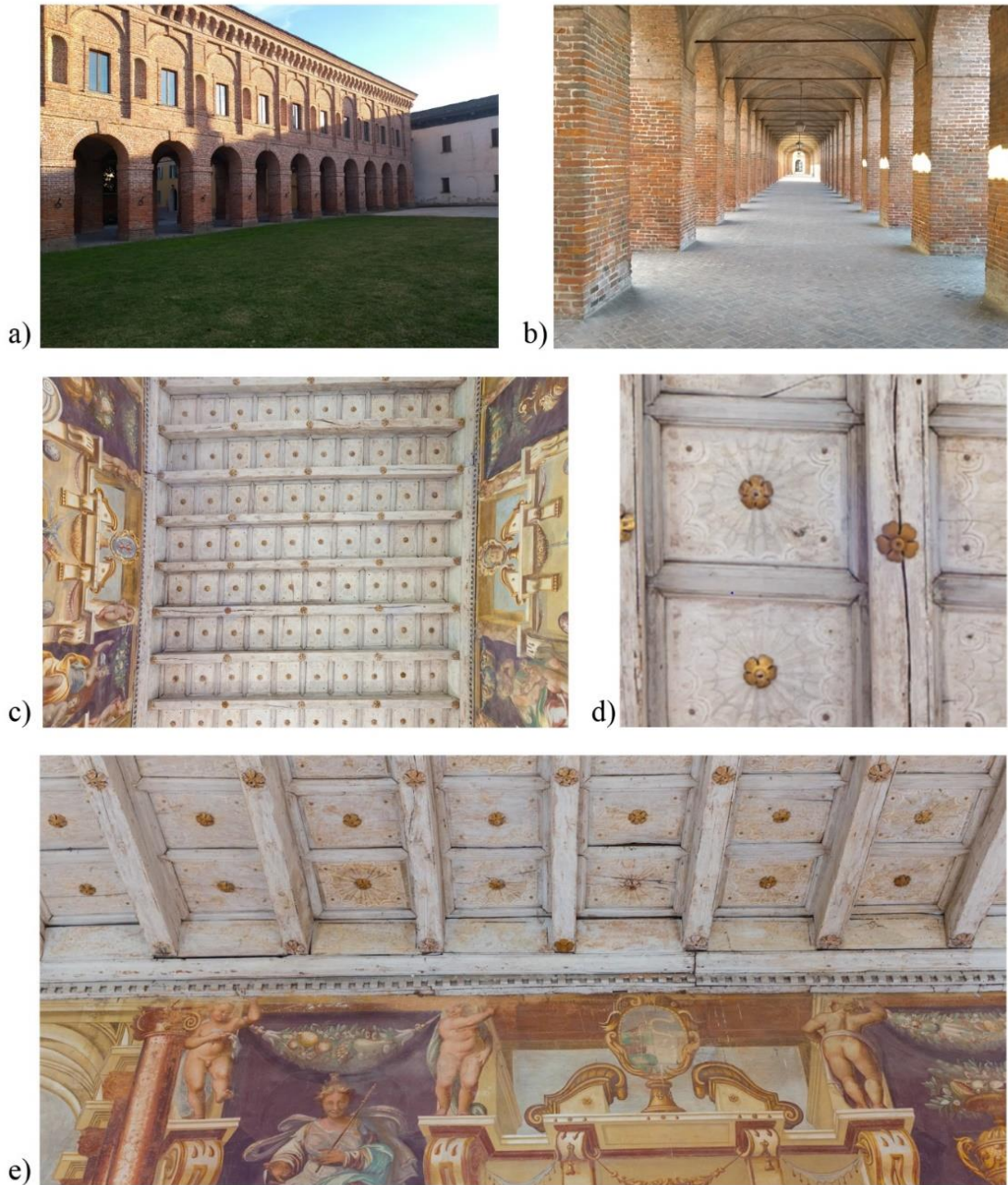
Source: Amigoni engineering studio (2012).

Figure 47 - Structural intervention after the 2012 earthquake: tie-rods on the top of the façades (a), steel profiles where the timber tie beam are introduced (b) and tie rods on the extrados of the coffered wooden floor (b) and (c).



Source: Amigoni engineering studio (2012).

Figure 48 - As-built state: change in colour of the columns (a, b), configuration of the lacunar wooden ceiling (c, d) and connection with the masonry walls (e).



Source: Dal Barco, Perobelli, Sartor (2012) modified by the author.

The connection between the lacunar ceiling and masonry walls was improved by perimetral steel beams, diagonal steel ties and transversal wooden beam integrated into such a system (figures 47.b and 47.c). Steel diagonal tie rods were also introduced in the intrados of the roof structures in the restoration interventions after the earthquake of 2012. Direct inspection images were found in Amigoni (2012). Moreover, longitudinal and transversal masonry walls were connected by steel tie rods, which seem to allow the building to improve

the box-behaviour. Such investigation is crucial for the following steps of the methodology since it allows supposing some relevant hypotheses that will be presented in Subsection 4.3.3

#### 4.2.2 From image data acquisition to thematic surveys

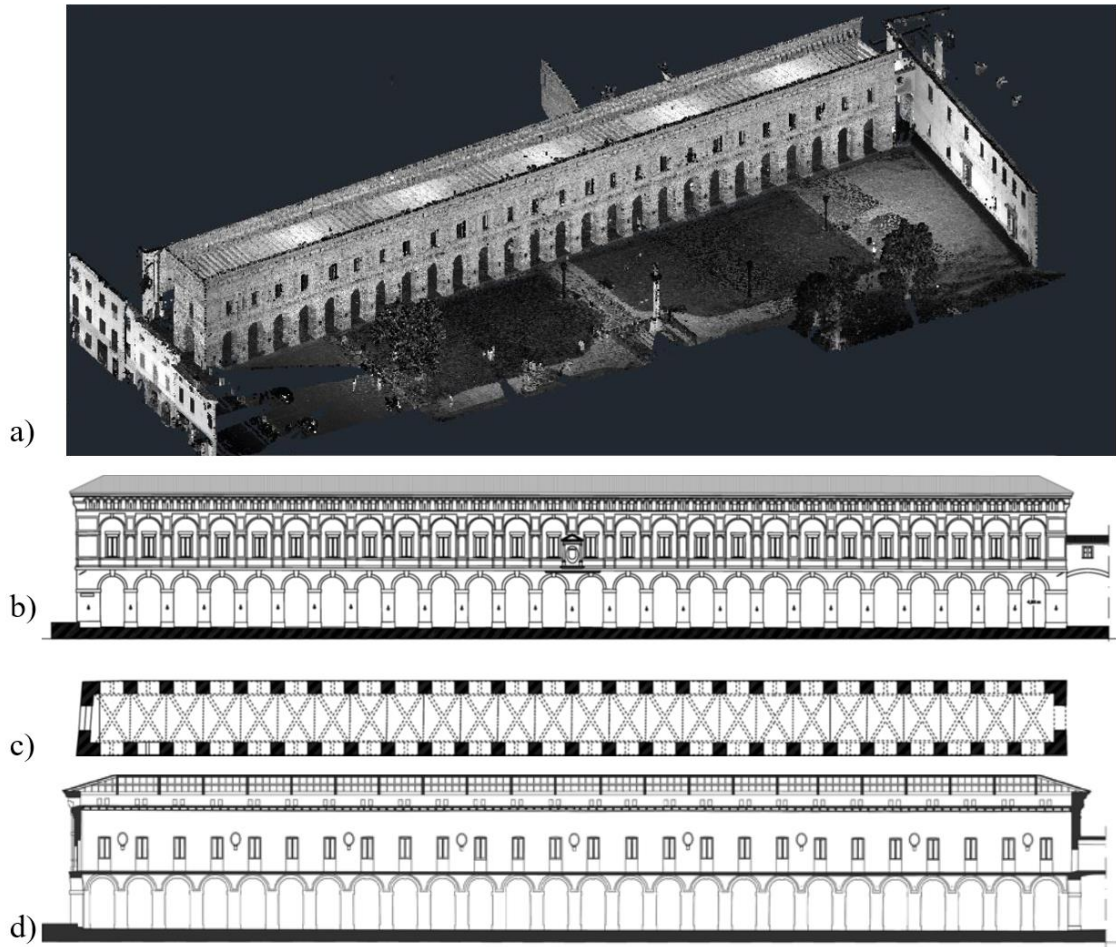
The available Point Cloud of *Galleria degli Antichi* (see Subsection 2.1.2.2.3 and Figure AN.A2) was obtained with the Laser Scanner and Theodolite tools (DAL BARCO; PEROBELLI; SARTOR, 2016). It was developed by Dal Barco, Perobelli and Sartor (2016), using Autodesk Recap<sup>®</sup> software (Figure 49.a). The elaborated file was imported in AutoCAD, where vectorial drawings were obtained and saved in DWG format (Figure 49) (DAL BARCO; PEROBELLI; SARTOR, 2016). Such files represent the geometrical survey, which is the base source upon the information collected were resumed (Annex A). An extensive *in-situ* inspection was already carried out and are described in Dal Barco, Perobelli and Sartor (2016) and Saisi, Terenzoni (2018). Such an investigation of the architectural complex was carried through visual inspection and described through the thematic surveys, *i.e.* the definition of materials, of their decay, of building technique, and structural condition (Figure 50) (DAL BARCO; PEROBELLI; SARTOR, 2016; SAISI; TERENZONI, 2018). Such primary sources allow simulating the case in which the researcher acquire information through existing data. However, a critical analysis must be done to compare such sources with the as-built state of the building

Most of the decay problems of the façade of the Gallery are caused by the rising damp. Such information is collected in the decay survey (Figure 50.c), showing the height of the dampness level and the typical decay of the masonry (figures 45.a and 45.b). In the interior of the palaces, traces of surface decay are explicable mainly to past leakages that occurred from the damaged roof. The water leakage from the roof damaged the ceiling structure as well. Furthermore, during heavy rain, the water leaks from the windows of the Gallery, damaging the decoration.

In Dal Barco, Perobelli, Sartor (2016), the survey and the interpretation of the crack pattern were also carried out by measurement of the out-of-plumb. Furthermore, the description of the past damage found in the archive documents was evaluated (DAL BARCO; PEROBELLI; SARTOR, 2016). The damage description on frescoes was carried out, together with the identification of the consequent repairs on the wall surfaces (DAL BARCO; PEROBELLI; SARTOR, 2016). This activity allowed distinguishing the effects of the strong earthquake which hit the area in 2012 (SAISI; TERENZONI, 2018).

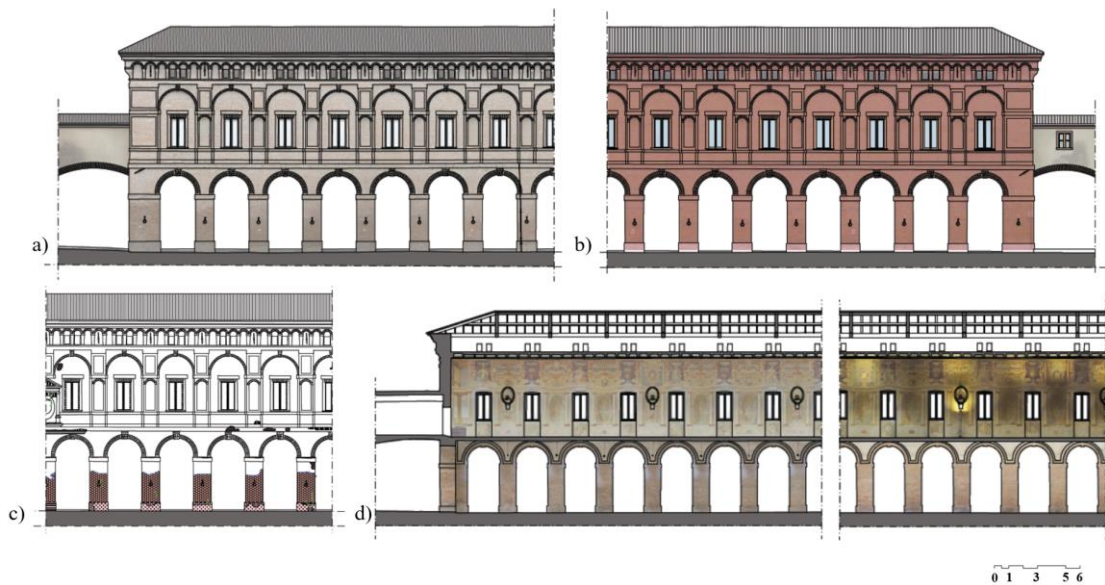


Figure 49 - Three-dimensional model obtained from the point cloud (a) and geometrical survey of the *Galleria degli Antichi*: west façade (b), plan (c) and longitudinal section (d).



Source: Dal Barco, Perobelli, Sartor (2016).

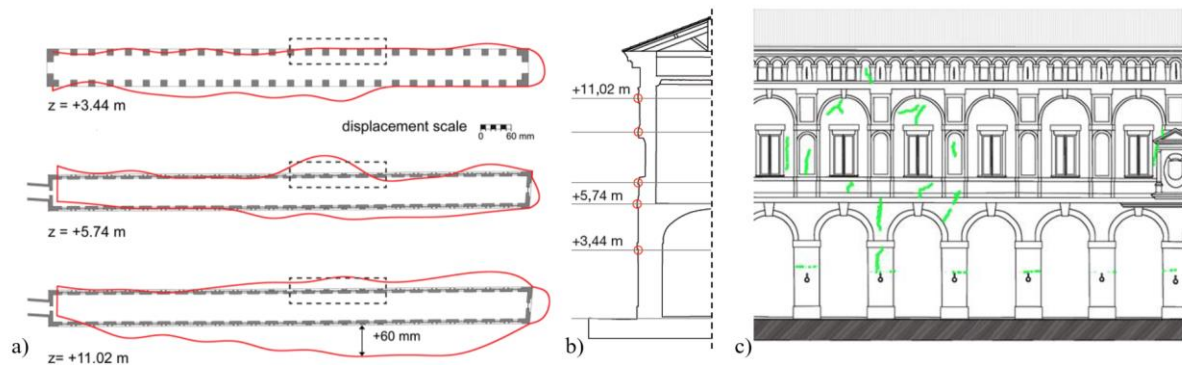
Figure 50 - Geometric surveys (a and d): a material survey (b) and material decay survey (c).



Source: Dal Barco, Perobelli, Sartor (2016).

In Figure 51.b, the out of plumb is compared at three different levels of the building. In such a survey, the deformations, represented in red, have different distributions for each level of the structure; they do not steadily increase with height. The survey of the out of plumb shows sharp deformation of the central part (Figure 51). Such sharp deformation was recorded at the level of the first floor at a height of 5.74 m (SAISI; TERENCEZONI, 2018). Moreover, deformations are concentrated mainly on the east side of the building. Furthermore, an asymmetric behaviour is recorded in terms of out-of-plane displacement, due to the presence of the flying passage from *Palazzo Giardino*.

Figure 51 - Structural survey of the out of plumb (in red) of *Galleria degli Antichi* (a) and (b) and crack pattern on the west façade (c).



Source: Dal Barco, Perobelli, Sartor (2016). Saisi, Terenzoni (2018).

### 4.3 HISTORIC-BUILDING INFORMATION MODELLING

The creation of the H-BIM model of the *Galleria degli Antichi* involves the organization of the acquired information. As previously mentioned, the leading source is a comprehensive geometric survey of the construction, including the pathology survey (DAL BARCO; PEROBELLI; SARTOR, 2016; SAISI; TERENCEZONI, 2018), but the visual inspection was crucial to critically analyse the already existing information. Information acquired in the previous phases of the proposed methodology is included in the H-BIM model, according to the workflow presented in the following subsections.

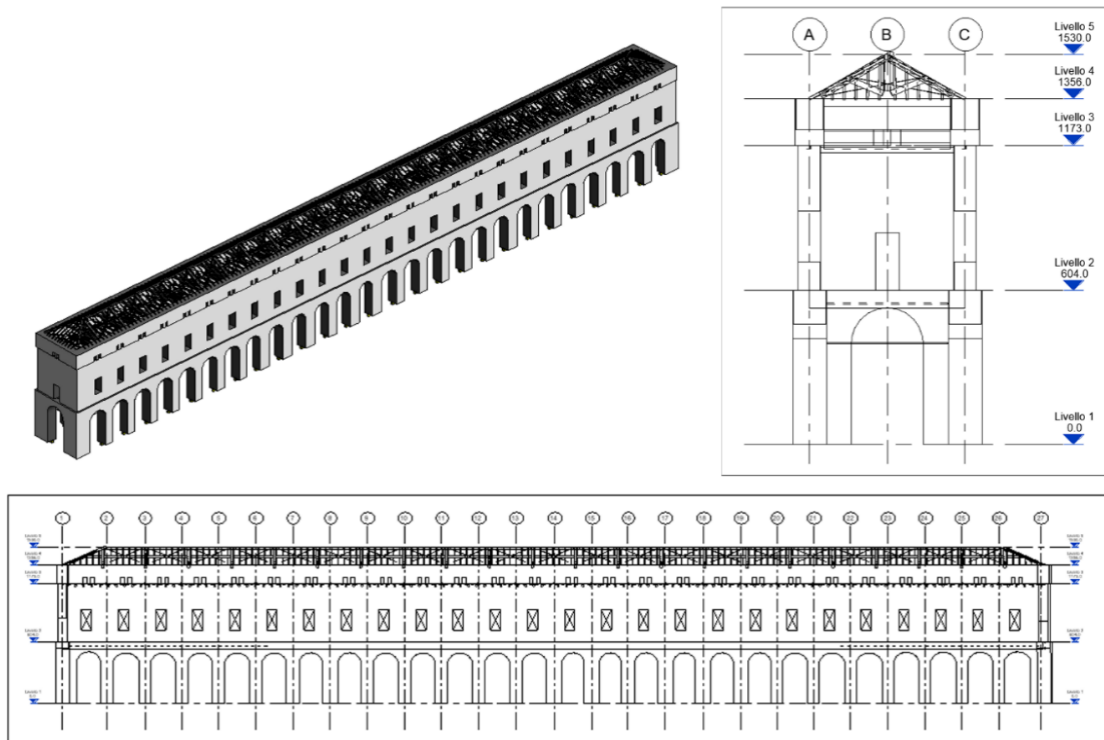
#### 4.3.1 H-BIM management: dimension and level of development

Modelling tolerance (see Subsection 3.4) was defined according to the structural purpose of the investigation. Hence, walls are simplified in their shapes (Figure 52) to provide

a level of information suitable for data exchange for limiting information loss from BIM to FEM software (BIAGINI *et al.*, 2016). Wall extrusions, decorations, or little change in thickness, *e.g.* spandrels below the windows and arches of the upper masonry level were simplified, and a homogenous thickness was given to the walls to avoid information loss. Similarly, masonry vaults are modelled as an equivalent horizontal deformable slab because it allows a correct direct integration between BIM and FEM software. Such simplifications were assumed because the instrumentation of the AVT setups recorded the structural response at the extrados level of the masonry vaults. However, the author is aware that such a choice could modify the structural response of the FEM model, and such modifications – together with the assumption of a homogenous thickness for each level - could be analysed in further researches.

In the proposed cases studies Revit® and Robot® are used since they have suitable interoperability for the research purpose (AUTODESK INC, 2010). It must be noticed that such simplifications must be assessed when the purpose of the analysis is different from the one proposed in this research, *e.g.* non-linear push-over analysis for damage identification and seismic assessment.

Figure 52 - H-BIM model: 3D view, longitudinal and transversal sections.

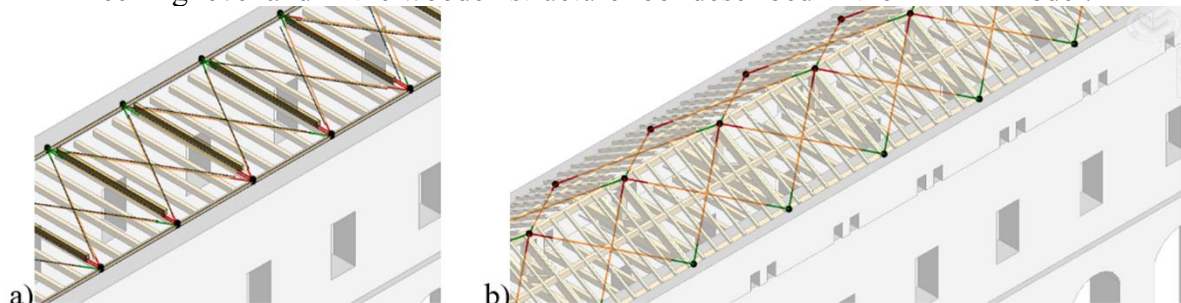


Source: the author.

The object elements were created according to the geometrical surveys and visual inspections (see Subsection 4.3.2). The information regarding the constructive phase was also implemented in each object. This procedure aims at the easy differentiation of the time-properties of each object. Furthermore, the physical and the mechanical properties of the structural elements are implemented in each object, improving the information regarding the safety dimension. In such an approach, the level of development of the objects could be considered as LOD 300 (see Subsection 2.3.1.2).

The information obtained from geometric surveys and visual inspections were implemented in the H-BIM model. The ‘phase filter’ Revit® option allows for the definition of each element according to its construction phases. In this building, two constructive phases were implemented for the description of each element, before and after the structural interventions of 2012 (Figure 53). As an example, the wooden and steel tie beams introduced during the 2012s interventions were implemented in Revit® according to their geometries and positions (Figure 53).

Figure 53 - Structural Intervention after the 2012 earthquake at the extrados of the coffered-ceiling level and in the wooden structure roof described in the H-BIM model.



Source: the author.

#### 4.3.2 The system configuration of the structural model

The geometric characteristics of the load-bearing walls and pillars were supposed according to the results of the direct inspections and geometric surveys (Figure 49.b). Since the *in-situ* investigation showed that the geometric characteristics of the walls differ for each level, three orders of walls are defined:

- a) at the ground level, the masonry pillars have a thickness of 1.275 m;
- b) at the second floor, the masonry walls have a thickness of 0.85 m;
- c) at the upper level, walls are characterized by masonry arches on the façade, and constant equivalent thickness of 1.2 m was assumed.



The same assumption is made for the masonry vaults, where an equivalent thickness of 0.70 m is defined. Such a value came from the information of the BIM model where the volume of the three-dimensional object of the masonry vaults was divided by its area. However, further research should assess the behaviour of masonry vaults represented in their real geometrical configuration.

Furthermore, structural behaviour of the masonry wall is supposed as single-leaf panel since no evidence of weak transversal connection within the wall was observed. However, for such a thickness the assumption of the single-leaf panel is not always valid, meaning that further researches should be done on such a hypothesis where more details on the structural response are required. Moreover, connection vertical to vertical structures - meaning wall-to-wall connection - is supposed as continuous. Indeed, such behaviour is enhanced by the presence of steel-tie rods between parallel masonry panels. Such elements ensure the box-behaviour of the overall system. Moreover, the flying passage from *Palazzo Giardino* (Figure 44.f) is considered as a boundary condition of the system. However, its influence on the overall structural behaviour is unknown and it will be modelled as springs elements and assessed in the further structural analysis (see Subsection 4.5.2). The foundations were supposed as fixed constraints due to the rigid ground foundation assumptions (BETTI, MICHELE, GALANO, 2015; CLEMENTE; BONTEMPI; BOCCAMAZZO, 2012; KILAR; PETROVČIČ, 2017).

The connection horizontal to vertical structures - meaning slab and roof connection with masonry walls - requires special care. The assessment concerning the type of structural element connections was developed through visual inspection. In the lacunar wooden ceilings, the absence of rigid connections between wall-beam and beam-beam elements allows assuming that supports are pinned in the vertical plane. Similarly, the timber trusses of the roof are assessed for the understanding of the structural model. Since the wooden structures of the roof are directly connected with the masonry walls, the stress distribution of the bending moment is not homogeneously transferred from tie beams to the walls. Such behaviour allows to supposing pinned connection in the vertical plane. On the contrary, masonry vaults are supposed as fixed to the orthogonal masonry walls. Such an assumption is due to vaults thickness and the continuity of the masonry material to the vertical walls. However, future researches should investigate such hypotheses.

Regarding the non-structural elements, they are modelled as loads acting on the structure, through their mass contribution, since non-structural elements are automatically neglected in the BIM-to-FEM integration. Hence such non-structural elements are simplified

by equivalent vertical loads. Such information was implemented in the H-BIM model. Moreover, properties and main assumptions regarding material behaviour are presented in the next subsection.

### 4.3.3 Material properties and assumptions

Since no experimental information was acquired on the materials, their properties and structural behaviours are assumed and must be confirmed by further experimental research. The Young Modulus of masonry structures is obtained, considering the average value suggested by NTC 2018 (Chart 6),  $E = 1.50$  GPa (CS.LL.PP., 2018). Such a value which was corrected by a factor of 1.2, corresponding to the hypothesis of good mortar. Such characteristic was confirmed by the visual inspection (Chart 7). For the masonry vault, an initial assumption was made since no available data are given. The Young Modulus was supposed an average value of 1.00 GPa (BOSCATO *et al.*, 2015). Masonry specific weight is assumed 18.00 kN/m<sup>3</sup>, according to NTC 2018 and further research (GENTILE; SAISI; CABBOI, 2015). Furthermore, in this research, materials are considered homogeneous and isotropic, linear elastic behaviour is assumed, and stiffness degradation is neglected (Table 1). A constant Poisson ratio  $\nu$  0.20 is supposed in the masonry structures (RAMOS *et al.*, 2013). Material properties of steel and timber structure are obtained from NTC 2018 and are resumed in Table 2.

Table 1 - Mechanical parameters of the masonry wall ( $E_m$ ,  $w_m$ ) and vaults ( $E_v$ ,  $w_v$ ).

	$E_m$ [GPa]	$E_v$ [GPa]	$w_m$ [kN/m <sup>3</sup> ]	$w_v$ [kN/m <sup>3</sup> ]
Masonry	1.80	1.00	18.00	18.00

Source: the author.

Table 2 - Mechanical parameters of the steel and wooden elements.

	$E$ [GPa]	$G$ [GPa]	$w$ [kN/m <sup>3</sup> ]
Steel	210.00	80.80	77.00
Wood	11.00	0.69	3.43

Source: the author.

## 4.4 FINITE ELEMENT MODEL

Direct integration of Revit<sup>®</sup> with Robot<sup>®</sup> allows that the information collected in the H-BIM model are transferred correctly in the FEM software. Moreover, they can be modified

in the subsequent FEM model, since the process of information updating is always possible, due to the interoperability of the software. In the following subsection, the phases of the definition of the FEM model are described, *i.e.* mesh generation through the definition of element type and size which influence the mesh quality and the number of degree of freedom of the problem to be solved.

#### 4.4.1 FE model and mesh element definition

In the FE model, the middle wall planes and masonry vaults are represented by thick-shell elements with shear deformation (KATILI, 1993a, 1993b), which are defined as 4-node quadrilateral elements (Q4). The beams are modelled as linear beam elements, with 6 degrees of freedom at each node. For the Q4 shell elements in connection with beam elements, pinned connections are generated – perpendicular to the plane of Finite Elements. The selected mesh type is Delaunay (GEORGE; BOROUCHE, 1998).

The number of degree of freedom, maximum out-of-plane displacement, base compressive stress, and vibrations modes are evaluated to define an adequate mesh size element. Table 3 shows the variation of the size element in the relation of the first vibration mode in the transversal and longitudinal vibration modes ( $Y$ ,  $X$ ), maximum compressive strength at the base of columns ( $\sigma$ ) and out-of-plane displacement at the top of the walls ( $\delta$ ), and degree of freedom ( $DOF$ ).

Table 3 - Influence of the element size in the transversal and longitudinal vibration modes ( $Y$ ,  $X$ ), maximum compressive strength ( $\sigma$ ), out-of-plane displacement ( $\delta$ ), degree of freedom ( $DOF$ ), and variation  $\Delta DOF$ .

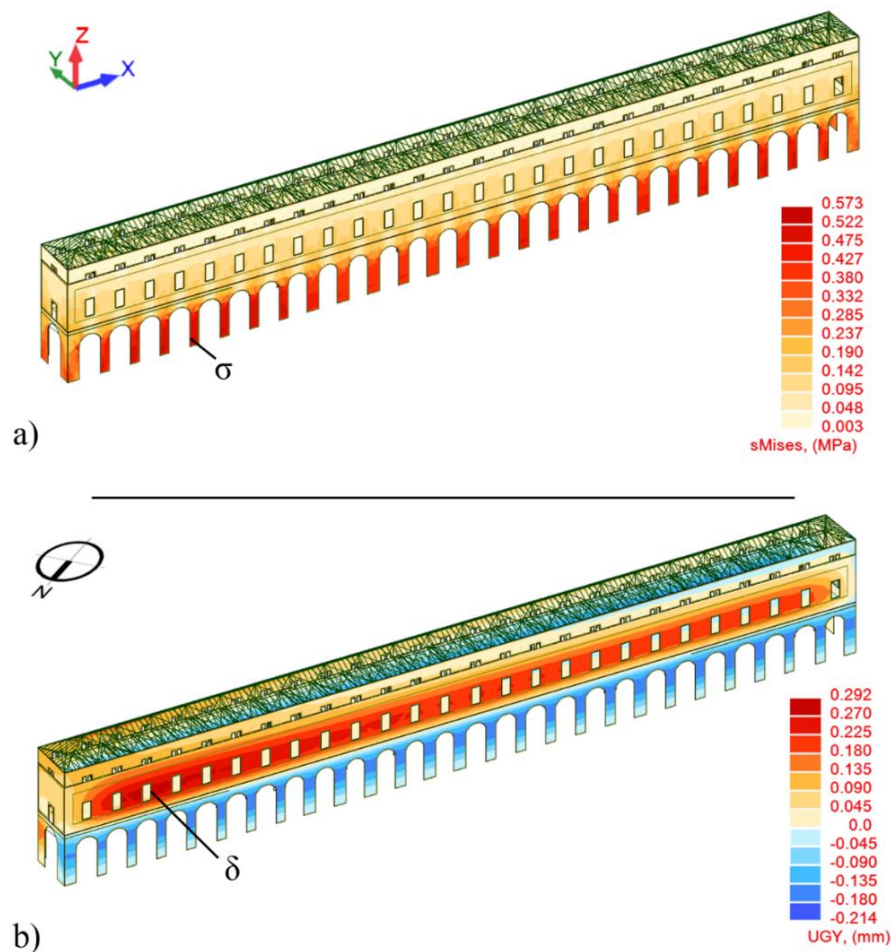
Element size	Y	X	$\sigma$	$\delta$	DOF	$\Delta DOF$
1.00	0.924	3.605	0.567	0.292	3.88E+04	-
0.90	0.923	3.488	0.562	0.277	4.36E+04	12%
0.80	0.923	3.440	0.542	0.270	4.71E+04	8%
0.70	0.922	3.441	0.530	0.271	5.27E+04	12%
0.60	0.920	3.408	0.532	0.278	6.35E+04	20%
0.50	0.920	3.390	0.533	0.281	7.91E+04	24%
0.40	0.919	3.362	0.533	0.283	1.09E+05	38%
0.30	0.918	3.338	0.533	0.284	1.85E+05	69%
0.20	0.916	3.321	0.538	0.285	4.12E+05	123%
0.10	0.915	3.308	0.538	0.287	1.60E+06	288%

Source: the author.

While the element size decreases continuously, the evaluated parameters have a sudden change of value for the element size 0.7 m, meaning that for such element size, the solution is not stable. For further refinement of the mesh, lower than 0.5 m, the solutions change slightly, meaning that the solution is stable. Such evaluation shows as was expected  $DOF$  increase ( $\Delta DOF$ ) (Table 3), while the other parameters converge when the element size decrease.

Equivalent Von Mises stress – based on the Von Mises failure criterion for masonry structures (LOURENÇO, 1996; MAVROULI et al., 2017; SYRMAKEZIS; ASTERIS, 2001) - are used to understand where maximum values of stresses are reached since they are qualitatively compared with the maximum value of compressive strength of the masonry structures. To provide such an assumption, the comparison between Mises stress and the compressive stresses must be done in the FEM model, confirming if the Mises stresses are reached due to the compressive stresses (Figure 54).

Figure 54 - Maximum Mises stresses (a) and maximum out-of-plane displacements (b) in the model with mesh size 1.00 m.



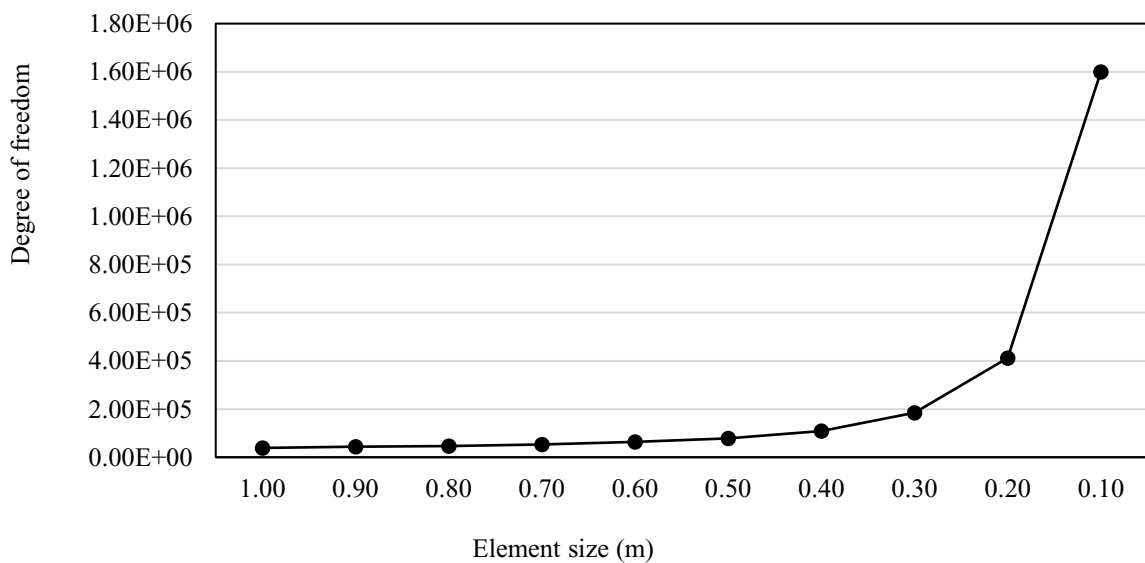
Source: the author.

Maximum values of Mises stresses are reached at approximately 1.00 m from the base of the columns, which is consistent with the insight of the visual inspection and historical-critical analysis. Indeed, some damages were observed in such part of the structural elements in the as-built configuration (Figure 45.e and 45.f). Maximum out-of-plane displacements are observed asymmetrically in the first-level masonry wall (Figure 54), which is also consistent with the out-of-plumb survey (Figure 51) developed by Dal Barco, Perobelli, Sartor (2016) and Saisi, Terenzoni (2018). Such behaviour should be carefully assessed in further research since it is a typical kinematic storey-mechanism of masonry buildings where floors have a stiffness function for the global structure.

#### 4.4.1 Mesh quality

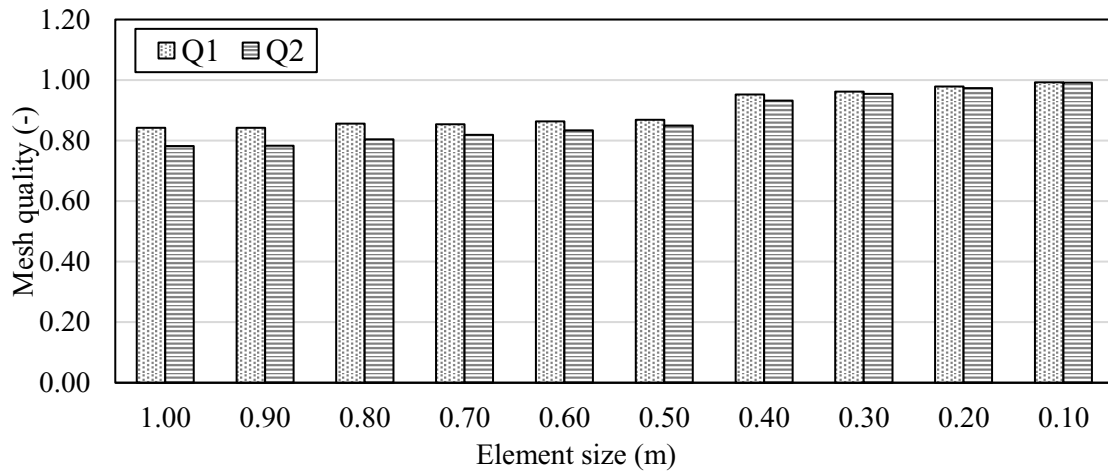
Mesh quality was assessed to obtain a good description of the structure. Averaged and weighted mesh quality are the parameters  $Q_1$  and  $Q_2$  selected for such investigation (see equations 30 and 31). In Figure 55, the variation of  $Q_1$  and  $Q_2$ , according to the degrees of freedom is described. Element size 0.2 corresponds to approximately 0.4 million DOF, allowing an increase of  $Q_1$  and  $Q_2$  of 14% and 22%, respectively. However, element size 0.1 m corresponds to 1.6 million of DOF, with an increase of 288% more than size 0.2. However, the mesh qualities increase only 16 and 24% (Figure 55).

Figure 55 - Exponential increase of degrees of freedom with the element size.



Source: the author.

Figure 56 - Average ( $Q_1$ ) and weighted ( $Q_2$ ) quality mesh according to the mesh size variation.



Source: the author.

Previous analyses allow selecting element size 0.2 m as consistent value for the representation of the structure. Such size avoids the time-consuming analysis of element size 0.1 m since no consistent variation in the results was obtained. Such a meshing process led the FE model to have 69179 nodes, with 67169 plane elements and 2676 bar elements; the total number of degrees of freedom is 412482. The obtained mesh quality of the proposed FE model is resumed by the parameters  $Q_1=0.979$  and  $Q_2=0.973$ .

#### 4.5 PRELIMINARY STRUCTURAL GLOBAL ASSESSMENT

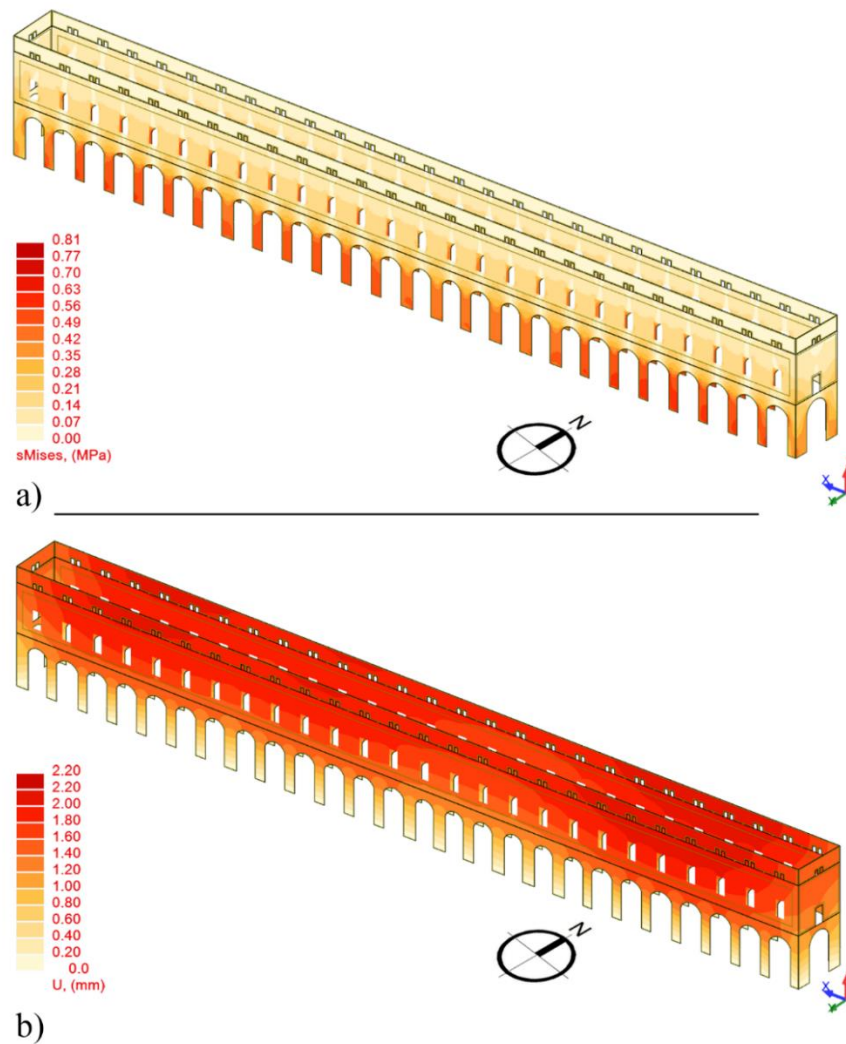
In the structural assessment of historical constructions, linear elastic analysis is always performed, before the application of more refined approaches. The linear elastic analysis was carried out to verify the consistency of the automatic exportation process of the H-BIM model. Such an approach aimed at increasing the accuracy of the H-BIM and FEM models, through the correction of the geometric errors and the structural element connections. Furthermore, once the errors were fixed, linear elastic self-weight and modal analyses were developed considering the dead loads to identify where maximum values of stress and strains were reached.

##### 4.5.1 Self-weight analysis

The self-weight analysis was carried out to verify the consistency of the geometrical building description and the material properties (PEÑA *et al.*, 2010), after the H-BIM-to-FEM integration. Total weight of the structure is about 50000 kN. The results of such analysis allow

the analyst to understand the general stress pattern (Figure 57.a). Stress pattern is consistent with the type of approaches which model the overall structure through its structural component, *e.g.* lumped mass, beams, panels (see Subsection 2.2.1). Hence, stresses (Von-Mises theory) are concentrated in the vertical axes of the columns, where the maximum value of 0.81 MPa is reached. Such value is five times less of the compressive strength corresponding to Young Modulus of 1800 MPa,  $f_m=4.00$  MPa. Moreover, it is three times less than the minimum value suggested by Circolare 617/09 (and further modification). Such results confirm that linear analysis is consistent with the hypotheses of the elastic range (PEÑA *et al.*, 2010). Total displacement results show that the deformations of the structure reach maximum values in the higher part of walls, asymmetrically, in the south-east side of the construction in according to the out-of-plumb surveys (Figure 57.b and 51.a)

Figure 57- Maximum Mises stresses (MPa) (a) and total displacements (mm) (b).



Source: the author.

Furthermore, dynamic behaviour was investigated in the range of 0-10 Hz since it allows to overcome the Italian standard threshold of 85% of participating mass (Table 4). Such a procedure allows identifying 30 modal shapes, obtained with the subspace iteration (AUTODESK, 2015). The evaluation of vibration modes on the main directions (Figure 58), in terms of frequencies and modal shapes, allows validating the models in the elastic field (PEÑA *et al.*, 2010). Moreover, the longitudinal mode has a participating mass  $RMX = 91.74\%$ . Such value is greater than 85%, which is the threshold allowed by the Italian National Standard (see Subsection 2.1.4.4.2) to describe the longitudinal dynamic behaviour of the structure.

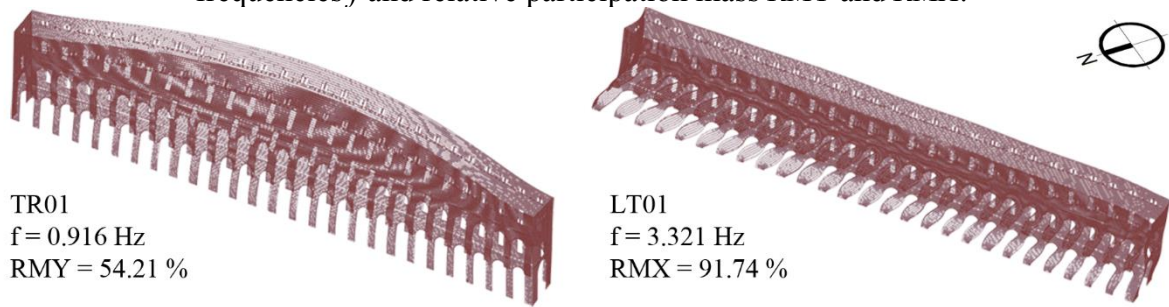
Table 4 - Vibration modes in the range of 0-10 Hz.

<b>Mode</b>	<b>f (Hz)</b>	<b>CMX (%)</b>	<b>CMY (%)</b>	<b>CMZ (%)</b>	<b>RMX (%)</b>	<b>RMY (%)</b>	<b>RMZ (%)</b>
1	0.916	0.00	54.21	0.00	0.00	54.21	0.00
2	1.146	0.00	54.21	0.00	0.00	0.00	0.00
3	1.514	0.00	62.02	0.00	0.00	7.81	0.00
4	1.908	0.00	62.02	0.00	0.00	0.00	0.00
5	2.327	0.00	66.95	0.00	0.00	4.93	0.00
6	2.766	0.00	66.95	0.00	0.00	0.00	0.00
7	3.208	0.00	71.01	0.00	0.00	4.05	0.00
8	3.321	91.74	71.01	0.00	91.74	0.00	0.00
9	3.700	91.74	71.01	0.00	0.00	0.00	0.00
10	3.829	91.74	85.81	0.00	0.00	14.80	0.00
11	4.172	91.75	85.81	0.00	0.00	0.00	0.00
12	4.222	91.75	87.59	0.00	0.00	1.78	0.00
13	4.827	91.75	87.92	0.00	0.00	0.33	0.00
14	4.840	91.75	88.39	0.00	0.00	0.47	0.00
15	5.220	91.80	88.39	0.03	0.05	0.00	0.03
16	5.529	91.80	88.91	0.03	0.00	0.52	0.00
17	5.577	93.09	88.91	0.03	1.29	0.00	0.00
18	5.682	93.09	88.91	0.03	0.00	0.00	0.00
19	6.302	93.09	88.91	0.03	0.00	0.00	0.00
20	6.630	93.09	89.35	0.03	0.00	0.44	0.00
21	7.198	93.09	89.40	0.03	0.00	0.05	0.00
22	7.556	93.09	89.40	0.03	0.00	0.00	0.00
23	7.702	93.09	89.40	0.19	0.00	0.00	0.16
24	8.183	93.09	89.40	0.19	0.00	0.00	0.00
25	8.507	93.09	89.65	0.19	0.00	0.25	0.00
26	8.671	93.16	89.65	0.19	0.07	0.00	0.00
27	9.080	93.16	89.65	0.19	0.00	0.00	0.00
28	9.260	93.16	89.66	0.19	0.00	0.01	0.00
29	9.349	93.16	89.66	0.19	0.01	0.00	0.00
30	9.965	93.16	89.66	17.59	0.00	0.00	17.40

Source: the author.



Figure 58 - Main vibration modes in the transversal ( $TR_{01}$ ) and longitudinal ( $LT_{01}$ ) directions: frequencies  $f$  and relative participation mass  $RM_Y$  and  $RM_X$ .



Source: the author.

#### 4.5.2 Built Environment evaluation

In the path to the knowledge of the structural behaviour understanding the relation of the analysed system with the built environment must be assessed. Hence, springs are introduced to simulate the boundary condition of the flying passage from the *Palazzo Giardino*. They were modelled in the middle plane of the walls and slab of such structural element. Range of values between  $10^3$  kN/m and  $10^5$  kN/m is investigated, according to similar researches (GENTILE; SAISI; CABBOI, 2015; IVORRA; PALLARÉS, 2006). Such values simulate the stiffness of the considered structural elements.

As expected, the longitudinal structural behaviour - in terms of frequencies and participating masses - is not influenced by such springs (Table 5). While transversal behaviour is slightly influenced, with increases lesser than 5%, the other transversal vibration modes have similar behaviour to the first transversal mode  $TR_{01}$  and springs have a negligible influence. Comparing the case in which no springs are modelled and the case in which springs have  $10^4$  kN/m, only the second longitudinal mode slightly vary (mode 17 in Table 4). As a result, second longitudinal mode frequency changes from 5.577 to 5.970 Hz, and its participating mass  $RM_Y$  increases of 5 %.

Table 5 - Influence of springs in the dynamic behaviour of the structure.

$k$ (kN/m)	$TR_{01}$ (Hz)	$LT_{01}$ (Hz)	$RM_X$ (%)	$RM_Y$ (%)	$\Delta f_{TR_{01}}$ (%)	$\Delta f_{LT_{01}}$ (%)
none	0.916	3.321	54.21	91.74	-	-
$10^3$	0.916	3.353	54.21	91.53	0.00	0.96
$10^4$	0.917	3.499	54.20	89.25	0.11	4.35
$10^5$	0.918	3.644	54.15	84.27	0.11	4.14

Source: the author.

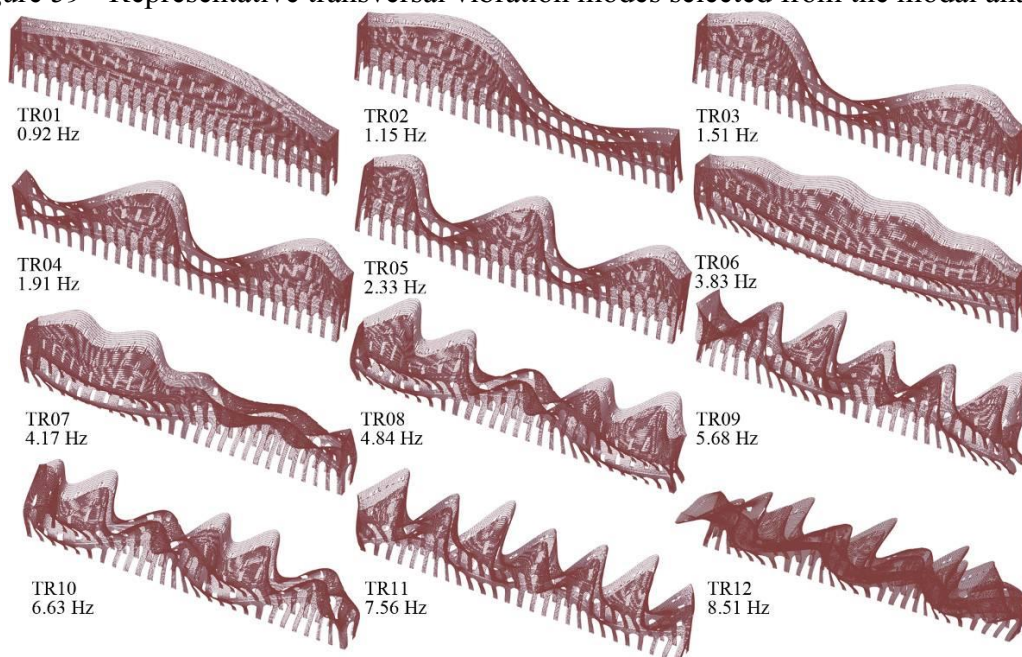
#### 4.6 MODAL ANALYSIS FOR THE DESIGN OF AMBIENT VIBRATION TESTS

As presented in the previous section, modal analysis (see subsections 2.2.2.5 and 3.2.3) was carried out to understand the mechanical behaviour of the structural model of *Galleria degli Antichi*. The results show as modes one and mode eight are the main modes in the transversal (Y) and longitudinal (X) directions, with current mass CMY of 54.21 % and CMX 91.74 % (Table 4), respectively. The first 30 modes reach a cumulative representative mass of RMX 93% and RMY 90% (Table 4). As was expected, most of the vibration modes involve the transversal direction of the building, which can be considered as the weakest one.

##### 4.6.1 Understanding of the overall structural behaviour

The structure seems to behave like a beam supported by springs in the transversal direction and like a cantilever beam in the vertical direction. Regarding the vertical direction, no representative modes were found in such a range, meaning that in such a range the structural behaviour involves mainly the horizontal plane. The only mode involving the vertical direction - which relative mass RMZ is 17.40 - is found with a frequency value of 9.965 Hz (Table 4). For these reasons, the understanding of the horizontal behaviour of *Galleria degli Antichi* will be relevant for the structural assessment.

Figure 59 - Representative transversal vibration modes selected from the modal analysis.

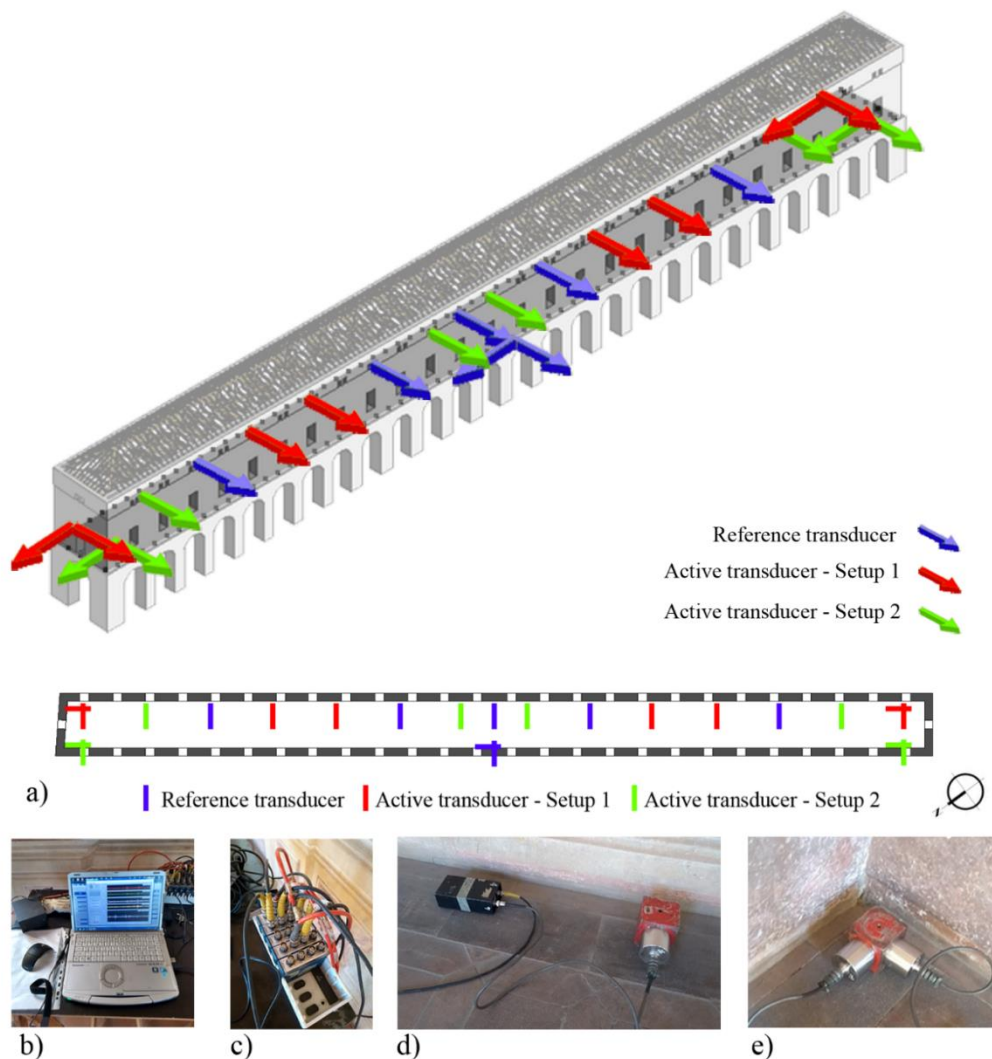


Source: the author.

#### 4.6.2 Design of the ambient vibration test

Modal analysis is used to design the setups of the ambient vibration test. Such a procedure mainly consists of the choice of the accelerometer location, to identify the vibration modes, differentiating one from the other (Figure 60). The extrados of the masonry vaults is selected as suitable for the monitoring, since it is a safe place to access, and it is already equipped with an electrical connection required for the AVT. Furthermore, the third level is not accessible, and the ground level is an open space and the control on the equipment represent an issue.

Figure 60 - Configurations of the two setups of the accelerometers in the ambient vibration test: piezoelectric accelerometer in uniaxial or bi-axial configuration (d) and (e) connected to a power unit/amplifier (d), whom signal is received from a data acquisition system (c) and elaborated in the acquisition computer Panasonic Toughbook CF-F9 (b).



Source: the author.

## 4.7 OPERATIONAL MODAL ANALYSIS

In this section, the operational modal analysis is developed to elaborate the results of the ambient vibration test carried out for the *Galleria degli Antichi*. Frequency Domain Decomposition was selected to obtain dynamic information of the structure, *.i.e.* frequencies and modal shapes. Such parameters allow comparing the numerical results to the experimental ones, providing insight concerning the consistency of the proposed methodology.

### 4.7.1 Ambient vibration test

The ambient vibration tests were conducted in February 2019. The data acquisition system was composed by 5 four-channel dynamic acquisition module NI 9234 (Figure 60.e) and 15 piezoelectric accelerometers Wilcoxon Research (WR) 731A (Figure 60.b), connected to a WR P31 power unit/amplifier (Figure 60.a). Each four-channel dynamic acquisition has a sampling frequency at 50 Hz. The piezoelectric accelerometer has a nominal sensitivity of 10 V/g peak acceleration  $\pm 0.5$  g.

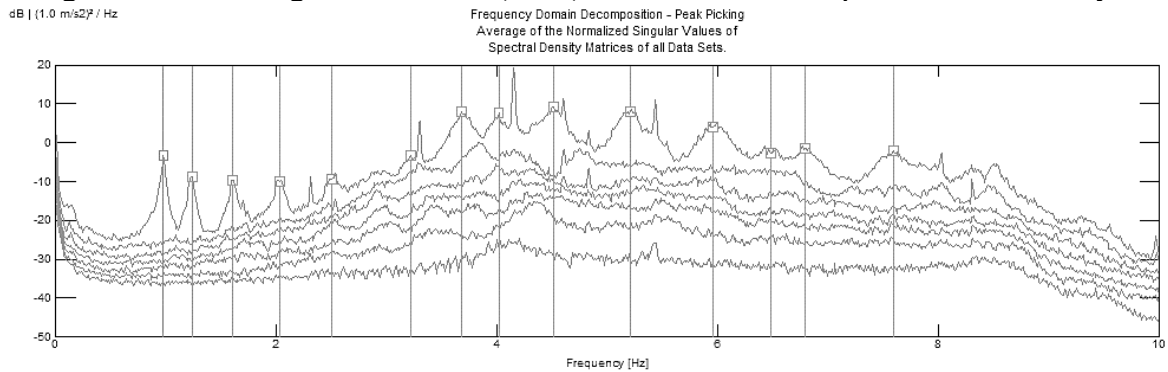
The AVT was carried out at the first-floor level (5.75 m). A series of two set-ups were required to cover the selected 23 measurement points (Figure 60): 15 accelerometers for each setup were available for the testing, which means that seven sensors were held stationary as reference transducers (Figure 60). In the tests, acceleration time-histories induced by ambient excitation were recorded for 2700 s each test at an interval of 0.005 s (200 Hz) to obtain accurate estimates of the modal parameters from OMA techniques. Signals converted to digital form were stored in a Panasonic Toughbook CF-F9 (Figure 60.d). The elaboration of the results of ATVs was carried out through the Operation Modal Analysis by the Frequency Domain Decomposition, which is presented in the next subsection.

### 4.7.2 Frequency Domain Decomposition

The software used for Frequency Domain Decomposition was Artemis (SVS, 2020). FDD allowed for the collection of time series led to the identification of the experimental vibration modes. The results of OMA in terms of frequencies are shown in Figure 61, where the first singular value lines (SV) of the spectral matrix is presented. As confirmed by the numerical modal analysis, the obtained vibration modes are in the horizontal directions (Table

6): 13 transversal and 1 longitudinal modal shapes ( $f = 3.213$  Hz). Their characteristics were resumed in Table 6. Frequencies, amplitudes, and phases in the two horizontal directions were elaborated to understand the experimental behaviour of the structure. Frequency and modal shapes of the extrados of the masonry vaults are represented in Figure 62.

Figure 61 - First singular value line (SVD) obtained from the operation modal analysis.



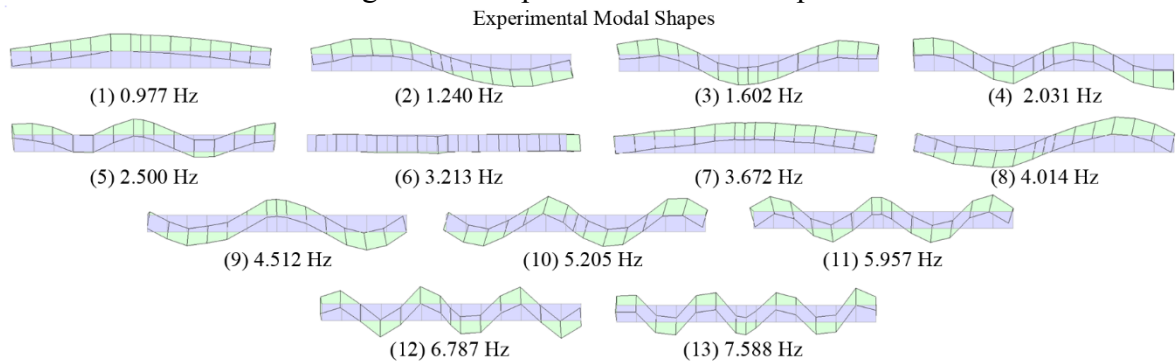
Source: the author.

Table 6 - Vibration modes obtained from the Frequency Domain Decomposition.

	1	2	3	4	5	6 (long)	7	8	9	10	11	12	13
f [Hz]	0.977	1.240	1.602	2.031	2.500	3.213	3.672	4.014	4.512	5.205	5.957	6.787	7.588

Source: the author.

Figure 62 - Experimental modal shapes.



Source: the author.

The Modal Assurance Criterion values are checked for the comparison of the experimental modes, where higher values mean that two modes are similar. In Figure 63, values are scaled from white to red, from minimum to maximum values of MAC, for the visual understanding of the results. As expected, since the vibration modes have two vertical orders before and after the longitudinal mode (Figure 59), some of those modal shapes are very similar

since they are experimentally obtained in the extrados of the masonry vaults, *e.g.* mode 1 and 7, 2 and 8, 3 and 9, 4 and 10, 5 and 11. Such results represent an issue for the comparison between experimental and numerical modes, whose solution is presented in the following section.

Figure 63- Modal Assurance Criterion obtained in Artemis®.

Mode	1	2	3	4	5	6	7	8	9	10	11	12	13	freq
1	1.00	0.05	0.10	0.04	0.50	0.04	0.98	0.07	0.09	0.06	0.16	0.02	0.06	0.977
2	0.05	1.00	0.04	0.17	0.26	0.04	0.08	0.95	0.05	0.11	0.01	0.05	0.05	1.240
3	0.10	0.04	1.00	0.02	0.10	0.02	0.15	0.18	0.86	0.03	0.09	0.02	0.13	1.602
4	0.04	0.17	0.02	1.00	0.08	0.07	0.02	0.09	0.21	0.80	0.02	0.14	0.12	2.031
5	0.50	0.26	0.10	0.08	1.00	0.18	0.44	0.25	0.25	0.18	0.68	0.08	0.19	2.500
6	0.04	0.04	0.02	0.07	0.18	1.00	0.03	0.05	0.07	0.06	0.15	0.11	0.03	3.213
7	0.98	0.08	0.15	0.02	0.44	0.03	1.00	0.04	0.10	0.06	0.14	0.08	0.08	3.672
8	0.07	0.95	0.18	0.09	0.25	0.05	0.04	1.00	0.19	0.06	0.05	0.01	0.07	4.014
9	0.09	0.05	0.86	0.21	0.25	0.07	0.10	0.19	1.00	0.17	0.12	0.01	0.03	4.512
10	0.06	0.11	0.03	0.80	0.18	0.06	0.06	0.06	0.17	1.00	0.27	0.08	0.13	5.205
11	0.16	0.01	0.09	0.02	0.68	0.15	0.14	0.05	0.12	0.27	1.00	0.18	0.11	5.957
13	0.02	0.05	0.02	0.14	0.08	0.11	0.08	0.01	0.01	0.08	0.18	1.00	0.03	6.787
14	0.06	0.05	0.13	0.12	0.19	0.03	0.08	0.07	0.03	0.13	0.11	0.03	1.00	7.588
freq	0.977	1.240	1.602	2.031	2.500	3.213	3.672	4.014	4.512	5.205	5.957	6.787	7.588	Hz

Source: the author.

#### 4.8 THE MAC-BASED SEMI-AUTOMATIC IDENTIFICATION PROCEDURE

The modal assurance criterion (MAC) was carried out for the identification of the numerical model according to the experimental results. Since experimental displacements are recorded at the extrados of the masonry vaults, the displacements of the numerical modal shapes were extracted in the Finite Element model nodes representing the experimental setup. Such an approach allows understanding which numerical modes have a higher level of correlation with the experimental modes. Furthermore, the evaluation of the experimental modal shapes - carried out at extrados of the masonry vaults - showed some similarities between the vibration modes before and after the longitudinal one (figures 59, 62 and 63).

Another issue was that comparing the numerical masonry vault extrados displacement to the experimental one, some modes are similar, and a visual comparison is not sufficient to assess the unique correspondence between experimental and numerical modes. Hence, the selection of the numerical modes corresponding to the experimental is solved through the MAC-based semi-automatic identification. The results of such a procedure are shown in terms of MAC in Figure 64.

Numerical modes 13 and 14 are similar - non-zero values of MAC - to the experimental mode 9, similarly 18-19 with 10, 20-21 with 11. Such cases are essential for the identification of numerical modes to be compared to experimental ones. Other crucial identifications concern



the numerical modes 22 and 24 in comparison with the experimental mode 12. Moreover, the numerical modes 25 and 28 compared with the experimental mode 13. Such a comparison cannot be done graphically, and the MAC-based procedure allowed such an issue.

Figure 64 - Modal assurance criterion of the experimental modes.

MAC		Experimental modes													f <sub>FEM</sub>
		1	2	3	4	5	6	7	8	9	10	11	12	13	
N u m e r i c a l  m o d e s	1	1.00	0.00	0.03	0.01	0.22	0.00	0.98	0.00	0.04	0.00	0.06	0.00	0.02	0.916
	2	0.00	0.99	0.00	0.04	0.05	0.00	0.01	0.87	0.00	0.00	0.00	0.00	0.00	1.146
	3	0.02	0.00	0.98	0.00	0.01	0.00	0.03	0.05	0.76	0.00	0.00	0.00	0.07	1.514
	4	0.00	0.10	0.00	0.98	0.00	0.00	0.00	0.01	0.04	0.60	0.00	0.03	0.00	1.908
	5	0.06	0.00	0.15	0.00	0.81	0.00	0.03	0.01	0.01	0.04	0.55	0.01	0.06	2.327
	6	0.00	0.13	0.00	0.49	0.00	0.00	0.00	0.01	0.01	0.02	0.00	0.42	0.00	2.766
	7	0.01	0.00	0.36	0.00	0.40	0.00	0.00	0.01	0.03	0.03	0.02	0.00	0.50	3.208
	8	0.00	0.00	0.00	0.00	0.01	0.97	0.00	0.00	0.00	0.00	0.01	0.00	0.00	3.321
	9	0.00	0.32	0.00	0.52	0.01	0.00	0.00	0.09	0.01	0.04	0.00	0.06	0.00	3.700
	10	0.99	0.00	0.04	0.00	0.17	0.00	0.99	0.01	0.03	0.00	0.05	0.00	0.03	3.829
	11	0.00	0.92	0.00	0.00	0.06	0.00	0.01	0.93	0.00	0.00	0.00	0.00	0.00	4.172
	12	0.00	0.00	0.60	0.00	0.29	0.00	0.01	0.04	0.11	0.01	0.04	0.00	0.14	4.222
	13	0.04	0.00	0.59	0.19	0.03	0.00	0.05	0.09	0.53	0.05	0.01	0.04	0.01	4.827
	14	0.04	0.00	0.71	0.12	0.03	0.00	0.05	0.01	0.91	0.01	0.01	0.00	0.01	4.840
	15	0.00	0.00	0.00	0.00	0.01	0.03	0.00	0.00	0.01	0.00	0.00	0.00	0.00	5.220
	16	0.04	0.00	0.00	0.00	0.67	0.00	0.02	0.00	0.25	0.02	0.18	0.00	0.12	5.529
	17	0.00	0.00	0.00	0.00	0.04	0.91	0.00	0.00	0.00	0.01	0.02	0.00	0.00	5.577
	18	0.00	0.01	0.00	0.73	0.00	0.00	0.00	0.00	0.03	0.91	0.00	0.00	0.00	5.682
	19	0.00	0.01	0.00	0.00	0.00	0.00	0.00	0.00	0.00	0.35	0.00	0.18	0.00	6.302
	20	0.08	0.00	0.00	0.00	0.67	0.00	0.06	0.00	0.12	0.03	0.91	0.03	0.00	6.630
	21	0.02	0.00	0.06	0.00	0.03	0.00	0.03	0.00	0.01	0.00	0.59	0.04	0.23	7.198
	22	0.00	0.02	0.00	0.10	0.00	0.00	0.00	0.00	0.00	0.04	0.00	0.77	0.00	7.556
	23	0.00	0.00	0.00	0.00	0.02	0.04	0.00	0.00	0.01	0.00	0.00	0.00	0.00	7.702
	24	0.00	0.00	0.00	0.00	0.00	0.00	0.00	0.00	0.00	0.00	0.00	0.67	0.00	8.183
	25	0.01	0.00	0.13	0.01	0.04	0.00	0.03	0.00	0.01	0.01	0.11	0.02	0.81	8.507
	26	0.00	0.00	0.00	0.00	0.00	0.25	0.00	0.00	0.00	0.00	0.00	0.00	0.00	8.671
	27	0.00	0.00	0.00	0.05	0.00	0.00	0.00	0.01	0.00	0.03	0.00	0.10	0.01	9.080
	28	0.09	0.00	0.06	0.03	0.01	0.00	0.11	0.00	0.09	0.03	0.02	0.03	0.66	9.260
	29	0.00	0.00	0.00	0.00	0.00	0.42	0.00	0.00	0.00	0.00	0.01	0.00	0.01	9.349
	30	0.06	0.07	0.05	0.00	0.02	0.10	0.07	0.08	0.08	0.01	0.00	0.00	0.01	9.965
f <sub>EXP</sub>		0.977	1.240	1.602	2.031	2.500	3.213	3.672	4.014	4.512	5.205	5.957	6.787	7.588	Hz

Source: the author.

The results of the identification procedure are shown in Table 7 and Figure 65. Once the dynamic characteristics of the heritage building were identified through AVT and OMA, further comparison with the FEA results is carried out. Such a comparison is aimed at assessing if the geometric, physical, and mechanical assumptions adopted in establishing the FE model have been chosen with a reasonable degree of approximation. Since the FE model was implemented through an H-BIM model, analysing the numerical model also provides a partial validation of the entire methodology.

Figure 65 - Comparison between experimental and numerical modes, in terms of frequency and modal shapes.

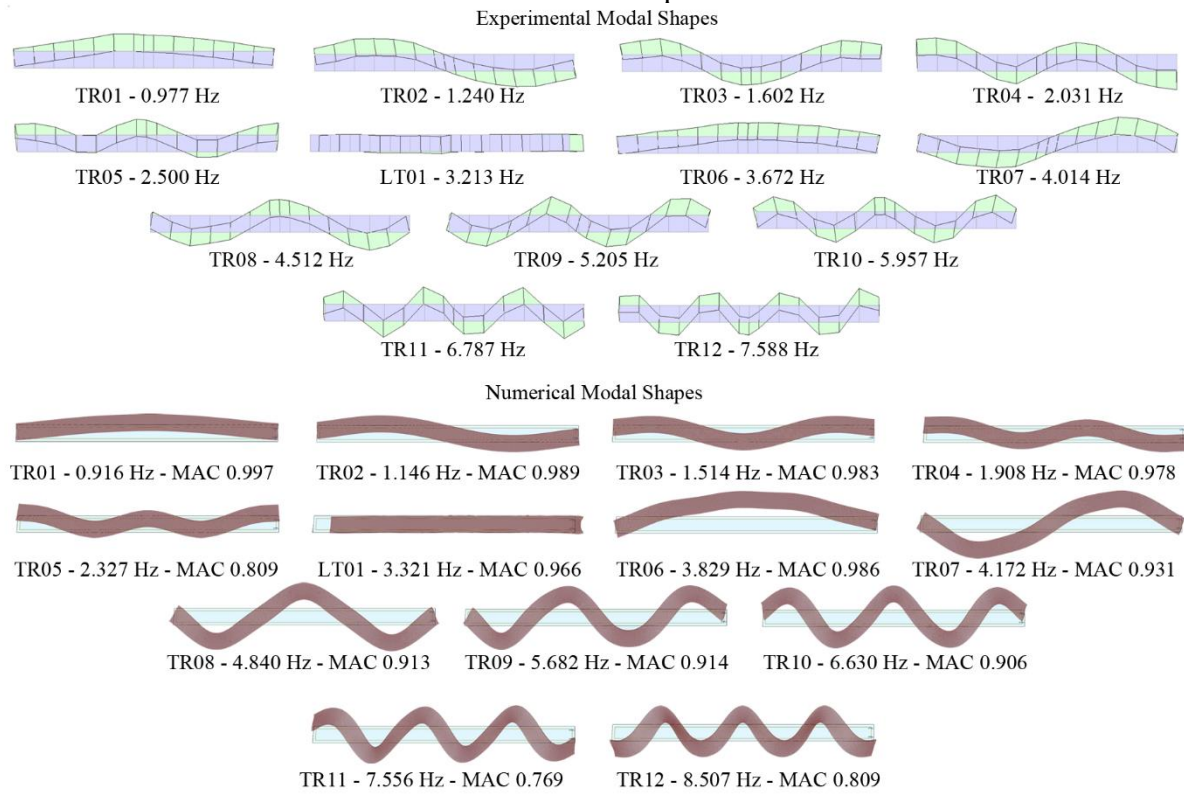


Table 7 - Modal assurance criterion and comparison between experimental (EXP) and numerical (FEM) modes.

EXP mode	Mode type	EXP f [Hz]	FEM mode	Mode type	FEM f [Hz]	MAC	DF (FEM/EXP)
1	TR01	0.977	1	TR01	0.916	0.997	-6.17%
2	TR02	1.240	2	TR02	1.146	0.989	-7.61%
3	TR03	1.602	3	TR03	1.514	0.983	-5.49%
4	TR04	2.031	4	TR04	1.908	0.978	-6.08%
5	TR05	2.500	5	TR05	2.327	0.809	-6.92%
6	LT01	3.213	8	LT01	3.321	0.966	3.37%
7	TR06	3.672	10	TR06	3.829	0.986	4.27%
8	TR07	4.014	11	TR07	4.172	0.931	3.95%
9	TR08	4.512	14	TR08	4.840	0.913	7.27%
10	TR09	5.205	18	TR09	5.682	0.914	9.16%
11	TR10	5.957	20	TR10	6.630	0.906	11.29%
12	TR11	6.787	22	TR11	7.556	0.769	11.32%
13	TR12	7.588	25	TR12	8.507	0.809	12.11%
average						0.919	7.31%

Source: the author.

Hence, the Modal Assurance Criterion (MAC) was used to compare experimental and numerical modal characteristics. The correlation between the dynamic characteristics of the



base FE model and the experimental results is shown in Figure 65 and Table 7. Correspondence between the mode shapes is one-to-one, with the worst MAC value being 0.77 and maximum frequency discrepancy 12.11%. The correlation between numerical and experimental behaviour seems to provide sufficient verification of the model main assumptions for this preliminary structural global assessment. Such insights are useful to increase the understanding of the overall structural behaviour of the analysed heritage building. However, further phases of the proposed methodology aim at improving such results.

#### 4.9 PARAMETER EVALUATION OF HISTORICAL CONSTRUCTION THROUGH SENSITIVITY ANALYSIS

The understanding of the influence of mechanical parameters on the structural behaviour of *Galleria degli Antichi* was carried out through the Sensitivity Analysis (SA). Furthermore, such an analysis allows understanding how the different structural element parameters influence the vibration modes.

##### 4.9.1 Definition of the uncertainty value range

The definition of the uncertainty value range is useful to understand the order of magnitude of each parameter, according to the assumption of the structural model. The structure is subdivided according to its geometry, and three levels of masonry walls are observed. For each level, the variation of the Young Modulus and the material density was investigated. As confirmed from similar researches (GENTILE; SAISI, 2007; RAMOS *et al.*, 2010; STANDOLI *et al.*, 2020), masonry Young modulus  $E$  has broad range values, for this reason, the range between 1.20 and 2.50 was analysed (Table 8), where 1.80 is the value assumed in the preliminary model (Table 1). Since the masonry vaults are simplified by their middle plane, an equivalent thickness was supposed, and its variation was evaluated. In the third level walls, the presence of cantilever arches (Figure 44.b) was assessed with an equivalent thickness variation. In the proposed SA, experimental modes are compared with FEM models, which numerical results vary according to the assessed parameter. Such a comparison is carried out through the MAC procedure (see Section 4.8)

Moreover, elastic springs of the boundary condition were investigated in Subsection 4.5.2. Springs have no influence on the transversal behaviour and very lightly influence on the

longitudinal behaviour. Furthermore, such type of information is lost in the direct integration between Robot<sup>®</sup> and Revit<sup>®</sup>. For these reasons, the assessment of such elements should be assessed in further research.

Table 8 - Definition of parameter values of Sensitivity Analysis: lower and upper bounds.

Parameter	Min	Base	Max	Unit	Description
$E_m$	1.20	1.80	2.50	GPa	Young Modulus - Masonry
$E_1$	1.20	1.80	2.50	GPa	Young Modulus - First level masonry pillars
$E_2$	1.20	1.80	2.50	GPa	Young Modulus - Second level masonry walls
$E_3$	1.20	1.80	2.50	GPa	Young Modulus - Cornice masonry walls
$E_v$	0.50	1.00	1.50	GPa	Young Modulus - Masonry vaults
$w_m$	16.00	18.00	20.00	kN/m <sup>3</sup>	Specific weight - Masonry
$w_1$	15.00	18.00	23.00	kN/m <sup>3</sup>	Specific weight - First level masonry pillars
$w_2$	15.00	18.00	23.00	kN/m <sup>3</sup>	Specific weight - Second level masonry walls
$w_3$	10.00	12.00	10.00	kN/m <sup>3</sup>	Equivalent specific weight - Cornice masonry walls
$w_v$	10.00	12.00	10.00	kN/m <sup>3</sup>	Equivalent specific weight - Masonry vaults
$t_c$	0.70	1.20	1.60	m	Equivalent thickness of cornice walls
$t_v$	0.50	0.60	0.80	m	Equivalent thickness of masonry vaults

Source: the author.

#### 4.9.2 Sensitivity analysis

Due to the considerations presented in the previous subsection, 12 parameters were selected for the SA. Consequently, 25 models were evaluated (2N+1). The “base” model has the values assumed as most suitable for the analysis. In the other 25 models, the unknown parameters are modified between their lower (min) and upper (max) bounds (Table 8). As previously mentioned, the modes to be compared of the 25 models were estimated carrying out the MAC comparison between each model with the experimental results.

Results of the SA coefficient (see Equation 57) are presented in Table 9. As expected, Young Moduli ( $E_m$ ,  $E_1$ ,  $E_2$ ,  $E_3$ , and  $E_v$ ) and specific weights ( $w_m$ ,  $w_1$ ,  $w_2$ ,  $w_3$ , and  $w_v$ ) are mostly affecting the structural response behaviour (figures 66 and 67). The analyses also suggest how the five modes corresponding to the first vertical order have similar behaviour (from TR01 to TR05). Furthermore, also the vibration modes of the second vertical order (from TR06 to TR12) behave similarly. Both groups of vibration modes depend on the Young Modulus of the masonry walls at the second and third levels of the construction ( $E_2$ ). Besides, only the specific weight of such walls ( $w_2$ ) is influencing all vibration modes (TR01 - TR12 and LT01).

Moreover, the masonry vault equivalent thickness influences the five vibration modes almost linearly, decreasing from the first to the 5th modes. The 7 modes of the vertical second-

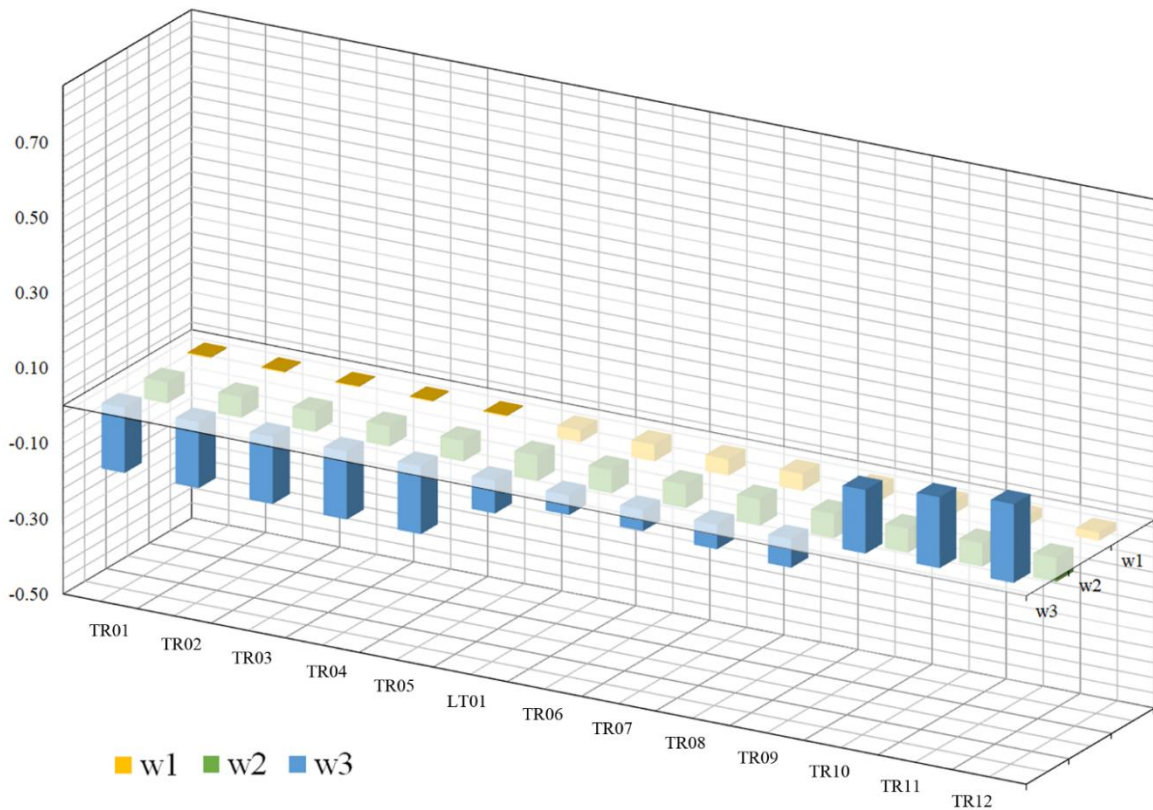
order (from TR06 to TR12) are influenced mostly by  $E_2$  and  $w_2$ . However, they also depend on the specific weight of pillars and vaults ( $w_1$  and  $w_v$ ) and the equivalent thickness of the third level masonry walls ( $t_c$ ).

Table 9 - Sensitivity coefficient for each assessed parameter.

	TR01	TR02	TR03	TR04	TR05	LT01	TR06	TR07	TR08	TR09	TR10	TR11	TR12
$E_m$	0.34	0.34	0.33	0.34	0.34	0.48	0.51	0.47	0.43	0.36	0.38	0.39	0.38
$E_1$	0.13	0.11	0.08	0.08	0.07	0.35	0.19	0.12	0.12	0.11	0.08	0.05	0.04
$E_2$	0.11	0.13	0.14	0.15	0.15	0.04	0.21	0.19	0.18	0.17	0.16	0.15	0.16
$E_3$	0.01	0.03	0.04	0.05	0.07	0.01	0.02	0.04	0.08	0.06	0.08	0.11	0.12
$E_v$	0.15	0.12	0.09	0.07	0.05	0.02	0.02	0.02	0.05	0.08	0.06	0.09	0.07
$w_m$	-0.31	-0.31	-0.30	-0.29	-0.29	-0.35	-0.35	-0.34	-0.32	-0.29	-0.25	-0.25	-0.21
$w_1$	-0.01	-0.01	-0.01	-0.01	-0.01	-0.09	-0.12	-0.10	-0.07	-0.08	-0.07	-0.05	-0.04
$w_2$	-0.15	-0.15	-0.14	-0.14	-0.14	-0.18	-0.16	-0.14	-0.16	-0.17	-0.16	-0.17	-0.18
$w_3$	-0.15	-0.15	-0.16	-0.16	-0.16	-0.07	-0.05	-0.10	-0.09	-0.07	-0.10	-0.10	-0.11
$w_v$	0.30	0.23	0.17	0.13	0.10	-0.02	-0.05	-0.02	0.05	0.09	0.09	0.14	0.12
$t_c$	-0.12	-0.08	-0.05	-0.02	0.03	-0.06	-0.04	0.02	0.15	0.12	0.13	-0.13	-0.10
$t_v$	0.44	0.31	0.20	0.14	0.10	-0.03	-0.03	-0.02	0.02	0.03	0.03	0.06	0.06

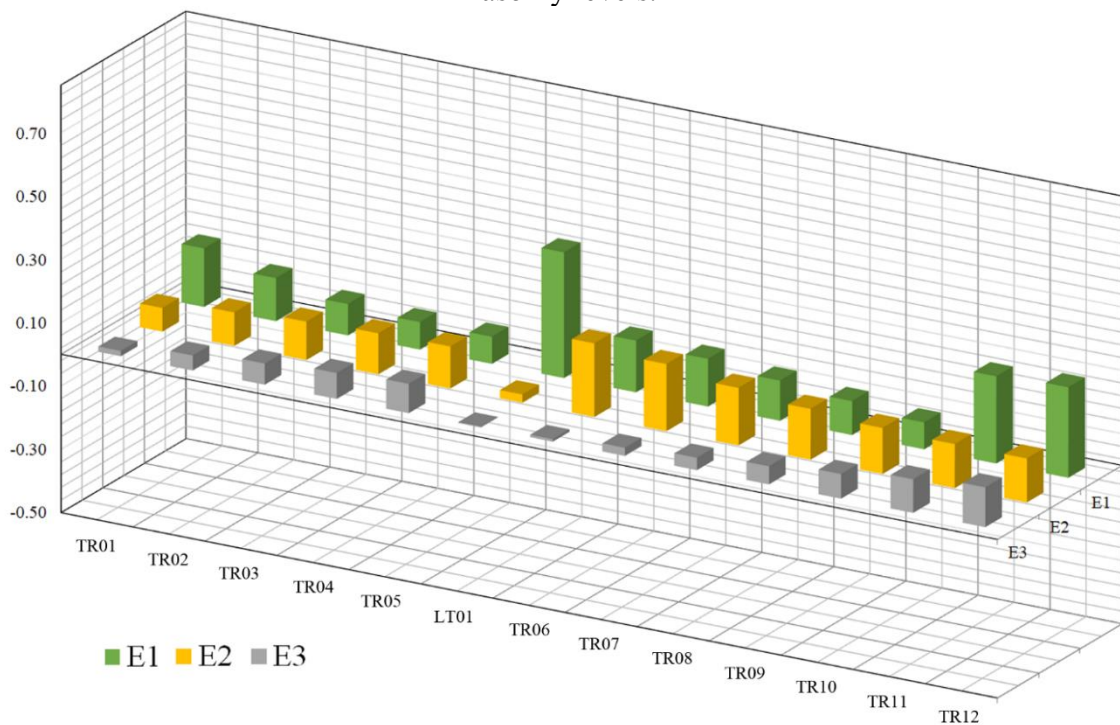
Source: the author.

Figure 66 - Sensitivity coefficients according to the variation of the weight of the three masonry levels.



Source: the author.

Figure 67 - Sensitivity coefficients according to the variation of Young Modulus of the three masonry levels.



Source: the author.

The longitudinal behaviour of the structure - in terms of first longitudinal modes (LT01) - mostly depends on the Young Modulus of the pillars,  $E_1$  (35%). The specific weight  $w$  of the masonry walls influences the longitudinal mode of -35%. The specific weight of masonry walls  $w_2$  has a sensitivity coefficient of 18%, meaning that such elements influence the longitudinal behaviour. Hence, in the proposed methodology, Sensitivity Analysis is carried out to understand the uncertainties of the structural model. However, SA also allows understanding which parameters should be updated to a better numerical representation of the structural behaviour. Such a procedure of Finite Element model tuning is presented in the following section.

#### 4.10 FINITE ELEMENT MODEL TUNING

The Douglas and Reid method (DOUGLAS; REID, 1982) was carried out to update the mechanical parameter of the model, searching for a better solution between initial upper and lower bounds (see subsections 2.2.5 and 3.3.2). The model uncertainties are investigated to assess which parameters mostly affect the structural behaviour results. Such an investigation allows understanding which parameters must be tuned to obtain the optimal FE model.

#### 4.10.1 Selection of the boundary condition range values

According to the results of the Sensitivity Analysis (Table 9), 7 parameters were selected for the FEM model updating: Young Modulus of column and wall masonry structures ( $E$ ), Young Modulus of masonry wall of the upper level ( $E_c$ ), Young Modulus of masonry vaults ( $E_v$ ), the specific weight of masonry wall of the upper level ( $w_c$ ), the specific weight of masonry vaults ( $w_v$ ), as the thickness of masonry wall of the upper level ( $t_c$ ), and the thickness of the masonry vaults ( $t_v$ ). The influence of such parameters on the structural behaviour is resumed in Subsection 4.10.3.

The parameters of the cornice walls of the upper level ( $w_c$ ,  $t_c$ ) and the masonry vaults ( $w_v$ ,  $t_v$ ) must be considered as equivalent parameters since the shell-type of Finite Elements required the simplifications of the structural model that were explained in Section 4.4. For the masonry column and second-floor walls, specific weight of 18.00 kN/m<sup>3</sup> was considered (Table 10). Furthermore, even in the further phase of updating  $w$  will be considered as fixed, its sensitivity coefficient is evaluated to increase the knowledge of such parameter on the model response. Such a parameter - referred to the masonry column and second-floor walls - is evaluated in the range of 16 to 20 kN/m<sup>3</sup>, according to NTC 2018 (CS.LL.PP., 2018).

Table 10 - Selected parameters to be updated.

	Lower bound	Base	Upper bound	Units
$E$	1.20	1.80	2.50	GPa
$E_c$	1.20	1.80	2.50	GPa
$E_v$	0.50	1.00	1.50	GPa
$w_c$	15.00	18.00	23.00	kN/m <sup>3</sup>
$w_v$	15.00	18.00	23.00	kN/m <sup>3</sup>
$t_v$	0.50	0.60	0.80	m
$t_c$	0.70	1.20	1.60	m

Source: the author.

#### 4.10.2 MAC-based semi-automatic identification

Since the experimental results were obtained at the extrados of the masonry vaults, the selection of the numerical modes was carried out at the same level. The choice of the vibration mode in each model - corresponding to the relative parameter modification - was efficiently carried out.

Some modal shapes seem to be similar in the transversal direction. For these reasons, the selection of the transversal modal shapes was carried out with the Modal Assurance

Criterion (MAC) (see subsections 3.2.4 and 4.8), comparing the numerical modes with the experimental results.

In Table 11, the MAC values of such semi-automatic identification are shown, which allow obtaining the frequencies of the identified numerical modes (Table 12). The evaluation of the minimum and maximum range values of the numerical frequencies allows obtaining insight on the FE model tuning. Indeed, it is suitable that the experimental frequencies are within such a range of numerical values (Table 12). Such frequencies will be used for the procedure of Model Updating, which will be presented in Subsection 4.10.4.

Table 11 - MAC values of numerical modes compared to the experimental data.

	TR01	TR02	TR03	TR04	TR05	LT01	TR06	TR07	TR08	TR09	TR10	TR11	TR12	min	max
Base	1.00	0.99	0.98	0.98	0.81	0.97	0.99	0.93	0.91	0.91	0.91	0.77	0.81	0.77	1.00
$E_{\min}$	1.00	0.99	0.99	0.97	0.79	0.96	0.98	0.92	0.94	0.92	0.93	0.80	0.82	0.79	1.00
$E_{\max}$	1.00	0.99	0.97	0.96	0.81	0.97	0.98	0.92	0.91	0.87	0.87	0.73	0.80	0.73	1.00
$E_{c,\min}$	1.00	0.99	0.98	0.97	0.81	0.97	0.98	0.92	0.90	0.78	0.90	0.89	0.88	0.78	1.00
$E_{c,\max}$	1.00	0.99	0.98	0.98	0.81	0.96	0.98	0.93	0.94	0.93	0.96	0.90	0.93	0.81	1.00
$E_{v,\min}$	1.00	0.98	0.96	0.95	0.81	0.97	0.99	0.94	0.94	0.93	0.96	0.90	0.91	0.81	1.00
$E_{v,\max}$	1.00	0.99	0.99	0.98	0.79	0.97	0.99	0.92	0.93	0.83	0.88	0.89	0.97	0.79	1.00
$w_{c,\min}$	1.00	0.99	0.98	0.98	0.81	0.97	0.99	0.93	0.93	0.95	0.94	0.84	0.88	0.81	1.00
$w_{c,\max}$	1.00	0.99	0.98	0.98	0.81	0.97	0.99	0.93	0.92	0.85	0.82	0.85	0.84	0.81	1.00
$w_{\min}$	1.00	0.99	0.98	0.98	0.81	0.97	0.99	0.95	0.94	0.89	0.87	0.76	0.82	0.82	1.00
$w_{\max}$	1.00	0.99	0.98	0.98	0.81	0.97	0.99	0.93	0.92	0.93	0.93	0.82	0.86	0.82	1.00
$w_{v,\min}$	1.00	0.99	0.98	0.98	0.81	0.97	0.99	0.94	0.93	0.89	0.87	0.75	0.76	0.75	1.00
$w_{v,\max}$	1.00	0.99	0.98	0.98	0.81	0.97	0.99	0.93	0.93	0.95	0.94	0.86	0.89	0.81	1.00
$t_{v,\min}$	1.00	0.99	0.98	0.97	0.81	0.97	0.99	0.95	0.95	0.92	0.93	0.82	0.86	0.81	1.00
$t_{v,\max}$	1.00	0.99	0.99	0.98	0.79	0.97	0.97	0.93	0.92	0.92	0.87	0.76	0.87	0.76	1.00
$t_{c,\min}$	1.00	0.99	0.98	0.97	0.80	0.97	0.98	0.91	0.86	0.83	0.95	0.94	0.90	0.80	1.00
$t_{c,\max}$	1.00	0.99	0.99	0.98	0.81	0.97	0.99	0.93	0.93	0.92	0.92	0.79	0.76	0.76	1.00
min	1.00	0.98	0.96	0.95	0.79	0.96	0.97	0.91	0.86	0.78	0.82	0.73	0.76		
max	1.00	0.99	0.99	0.98	0.81	0.97	0.99	0.95	0.95	0.95	0.96	0.94	0.97		

Source: the author.

Table 12 - Frequencies of the 2N+1 analyses, with N = 7 number of the parameters.

	TR01	TR02	TR03	TR04	TR05	LT01	TR06	TR07	TR08	TR09	TR10	TR11	TR12
EXP	0.977	1.240	1.602	2.031	2.500	3.213	3.672	4.014	4.512	5.205	5.957	6.787	7.588
Base	0.916	1.146	1.514	1.908	2.327	3.321	3.829	4.172	4.840	5.682	6.630	7.556	8.507
$E_{\min}$	0.817	1.029	1.368	1.722	2.094	2.727	3.191	3.538	4.190	5.016	5.945	6.850	7.748
$E_{\max}$	1.016	1.259	1.650	2.077	2.535	3.882	4.450	4.791	5.450	6.292	7.240	8.820	9.172
$E_{c,\min}$	0.910	1.125	1.474	1.845	2.238	3.317	3.815	4.129	4.744	5.496	6.830	7.824	8.831
$E_{c,\max}$	0.922	1.167	1.553	1.969	2.411	3.324	3.840	4.213	4.913	5.808	6.829	7.867	8.921
$E_{v,\min}$	0.848	1.072	1.426	1.811	2.227	3.318	3.796	4.077	4.602	5.284	6.079	6.926	7.838
$E_{v,\max}$	0.971	1.198	1.567	1.962	2.380	3.324	3.855	4.232	4.971	5.882	7.459	8.587	9.700
$w_{\min}$	0.932	1.166	1.539	1.939	2.366	3.420	3.953	4.307	4.990	5.857	6.818	8.418	9.536
$w_{\max}$	0.901	1.127	1.489	1.877	2.289	3.229	3.719	4.053	4.696	5.522	6.453	7.372	8.308

$W_{c,min}$	0.946	1.184	1.565	1.973	2.406	3.372	3.869	4.220	4.893	5.758	6.735	7.713	8.705
$W_{c,max}$	0.872	1.090	1.439	1.812	2.210	3.241	3.773	4.107	4.752	5.562	6.940	7.951	9.001
$W_{v,min}$	0.918	1.148	1.516	1.911	2.330	3.356	3.904	4.251	4.921	5.771	6.711	8.259	9.346
$W_{v,max}$	0.913	1.142	1.509	1.903	2.321	3.266	3.714	4.052	4.704	5.540	6.488	7.441	8.411
$t_{v,min}$	0.864	1.101	1.475	1.872	2.295	3.354	3.881	4.214	4.851	5.665	6.588	7.495	8.438
$t_{v,max}$	1.065	1.270	1.615	1.994	2.401	3.243	3.725	4.084	4.790	5.688	6.674	8.368	9.489
$t_{c,min}$	0.959	1.178	1.533	1.905	2.293	3.407	3.878	4.177	4.760	5.852	6.759	7.725	8.682
$t_{c,max}$	0.785	1.008	1.357	1.740	2.152	4.140	3.653	4.028	4.725	5.613	6.608	7.552	8.519
min	0.785	1.008	1.357	1.722	2.094	2.727	3.191	3.538	4.190	5.016	5.945	6.850	7.748
max	1.065	1.270	1.650	2.077	2.535	4.140	4.450	4.791	5.450	6.292	7.459	8.820	9.700

Source: the author.

### 4.10.3 Sensitivity coefficients for the understanding of the model parameters

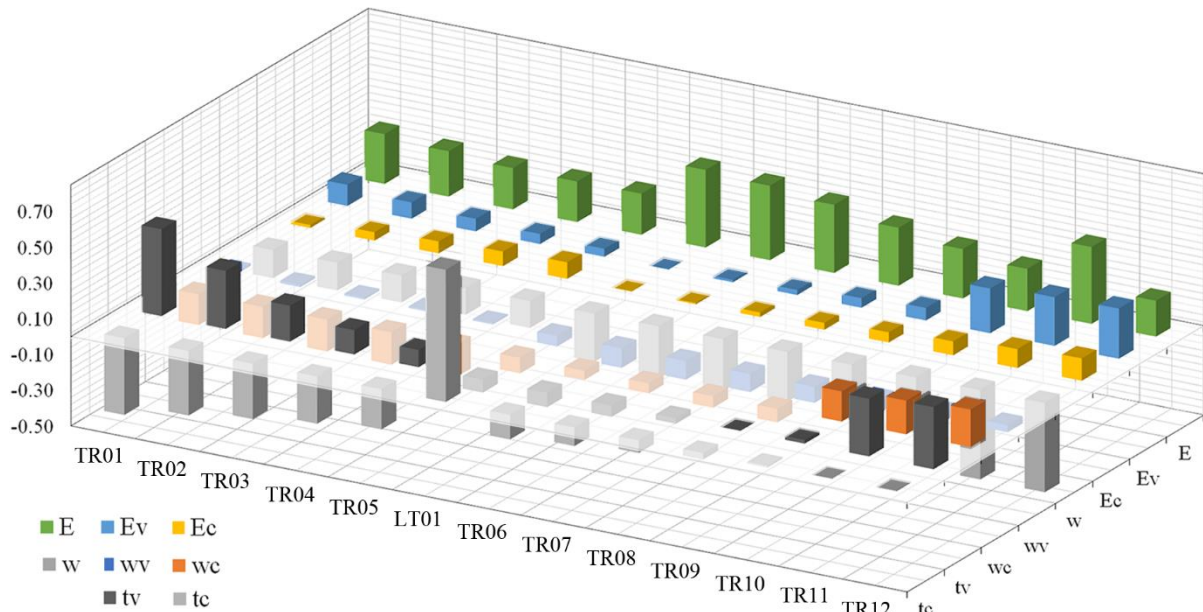
Sensitivity coefficients show how the model parameters affect the structural numerical response. In Figure 68 and Table 13, the influence of the selected parameters in the global structural response is resumed.

As expected,  $E$  influences all the vibration modes in the transversal and longitudinal directions (Figure 68), from 0.20 to 0.43 (Table 13). Moreover,  $E_v$  affects mostly the first transversal mode (0.12) and the modes TR10, TR11 and TR12 (0.25, 0.27, and 0.28, respectively). The weight of masonry vaults  $w_v$  affects mostly the global numerical response of the vibration modes from TR06 to TR12. On the contrary, the weight of the upper level of cornice masonry walls,  $w_c$ , affects mostly the vibration modes from TR01 to TR05. The geometrical parameters  $t_v$  and  $t_c$  also affect mostly the vibrational modes before the longitudinal mode.

Table 13 - Sensitivity coefficients of the selected parameters:  $E$ ,  $E_v$ ,  $E_c$ ,  $w$ ,  $w_v$ ,  $w_c$ ,  $t_v$ ,  $t_c$ .

	TR01	TR02	TR03	TR04	TR05	LT01	TR06	TR07	TR08	TR09	TR10	TR11	TR12
$E$	0.28	0.25	0.23	0.23	0.23	0.43	0.42	0.38	0.32	0.28	0.24	0.43	0.20
$E_v$	0.12	0.09	0.07	0.06	0.05	0.00	0.01	0.03	0.05	0.07	0.25	0.27	0.28
$E_c$	0.02	0.05	0.07	0.08	0.09	0.00	0.01	0.03	0.04	0.06	0.08	0.11	0.13
$w$	-0.15	-0.15	-0.14	-0.14	-0.15	-0.25	-0.26	-0.26	-0.27	-0.25	-0.24	-0.22	-0.21
$w_v$	-0.01	-0.01	-0.01	-0.01	-0.01	-0.06	-0.11	-0.10	-0.10	-0.09	-0.08	-0.05	-0.04
$w_c$	-0.17	-0.18	-0.18	-0.18	-0.18	-0.09	-0.05	-0.06	-0.07	-0.08	0.17	0.19	0.21
$t_v$	0.49	0.32	0.20	0.14	0.10	-0.07	-0.08	-0.06	-0.03	0.00	0.02	0.32	0.35
$t_c$	-0.43	-0.36	-0.31	-0.26	-0.23	0.74	-0.14	-0.10	-0.07	-0.04	-0.01	0.00	0.00

Source: the author.

Figure 68 - Sensitivity coefficient of the selected parameters:  $E$ ,  $E_v$ ,  $E_c$ ,  $w$ ,  $w_v$ ,  $w_c$ ,  $t_v$ ,  $t_c$ .

Source: the author.

#### 4.10.4 FE model updated

The solution of the model updating is carried out through the minimization of the selected frequency function (see equations 60 and 61). In Table 14, the results of Douglas and Reid method (1982) are given. The model updated with the optimized parameters (Table 14) was further analysed, and the obtained frequencies are as shown in Figure 69. The modes are automatically selected, where the highest MAC values are reached. Each numerical modal shape of the updated model was compared with the experimental modal shape to obtain such MAC values (Figure 69). Moreover, the functional discrepancies were calculated comparing the numerical mode frequencies with the experimental data (Figure 72).

Table 14 - Optimized parameters obtained from the DR algorithm.

$E$ [GPa]	$E_c$ [GPa]	$E_v$ [GPa]	$w_c$ [kN/m <sup>3</sup> ]	$w_v$ [kN/m <sup>3</sup> ]	$t_v$ [m]	$t_c$ [m]
1.74	1.97	0.59	15.1	21.61	0.71	1.08

Source: the author.

The obtained modal shapes of the updated model were compared with the experimental modal shapes through the Modal Assurance Criterion to verify how the updated model describes the structural behaviour of *Galleria degli Antichi*. The previous analysis shows that all modal shapes of the updated FEM model have an improved MAC value, meaning that the numerical modal shapes fit better with the experimental data (Figure 69). The optimization



improves the accordance between the numerical and experimental model in terms of frequencies and MAC, meanings that the updated model represents the experimental structural better than the base model (figures 69 to 71).

Figure 69 - MAC-based semi-automatic selection of numerical modes of the updated model.

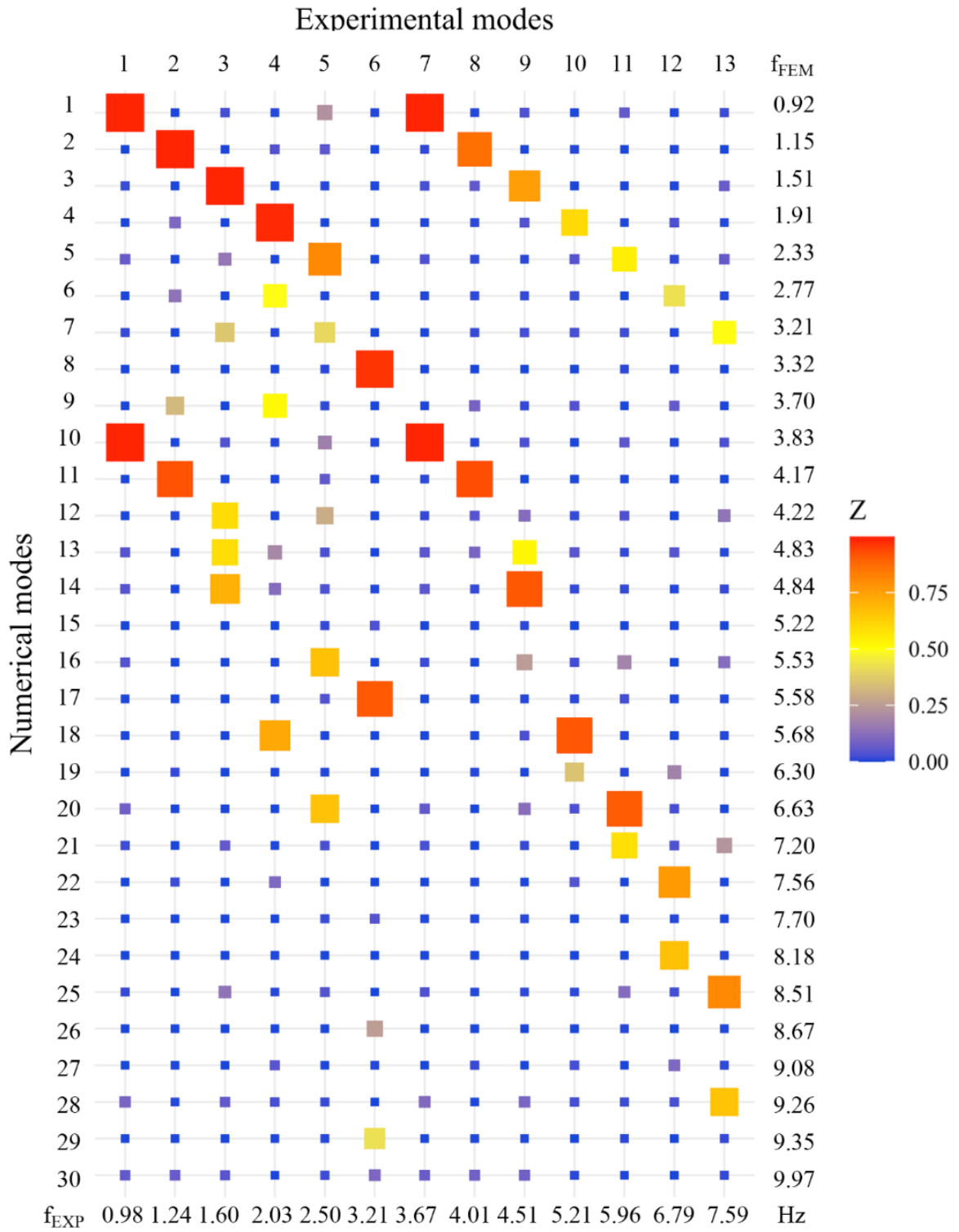
MAC	Experimental modes														f <sub>FEM</sub>	
	1	2	3	4	5	6	7	8	9	10	11	12	13	14		
N u m e r i c a l  m o d e s	1	1.00	0.00	0.03	0.01	0.22	0.00	0.98	0.00	0.04	0.00	0.06	0.00	0.00	0.02	<b>0.938</b>
	2	0.00	0.99	0.00	0.03	0.05	0.00	0.01	0.87	0.00	0.00	0.00	0.00	0.00	0.00	<b>1.161</b>
	3	0.02	0.00	0.98	0.00	0.00	0.00	0.03	0.05	0.79	0.00	0.00	0.00	0.00	0.06	<b>1.522</b>
	4	0.00	0.09	0.00	0.97	0.00	0.00	0.00	0.01	0.04	0.66	0.00	0.01	0.02	0.00	<b>1.912</b>
	5	0.07	0.00	0.12	0.00	0.81	0.00	0.04	0.01	0.01	0.04	0.62	0.00	0.01	0.04	<b>2.330</b>
	6	0.00	0.12	0.00	0.46	0.00	0.00	0.00	0.01	0.01	0.01	0.00	0.02	0.49	0.00	2.767
	7	0.01	0.00	0.34	0.00	0.37	0.00	0.00	0.01	0.03	0.03	0.01	0.01	0.00	0.56	3.204
	8	0.00	0.00	0.00	0.00	0.01	0.97	0.00	0.00	0.00	0.00	0.01	0.94	0.00	0.00	<b>3.252</b>
	9	0.98	0.00	0.04	0.01	0.16	0.00	0.98	0.01	0.04	0.00	0.05	0.00	0.00	0.04	<b>3.652</b>
	10	0.00	0.45	0.00	0.43	0.01	0.00	0.01	0.18	0.01	0.03	0.00	0.01	0.04	0.00	3.686
	11	0.00	0.86	0.00	0.00	0.05	0.00	0.01	0.93	0.00	0.00	0.00	0.00	0.00	0.00	<b>3.953</b>
	12	0.00	0.00	0.77	0.00	0.18	0.00	0.02	0.04	0.27	0.01	0.02	0.00	0.00	0.10	4.190
	13	0.06	0.00	0.68	0.00	0.11	0.00	0.07	0.03	0.94	0.00	0.04	0.00	0.00	0.00	<b>4.527</b>
	14	0.00	0.01	0.00	0.86	0.00	0.00	0.00	0.02	0.04	0.28	0.00	0.01	0.06	0.00	4.786
	15	0.00	0.00	0.00	0.00	0.01	0.03	0.00	0.00	0.01	0.00	0.00	0.01	0.00	0.00	5.083
	16	0.00	0.00	0.00	0.49	0.00	0.00	0.00	0.00	0.03	0.93	0.00	0.00	0.01	0.00	<b>5.258</b>
	17	0.03	0.00	0.02	0.00	0.75	0.00	0.01	0.00	0.11	0.06	0.33	0.00	0.00	0.10	5.461
	18	0.00	0.00	0.00	0.00	0.02	0.93	0.00	0.00	0.00	0.00	0.02	0.91	0.00	0.00	5.561
	19	0.07	0.00	0.01	0.00	0.41	0.00	0.06	0.00	0.08	0.02	0.96	0.00	0.03	0.04	<b>6.108</b>
	20	0.00	0.03	0.00	0.11	0.00	0.00	0.00	0.01	0.00	0.09	0.00	0.01	0.35	0.00	6.181
	21	0.00	0.00	0.10	0.00	0.08	0.00	0.01	0.00	0.00	0.01	0.12	0.00	0.05	0.44	6.993
	22	0.00	0.01	0.00	0.03	0.00	0.00	0.00	0.00	0.00	0.01	0.00	0.01	0.91	0.01	<b>7.013</b>
	23	0.00	0.00	0.00	0.00	0.01	0.04	0.00	0.00	0.00	0.00	0.00	0.02	0.00	0.01	7.666
	24	0.00	0.01	0.00	0.10	0.00	0.00	0.00	0.01	0.00	0.01	0.00	0.00	0.12	0.00	7.769
	25	0.04	0.00	0.09	0.01	0.00	0.00	0.05	0.00	0.05	0.01	0.06	0.00	0.01	0.93	<b>7.965</b>
	26	0.00	0.01	0.00	0.00	0.00	0.32	0.00	0.01	0.00	0.00	0.00	0.31	0.00	0.00	8.358
	27	0.04	0.00	0.01	0.00	0.02	0.21	0.04	0.00	0.01	0.01	0.00	0.19	0.00	0.00	8.416
	28	0.00	0.00	0.00	0.00	0.00	0.25	0.00	0.00	0.00	0.00	0.00	0.25	0.00	0.00	8.475
	29	0.00	0.00	0.01	0.00	0.00	0.24	0.00	0.00	0.02	0.01	0.00	0.20	0.00	0.00	8.509
	30	0.00	0.00	0.00	0.07	0.00	0.38	0.00	0.01	0.00	0.04	0.00	0.39	0.00	0.00	8.619
f <sub>EXP</sub>	0.977	1.240	1.602	2.031	2.500	3.213	3.672	4.014	4.512	5.205	5.957	6.475	6.787	7.588	Hz	

Source; The author.

Graphical comparison of the MAC-base structural identification of the experimental with the numerical modes of the base model (Figure 70) and the updated model (Figure 71) is useful to understand the accuracy of the proposed methodology. In such graphical comparison, each square is scaled in shape and colour according to the MAC value obtained from the comparison of experimental and numerical modes. Indeed, frequency discrepancies DF (Figure 72) and MAC values (Figure 71) of the updated model confirm the improvement of the

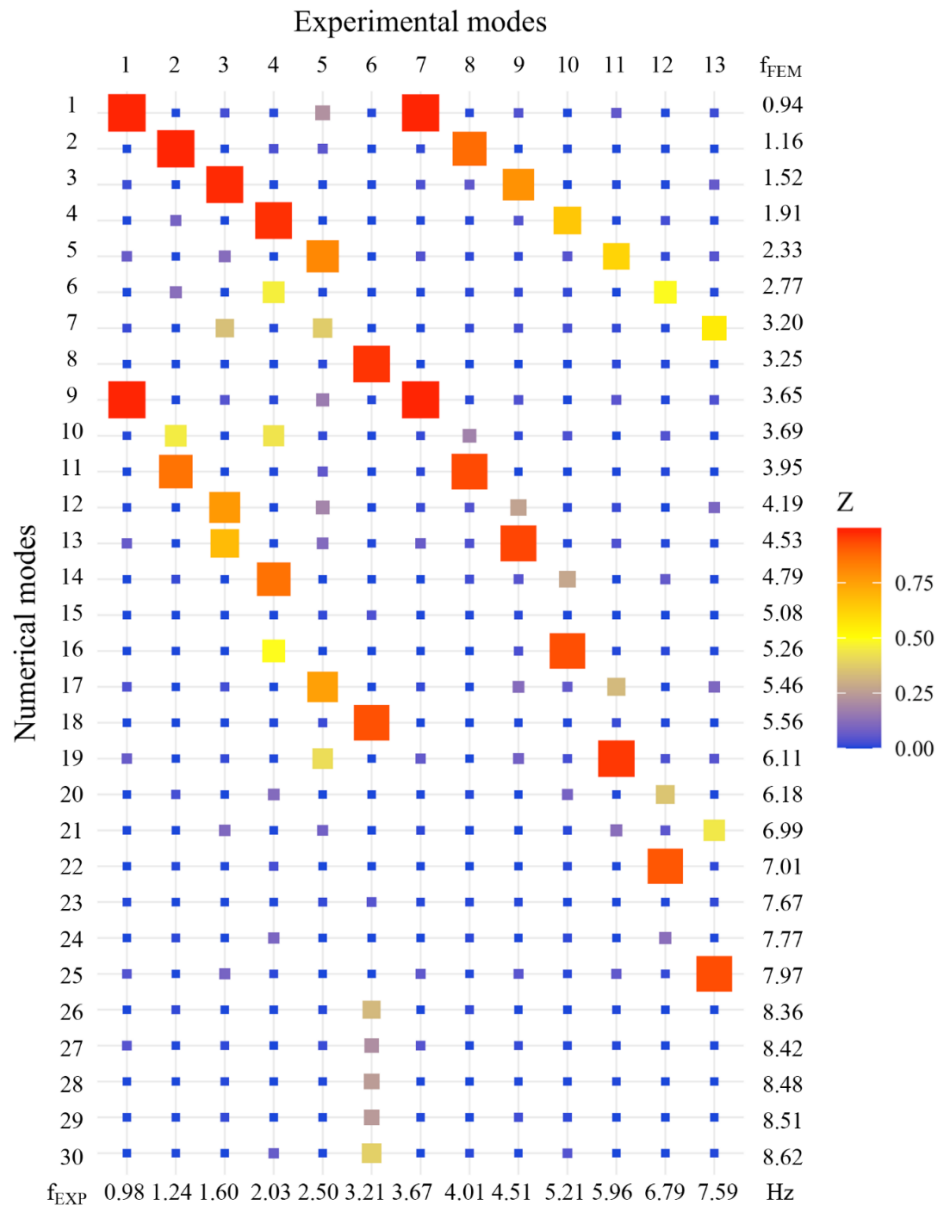
numerical representation of the heritage building structural behaviour that the numerical model fits better with the real behaviour of the structure.

Figure 70 - Comparison of numerical and experimental modes for the Base model.



Source: the author.

Figure 71 - Comparison of numerical and experimental modes for the Updated model.



Source: the author.

In Figure 72, Frequency Modal Assurance Criterion (FMAC) is shown. In Table 15, the numerical and experimental results are compared in terms of MAC, DF, and their percentage increasing,  $\Delta MAC$  and  $\Delta DF$ , respectively. In each point of Figure 7, numerical and experimental vibration modes are compared through a scaled circle representing the MAC value (Table 15), which colour is linearly ranged from red (minimum MAC value) to blue (maximum MAC value). In terms of geometrical description of the vibration modes, MAC values of the base model were higher than the threshold value 0.8, usually considered as a good result (GENTILE; SAISI; CABBOI, 2015). However, the mode TR11 of the base model has a value lower than

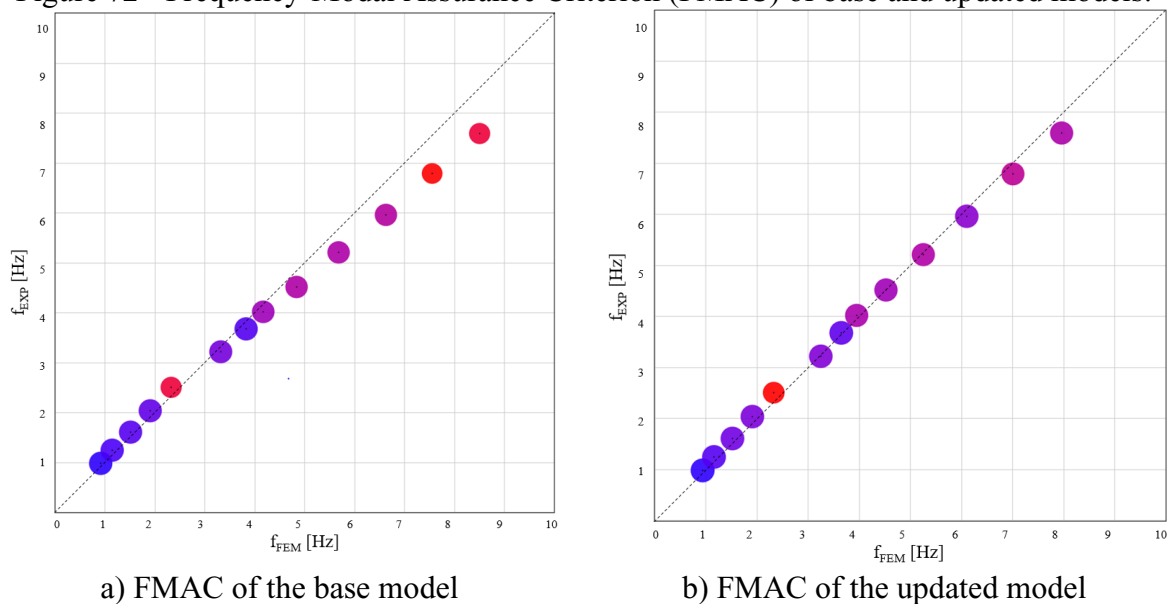
such a threshold. In the updated model, the MAC values increased in any vibration mode up to 19% in TR11 (Table 15). After the updating process, the MAC values - except for the mode TR05 which MAC does not vary from the base model - reached values higher than 0.9, matching the experimental structural behaviour of the historic building. The frequency discrepancies of the base model ( $DF_{BM}$ ) has an average error of 7.31 %, exceeding 10% in the last 3 modes, TR10, TR11 and TR12. After the updating process, the percentage increasing improves up to 95% for the mode TR08, with an average improvement of 54%, and a maximum value of  $DF_{UM}$  of 6,39 in the TR02. The description of the modes TR10, TR11, and TR12 was improved in terms of modal shape and frequency following the experimental results. The updating process increased the numerical match with the experimental structural behaviour of the construction in terms of MAC and DF.

Table 15 – Numerical comparison by modal assurance criterion and frequency discrepancy between the base model ( $MAC_{BM}$ ,  $DF_{BM}$ ) and the updated model ( $MAC_{UM}$ ,  $DF_{UM}$ ).

	TR01	TR02	TR03	TR04	TR05	LT01	TR06	TR07	TR08	TR09	TR10	TR11	TR12	average
$MAC_{BM}$	0.997	0.989	0.983	0.978	0.809	0.966	0.986	0.931	0.913	0.914	0.906	0.769	0.809	0.919
$MAC_{UM}$	0.997	0.987	0.976	0.969	0.813	0.966	0.983	0.934	0.942	0.928	0.96	0.914	0.932	0.946
$\Delta MAC$	0%	0%	-1%	-1%	0%	0%	0%	0%	3%	2%	6%	19%	15%	3%
$DF_{BM}$ [%]	-6.17	-7.61	-5.49	-6.08	-6.92	3.37	4.27	3.95	7.27	9.16	11.29	11.32	12.11	7.31
$DF_{UM}$ [%]	-3.97	-6.39	-4.95	-5.85	-6.81	1.21	-0.53	-1.5	0.33	1.02	2.53	3.33	4.97	3.34
$\Delta DF$	36%	16%	10%	4%	2%	64%	88%	62%	95%	89%	78%	71%	59%	54%

Source; The author.

Figure 72 - Frequency-Modal Assurance Criterion (FMAC) of base and updated models.



Source: the author.

Results confirm that the correspondence between numerical and experimental modes follows the hypothetical trend of a perfect match, along the diagonal. In the base model for the higher modes frequency discrepancies increase, and MAC values decrease, meaning that a loss of correspondence occurs (Figure 72.a). Such behaviour was optimized through the proposed methodology. As a result, the updating of the FE model with the experimental investigation results allowed obtaining a refinement of the numerical model (Figure 72.b). The proposed FE model tuning procedure permits a better understanding of the overall structural behaviour, also increasing the knowledge of the heritage building. Furthermore, the FE updated model could represent the so-called ‘numerical twin’ of the *Galleria degli Antichi*, which is a reliable reference for further research of Structural Health Monitoring.

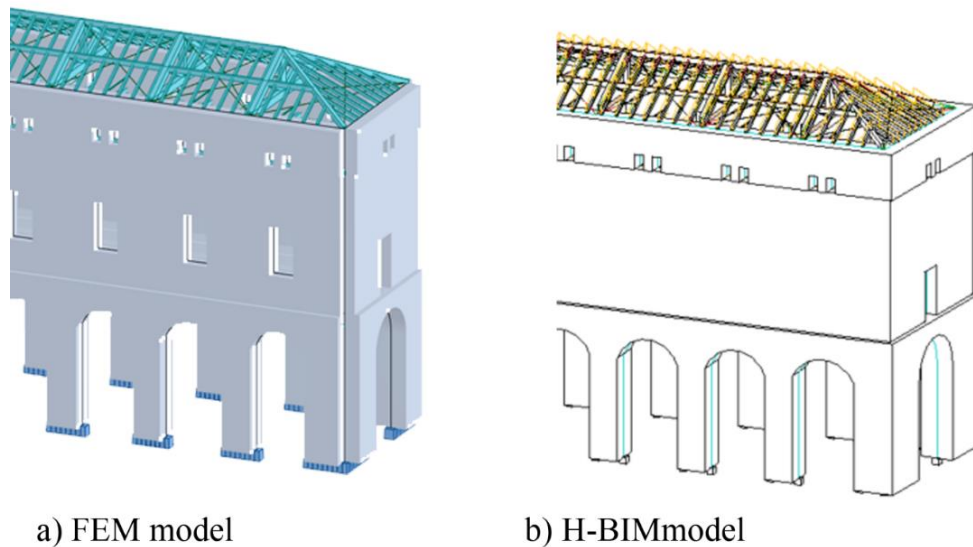
#### 4.11 H-BIM OPTIMAL MODEL

The information acquired with the FE model updating is subsequently uploaded in the H-BIM model. The procedure of information exchange between Robot<sup>®</sup> and Revit<sup>®</sup> is not trivial and requires special care, and it will briefly be presented in this section.

The FEM model can be directly imported from Robot<sup>®</sup> to Revit<sup>®</sup>, however, information loss can occur (Figure 73). Such an issue is overcome if, from the H-BIM model - from which the FE model was exported - model updating through direct integration is selected while both software Revit<sup>®</sup> and Robot<sup>®</sup> are running. Such a procedure allows the H-BIM model to acquire information about geometries, material properties, loads, type of connections and results of the FE analysis.

Information acquired in the FE Analysis can be explored, managed and represented directly in Revit<sup>®</sup> to facilitate the understanding of the global behaviour for future users, or uses. However, modal analysis results are not available directly in Revit<sup>®</sup>. Hence, external files - e.g. documentation, images, and technical report - must be associated with the H-BIM model through BIM objects defined according to the requirement of the user. In Appendix A, the procedure to create the family objects is described. It enhances the H-BIM model with the information acquired within the proposed methodology. As an example, the accelerometers are created in H-BIM model to represent setups of the AVT and to manage the information regarding the dynamic behaviour of the structure. However, this type of use of the BIM was presented in the literature review and extensively investigated by researchers. Hence, the application of the methodology to the case study of *Galleria degli Antichi* is concluded.

Figure 73 - Loss of the information in the FEM-to-BIM direct integration for a new H-BIM project.



Source: the author.

#### 4.12 PARTIAL CONCLUSION

The methodology involving historical and architectural research complemented by H-BIM and operational modal testing has been applied to the significant heritage building of *Galleria degli Antichi*, Sabbioneta (Italy). Such an application was useful to develop and to validate the proposed methodology (Section 3).

The experience collected in the present investigation allows drawing some conclusions:

- a) merging the information collected by historical and architectural research, H-BIM and dynamic tests allow solving the main uncertainties of the numerical models and assessing the structural state of preservation of the building, in a fully non-destructive way;
- b) *in-situ* inspections, thematic surveys and comparison of the archive documents with the visual inspection resumed within the H-BIM model improve the knowledge of overall structural behaviour of heritage buildings;
- c) experimental tests in operational conditions provide quantitative parameters (resonant frequencies and mode shapes), which are representative of the structural condition and contribute to the knowledge of the as-built configuration;

d) further steps of FE model refinement increases the level of knowledge; main parameters affecting the global structural behaviour were updated by Douglas and Reid method. As a result, an improvement of the numerical results was obtained. The percentage increasing of modal assurance criterion values,  $\Delta MAC$ , reached up to 19%, improving the average values of 3%. The percentage increasing of frequency discrepancy,  $\Delta DF$ , reached up to 95%, improving the average values of 54%. Indeed, the numerical representation of the experimental behaviour was improved, both in terms of frequencies and modal shapes.

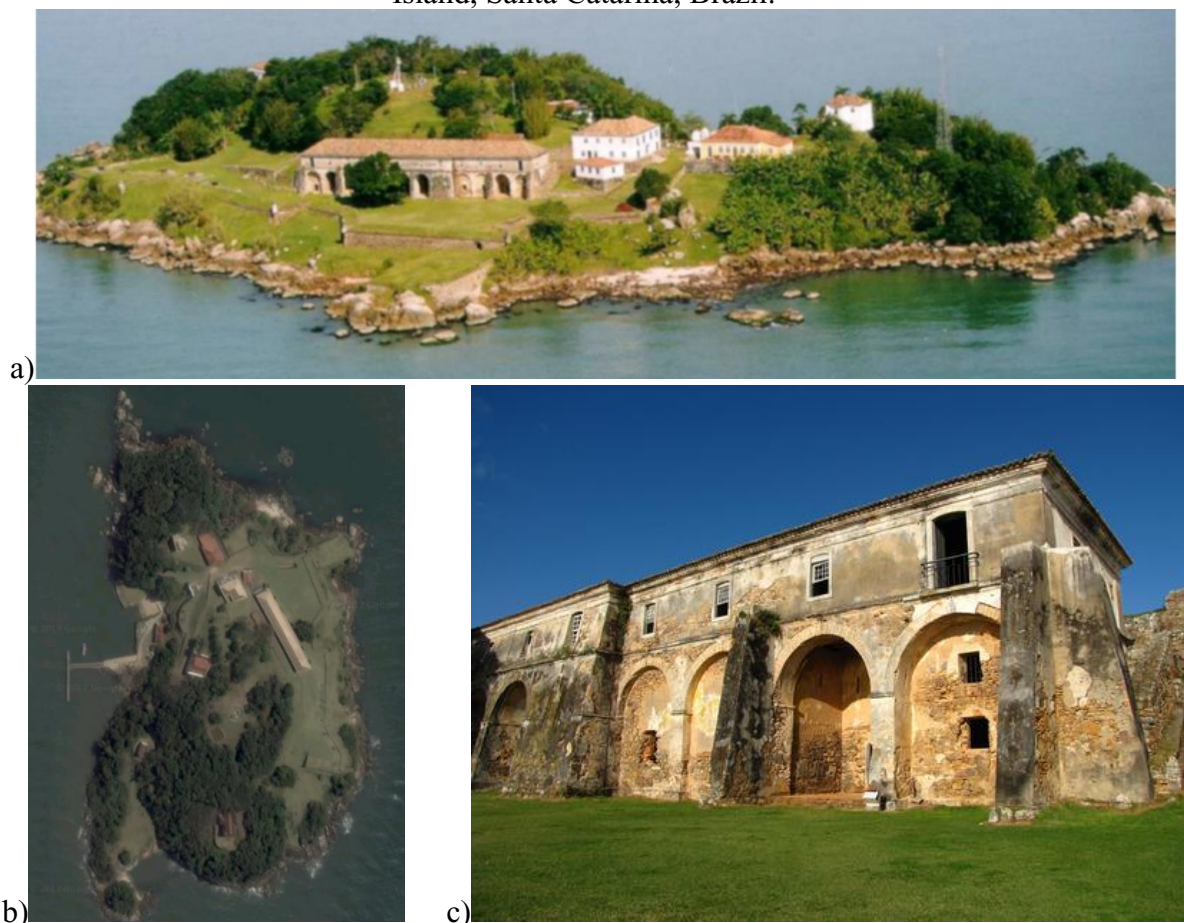




## 5 UNDERSTANDING THE STRUCTURAL BEHAVIOUR OF HISTORICAL BUILDINGS AND THE TEST PLANNING: THE CASES OF THE *QUARTEL DA TROPA*

In this chapter, the proposed case study of the *Quartel da Tropa* is presented. Such heritage building - belonging to the fortress of Anhatomirim Island (SC), Brazil - was chosen to apply the proposed methodology (Figure 74). The construction is one of the main buildings of the Fortress of Santa Cruz, located on Anhatomirim Island, municipality of Governador Celso Ramos, State of Santa Catarina, Brazil. Such an approach also leads to suggest possible special cares for the test planning and future structural intervention proposals.

Figure 74 - Overall view (a) and north-facing orthophoto (b) of the fortress of Anhatomirim Island, Santa Catarina, Brazil.



Sources: Backert and Sartori from Tonera (2010) (a, c). Google (b).

The objective of this chapter is to show how to improve the path to knowledge of a historic building through the proposed H-BIM-oriented methodology (CALÌ; DIAS DE

MORAES; DO VALLE, 2019). Furthermore, such an application aims at the development of the proposed H-BIM workflow during the process between architectural and structural modelling of a heritage built. Such an approach allows understanding the influence of the constructive phases in the structural behaviour of a historical building and investigating the possible reasons for such modifications (CALÌ; DIAS DE MORAES; DO VALLE, 2020).

In this case study, the increase of the level of knowledge of a historical building also allows understanding the evolution of constructive phases through the use of HBIM (H-BIM) (ANTONOPOULOU; BRYAN, 2017) and Finite Element method analysis (BATHE, 2006; ZIENKIEWICZ, O. C., TAYLOR, 2000). Furthermore, a systematic approach to the design of the *in-situ* test is proposed, through the sensitivity analysis aimed at the understanding of the most relevant parameters.

## 5.1 MAIN HYPOTHESES OF THE RESEARCH CASE STUDY

The validation of the proposed methodology was presented in Chapter 4. It showed how the H-BIM oriented approach allows developing FE models that are consistent with the real structural behaviour. Indeed, even the untuned FE model helps in the understanding of structural behaviour, giving reliable results (see Subsection 4.5.1). Such hypotheses allow supposing that after the identification of the as-built configuration - where the numerical model is consistent with the real behaviour of the structure - a regressive knowledge procedure can be carried out to understand the constructive evolution of the heritage building.

The H-BIM model can be obtained directly from point clouds - generated by laser scanning or photogrammetry processing- or from 2D technical drawings. In this case study research, the author chooses a heritage building where only technical drawings are available. Such an approach allows extending the proposed methodology to the general case where the analyst does not have the laser scanning or photogrammetric surveys. In the proposed case studies, the author used Revit<sup>®</sup> and Robot<sup>®</sup> as H-BIM and FEM software, respectively. Such a procedure is explained in the following subsections. Furthermore, the approach proposed to the *Galleria degli Antichi* - where the design of the experimental test (AVT) was carried out in relation with the structural analysis results - is developed for the design of several non-destructive tests. In such a way, the results obtained from the AVT test (see Subsection 4.7.1) could be improved by the adoption of a comprehensive experimental campaign to increase the level of knowledge of the heritage building.

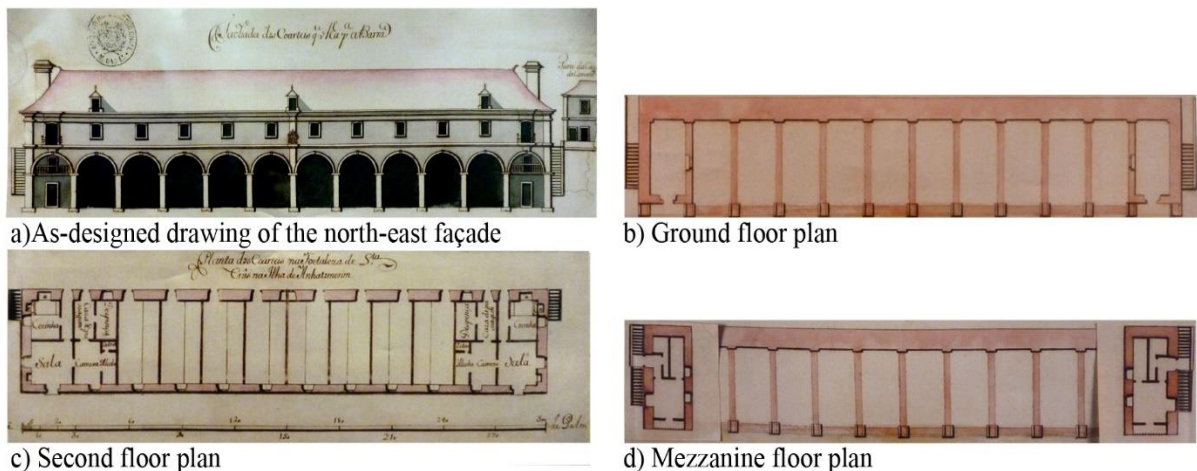
## 5.2 HISTORIC AND DOCUMENTARY RESEARCH

A historical masonry structure is selected as an example to apply the proposed multidisciplinary methodology. Such a case study is the *Quartel da Tropa* (literally Troop Barracks), which is the largest among Brazilian fortifications (Figure 74). The construction was designed by the Portuguese military engineer José da Silva Paes. In the 18<sup>th</sup>-century, the fortress belonged to one of the cornerstones of the triangular defence system, still formed by the Fortresses of São José da Ponta Grossa and Santo Antônio de Ratonés. This system was designed to protect the northern side of Santa Catarina Island from foreign attacks - mainly from Spain - and consolidate the Portuguese occupation of Southern Brazil in the eighteenth century.

### 5.2.1 Understanding the constructive evolution of the structure

The evaluation of constructive evolutions and construction identification was obtained through the historical-critical analysis of the documental sources (CALÌ *et al.*, 2019; TONERA, 2010; TONERA; FRAGOSO, 2013). The as-designed project demonstrates the influence of Renaissance architecture (TONERA, 2010; TONERA; FRAGOSO, 2013) (Figure 75.a). Such evaluation helps to understand the structural performances of the construction and the possible modifications caused by each constructive phase (MAGENES; MENON, 2009).

Figure 75 - As-designed representation of the *Quartel da Tropa*: a) north-east façade, b) ground floor plan, c) second-floor plan and d) mezzanine floor plan.



Source: Arquivo Histórico Ultramarino, Lisbon from Tonerá (2010).



The structure - length 66.8 m, width 9.85 m, height 10.5 m - is characterized by the presence of masonry arches in the longitudinal direction (figures 74 and 77.a) - north-east façade - and in the transversal direction (Figure 77.b), connecting the thick slope-shaped retaining wall to the main façade (Figure 77.c). A central slope-shaped masonry element and buttresses were introduced in the north-east façade along with the constructive history of the building (Figure 77.e), but no information about the reasons for such intervention was found in the documentary research (TONERA, 2010; TONERA; FRAGOSO, 2013).

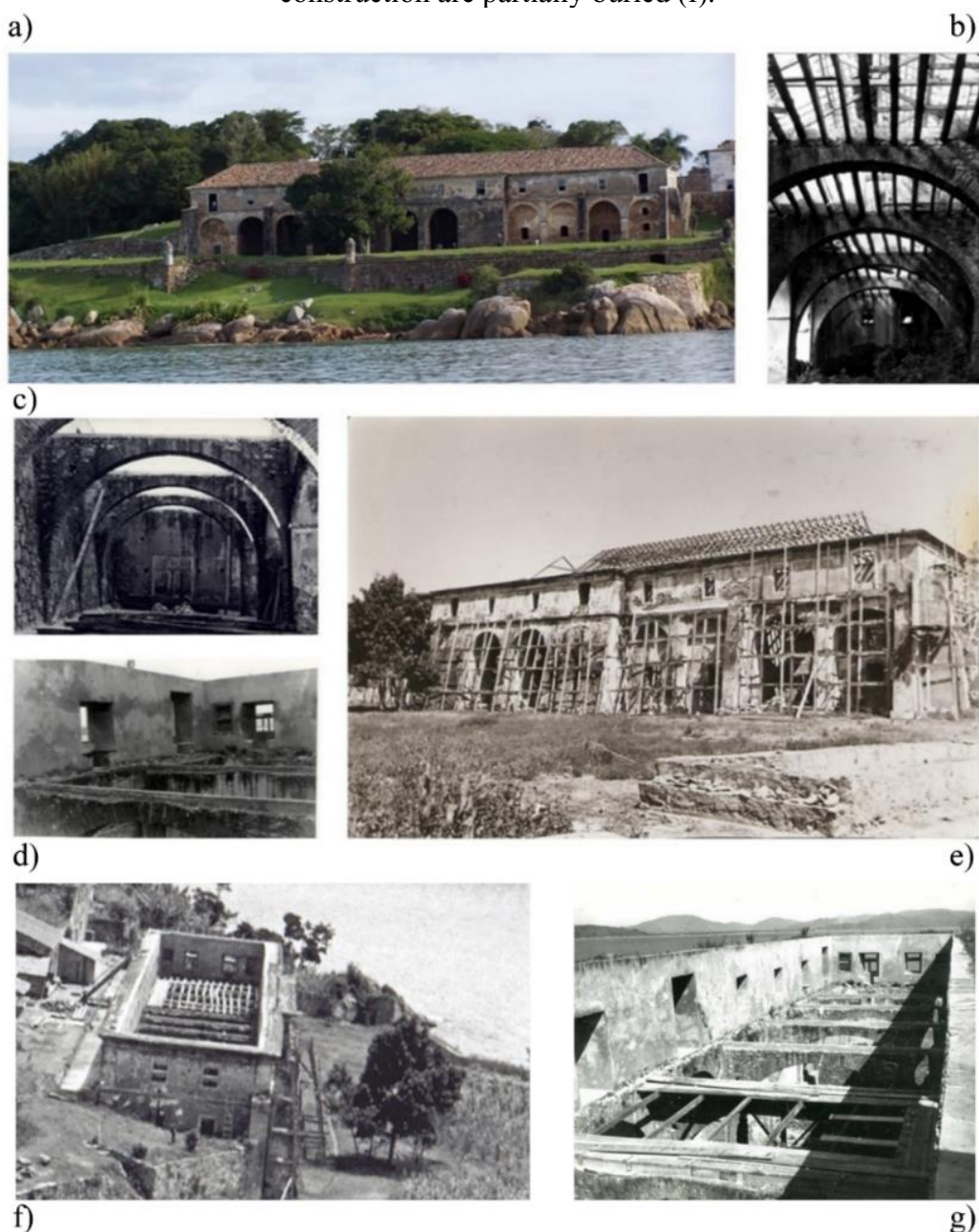
Figure 76 - *Quartel das Tropas* in the 1970s structural interventions (a, b, c, and d). Lateral partially buried façades in three sides of the construction (b, c, e and f).



Source: the author (a, b). Archive of IPHAN (c, d, e, f) from Tonera (2010).

The structure had two symmetrical mezzanines at the opposite side of the main façade (Figure 83). However, in the as-built configuration (Figure 83.d), only the mezzanine of the north-west part still exists (Figure 76). The access to such mezzanines was in the partially buried lateral façades (Figure 77.f). The first level of the south-west façade is buried, and a thick slope shaped wall retains the soil action (Figure 77.c).

Figure 77 - *Quartel da Tropa* (a) in the ‘as-built’ configuration after the 1970s restorations (b, c, d, e) where the simple trussed roof structure (b) was replaced with a collar tie beam (e) and concrete beams (d) were introduced on the masonry arches (c) and (g); three sides of the construction are partially buried (f).



Source: Archive of IPHAN, from Tonerá (2010).

### 5.2.2 Historical-critical analysis and survey

Historical-critical analysis of the documental researches and existing geometric surveys (TONERA, 2010; TONERA; FRAGOSO, 2013) allow increasing the knowledge of the heritage structure and creating the H-BIM model where the constructive building evolution. Such an evolution is resumed and represented by four main phases (TONERA, 2010; TONERA; FRAGOSO, 2013). According to the historical researches in the archives of the *Instituto de Patrimônio Histórico e Artístico Nacional* (IPHAN), the slope-shaped masonry element and the buttresses of the north-east façade are not represented in the original drawings of 1747 (TONERA, 2010; TONERA; FRAGOSO, 2013). Such elements are represented in further drawings and documents (TONERA, 2010; TONERA; FRAGOSO, 2013). It is possible to suppose that they were implemented in further constructive phases: the central masonry element was probably introduced in 1760 and the buttresses in 1843 (TONERA, 2010; TONERA; FRAGOSO, 2013).

The survey of pathologies on the characteristics of wood and masonry was widely represented by Arch. Toner, head chef of the “*Projeto Fortaleza*” - which is the program of the management of the Fortress of Santa Catarina, provided by the Universidade Federal de Santa Catarina, Florianópolis, Brazil. Such a set of files reaches about 1000 files created in the CAD environment (TONERA, 2010). The level of detail and knowledge of these structures can be considered very good. However, the use of this information can be challenging to read for professionals who receive this database. The use of an H-BIM-oriented methodology manages to gather such information in a single database, which can be accessed by the different project actors.

The analysis of the documental sources also shows that, during the restoration of 1970, the wooden horizontal structural elements underwent profound modifications (TONERA, 2010; TONERA; FRAGOSO, 2013) (figures 77.b, 77.e, and 77.g), according to a trend found in other architectural heritage sites in Brazil (LOPES, 2007). The roof structure was simply trussed, with king posts and struts (Figure 77.b). It was replaced with trusses with a collar tie beam (Figure 77.e). In the same restoration of 1970, the beams of the wooden slabs, which were fixed in the masonry walls (Figure 77.b), were substituted by simply supported beams resting on new reinforced concrete beams, leaning on the masonry arches (Figure 77.b) (TONERA, 2010; TONERA; FRAGOSO, 2013).

### 5.3 INFORMATION ACQUISITION

In the case of heritage buildings, an essential step is the characterization of the materials of the structure. Such a stage is challenging for the different type of information source, requiring special care. Regarding the *Quartel da Tropa*, the masonry and wood structures have a high level of heterogeneity, both geometric and constructive. It does not allow the exact definition of all physical and mechanical characteristics. A tool that can represent the preliminary basis for this process is visual inspection, and it will be described in Subsection 5.3.1.

The research developed by the Interdisciplinary Group of Studies of Madeira (GIEM) of the Federal University of Santa Catarina was analysed for the wooden element assessment (Annex B). The investigation carried out on the wooden elements of the *Quartel* aims to characterize their physical and mechanical properties. Finally, experimental tests were carried out for the assessment of the soil characteristics (Subsection 5.3.2 and Appendix B). Such topics will be presented in the following subsections.

#### 5.3.1 Visual inspection

Visual inspection was developed by the author to increase the path to knowledge of the historical building of the *Quartel da Tropa*. In the absence of quantitative data on the structural elements, the first approach through visual inspection is a useful tool for professionals working with heritage buildings. The Italian Standards Circolare 617/09 (CS.LL.PP., 2009) and the Technical Standards NTC 2018 (CS.LL.PP., 2019) were used to define the elements to be assessed in the *Quartel*, *i.e.* masonry geometry and texture, type and quality of mortar, transversal connection. Such characteristics are evaluated, employing a geometric and photographic survey.

##### 5.3.1.1 Evaluation of the masonry structures

Different textures of masonry define the structural elements (Figure 78.a). Arches and column are characterized by brick and mortar layers with some stone elements (Figure 78.a). The retaining masonry wall in connection with the soil is made by rubble masonry, and no connections between orthogonal masonry arches are observed (Figure 78.b). The presence of



growing vegetation confirms such an assumption (Figure 78.b). The wall thickness varies between 0.70 m and 1.15 m, and the broad core of the walls is shown in the second level masonry walls (Figure 79). Structural masonry has a discontinuous configuration, making it challenging to define its stratigraphy (Figure 78).

Figure 78 - Stratigraphy of a masonry wall and transversal connection with the retaining wall.



Source: the author.

The mortar can be considered good, as it has shown to have adequate strength, even where the bricks had advanced degradation (Figure 79.c). Through visual inspection, it is evident how the constructive evolution of the structure profoundly affected masonry construction. The structural elements that were added over time, the central masonry slope-shaped element and the buttresses (Figure 86), present different stratigraphy from the other



walls, and the use of different materials leads to different performance states of the structural elements. The hypotheses of the different constructive phases are confirmed by the presence of growing vegetation between the masonry walls and the central slope-shaped element (Figure 78.c). Moreover, it is also remarked by the difference of texture between the column and the buttresses (Figure 78.d).

Figure 79 - Stratigraphy of second-level masonry walls (a, b), presence of voids due to the pre-existing chimney. Mortar in good condition in arches (c) and columns (d), while bricks in an advanced state of degradation.



Source: the author.

### 5.3.1.2 Evaluation of the timber structures

In the evaluation of the timber structures, the assessment of the type of connection is crucial. Connections between beams and masonry walls were modified after the restoration

intervention, and the double embedded beam system was replaced by systems with double-supported beams, placed above reinforced concrete beams (figures 80.a, 80.b, 80.c and 81).

Figure 80 - Current state of the wooden slab elements (a, b), supports of the wooden slab (c) and the wooden tie-beams of the roof (d).

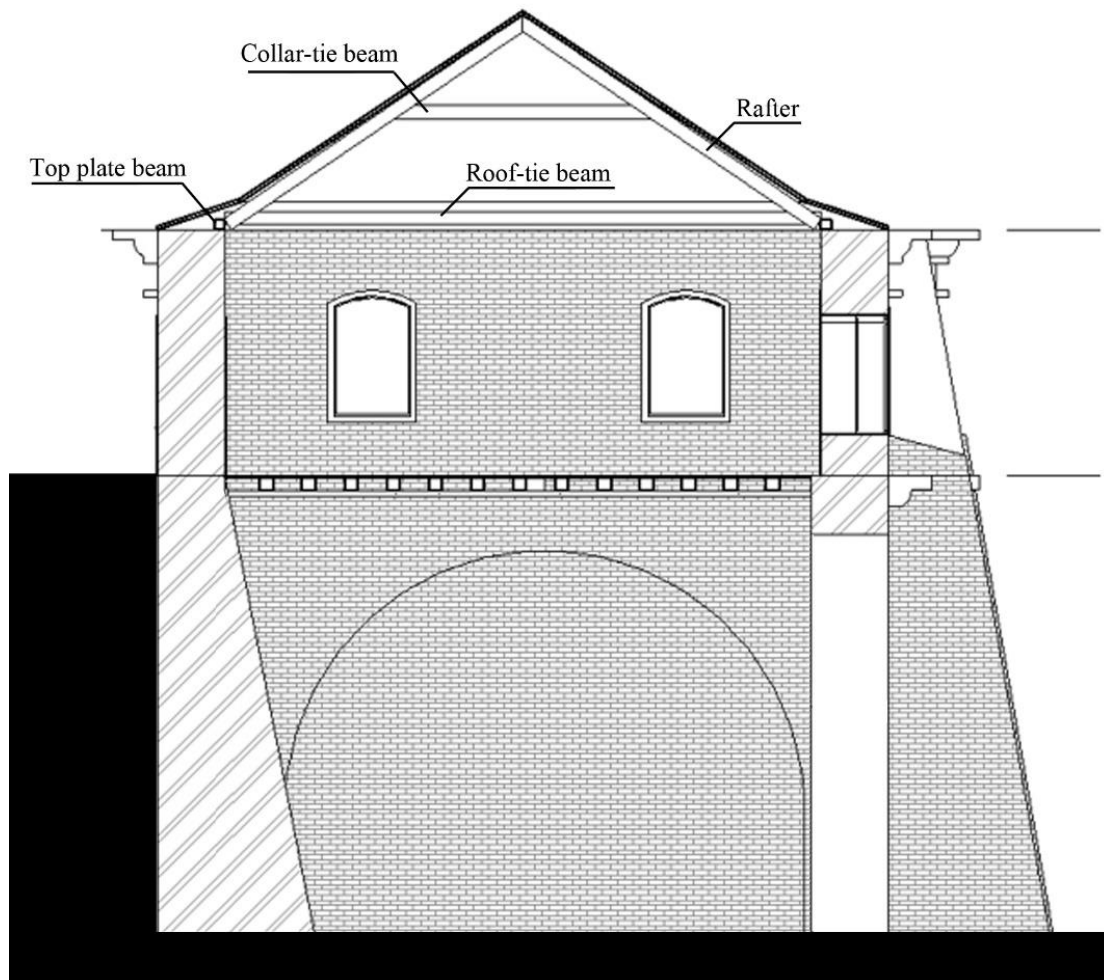


Source: the author (a, b, c, and d). Tonera (2010) (e).

Available data - from the survey campaign of the research group *Grupo Interdisciplinar de Estruturas de Madeira* (GIEM), of the Federal University of Santa Catarina

- was used to evaluate the physical and mechanical characteristics of the wooden elements (TEREZO, 2005). Such experimental campaign is described and analysed in Annex B. The estimation of the quality of the wooden pieces was possible through visual inspection, assessing defects such as knots and inclined fibres, in addition to the detection of signs of mechanical cracks. It was observed that most of the wooden pieces were attacked by fungi, followed by superficial moisture and termite attacks. Some elements were infested entirely with fungi, in an advanced stage of degradation.

Figure 81 - Section of the *Quartel da Tropa*, with identification of the structural elements of the roof after the intervention of 1970.



Source: the author.

Furthermore, beams - in the proximity of the north-west retaining wall - suffered severe decay. It also occurred in some roof tie-beams (Figure 81 and 88). However, most pieces have a superficial fungus attack, which only causes a superficial stain without causing loss of resistance of the wooden pieces.



Figure 82 - Advanced degradation of floor joists caused by fungi (a), moisture stains on roof rafters (b) and floor (c). Termite degradation in wooden joists (d) and roof tie-beams (e).



Source: Terezo (2005).

### 5.3.1 Wooden characteristic investigation

An extensive pathology survey of the wooden pieces was defined and represented in CAD drawings collected in the Fortalezas Multimedia Project (TONERA, 2010). These files describe the pathology of each constructive element, that was recorded and numbered (TONERA, 2010). However, such a database is detailed since each wooden structural elements

is represented for each file. Due to the huge amount of CAD drawings and technical reports, a comprehensive understanding of the as-built state of the heritage building is challenging.

Terezo (2005) carried out the definition of the wooden species by sampling, humidity assessment and sonic tests (see Annexe B). Terezo (2005) discusses how humidity phenomena can only be observed after the occurrence of rain in the place, leading to believe that such stains are seasonal and do not alter the moisture content of the wooden pieces (Figure 82). Moisture stains are less frequent than the presence of fungi (Annex B). The termite attack was also observed in some pieces of rafters, lines and bars: the highest occurrence was in bars of the deposits and close to the deposits (Figure 82) (TEREZO, 2005). It is important to note that after the investigation of GIEM, damaged elements were replaced. However, in the as-built state, similar pathologies appeared again in the same previous position, showing how the humidity and moisture condition of the structure still affect the building (Figure 80).

### 5.3.2 Soil characteristic investigation

Experimental tests on the soil were carried out by the author together with the support of the *Laboratório de Mapeamento Geotécnico* of the Federal University of Santa Catarina (LAMGEO, 2018). Such tests increase the understanding of historical construction and its environment (RELUIS, 2010). Direct shear tests, granulometric analysis, and humidity tests were carried out to obtain cohesion  $C$ , friction angle  $\Phi$ , density soil  $\gamma$  (Appendix B). Such tests suggest that the soil type is red, yellow podzols and the soil lithology is granitic rock type which is considered as cohesive soil. Contribution of the soil will be considered terms of horizontal soil actions and will be introduced as a load of the structural model (see Subsection 5.5.2).

Table 16 - Characteristics of the physical and mechanical parameters of the soil.

	$\gamma$ [kN/m <sup>3</sup> ]	$C$ [kPa]	$\Phi$ [°]
Soil	15.50	14.70	18.40

Source: the author.

## 5.4 HISTORIC-BUILDING INFORMATION MODELLING

The creation of the H-BIM model of the *Quartel da Tropa* begins with the management of the available information. The leading source is a comprehensive geometric survey of the construction, including the pathology survey (TONERA, 2010; TONERA; FRAGOSO, 2013),

the identification of the wooden structures (TEREZO, 2005) and experimental test on the soil (LAMGEO, 2018). The existing 2D CAD drawings (TONERA, 2010; TONERA; FRAGOSO, 2013) represent the primary sources of the architectural H-BIM model. Such a model was developed in Autodesk Revit® (AUTODESK INC, 2010). Such software allows for the creation of structural analytical models - elaborated from the architectural model - and analysing it through default structural tools. Furthermore, the analytical model can be exported to other structural analysis software. In the proposed workflow, the analytical model was exported in Autodesk Robot®, software based on the Finite Element method (BATHE, 2006; ZIENKIEWICZ, O. C., TAYLOR, 2000). The use of BIM process allows understanding and defining the system configuration of the structural model before the creation of the FEM software. Such a definition is described in the following subsection.

#### **5.4.1 The system configuration of the structural model**

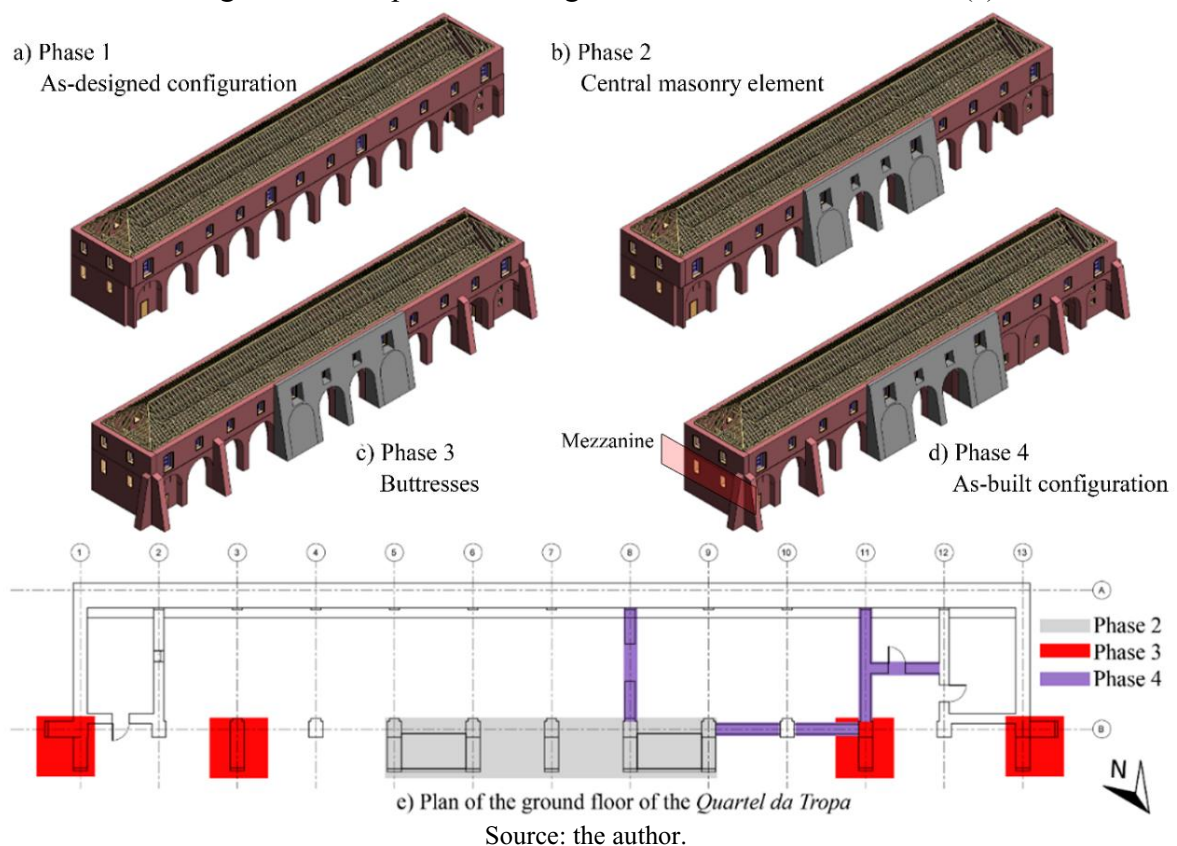
The geometric characteristic of the structural model was elaborated according to the visual inspection and the geometric surveys. The evaluation of the configuration of the structural model requires special care due to the different structural elements. The ground level is characterized by a trapezoidal retaining wall (Figure 81), tapered on one side along with the height of 6.80 m. Such a wall have a variable thickness, from 1.80 m at the base to 1.00 at the top. On the opposite side, the north-east façade is characterized by masonry arches with a thickness of 1.15 m. However, such a façade is divided into three parts by the presence of the central masonry slope-shaped element. Such an element has a variable thickness from 2.40 m to 1.00 m at the top. Such an element - which is continuous to the vertical walls - has a trapezoidal shape, tapered on one side along with the height of the whole building, 10.50 m. The second-level masonry walls have a thickness of 1.00 m. The buttresses, instead, have a thickness of 1.00 m and are assumed as a continuum with the masonry walls. However, the last assumption should be investigated in further *in-situ* tests and validated through experimental data.

Structural behaviour of the masonry walls is supposed as single-leaf. Connection wall-to-wall is considered as fixed since buttresses enhance such behaviour. Furthermore, the assessment concerning the type of wall-beam and beam-beam connections of the structure was developed through visual inspection. The absence of rigid connections between the elements mentioned above allows the supposition that rotations at each node are released. Connections

beam-to-wall are considered as pinned. The foundation supports were supposed as fixed constraints due to the rigid ground foundation assumptions (BETTI, MICHELE, GALANO, 2015; CLEMENTE; BONTEMPI; BOCCAMAZZO, 2012; KILAR; PETROVČIČ, 2017). The simplifications are also validated by the visual inspection, that showed how the vertical masonry elements are in contact with the soil, at a deeper level than the considered construction ground floor (Figure 78.d).

The analysis of the constructive evolution relies on the information acquired in the historical-critical analysis. Through such an analysis, four main phases of the structural model are identified. Each of the phase - described in Subsection 5.2.2 - is represented in the H-BIM model (Figure 83).

Figure 83 - Constructive evolution in the H-BIM: 'as-designed' project (a), the introduction of the central masonry element (b), the introduction of the buttresses (c), 'as-built' project (d) and ground-level plan according to the constructive evolution (e).



Phase 1 represents the as-designed project of 1747 (Figure 83.a), Phase 2 shows the central masonry slope-shaped element of 1760 (Figure 83.b), Phase 3 represents the introduction of buttresses of 1843 (Figure 83.c) and Phase 4 corresponds to the as-built construction, after the restoration interventions of 1970 (Figure 83.d). Indeed, during its history,

the *Quartel* was used in different ways, for example as a military jail or as a military hospital (TONERA, 2010; TONERA; FRAGOSO, 2013), meaning that the distributive configuration of the spaces was modified according to the function it had to supply (Figure 83.e).

#### 5.4.2 Material properties and assumptions

An appropriate approach to structural risk assessment involves an adequate definition of material characteristic parameters through comprehensive research campaigns (M. IOANNIDES; E. FIN; R. BRUMANA; P. PATIAS; A. DOULAMIS; J. MARTINS MANOLIS WALLACE, 2018; RELUIS, 2010; VAN BALEN, K.; VANDESANDE, 2017). However, simulating the case where researchers cannot develop such extensive experimental campaigns, simplifications of the material behaviour were done. Material characteristics were estimated from experimental results (LAMGEO, 2018; TEREZO, 2005), national standards (ABNT, 2005; NTC, 2008) or obtained from proved scientific literature (FERRITO; MILOSEVIC; BENTO, 2016; ROCCO LAHR *et al.*, 2015; ROSS; USDA FOREST SERVICE., 2010; ZENID, 2009).

Despite Brazilian research studies on this type of masonry structures being found (ARASH, 2012; CARVALHO *et al.*, 2014), significant variability in the results was observed (CARVALHO *et al.*, 2014). For these reasons, material properties were implemented according to the suggested values of the Italian Standard (NTC, 2008) and proved scientific researches in this field (GESUALDO; NUNZIANTE, 2005; LOURENÇO, 2002; ROCA *et al.*, 2010). Such references allow the adoption of an average value of 1.40 MPa - the interval is defined between 1.00 and 1.80 MPa - for the compressive strength of the masonry structures (NTC, 2008). The compressive strength will be considered to check if the results obtained from the static analysis are sufficiently distant from these values, meaning that the linear static behaviour also has a physical meaning.

Concerning the wooden structure, a geometric and physical survey confirms that there are several types of wooden species in the different structural elements (TEREZO, 2005). Despite this heterogeneity, most of the wooden beam elements are made of the same wood species, *Peroba rosa* (technically known as *Aspidosperma pirycollum*) (TEREZO, 2005). The material characteristics implemented in the model are summarized in Table 17. In this phase of analysis, materials are considered homogeneous and isotropic, linear elastic behaviour is



assumed, and stiffness degradation is neglected (HACIEFENDIOĞLU; DEMIR; ALPASLAN, 2016).

Table 17 - Characteristics of the physical and mechanical parameters.

	<b>E [MPa]</b>	<b>v</b>	<b><math>\gamma</math> [kN/m<sup>3</sup>]</b>
Masonry structures	1309.50	0.25	19.00
Wooden structures	10500.00	0.27	6.38
Concrete beams	18435.00	0.20	25.00

Source: the author.

## 5.5 FINITE ELEMENT MODEL

The BIM software Revit<sup>®</sup> simplifies the structural analytical model representing walls by their middle planes and beams by their longitudinal axes. After such a phase, direct integration allows exporting the H-BIM model in the FEM software. The definition of the Finite Element model was developed in Robot<sup>®</sup> (AUTODESK, 2015a). It allows the user to modify the Finite Element meshing discretization, that in Revit<sup>®</sup> is not customizable (AUTODESK, 2012b). Such an H-BIM workflow allows updating both architectural and structural models using compatible software. Indeed, as mentioned in the methodology Subsection 2.3.1.3, a fundamental characteristic of the H-BIM workflow is that the compatibility between the two software allows modification of the FEM model and consequently updating the H-BIM model at a later stage (Autodesk, 2012b). The process of the definition of the FE model will be presented in the following subsections.

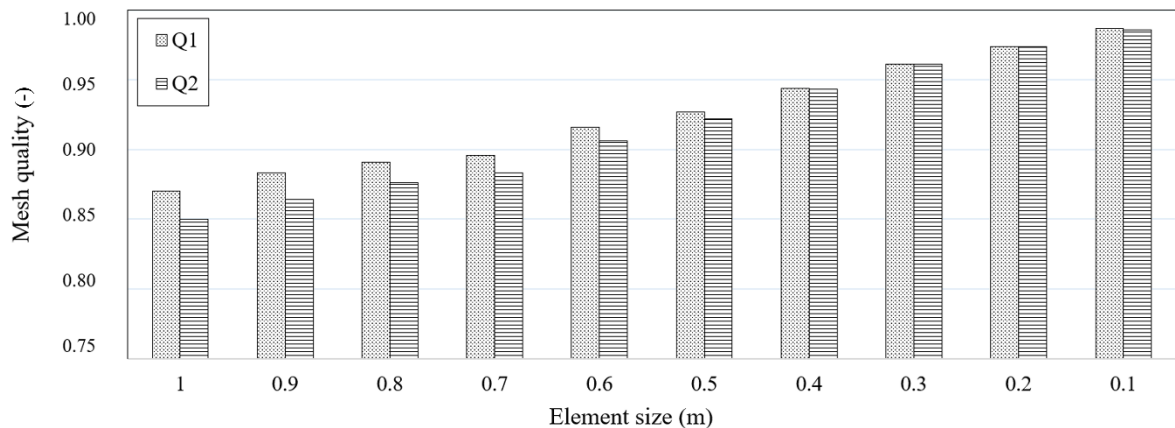
### 5.5.1 Definition and calibration of the mesh

In the FEM model, the middle wall planes are discretized by thick-shell meshes, which are defined as 4-node quadrilateral elements (Q4). This type of mesh is defined according to the discrete Kirchhoff - Mindlin element based on Mindlin-Reissner (Discrete Kirchhoff - Mindlin Quadrilateral, DKMQ) plate theory and assumed shear strain fields (HO-LE, 1988; KATILI, 1993a). The beams are modelled as linear bar elements, with 6 degrees of freedom at each node. Regarding the behaviour of Q4 elements in connection with bar elements - perpendicular to the plane of FE (in the direction of drilling rotation), pinned connections are generated.

In the FEM software Robot<sup>®</sup>, the main methods of Finite Element mesh discretization are Delaunay (HO-LE, 1988) and Coons (COONS, 1967; PROVATIDIS; KANARACHOS, 2000). As already pointed out, the type of mesh element automatically chosen during the exportation from Revit<sup>®</sup> to Robot<sup>®</sup> is the shell element for the masonry panels and the beams for the wooden and concrete elements (AUTODESK, 2012b). Due to the complexity of the analytical model, the process of mesh refinement is important to validate the Finite Element model and to obtain consistent results. However, in this research, the number of degrees of freedom (DoF) of the model was considered as a fundamental parameter. A good balance between mesh quality (KOLCUN, 1999) and DoF allows the creation of a consistent analytical model that can be analysed without a high computational effort.

Several models are analysed to define and calibrate the mesh. The chosen parameters defining each model are mesh type and quality, size and number of Finite Elements, number of degrees of freedom and time of elaboration of linear elastic analysis. The mesh quality parameters  $Q_1$  and  $Q_2$  increase according to the reduction of the element size (Figure 84).

Figure 84 - Evolution of the mesh quality dimensionless parameters  $Q_1$  e  $Q_2$  of the Coons mesh method according to the element size.



Source: the author.

However, while the element size decreases the number of degrees of freedom grows exponentially. It causes an increase in the computational effort of the analysis, even in the phases of linear elastic analysis. The use of the Coons element method was selected because the time analysis is almost three times less than the Delaunay method. The element size 0.3 m was chosen due to the combination of convergence of the results, good mesh quality ( $Q_1=0.96$ ;  $Q_2=0.96$ ) and degrees of freedom (164358) that still ensures the quickness of the linear elastic analyses.

### 5.5.2 Definition of loads and boundary conditions

In the knowledge path of heritage buildings, the geotechnical context assessment is fundamental for the evaluation and modelling process of the boundary conditions and the loads interacting with the referred structure (DIRECTIVE OF THE PRIME MINISTER, 2007; M. IOANNIDES *et al.* 2018; VAN BALEN, K.; VANDESANDE, 2017). The considered loads acting on the building are the dead loads of structural elements and the lateral loads due to the presence of the soil on three partially buried lateral façades. The weight contribution of non-structural elements is simplified by equivalent vertical loads. Such loads are introduced in the H-BIM workflow through Revit<sup>®</sup>. As previously mentioned, the contribution of the soil was simplified in terms of horizontal soil actions, that are modelled in Robot<sup>®</sup>, since it allows for the creation of triangular horizontal loads. Such load represents the hypothesis of at-rest earth pressures in which little or no movement is acceptable (PRADEL, 1994), and the Jaky formulation was considered (MORGENSTERN, N.R.; EISENSTEIN, 1970). Furthermore, the presence of a thick retaining wall counteracting the soil action allows supposing that rotations or movements are not allowed.

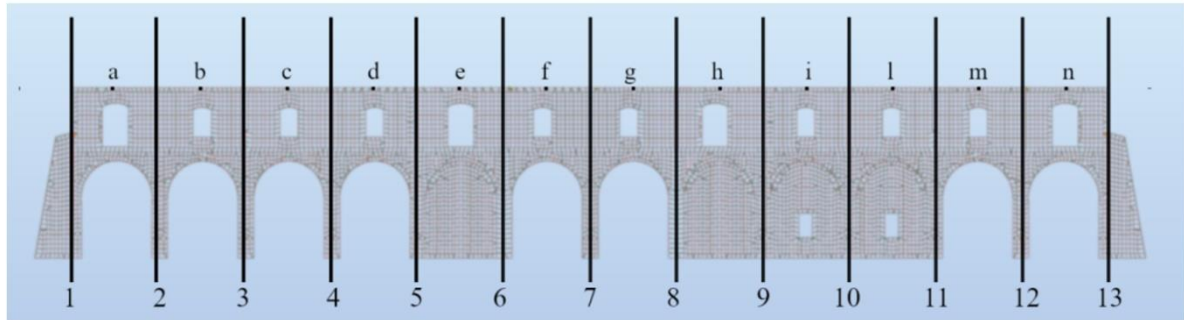
### 5.5.3 Preliminary structural global assessment

Linear elastic analysis of the *Quartel da Tropa* consents to understand the global structural behaviour and to hypothesize the causes of the different constructive configurations during the time. In Robot<sup>®</sup>, the linear elastic analysis is developed with the sparse method (BANK; DOUGLAS, 1993). The results of the previous analyses were recorded in the control points selected on the north-east façade, which was the most affected by the restoration interventions during the building life-cycle (Figure 85). The information collected - such as the historical-critical analysis, the surveys, and the physical-mechanical characterization of the materials - were implemented in the architectural H-BIM model and used to create the structural H-BIM model.

The linear static analyses were focused on the evaluation and the comparison of two main parameters in the constrictive evolution phases: the out-of-plane top displacement and the base compressive stress. In each constructive phase, the vibration modes are selected as qualitative parameters that characterize and summarize the structural behaviour in the two main directions. Moreover, the mode shapes are calculated in both directions to evaluate the stiffness

variation caused by the several interventions on the masonry structure. They also allow the investigation of the influence of the different interventions over time. Such an analysis is presented in the following subsections.

Figure 85 - Definition of axes and control-points in the Finite Element model in the north-east façade.



Source: the author.

#### 5.5.4 Self-weight analysis

In this case study, the linear elastic analysis was used as an auxiliary tool assisting in the diagnosis of the overall structure, through the self-weight analysis. After the mesh refinement process of the FEM model, the modal analysis was developed to resume the global behaviour in each constructive phase, in terms of overall stiffness. The static analyses were resumed through the evaluation of two main parameters, the top out-of-plane displacement, and the base compressive stress. Both analyses were developed to improve the knowledge path of the referred historical construction. The proposed qualitative analysis of the evolution of structural behaviour is developed to understand the constructive phases of historical construction. In case of a lack of information, such analysis allows understanding the modification occurred during the building life-cycle. The results obtained in the proposed research are shown in the following subsections.

##### 5.5.4.1 Evolution of first vibration modes through the constructive phases

The evolution of the global stiffness was evaluated through the main vibration modes, according to the construction phases. The results - resumed in Table 18 - showed an increase in the natural frequency of the main modes in the transversal and longitudinal direction (Figure 86). Some parameters are selected to describe each mode (Table 18):  $f$  and  $T$  are resonant

frequencies and periods  $T$ , respectively.  $RMX$  and  $RMY$  are the participating mass percentages in the longitudinal ( $X$ ) and transversal ( $Y$ ) directions.  $M$  is the total mass of the structure, while  $\Delta f$  and  $\Delta M$  are the increases in terms of frequency and mass.

The modal analysis suggests how, in each constructive phase, the value of the frequencies increased despite the masses increasing as well. Such a result suggests that global stiffness increased (Figure 86 and Table 18). The increase of the frequencies of the main modes occurs mainly in the longitudinal direction when the thick central masonry slope-shaped element is introduced,  $\Delta M$  6.57% and  $\Delta f$  54.44%. Such an increase is due to the thick section of the masonry element. Such an element increases stiffness in the longitudinal direction. A comparison is realized between the four phases, thus describing the constructive evolution. The identification of the first mode shape for each constructive phase allows the understanding of how the interventions of the masonry structures increase the global stiffness, modifying the mode shapes (Figure 86). As the first modes always appear in the transversal direction (Figure 86), it is considered as the weakest one.

Table 18 - Modal parameters according to the construction phases.

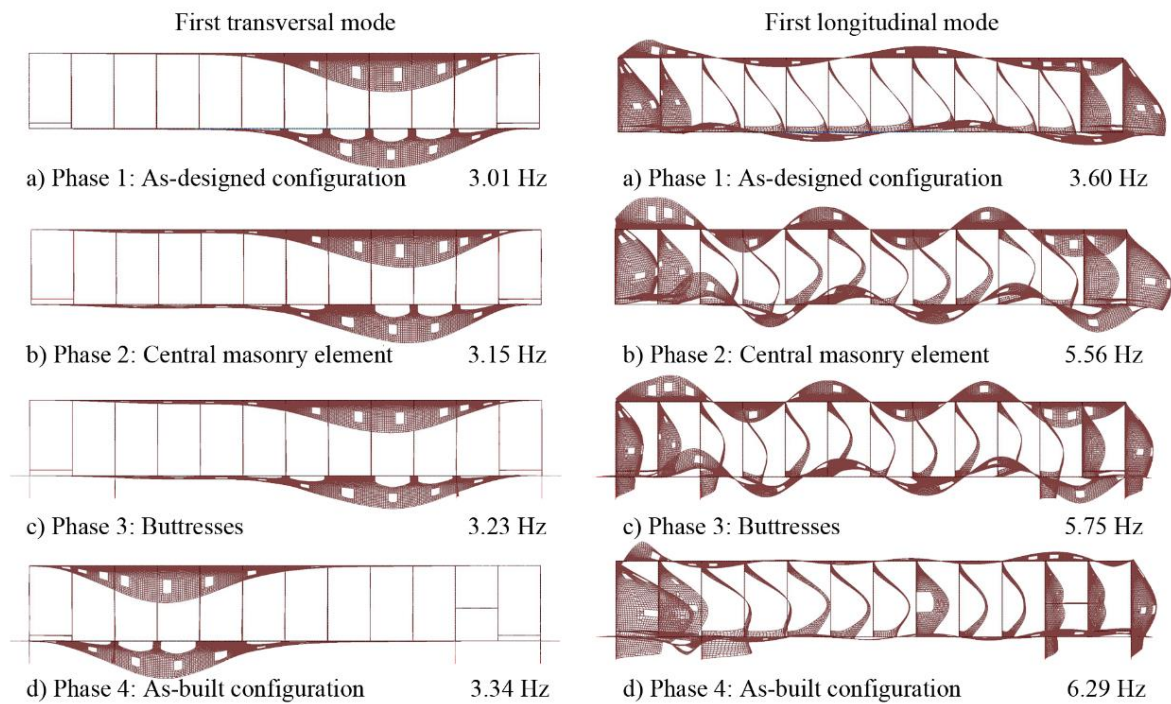
<b>Transversal direction</b>	$f$ (Hz)	$T$ (s)	$RMY$ (%)	$M$ (kg)	$\Delta f$ (%)	$\Delta M$ (%)
Phase 1	3.01	0.33	17.84	3593349.70	-	-
Phase 2	3.15	0.32	21.11	3829560.79	4.65	6.57
Phase 3	3.23	0.31	20.89	4023393.51	2.54	5.06
Phase 4	3.34	0.30	15.67	4219425.75	3.41	4.87
<b>Longitudinal direction</b>	$f$ (Hz)	$T$ (s)	$RMX$ (%)	$M$ (kg)	$\Delta f$ (%)	$\Delta M$ (%)
Phase 1	3.60	0.28	31.82	3593349.70	-	-
Phase 2	5.56	0.18	22.76	3829560.79	54.44	6.57
Phase 3	5.75	0.17	10.21	4023393.51	3.42	5.06
Phase 4	6.29	0.16	28.71	4219425.75	9.39	4.87

Source: the author.

The modification of the longitudinal modal shapes between the constructive Phases 1 and 2 (Figure 86.a and 87.b) also suggests that the dynamic behaviour of the construction was modified by the introduction of the slope-shaped central masonry element. In the same direction, the buttresses (Phase 3) do not modify the mode shape but cause a frequency increase  $\Delta f$  2.54%, despite a  $\Delta M$  5.06%, meaning a possible stiffness increase. The introduction of thick masonry walls, under the arches in the right part of the structure, lead to a  $\Delta f$  3.41%, modifying the first transversal mode shape (Phase 4). The as-built configuration (Phase 4) shows how the

introduction of masonry walls in the right part leads to an asymmetrical behaviour in terms of mode shape, and consequently in terms of frequency, distribution of the masses, and stiffness.

Figure 86 - Evolution of the most representative transversal) and longitudinal mode according to the constructive phases: 'as-designed' project (a), the introduction of the central masonry element (b), the introduction of the buttresses (c), 'as-built' project (d).



Source: the author.

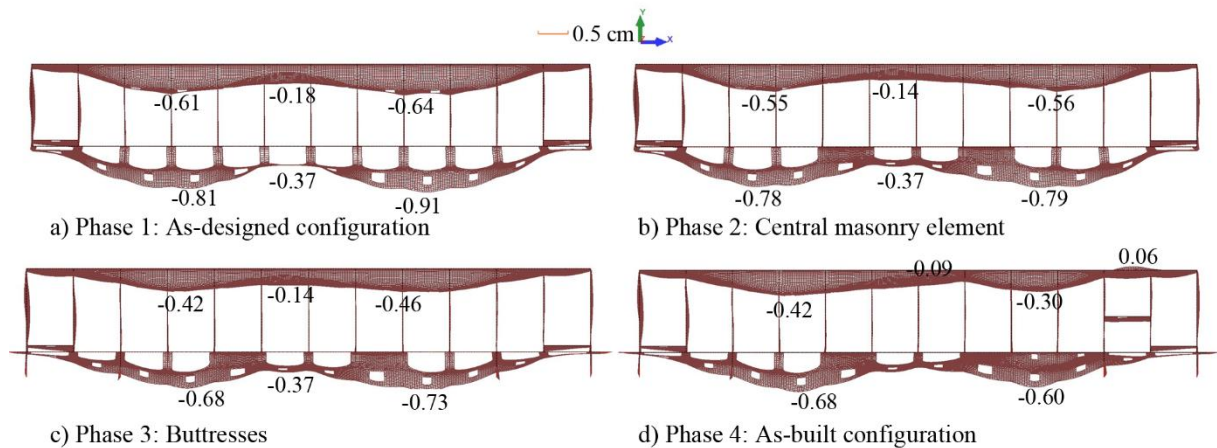
#### 5.5.4.2 Out-of-plane displacement

The top out-of-plane displacements obtained from the analysis of the permanent loads are presented in Figure 87. It is possible to understand how the horizontal soil action is the leading cause of the lateral displacement (Figure 87). Furthermore, the timber structures of the roof introduce lateral loads in the vertical masonry structure (LOPES, 2007). In the main façade, these two types of loads have the same direction, increasing the lateral displacement of the construction. In the opposite façade, south-west, these loads have opposite directions. The introduction of the central masonry element does not reduce the out-of-plane top displacement (Figure 72.b) considerably. The introduction of the buttresses - axes 3<sup>rd</sup> and 11<sup>th</sup> (Figure 85)- reduced the out-of-plane displacement in the transversal direction (Figure 87.c). In the 'as-built' constructive configuration, walls - introduced in the lower level of the right part of the construction - reduced the out-of-plane displacement, in the right part of the façade (Figure

87.d). Consequently, the ‘as-built’ configuration led to an asymmetrical behaviour of the structure, confirming the results of the modal analysis.

The analyses of the different constructive phases allow the understanding of how the restorations affected the global structural behaviour of the construction. The interventions modified the configuration of the north-east façade. For these reasons, focusing on the structural response of this façade in the main constructive phases was interesting. In the ‘as-designed’ configuration, the out-of-plane displacement reaches the maximum values of the north-east façade, in the control point *d* and *i* (figures 86 and 87).

Figure 87 - Out-of-plane top displacement (cm) of the north-east façade according to the constructive evolution: ‘as-designed’ project (a), the introduction of the central masonry element (b), the introduction of the buttresses (c), ‘as-built’ project (d).



Source: the author.

As expected, the buttresses - introduced where the high displacement values were reached at 3<sup>rd</sup> and 11<sup>th</sup> axes - reduced the out-of-plane displacements in these points (Figure 87.c). According to the simplification of the main constructive phases, the as-built configuration led to a displacement reduction in the right side of the façade (Figure 87.d).

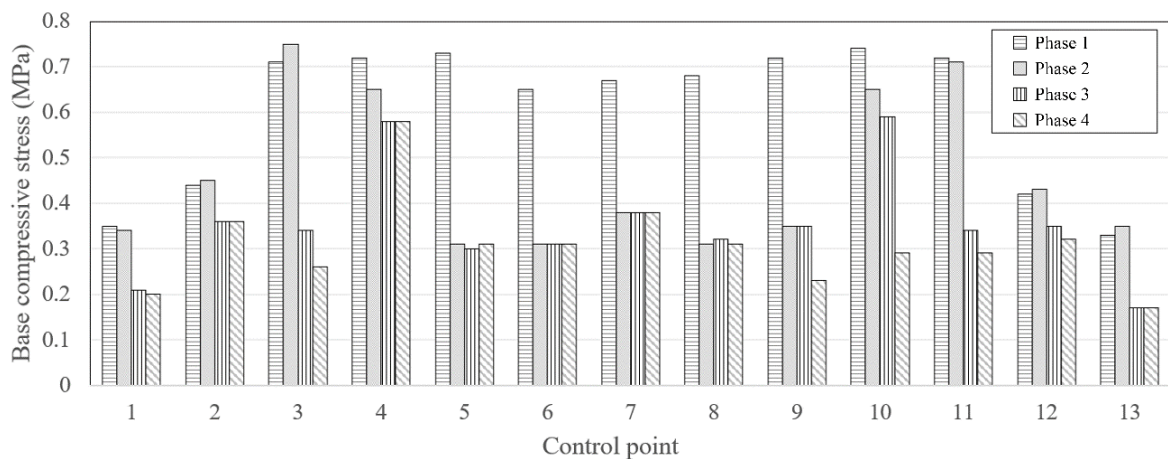
The results pointed out that the modification of the construction improved the structural behaviour in terms of top out-of-plane displacement, particularly in the buttresses - axes 3<sup>rd</sup> and 11<sup>th</sup> - of the façade. Moreover, the as-built structure (Figure 87.d) shows a high level of asymmetry due to the introduction of thick masonry walls under the arches on the right part of the construction, causing an asymmetric response to the acting loads. The results of the out-of-plane displacement confirm the main deformation configuration suggested by the first mode shape of the structure in the transversal direction.



### 5.5.4.3 Base compressive stress

The compressive stresses achieved at the base of each axis of the north-east façade are presented in Figure 88. The introduction of the central masonry element (Phase 2) caused a stress reduction - relating to the as-designed configuration (Phase 1) - of 43% in the central column on the 7<sup>th</sup> axis (Figure 88). This intervention also reduced the stresses in the north-east façade, from axis 4<sup>th</sup> to axis 10<sup>th</sup>. At the same time, it caused an increase in the compressive stress at the base of the 3<sup>rd</sup> axis. The introduction of the buttresses (Phase 3) caused a reduction of 55% and 52% at the base of the axes 3<sup>rd</sup> and 7<sup>th</sup> (Figure 88).

Figure 88 - Base compressive stress (MPa) in the control points of the north-east façade according to the constructive evolution.



Source: the author.

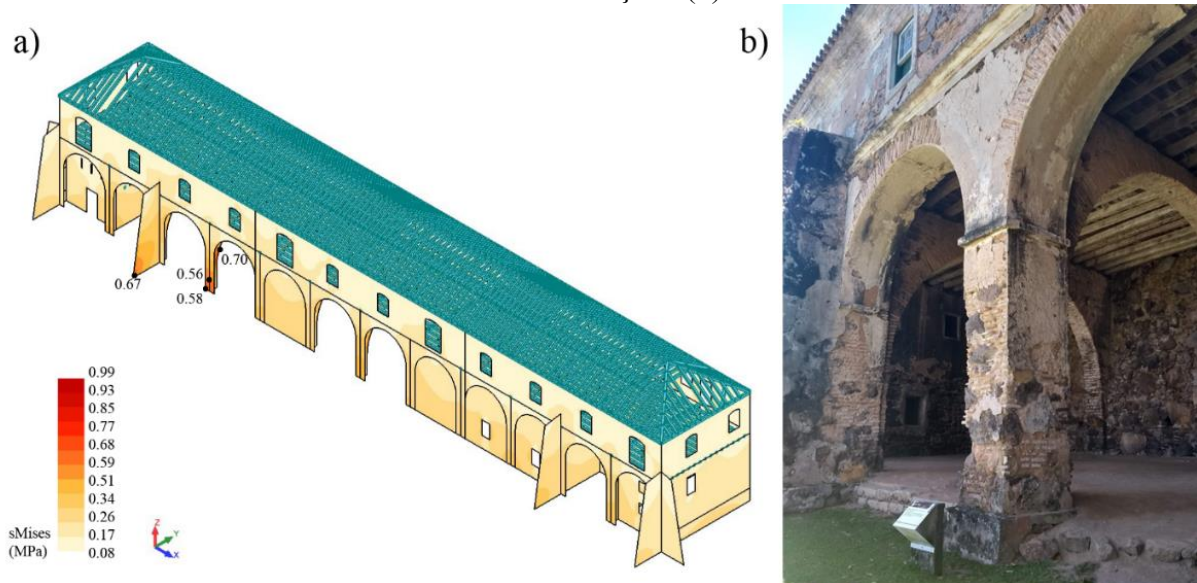
The analysis of the base compressive stress in the ‘as-built’ masonry structures (Phase 4) confirmed the asymmetrical structural behaviour in the ‘as-built’ configuration. The introduction of the central masonry element and the buttresses reduced both the top out-of-plane displacements and the compressive stresses of the structure in its main façade. The thick masonry walls introduced in the as-built configuration (Figure 83.d) reduced both displacements (Figure 87) and stresses (Figure 88). However, walls caused an asymmetrical global structural response of the masonry structures. Such behaviour leads to a concentration of the stresses on the left side of the building. Moreover, it affects mostly the arch and the column in the axis 4 (Figure 89). These results are confirmed by the current state of the building, where cracks and damages appear in the above-mentioned structural elements (Figure 89.b). However, such cracks and damages must be analyzed in further researches to understand if they depend on mechanical over-loading or they are due to material decay.



The results suggest that the constructive modifications - summarized in the phases 1, 2 and 3 (Figure 83) - were made to improve the global structural behaviour, aiming to counteract the horizontal actions - including the loads due to the soil. Those assumptions suggest how horizontal actions must be carefully considered in the structural assessment developed in any future restoration planning. Indeed, they were possibly the main reasons for the structural interventions made.

The results - obtained for the 'as-built' configuration - suggest that the introduction of longitudinal and transversal masonry walls modification was probably made according to the functional requirement in the spatial distribution of the lower level of the building, neglecting the structural consequences of the construction. Regarding the wooden horizontal elements, they improve the stiffness and the box behaviour of the building. However, they do not reduce the asymmetrical behaviour in terms of vibration modes, stresses, and displacements.

Figure 89 - Stress distribution in the 'as-built' configuration (a); damage in the column of the north-east façade (b).



Source: the author.

Furthermore, in the 'as-built' configuration base, compressive stresses reach values that are far from the considered average compressive strength of the masonry structures (1.40 MPa). Since the results obtained from the static analysis are sufficiently distant from this value, it means that the linear static analysis is consistent with a qualitative interpretation of the structural behaviour.

## 5.6 TEST PLANNING HISTORICAL CONSTRUCTION: FROM THE SENSITIVITY ANALYSIS TO THE PARAMETER UNDERSTANDING

This section aims to propose an approach that allows reducing the construction uncertainties through the understanding of the overall structural behaviour and the *in-situ* test planning. The combination of H-BIM process (ANTONOPOULOU; BRYAN, 2017) and knowledge path of historical constructions (RELUIS, 2010) offers useful tools to the proposed goal. Such an approach allows carrying out a sensitivity analysis that allows finding out which mechanical parameters influence the global structural behaviour of historical buildings.

The results of such analysis allow reducing invasiveness impacts, time (4D) and costs (5D) on an experimental testing campaign aimed to know the most relevant characteristics of the structure and its further intervention proposals. The proposed approach applied to the case study of the *Quartel da Tropa* shows how it can be adapted to heritage constructions.

### 5.6.1 Application of Sensitivity Analysis to historical construction test planning

In the case study of the *Quartel da Tropa*, the sensitivity analysis is used both as cognitive evaluation or improvement assessment (ASGARI; OSMAN; ADNAN, 2013). In the cognitive evaluation, the objective is to understand how each parameter influences the structural response; in the improvement assessment, the aim is to assess where interventions have significant improvement in the overall structural behaviour (LAGOMARSINO *et al.*, 2013; S.T.A. DATA, 2018). The first approach is used for the experimental test design to avoid performing tests in non-significant points and extending them in the most significant impact knowledge areas instead (LAGOMARSINO *et al.*, 2013; S.T.A. DATA, 2018). The second one allows optimizing the decision-making phase for further intervention proposal, revealing itself as a powerful aid by finding more effective interventions, thus improving the planning of the intervention and maximizing the return in terms of structural improvements (LAGOMARSINO *et al.*, 2013; S.T.A. DATA, 2018).

Due to the lack of knowledge about the characteristic parameters of the masonry structures, the proposed focus on the cognitive evaluation of the parameters aims at elaborating a comprehensive *in-situ* test planning. Indeed, the systematic use of non-destructive or minor destructive tests is essential to evaluate those essential factors within the building (BINDA; SAISI, 2001; RELUIS, 2010). For these reasons, the proposed research focused on tests that

are widely verified and applied to a wide range of cases of heritage field. The proposed tests are sonic (MIRANDA, L.; CANTINI, L.; GUEDES, J.; BINDA, L.; COSTA, 2013), tomographic tests (BINDA; SAISI, 2001), single and double flat-jack (CARPINTERI; INVERNIZZI; LACIDOGNA, 2009; GREGORCZYK; LOURENÇO, 2000), and AVT (GENTILE; SAISI, 2007; GENTILE; SAISI; CABBOI, 2015).

Furthermore, structural health monitoring is recommended for future research for the understanding of the influences of the environment on the dynamic behaviour of the structure (ZONNO *et al.*, 2019b). However, the number of tests that can be performed on a homogeneous wall type will generally be minimal and will not allow a statistical treatment of the results (CNR, 2014). Therefore, the interpretation of the results will be traced back to a synthetic judgment, in which the use of only one experimental data can be significant (CNR, 2014).

#### 5.6.1.1 Definition of the uncertainty value range

The definition of the uncertainty value range relies on the definition of the material properties. Such properties are chosen according to experimental results (TEREZO, 2005), the suggested values of the National Standards (ABNT NBR 6118:2003, 2005; ASSOCIAÇÃO BRASILEIRA DE NORMAS TÉCNICAS - ABNT, 1997; CS.LL.PP., 2009) and proved scientific researches (DIRECTIVE OF THE PRIME MINISTER, 2007; ROCA *et al.*, 2010; ROCCO LAHR *et al.*, 2015). Geometrical characteristics of the construction and soil parameters - obtained from the *in-situ* test - are assumed as deterministic (Table 19).

Table 19 - Deterministic and aleatory parameters of the proposed Sensitivity Analysis.

	Deterministic parameters		Epistemic parameters			Aleatory parameters of masonry structures		
	Soil	Concrete 1	Concrete 2	Wood C20	Wood C30	min	average	max
$E$ (MPa)	-	18435	23250	9500	14500	1035	1305	1575
$G$ (MPa)	-	7681	9964	475	725	345	435	525
$\nu$	-	0.20	0.17	0.27	0.27	0.10	0.25	0.5
$w$ (kN/m <sup>3</sup> )	15.50	25	23	6.5	8	17	19	21
$C$ (kPa)	14.70	-	-	-	-	-	-	-
$\phi$ [°]	18.40	-	-	-	-	-	-	-

Source: The author.

According to the results of the investigation presented in Annex B (TEREZO, 2005), the wooden element beams were modelled as dicotyledons C20. Such material parameters are

selected according to the Brazilian standard ABNT NBR 7190:1997 (ASSOCIAÇÃO BRASILEIRA DE NORMAS TÉCNICAS - ABNT, 1997). Due to the objective of the proposed research, the masonry parameters are defined as aleatory (Table 19), while concrete and wooden parameters are assumed as epistemic (Table 19). Regarding Equation 66, the minimum number of cases to evaluate the sensitivity coefficient for epistemic parameters is two, and for this reason, two types of concrete and wood are evaluated.

Regarding the evaluation of the epistemic parameters, 9 cases are investigated. In the average model, the connections are supposed as pinned, meaning that the rotations  $R_y$  and  $R_z$  are allowed. For the type of connection assessment, in case 1, all the connections are supposed as fixed, while, in case 2, only rotations  $R_y$  are allowed. Since, case 2 shows no significant modification in terms of structural response in cases 3, 4 and 5, fixed connections are supposed in the roof, slab, and reinforced concrete (RC) beams, respectively. In case 6, wooden elements are defined as C30, according to the Brazilian standard ABNT NBR 7190:1997 (ASSOCIAÇÃO BRASILEIRA DE NORMAS TÉCNICAS - ABNT, 1997). Similarly, in case 7, RC beams are assumed with different material characteristics according to the Brazilian standard ABNT NBR 6118:2007 (ABNT NBR 6118:2003, 2005) (Table 19). In cases 8 and 9, the hypotheses of different masonry characteristics are investigated, where the properties of buttresses and arches are defined according to the Italian standard *Circolare* 617/09 suggestions for brick masonry type,  $E = 1500$  MPa,  $G=500$  MPa and  $w=18$  kN/m<sup>3</sup> (CS.LL.PP., 2009).

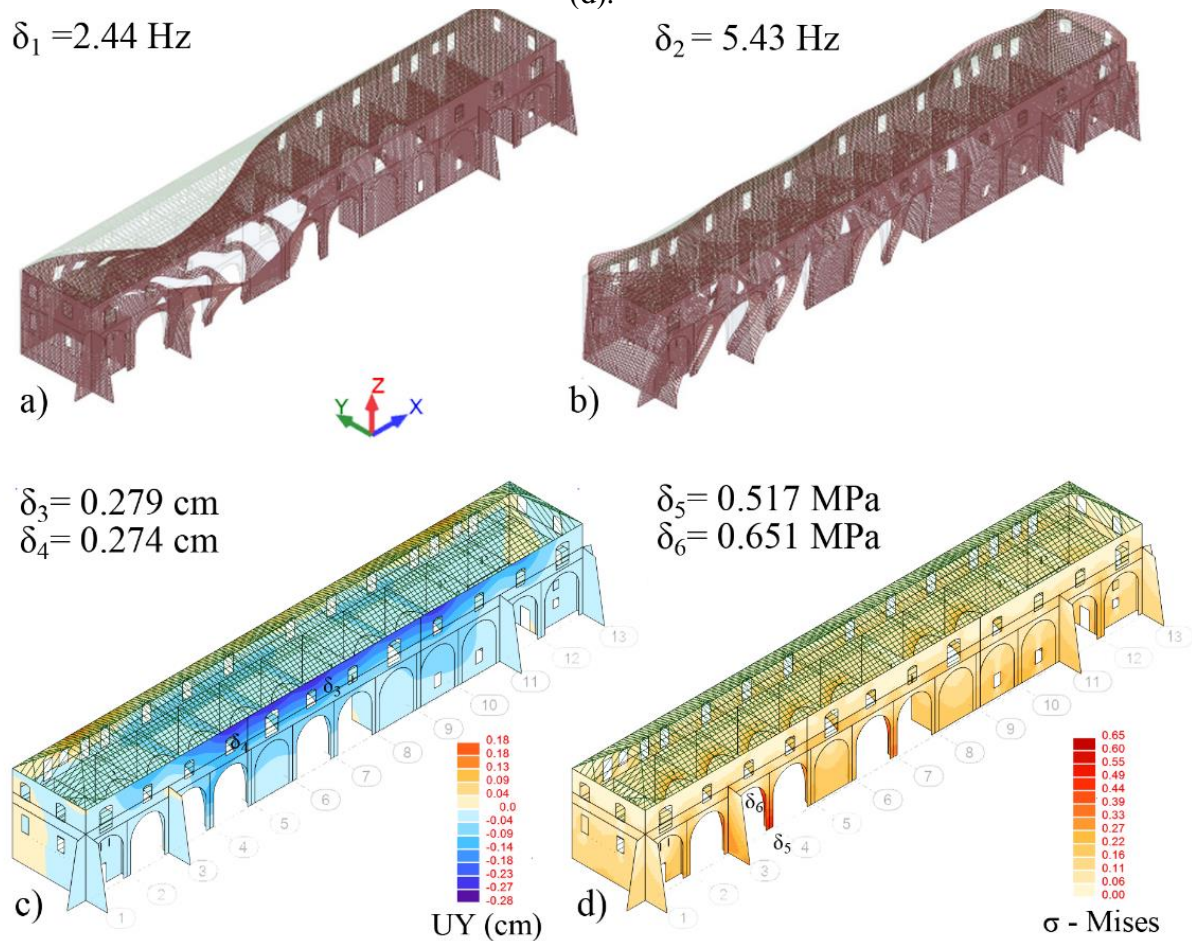
#### 5.6.1.2 Control point selection

The historical-critical analysis allowed defining the main phases of constructive evolution (CALÌ *et al.*, 2019). The as-designed building (18<sup>th</sup> century) was modified by the introduction of a masonry slope-shaped element and successively of the buttresses. The north-east façade (figures 74 and 75) was affected by several modifications through the pass of time and the different uses of the building (TONERA, 2010). For these reasons, it is interesting to analyse the result of the structure evolution focusing on the behaviour of the north-east façade (figures 83 and 86). The proposed linear elastic analyses allow approaching the global structural behaviour of historical construction. The static analysis shows the relevant points within the peak values of stresses and displacement are reached. The dynamic analysis - confirming structural evaluations obtained in previous researches - shows the asymmetrical behaviour of the structures (Figure 90).

The interpretation of the proposed analyses - obtained from the as-built model - allows for the control point selection where the parameters of the sensitivity analysis ( $\delta_1 - \delta_6$ ) will be recorded. The maximum displacement is reached at the top of the masonry wall in the 4<sup>th</sup> axis (Point A). Similarly, the maximum stress values - according to the Mises theory - are reached in the right base of the arch on the 4<sup>th</sup> axis compressive stresses (point B) (Figure 90). Parameters of the sensitivity analysis are defined as follow (Figure 90):

- a) first vibrational modes in transversal ( $\delta_1$ ) and longitudinal ( $\delta_2$ ) (b) directions;
- b) top out-of-plane displacements between axes 6<sup>th</sup> and 7<sup>th</sup> ( $\delta_3$ ) and between axes 4<sup>th</sup> and 5<sup>th</sup> ( $\delta_4$ );
- c) Mises stresses at the base of the column ( $\delta_5$ ) and the springing line of the arch in the 4<sup>th</sup> axis ( $\delta_6$ ).

Figure 90 - First vibrational modes in transversal ( $\delta_1$ ) (a) and longitudinal ( $\delta_2$ ) (b) directions. Top out-of-plane displacements  $\delta_3$  between axes 6<sup>th</sup> and 7<sup>th</sup> and  $\delta_4$  between axes 4<sup>th</sup> and 5<sup>th</sup> (c). Mises stresses at the base of the column  $\delta_5$  and the springing line of arch  $\delta_6$  in the 4<sup>th</sup> axis (d).



Source: the author.

### 5.6.1.3 Response variation of the aleatory and epistemic parameters

Response variation in terms of static ( $\delta_3, \delta_4, \delta_5, \delta_6$ ) and dynamic behaviour ( $\delta_1$  and  $\delta_2$ ) are shown in Table 20. Subsequently, the response variation coefficients  $\Delta'_1, \Delta'_2, \Delta'_3, \Delta'_4, \Delta'_5, \Delta'_6$  are calculated through sensitivity analysis (SA) both for aleatory and epistemic parameter (see equations 62 and 63 in Subsection 3.3.1). The SA was carried out to assess how the characterization of each one of the selected parameters affects the global structural behaviour. Parameters  $\delta_1$  and  $\delta_2$  are obtained as a preliminary evaluation of the overall stiffness in each direction, in terms of first vibrational modal frequencies, while parameters from  $\delta_3$  and  $\delta_6$  describe the static behaviour of the structure, in terms of displacements and stresses

Table 20 - Response variations  $\delta_i$  according to the sensitivity analysis of the aleatory and epistemic parameters.

Aleatory parameters	$\delta_1$ [Hz]	$\delta_2$ [Hz]	$\delta_3$ [cm]	$\delta_4$ [cm]	$\delta_5$ [MPa]	$\delta_6$ [MPa]
Base	2.4420	5.4334	0.2791	0.2740	0.5168	0.6505
$E_{min}$	2.2158	4.9735	0.3123	0.3076	0.5143	0.6456
$E_{max}$	2.6347	5.8379	0.2564	0.2513	0.5189	0.6548
$G_{min}$	2.4224	5.4011	0.2858	0.2805	0.5193	0.6585
$G_{max}$	2.4562	5.4566	0.2743	0.2693	0.5152	0.6450
$\nu_{min}$	2.4271	5.4828	0.2787	0.2738	0.5052	0.6535
$\nu_{max}$	2.5385	5.4200	0.2746	0.2693	0.5129	0.6449
$w_{min}$	2.5194	5.6092	0.2725	0.2765	0.4509	0.5942
$w_{max}$	2.3702	5.2707	0.2817	0.2754	0.5564	0.6927
Epistemic parameters	$\delta_1$	$\delta_2$	$\delta_3$	$\delta_4$	$\delta_5$	$\delta_6$
Case 1	2.4461	5.6863	0.2347	0.2294	0.5162	0.6527
Case 2	2.4357	5.6540	0.2776	0.2712	0.5165	0.6502
Case 3	2.4572	5.5383	0.2346	0.2293	0.5173	0.6539
Case 4	2.4274	5.5383	0.2788	0.2736	0.5156	0.6493
Case 5	2.4461	5.4603	0.2794	0.2746	0.5169	0.6506
Case 6	2.4466	5.6388	0.2433	0.2393	0.5199	0.6620
Case 7	2.4536	5.4502	0.2784	0.2737	0.5163	0.6482
Case 8	2.4439	5.4403	0.2790	0.2709	0.4868	0.6129
Case 9	2.4676	5.5502	0.2742	0.2708	0.4984	0.6957

Source: the author.

As expected, the main variations were obtained due to the uncertainty of Young's Modulus ( $E$ ) (Table 21 and Figure 91), related to the structure stiffness, up to  $\Delta'_1 = 0.17$  for the main vibration modes and up to  $\Delta'_4 = 0.21$  for the out-of-plane displacement. The variation of the specific weight of the masonry ( $w$ ) influences the results of the structural global behaviour, mostly the maximum stresses at the base of the construction, up to  $\Delta'_5 = 0.20$ . Instead, the variation of the Shear Modulus ( $G$ ) the Poisson's ratio ( $\nu$ ) does not affect considerably the

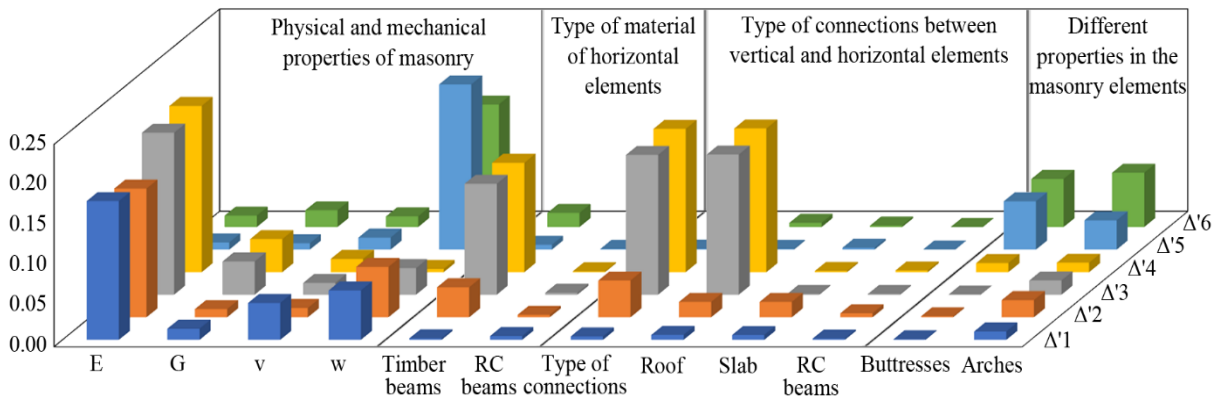
overall structure stiffness. The main differences in terms of out-of-plane displacements are obtained considering the structure connections as fixed (Table 21 and Figure 91), mainly in roof structure  $\Delta'_3 = 0.17$ ,  $\Delta'_4 = 0.18$ . The type of wooden beam also affects the static behaviour of the construction - in terms of displacements - and an in-depth investigation on the wooden physic and mechanical parameters should be done in further research. The RC beam type and connections, instead, seems to have a very low influence on the global behaviour of the structures, meaning also that their introduction in the restoration intervention is questionable. Furthermore, the uncertainty on the assumption of the different materials in buttresses and arches show influence in the response variation from 0.00 to 0.07.

Table 21 - Response variation coefficients  $\Delta'_k$  according to the sensitivity analysis of the aleatory parameters.

<b>Aleatory parameters</b>	$\Delta'_1$	$\Delta'_2$	$\Delta'_3$	$\Delta'_4$	$\Delta'_5$	$\Delta'_6$
<i>E</i>	0.17	0.16	0.20	0.21	0.01	0.01
<i>G</i>	0.01	0.01	0.04	0.04	0.01	0.02
<i>v</i>	0.05	0.01	0.01	0.02	0.01	0.01
<i>w</i>	0.06	0.06	0.03	0.00	0.20	0.15
<b>Epistemic parameters</b>	$\Delta'_1$	$\Delta'_2$	$\Delta'_3$	$\Delta'_4$	$\Delta'_5$	$\Delta'_6$
Timber beams	0.00	0.04	0.14	0.14	0.01	0.02
RC beams	0.00	0.00	0.00	0.00	0.00	0.00
Type of Connections	0.00	0.05	0.17	0.18	0.00	0.00
Roof Connection	0.01	0.02	0.17	0.18	0.00	0.01
Slab Connection	0.01	0.02	0.00	0.00	0.00	0.00
RC Beam Connection	0.00	0.00	0.00	0.00	0.00	0.00
Masonry buttresses	0.00	0.00	0.00	0.01	0.06	0.06
Masonry arches	0.01	0.02	0.02	0.01	0.04	0.07

Source: the author.

Figure 91 - Sensitivity coefficients of structural responses according to the aleatory and epistemic parameters.



Source: the author.



The proposed Sensitivity Analysis allows evaluating which model uncertainties mostly affect the selected structural response. Such an approach permits the cognitive evaluation for the *in-situ* test planning design and the improvement assessment, which are presented in the next subsections.

### 5.6.2 Cognitive evaluation for the *in-situ* test planning design

The approach presented to the cognitive evaluation is aimed at increasing the level of knowledge of historical construction. The previous results allow understanding the most relevant parameters of the structure. Elaborating an experimental campaign planning focused on these main characteristics allows reducing costs and time. The visual inspection had a crucial role in the cognitive evaluation of the structural characteristic of the construction. Such a tool confirmed the self-weight analyses through the observation of some damages in the structure of the *Quartel da Tropa*. As an example, the base of the column - selected as control point B - shows an extended crack pattern in the external part of the masonry (figures 92.a and 92.b).

Figure 92 - Damages in the column of the 4th axis of the structure (a, b), connection between column and buttresses (c) and connection of the central slope-shaped masonry with the main façade (d).



Source: the author.

The structural element of the column - situated in the 4<sup>th</sup> axis - has a high value of out-of-plane displacements and stresses (Figure 90), confirming the asymmetrical behaviour of the structure. An accurate geometric description will allow describing the damage patterns by thematical surveys. For such a reason, geometrical survey through laser scanning and orthophotos is useful to collect such information for further analysis. The use of orthophotos improves the damage pattern surveys recording the state of the art of the construction, simplifying the process of data collection in the knowledge path of the heritage built. The H-



BIM offers the possibility to improve the previous tools through the implementation of laser scanning and orthophoto for the creation of the three-dimensional informative model. Such a model permits a better geometrical description and representation of the historical construction. A laser scanning campaign should be done also to describe the displacement pattern of the structural elements, *i.e.* out-of-plumb survey. Such an approach is also suitable to be used for the calibration of the parameters of the structural model, comparing the displacements - recorded in the obtained point cloud - with the structural analysis results. Indeed, in the case of *Quartel da Tropa*, the obtained point cloud could confirm - or deny - the results of the developed structural and sensitivity analysis.

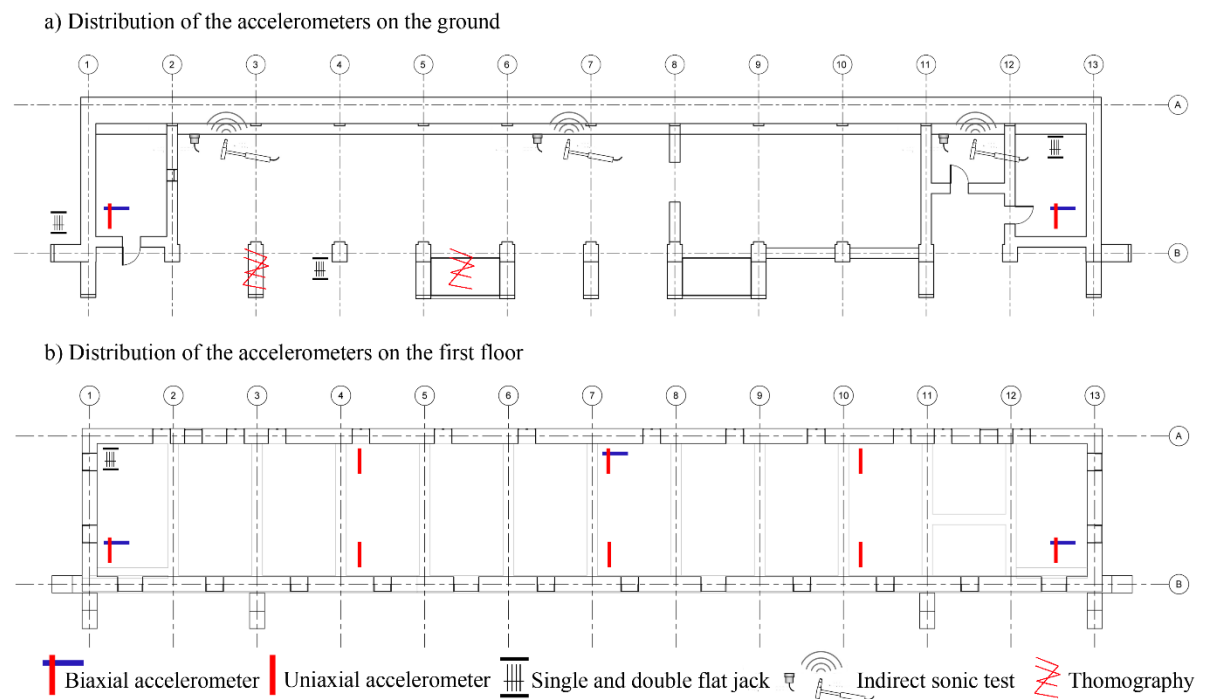
Furthermore, the identification of the vibration modes should be carried out through *in-situ* tests, AVT and OMA. Such identification will improve the process of calibration of the structural model, also through the aleatory and epistemic parameter evaluation (ASGARI; OSMAN; ADNAN, 2013; CATTARI *et al.*, 2015; GENTILE; SAISI; CABBOI, 2015). Such a type of experimental test is adequate for the historical construction due to the non-destructive characteristic. Moreover, such a procedure allows describing the global behaviour of the structure (BINDA; SAISI, 2001).

The set-up of the accelerometers is designed according to the results obtained from the modal analysis and the sensitivity analysis (Figure 93). Ten accelerometers is defined since the proposed MAC-based semi-automatic identification procedure (see Section 4.8) allows obtaining consistent results even with a limited number of accelerometers. Such accelerometers are defined as follow. Two biaxial accelerometers should be installed in the lateral parts of the ground floor - near the north-east façade - to understand the longitudinal and transversal displacements at the ground level. Similarly, two biaxial accelerometers should be set in the upper floor to describe the displacement variations in the two main directions. In the middle point of the structure - 7<sup>th</sup> axis - another biaxial accelerometer should be installed - with one uniaxial accelerometer on the opposite façade. Such a configuration allows assessing if the two façades are moving together or if some differential displacement is happening in the two directions. Furthermore, possible torsional effects should be assessed due to the asymmetry of the structure. In the 4<sup>th</sup> and 10<sup>th</sup> axes, unidirectional accelerometers could be set to assess the behaviour of the building in the points where structural analysis showed higher values of out-of-plane displacements. Concerning the set-up mentioned above, a structural health monitoring system should be defined in further research to assess the structural behaviour modifications. Frequency and modal shapes should be monitored to assess to the influence of the particular

environment where the *Quartel* is, considering winds, humidity and temperature variations (ZONNO *et al.*, 2019b) (Figure 93).

The setup system mentioned above could also give feedback in the case of further restoration projects, monitoring the structural behaviour variation due to the restoration modifications. Such monitoring analyses the structure before and after the interventions, also providing their effectiveness. Hence, once the vibration modes are obtained from the experimental results, the sensitivity analysis proposed in this research could be compared and improved according to the experimental vibration modes and the out-of-plane displacement survey obtained from the laser scanning. A process of model tuning of the main parameters should be adopted to assess the aleatory and epistemic parameters of the structure proposed in the further research (ASGARI; OSMAN; ADNAN, 2013; GENTILE; SAISI; CABBOI, 2015). Such a procedure will improve the correspondence between numerical and experimental results, increasing the level of knowledge of the heritage building.

Figure 93 - Experimental test set-up: accelerometer configuration for the modal parameter assessment and the health monitoring, and other non-destructive or minor destructive tests.



Source: the author.

As already mentioned, in heritage buildings, a non-destructive test should be preferred to destructive (or minor destructive) tests investigate the uncertainties of the structure. The geometrical depth of the retaining wall of the considered structure is unknown. Indirect sonic

tests could assess the geometry of such structural element (Figure 78) (LOURENÇO *et al.*, 2016; MIRANDA, L.; CANTINI, L.; GUEDES, J.; BINDA, L.; COSTA, 2013). Sonic tomography tests (BINDA; SAISI, 2001) could be evaluating the as-built state of the building and the stratification of the masonry elements, which was impossible to assess through visual inspection. Moreover, sonic tomography allows understandings the effectiveness of the connections of the structural element added in the different constructive phases, *e.g.* the connection between the buttresses and the masonry column (Figure 92.c) or the central slope-shape masonry element (Figure 83.b).

Furthermore, the carrying out the single and double flat-jack test (CARPINTERI; INVERNIZZI; LACIDOGNA, 2009; GREGORCZYK; LOURENÇO, 2000) allows the understanding of the mechanical parameters of the different masonry element (BINDA; SAISI, 2001). At the same time, flat-jack tests define the state of stress and strain, locally, from which can be evaluated the Young Modulus  $E$ , which was one of the main parameters affecting the structural behaviour.

Furthermore, two assumptions were investigated regarding the presence of different masonry properties, as confirmed from the constructive evolution of the *Quartel* shows. Case 8 and 9 were developed considering that different material properties were used in the buttresses and the arches, respectively. Such an assumption had a low influence on the results (Figure 91). However, other uncertainties could be introduced and investigated in further research. Such uncertainties understanding should concern the presence of a different type of masonry elements, increasing the knowledge of the structural behaviour (GENTILE; SAISI, 2007; GENTILE; SAISI; CABBOI, 2015).

### 5.6.3 Improvement assessment

The improvement assessment of the possible intervention was evaluated according to the sensitivity analysis of the epistemic factors. It was obtained considering the quality of the connections between different structural elements. This evaluation shows how the main differences - in terms of out-of-plane displacements (Table 21 and Figure 91) - are obtained considering the structure connections as fixed more than pinned, mainly in roof structure  $\Delta'_3=0.20$ ,  $\Delta'_4=0.15$ . In other terms, interventions developed to create stiffer connections in the roof elements could improve the overall structural box-behaviour. As expected, the main variations were obtained due to the uncertainty of Young's Modulus ( $E$ ) (Table 21 and Figure

91), related to the structure stiffness. The variation of the Shear Modulus ( $G$ ) the Poisson's ratio ( $\nu$ ) does not affect the overall structure stiffness considerably. Instead, the assessment of the specific weight of the masonry ( $w$ ) influences the results of the structural model global behaviour.

As expected, the type of connection in the wooden beam also affects the static behaviour of the construction - in terms of displacements - and a further investigation on the wooden physic and mechanical parameters should be done. The RC beam type and connections, instead, seems to have a shallow influence on the global behaviour of the structures, meaning also that their introduction in the restoration intervention is questionable.

## 5.7 PARTIAL CONCLUSION

The application of the H-BIM methodology on the case study of the *Quartel da Tropa* showed how the proposed multidisciplinary approach allows the understanding of the constructive phase evolution of a historical building and the possible reasons that caused modifications during the lifecycle of such construction. The obtained results lead to the following conclusions:

- a) the proposed methodology allows the creation of a structural model from the architectural model with fewer uncertainties and less simplification, improving the knowledge path of historical constructions;
- b) the lack of information about the physical and mechanical characteristics increases the level of uncertainties in the structural analysis; the linear analysis provides insights about the overall structural behaviour of the construction while it does not represent the real behaviour of complex buildings;
- c) the analysis of the constructive evolution allows the definition of how the restoration interventions modified the structural behaviour of a building, and it is useful to understand the reasons for the different modifications during the time;
- d) the sensitivity analysis is useful to understand which parameters mostly influence the structural behaviour of heritage buildings; the sensitivity related to the Young Modulus affected the structural numerical behaviour up to  $\Delta'_{1} = 0.17$  for the main vibration modes and up to  $\Delta'_{4} = 0.21$  for the out-of-plane displacement. The sensitivity of the specific weight of the masonry ( $w$ )

influences the results of the structural global behaviour, mostly in terms of maximum stresses at the base of the construction, up to  $\Delta'_5 = 0.20$ . Moreover, the assumption of the fixed roof connection could influence the results in terms of out-of-plane displacements up to  $\Delta'_3 = 0.17$ ,  $\Delta'_4 = 0.18$ ;

- e) the cognitive evaluation allows improving the test planning, focusing on the assessment on the main parameters localizing the impact of the experimental test of the relevant structural elements;
- f) the proposed methodology allowed increasing the level of knowledge of the historical construction of the *Quartel da Tropa*, through the sensitivity analysis and the experimental test campaign of the structure; such an approach also led to the definition of further specific structural analysis to be carried out.



## 6 GENERAL CONCLUSIONS

The proposed H-BIM-oriented methodology shown to be suitable as a paradigm for the path to knowledge. It also proves to fit with a multidisciplinary field in which several types of information must be collected and summarized in an informative database for the decision-making process. Such a methodology was developed and validated through the application to significant heritage buildings, *Galleria degli Antichi* (Italy) and *Quartel da Tropa* (Brazil).

The insights collected in the proposed research allow drawing some conclusions:

- a) merging the information collected by historical and architectural research, H-BIM and experimental tests should allow solving the main uncertainties of the numerical models and to assess the structural state of preservation of the building, in a fully non-destructive way;
- b) *in-situ* inspections, thematic surveys and the comparison of the archive documents with the visual inspection resumed within the H-BIM model improve the knowledge of overall structural behaviour of heritage buildings;
- c) experimental tests in operational conditions (AVT) provide quantitative parameters, which are representative of the structural condition and contribute to the knowledge of the as-built configuration;
- d) further steps of FE tuning increases the level of knowledge. The percentage increasing of modal assurance criterion values,  $\Delta MAC$ , reached up to 19%, improving the average values of 3%. The percentage increasing of frequency discrepancy,  $\Delta DF$ , reached up to 95%, improving the average values of 54%. As a result, an improvement of the correspondence between experimental and numerical parameters was obtained.

Furthermore, the proposed research confirms how the structural behaviour of historical buildings depends on the level of knowledge of the material mechanical parameters and structural behaviour in terms of stress, deformations, and stiffness. The results of the proposed research allow drawing some considerations:

- a) the sensitivity analysis is useful to understand which parameters mostly influence the structural behaviour of heritage buildings; the sensitivity related to the Young Modulus affected the structural numerical behaviour up to  $\Delta'_1 = 0.17$  for the main vibration modes and up to  $\Delta'_4 = 0.21$  for the out-of-plane displacement. The sensitivity of the specific weight of the masonry ( $w$ )

influences the results of the structural global behaviour, mostly in terms of maximum stresses at the base of the construction, up to  $\Delta'_5 = 0.20$ . Moreover, the assumption of the fixed roof connection could influence the results in terms of out-of-plane displacements up to  $\Delta'_3 = 0.17$ ,  $\Delta'_4 = 0.18$ ;

- b) the sensitivity analysis also allows developing an extensive test campaign reducing the great effort in terms of time and costs;
- c) the cognitive evaluation allows improving the test planning, focusing on the assessment on the main parameters localizing the impact of the experimental test of the relevant structural elements;
- d) the increase of knowledge of heritage buildings relies on the assessment of the as-built configuration obtained through experimental results;
- e) the assessment of the construction model is crucial. Such an assessment is fundamental for the decision making phase where restoration intervention is required;
- f) the methodology proposed allows increasing the level of knowledge of the historical construction, through the sensitivity analysis and the experimental test campaign of the structure. Such an approach led to carry out further specific structural analysis to assess the as-built state of preservation of the historic construction.

Moreover, the proposed methodology allows for the design of comprehensive *in-situ* investigations, which ensures the development of structural models characterized by increasing accuracy. Subsequently, the structural identification and the model updating increase the level of knowledge, allowing for the execution of further analysis, more reliable and better representative for the safety assessments of the structural behaviour of the building. Hence, based on the level of knowledge achieved, an appropriate confidence factor will be defined, to graduate the level of uncertainty of the model. Consequently, the use of gradually smaller confidence factors and partial factors can be done in further analyses, when experimental results confirm the consistency of the updated models. In such a way, more sophisticated analyses acquire a crucial role since they rely on numerical twin models that better fit with the real structural behaviour.

Furthermore, the preliminary assessment of global behaviour leads to better selection of the type of analyses to be carried out, e.g. static, dynamic or kinematic approaches. As an example, the use of the well-known predictive kinematic models for the collapse assessment



could be implemented directly in BIM software where all the required information are already collected. Such kinematic models rely on the combination of geometric, physical and mechanical parameters in predefined formulations. Such formulations can be implemented in the H-BIM model through simple formulations. Such characteristics of the heritage construction should represent a direct source of consultation for further researchers.

Besides, simplified approaches through the structural component - *i.e.* lumped mass, beam, panels - could be done, when consistent with the results of such methodology. The adoption of such simplified models for further researches, although affected by uncertainties, has the advantage of providing a homogeneous and comparable assessment on a territorial scale. Such a simplified approach could give significant insight to plan *in-situ* investigations, structural health monitoring systems or restoration interventions. Moreover, the updated model obtained from the proposed methodology could be considered as a reliable reference model for a structural health monitoring aimed at further understanding of environmental aspect on the dynamic behaviour. Furthermore, the understanding of the dynamic behaviour of the structure can be used in the further analysis where the optimal sensor location could offer reliable models for structural health monitoring.



## REFERENCES

- AMERICAN INSTITUTE OF ARCHITECTS (AIA). Project building information modeling protocol form. 2013.
- ABDEL-GHAFFAR; A. M.; HOUSNER, G. W. Ambient vibration tests of suspension bridge. **Journal of the Engineering Mechanics Division**, 1978, 104.5: 983-999.
- ABDEL-GHAFFAR; A. M.; SCANLAN, R. H. Ambient vibration studies of golden gate bridge: I. Suspended structure. **Journal of Engineering Mechanics**, 1985, 111.4: 463-482.
- ACITO, M.; BOCCIARELLI, M.; CHESI, C. and MILANI, G. Collapse of the clock tower in Finale Emilia after the May 2012 Emilia Romagna earthquake sequence: Numerical insight. **Engineering Structures**, 2014, 72: 70-91.
- AGUILAR, R.; ZONNO, G.; LOZANO, G.; BOROSCHEK, R. and LOURENÇO, P.B. *et al.* Vibration-Based Damage Detection in Historical Adobe Structures: Laboratory and Field Applications. **International Journal of Architectural Heritage**, 2019, 13.7: 1005-1028.
- ALLEMANG, R. J. The modal assurance criterion-twenty years of use and abuse. **Sound and vibration**, 2003, 37.8: 14-23.
- AMIGONI, C. **Technical drawings on the restoration intervention of Galleria degli Antichi, Mantua** (Italy). Studio di Ingegneria Amigoni. 2012. Available on-line at [http://www.studioamigoni.com/?page\\_id=prodotti&idcontenuto=279&idparent=480&iddetail=512&LID=0](http://www.studioamigoni.com/?page_id=prodotti&idcontenuto=279&idparent=480&iddetail=512&LID=0)
- ANDERSEN, P. **Technical Paper on the Stochastic Subspace Identification Techniques**. ARTeMIS Extractor Online Help. Version, 2010.
- ANTONOPOULOU, S.; BRYAN, P. **Historic England BIM for Heritage: Developing a Historic Building Information Model**. Swindon: Historic England. 2017, 10: 2019.
- APOLLONIO, F. I. Il disegno di Sabbioneta. Rilievo urbano e immagine della città. **Disegnarecon**, 2008, 1(1).
- ARAS, F., *et al.* Experimental and numerical modal analyses of a historical masonry palace. **Construction and Building Materials**, 2011, 25.1: 81-91.
- ARASH, S. Mechanical properties of masonry samples for theoretical modelling. In: **15th International Brick and Block Masonry Conference**. 2012.1.
- ARAYICI, Y.; TAH, J. Towards building information modelling for existing structures. **Structural Survey**, 2008.
- ASGARI, B.; OSMAN, S. A.; ADNAN, A. Sensitivity analysis of the influence of structural parameters on dynamic behaviour of highly redundant cable-stayed bridges. **Advances in Civil Engineering**, 2013, 2013.

ASSOCIAÇÃO BRASILEIRA DE NORMAS TÉCNICAS. **NBR 8800**: Projeto de estruturas de aço e de estruturas mistas de aço e concreto de edifícios. Rio de Janeiro, Brazil. 2008.

ASSOCIAÇÃO BRASILEIRA DE NORMAS TÉCNICAS. **NBR 6118**: Projeto de estruturas de concreto: procedimento. Rio de Janeiro, Brazil. 2003.

ASSOCIAÇÃO BRASILEIRA DE NORMAS TÉCNICAS. **NBR 7181**: Análise Granulométrica - Métodos de Ensaio. Rio de Janeiro. Brazil. 1984

ASSOCIAÇÃO BRASILEIRA DE NORMAS TÉCNICAS. **NBR 7190**: Projeto de estruturas de madeira. Rio de Janeiro, Brazil. 1997.

AUGARDE, C. E. Soil mechanics and earthen construction: strength and mechanical behaviour. In: **Modern Earth Buildings**. Woodhead Publishing, 2012. p. 204-221.

AUTODESK INC. Integrating Revit Structure® and Robot® Structural Analysis Professional. Available at:  
[https://www.cadstudio.cz/dl/Linking\\_Autodesk\\_Revit\\_Revit%20Structure\\_and\\_Robot\\_Structural\\_Analysis\\_Professional-Whitepaper.pdf](https://www.cadstudio.cz/dl/Linking_Autodesk_Revit_Revit%20Structure_and_Robot_Structural_Analysis_Professional-Whitepaper.pdf)

AVDELIDIS, N. P.; MOROPOULOU, A. Applications of infrared thermography for the investigation of historic structures. **Journal of Cultural Heritage**. 2004, 5, 1.1: 119-127.

BANK, R. E.; DOUGLAS, C. C. Sparse matrix multiplication package (SMMP). IBM Thomas J. Watson Research Division, 1992.

BARAZZETTI, L., *et al.* Cloud-to-BIM-to-FEM: Structural simulation with accurate historic BIM from laser scans. **Simulation Modelling Practice and Theory**, 2015, 57: 71-87.

BARAZZETTI, L., *et al.* BIM from laser clouds and Finite Element analysis: combining structural analysis and geometric complexity. 2015. In: **The International Archives of the Photogrammetry, Remote Sensing and Spatial Information Sciences**, Volume XL-5/W4, 2015 3D Virtual Reconstruction and Visualization of Complex Architectures, 25-27 February 2015, Avila, Spain.

BARAZZETTI, L., *et al.* HBIM and augmented information: towards a wider user community of image and range-based reconstructions. 2015. In: **The International Archives of the Photogrammetry, Remote Sensing and Spatial Information Sciences**, Volume XL-5/W7, 2015 25th International CIPA Symposium 2015, 31 August - 04 September 2015, Taipei, Taiwan.

BATHE, K. J. *Finite Element Procedures for Solids and Structures-Nonlinear Analysis: Video Course Study Guide*. Beil. MIT Center for Advanced Engineering Study, 1986.

BECHTUM, T. **Automation and further development of the borehole shear test**. Master thesis, Department of Civil, Construction and Environmental Engineering, Iowa State University, Iowas, USA, 2012.

BELLINO, A.; FASANA, A.; GARIBALDI, L. and MARCHESIELLO, S. PCA-based detection of damage in time-varying systems. **Mechanical Systems and Signal Processing**, 2010, 24.7: 2250-2260.

BENDAT, J. S.; PIERSOL, A. G. Engineering applications of correlation and spectral analysis. New York, **Wiley-Interscience**, 1980. 315 p., 1980.

BENNATI, S.; NARDINI, L.; SALVATORE, W. Dynamic behaviour of a medieval masonry bell tower. II: Measurement and modelling of the tower motion. **Journal of structural engineering**, 2005, 131.11: 1656-1664.

BESSELING, J. F. Non-linear analysis of structures by the Finite Element method as a supplement to a linear analysis. *Computer Methods in Applied Mechanics and Engineering*, v. 3, n. 2, p. 173-194, 1974.

BETTI, M.; GALANO, L.; VIGNOLI, A.. Finite Element modelling for seismic assessment of historic masonry buildings. *In: Earthquakes and their impact on society*. Springer, Cham, 2016. p. 377-415.

BIAGINI, C., *et al.* Towards the BIM implementation for historical building restoration sites. **Automation in Construction**, 2016, 71: 74-86.

BINDA, L.; CANTINI, L.; FERNANDES, F.; SAISI, A.; TEDESCHI, C. and ZANZI, L. Diagnostic Investigation on the Historical Masonry Structures of a Castle by the complementary use of non-destructive techniques. *In: Proceedings of the 13th International Brick and Block Masonry Conference Amsterdam*, Amsterdam. 2004.

BINDA, L., *et al.* **Experimental and numerical investigation on a brick masonry building prototype-Report 5.0-Measuring masonry materials properties**: Detailed results from an extensive experimental research. Department of Structural Engineering, University of Milano Politecnico, Milan, 1995.

BINDA, L.; ROBERTI, G. M.; ABBANEO, S. The diagnosis research project. **Earthquake Spectra**, 1994, 10.1: 151-170.

BINDA, L.; CANTINI, L.; TIRABOSCHI, C. and AMIGONI, C. Non Destructive investigation for the conservation design of a monastery near Bergamo (Italy). *In: RILEM Symposium on the On Site Assessment of Concrete, Masonry and Timber Structures-SACoMaTiS 2008*. RILEM Publications SARL, 2008. p. 797-806.

BINDA, L.; SAISI, A. Non Destructive testing applied to historic buildings: The case of some Sicilian Churches. **Historical Constructions**, 2001, 29-46.

BINDA, L.; SAISI, A. Knowledge of the building, on site investigation and connected problems. *In: Eurocode Volume 8*. 2009. p. 213-224.

BINDA, L.; SAISI, A. Application of NDTs to the diagnosis of Historic Structures. *In: 7th International Symposium on Non-destructive Testing in Civil Engineering*. 2009.

BINDA, L.; SAISI, A.; TIRABOSCHI, C. Investigation procedures for the diagnosis of historic masonries. **Construction and Building Materials**, 2000, 14.4: 199-233.

BIONDI, S. The knowledge level in existing buildings assessment. In: **Proceedings of 14th World Conference on Earthquake Engineering**. 2008. p. 12-17.

BODIG, J.; JAYNE, B. A. Mechanics of wood and wood composites. New York: Van Nostrand Reinhold, 1982.

BOEYKENS, S.; SANTANA QUINTERO, M.; NEUCKERMANS, H. Improving architectural design analysis using 3D modeling and visualization techniques. In: **Digital Heritage: Proceedings of the 14th International Conference on Virtual Systems and Multimedia**. Archeolingua; Hungary, 2008. p. 67-73.

BORNAZ, L.; RINAUDO, F. Terrestrial laser scanner data processing. In: **XXth ISPRS Congress**. Istanbul. 2004.

BOSCATO, G.; RUSSO, S.; CERAVOLO, R. and FRAGONARA, L.Z. Global sensitivity-based model updating for heritage structures. **Computer-Aided Civil and Infrastructure Engineering**, 2015, 30.8: 620-635.

BOSCHI, S.; GALANO, L.; VIGNOLI, A. Mechanical characterisation of Tuscany masonry typologies by in situ tests. **Bulletin of Earthquake Engineering**, 2019, 17.1: 413-438.

BRANCO, J. M.; PEIXOTO, T.; LOURENÇO, P.B. and MEDEIROS, P.M.B. Mechanical characterization of old chestnut beams. 2015.

BRENCICH, A.; SABIA, D. Experimental identification of a multi-span masonry bridge: The Tanaro Bridge. **Construction and Building Materials**, 2008, 22.10: 2087-2099.

BREYSSE, D. Non-destructive evaluation of concrete strength: An historical review and a new perspective by combining NDT methods. **Construction and Building Materials**, 2012, 33: 139-163.

BRINCKER, R.; ZHANG, L. Frequency domain decomposition revisited. In: **Proceedings of 3rd International Operational Modal Analysis Conference (IOMAC'09)**. 2009. p. 615-626.

BRINCKER, R.; ZHANG, L.; ANDERSEN, P. Modal identification from ambient responses using frequency domain decomposition. In: **Proceedings of the 18<sup>th</sup> International Modal Analysis Conference (IMAC)**, San Antonio, Texas. 2000.

BROWNJOHN, J.M.W. Ambient vibration studies for system identification of tall buildings. **Earthquake engineering and structural dynamics**, 2003, 32.1: 71-95.

BROWNJOHN, J. M. W.; DUMANOGLU, A. A.; SEVERN, R. T. Ambient vibration survey of the Fatih Sultan Mehmet (Second Bosphorus) suspension bridge. **Earthquake engineering and structural dynamics**, 1992, 21.10: 907-924.

BROWNJOHN, J. M. W.; XIA, P. Q. Dynamic assessment of curved cable-stayed bridge by model updating. **Journal of structural engineering**, 2000, 126.2: 252-260.

BRUMANA, R., *et al.* Strategy for integrated surveying techniques finalized to interpretive models in a byzantine church, Mesopotam, Albania. **International Journal of Architectural Heritage**, 2014, 8.6: 886-924.

BRUMANA, R.; DELLA TORRE, S.; PREVITALI, M.; BARAZZETTI, L.; CANTINI, L.; ORENI, D. and BANFI, F. Generative HBIM modelling to embody complexity (LOD, LOG, LOA, LOD): surveying, preservation, site intervention—the Basilica di Collemaggio (L'Aquila). **Applied Geomatics**, 2018, 10.4: 545-567.

BRUNO, S.; DE FINO, M.; FATIGUSO, F. Historic Building Information Modelling: performance assessment for diagnosis-aided information modelling and management. **Automation in Construction**, 2018, 86: 256-276.

BURMAN, A.; MAITY, D.; SREEDEEP, S. Iterative analysis of concrete gravity dam-nonlinear foundation interaction. **International Journal of Engineering, Science and Technology**, 2010, 2.4: 85-99.

CABBOI, A.; GENTILE, C.; SAISI, A. From continuous vibration monitoring to FEM-based damage assessment: application on a stone-masonry tower. **Construction and Building Materials**, 2017, 156: 252-265.

CALÌ, A. Seismic Assessment by Equivalent Frame Modelling of Palacio Pereira, Santiago de Chile. Master Thesis of Advanced Master in Historical Construction and Monuments, Universitat Politècnica de Catalunya, Barcelona, Spain, 2015.

CALÌ, A. Rigidez no plano dos elementos estruturais horizontais em madeira sob ação monotônica horizontal. In: **XV EBRAMEM - Encontro Brasileiro em Madeiras e em Estruturas de Madeira**. Curitiba, Brazil: 2016. [In Portuguese]

CALÌ, A.; DO VALLE, Â.; DIAS DE MORAES, P. Building Information Modelling and Structural Analysis in the Knowledge Path of a Historical Construction. In: **Structural Analysis of Historical Constructions**. Springer, Cham, 2019. p. 2071-2079.

CALÌ, A.; DIAS DE MORAES, P.; DO VALLE, Â. Understanding the structural behaviour of historical buildings through its constructive phase evolution using H-BIM workflow. **Journal of Civil Engineering and Management**, 2020, 26.5: 421-434.

CALLIARI, R., *et al.* User manual of ANDILWall, version 2.5. Rome: ANDIL Assolaterizi, 2010.

CÂMARA BRASILEIRA DE INDÚSTRIA DE CONSTRUÇÃO, CBIC. Coletânea Implementação do BIM Para Construtoras e Incorporadoras. Volume 2. **Implementação BIM**. Brasília, June 2016. Available at: [http://sindusconbc.com.br/wp-content/uploads/2016/10/VOLUME-\\_2.pdf](http://sindusconbc.com.br/wp-content/uploads/2016/10/VOLUME-_2.pdf)

CAMATA, G., *et al.* Safety analysis of the bell tower of S. Maria Maggiore Cathedral in Guardiagrele (Italy). In: **Proceedings of the 14th World Conference on Earthquake Engineering**. 2008. p. 12-17.

CARPINTERI, A.; INVERNIZZI, S.; LACIDOGNA, G. Historical brick-masonry subjected to double flat-jack test: Acoustic emissions and scale effects on cracking density. **Construction and Building Materials**, 2009, 23.8: 2813-2820.

CARVALHO, J., *et al.* Safety analysis of modern heritage masonry buildings: Box-buildings in Recife, Brazil. **Engineering structures**, 2014, 80: 222-240.

CASARIN, F.; MODENA, C. Seismic assessment of complex historical buildings: application to Reggio Emilia Cathedral, Italy. **International Journal of Architectural Heritage**, 2008, 2.3: 304-327.

CASOLO, S.; DIANA, V.; UVA, G. Influence of soil deformability on the seismic response of a masonry tower. **Bulletin of Earthquake Engineering**, 2017, 15.5: 1991-2014.

CATTARI, S., *et al.* Sensitivity analysis for setting up the investigation protocol and defining proper confidence factors for masonry buildings. **Bulletin of Earthquake Engineering**, 2015, 13.1: 129-151.

CENDES, Z. J.; SHENTON, D.; SHAHNASSER, H. Magnetic field computation using Delaunay triangulation and complementary Finite Element methods. **IEEE Transactions on Magnetics**, 1983, 19.6: 2551-2554.

CHI, H. L.; WANG, X.; JIAO, Y. BIM-enabled structural design: impacts and future developments in structural modelling, analysis and optimisation processes. **Archives of computational methods in engineering**, 2015, 22.1: 135-151.

CHIABRANDO, F.; LO TURCO, M.; SANTAGATI, C. Digital invasions: from point clouds to historical building object modeling (H-BOM) of a UNESCO WHL site. **International Archives of the Photogrammetry, Remote Sensing and Spatial Information Sciences**, 2017, 42.2/W3.

CHIABRANDO, F., SPANÒ, A. Points clouds generation using TLS and dense-matching techniques. A test on approachable accuracies of different tools. In: **XXIV International CIPA Symposium**, Strasbourg. 2013. p. 2-6.

CHURILOV, S.; MILKOVA, K.; DUMOVA, E. Dynamic identification analysis for the FE model updating of masonry buildings. Modena, da Porto and Valluzi (coordinators), **Brick and Block Masonry-Trends, Innovations and Challenges**. London, Taylor and Francis Group. DOI, 2016, 10.

CLEMENTE, P.; BONTEMPI, F.; BOCCAMAZZO, A. Design and Optimization of Base Isolated Masonry Buildings. In: **15th World Conference on Earthquake Engineering**. 2012.

CNR, D. T. 212 2013. **Istruzioni per la Valutazione Affidabilistica della Sicurezza Sismica di Edifici Esistenti**. Consiglio nazionale delle ricerche, 2014, 14. [In Italian]



COLLINS, J. D., *et al.* Statistical identification of structures. **AIAA Journal**, 1974, 12.2: 185-190.

COMPAN, V.; PACHÓN, P.; CÁMARA, M. Ambient vibration testing and dynamic identification of a historical building. Basilica of the Fourteen Holy Helpers (Germany). **Procedia Engineering**, 2017, 199: 3392-3397.

COONS, S. A. Surfaces for computer-aided design of space forms. **Massachusetts Institute of Tech Cambridge Project MAC**, 1967.

OLIVEIRA, J. P. C. **Normalização BIM: Especificação do Nível de Desenvolvimento e Modelação por Objetivos**. M.SC. Thesis, Civil Engineering. Porto University, Porto, Portugal, 2016. Disponível em: <[https://paginas.fe.up.pt/~gequaltec/w/images/Global\\_v7.01-Final.pdf](https://paginas.fe.up.pt/~gequaltec/w/images/Global_v7.01-Final.pdf)>

COULOMB, C. A. Essai sur une application des regles de maximis et minimis a quelques problemes de statique relatifs a l'architecture (essay on maximums and minimums of rules to some static problems relating to architecture). 1973.

CRESPI, P., *et al.* From BIM to FEM: The analysis of an historical masonry building. **WIT Transactions on The Built Environment**, 2015, 149: 581-592.

CS.LL.PP. Norme tecniche per le costruzioni. Gazzetta Ufficiale della Repubblica Italiana, 29. 2008. [In Italian]

CS.LL.PP. CIRCOLARE 617 2009. Istruzioni per l'applicazione delle Norme Tecniche per le Costruzioni di cui al DM 14 gennaio 2008. Gazzetta Ufficiale Della Repubblica Italiana, 2009. [In Italian]

CS.LL.PP. Aggiornamento delle Norme tecniche per le costruzioni. Gazzetta Ufficiale della Repubblica Italiana, 42. 2018. [In Italian]

CS.LL.PP. Istruzioni per l'applicazione dell'«Aggiornamento delle “Norme tecniche per le costruzioni”», Gazzetta Ufficiale della Repubblica Italiana, 35. 2019. [In Italian]

CS.LL.PP. Linee Guida per la classificazione e gestione del rischio, la valutazione della sicurezza ed il monitoraggio dei ponti esistenti. 2020. [In Italian]

DAL BARCO, G.; PEROBELLI, S.; SARTOR, T. **Palazzo del Giardino e Galleria degli Antichi a Sabbioneta**. Master's Thesis, Politecnico di Milano, Milano, Italy, 2016.

DANESE, M., *et al.* Investigating Material Decay of Historic Buildings Using Visual Analytics with Multi-Temporal Infrared Thermographic Data. **Archaeometry**, 2010, 52.3: 482-501.

DE LIMA, J. A. S.; SANTOS, J. Generalized Stefan-Boltzmann law. **International Journal of Theoretical Physics**, 1995, 34.1: 127-134.

DE MATTEIS, G.; MAZZOLANI, F. M. The Fossanova Church: seismic vulnerability assessment by numeric and physical testing. **International Journal of Architectural Heritage**, 2010, 4.3: 222-245.

DEL GIUDICE, M.; OSELLO, A. BIM for Cultural Heritage. *International Archives of the Photogrammetry, Remote Sensing and Spatial Information Sciences*, 2013, 5.2: 225-229.

DEL PIERO, G. Constitutive equation and compatibility of the external loads for linear elastic masonry-like materials. **Meccanica**, 1989, 24.3: 150-162.

DIRECTIVE OF THE PRIME MINISTER. Italian Guidelines for risk classification and management, safety assessment and monitoring of existing bridges. *DM 14 January 2008*. Directive of PCM: Rome, Italy, 2011.

DIRECTIVE OF THE PRIME MINISTER. Italian Guidelines for evaluation and mitigation of seismic risk to Cultural Heritage. *DM 14 January 2008*. Directive of PCM: Rome, Italy, 2011. [In Italian]

DORE, C., *et al.* Structural simulations and conservation analysis-historic building information model (HBIM). *In: The International Archives of the Photogrammetry, Remote Sensing and Spatial Information Sciences*, Volume XL-5/W4, 2015 3D Virtual Reconstruction and Visualization of Complex Architectures, 25-27 February 2015, Avila, Spain. 2015, 40.5: 351.

DOUGLAS, B. M.; REID, W. H. Dynamic tests and system identification of bridges. **Journal of the Structural Division**, 1982, 108.ST10.

DWIVEDI, S. K.; VISHWAKARMA, M.; SONI, A. Advances and researches on non-destructive testing: A review. **Materials Today: Proceedings**, 2018, 5.2: 3690-3698.

EASTMAN, C. M., *et al.* BIM handbook: A guide to building information modelling for owners, managers, designers, engineers and contractors. John Wiley and Sons, 2011.

EL-EMAM, M. Experimental and numerical study of at-rest lateral Earth pressure of over consolidated sand. **Advances in Civil Engineering**, 2011, 2011.

ELYAMANI, A., *et al.* Dynamic investigation of a large historical cathedral. **Structural Control and Health Monitoring**, 2017, 24.3: e1885.

EUROCODE 0: European Standard EN 1990: 2001. Basis of structural design. *Comite Europeen de Normalisation*, Brussel, 1990.

EUROCODE 8. European Standard EN 1998-3:2005: Design of structures for earthquake resistance - Part 3: Assessment and retrofitting of buildings. *Comite Europeen de Normalisation*, Brussels, 2005.

FARRAR, C. R.; WORDEN, K. An introduction to structural health monitoring. **Philosophical Transactions of the Royal Society A: Mathematical, Physical and Engineering Sciences**, 2007, 365.1851: 303-315.

FEDA, J. K<sub>0</sub>-Coefficient of Sand in Triaxial Apparatus. **Journal of Geotechnical Engineering**, 1984, 110.4: 519-524.

FERRITO, T.; MILOSEVIC, J.; BENTO, R. Seismic vulnerability assessment of a mixed masonry-RC building aggregate by linear and nonlinear analyses. **Bulletin of Earthquake Engineering**, 2016, 14.8: 2299-2327.

FOTI, D., *et al.* Ambient vibration testing, dynamic identification and model updating of a historic tower. **NDT & E International**, 2012, 47: 88-95.

FRAGONARA, Z. **Dynamic model for ancient heritage structures**. Doctoral Thesis. Polytechnic University of Torino, DOI: 10.6092/polito/porto/2502121. Torino, Italy, 2012.

FRISWELL, M.; MOTTERSHEAD, J. E. **Finite Element model updating in structural dynamics**. Volume 38. DOI: 10.1007/978-94-015-8508-8. Springer Netherlands, 2013.

GADE, S., *et al.* Frequency domain techniques for operational modal analysis. *In: 1st IOMAC Conference*. 2005.

GENTILE, C.; MARTINEZ Y CABRERA, F. Dynamic investigation of a repaired cable-stayed bridge. **Earthquake engineering and structural dynamics**, 1997, 26.1: 41-59.

GENTILE, C.; CABRERA, F. M. Y. Dynamic performance of twin curved cable-stayed bridges. **Earthquake engineering and structural dynamics**, 2004, 33.1: 15-34.

GENTILE, C.; SAISI, A. Ambient vibration testing of historic masonry towers for structural identification and damage assessment. **Construction and building materials**, 2007, 21.6: 1311-1321.

GENTILE, C.; SAISI, A. Operational modal testing of historic structures at different levels of excitation. **Construction and Building Materials**, 2013, 48: 1273-1285.

GENTILE, C.; SAISI, A.; CABBOI, A. Structural identification of a masonry tower based on operational modal analysis. **International Journal of Architectural Heritage**, 2015, 9.2: 98-110.

GESUALDO, A.; NUNZIANTE, L. Omogeneizzazione di murature storiche. *In: Proceedings XVII National Congress AIMETA*, Florence, Italy. 2005. <http://hdl.handle.net/11588/120132>

GONÇALVES, R.; TRINCA, A. J.; CERRI, D. G. P. Comparison of elastic constants of wood determined by ultrasonic wave propagation and static compression testing. **Wood and fiber science**, 2011, 43.1: 64-75.

GREGORCZYK, P.; LOURENÇO, P. B. A review on flat-jack testing. **Engenharia Civil, Número 9**, 2000.

Available at: [https://repositorium.sdum.uminho.pt/bitstream/1822/2504/1/Pag\\_39-50.pdf](https://repositorium.sdum.uminho.pt/bitstream/1822/2504/1/Pag_39-50.pdf)

HACIEFENDIOĞLU, K.; DEMIR, G.; ALPASLAN, E. Determination of Modal Parameters of Historical Masonry Minarets by using Operational Modal Analysis. *In: Proceedings of the World Congress on Civil, Structural, and Environmental Engineering (CSEE'16)*. 2016. Available at: [http://avestia.com/CSEE2016\\_Proceedings/files/paper/ICSENM/104.pdf](http://avestia.com/CSEE2016_Proceedings/files/paper/ICSENM/104.pdf)

HANDY, R. L. Borehole shear test manual. **Handy Geotechnical Instruments**, Inc., Madrid, 2002.

HANDY, R. L.; FOX, N. S. A soil bore-hole direct-shear test device. **Highway Research News**, 1967.

HANNA, A.; AL-ROMHEIN, R. At-rest earth pressure of over consolidated cohesionless soil. **Journal of geotechnical and geo-environmental engineering**, 2008, 134.3: 408-412.

HO-LE, K. Finite Element mesh generation methods: a review and classification. **Computer-aided design**, 1988, 20.1: 27-38.

HOSFORD, W. F. **Solid mechanics**. Cambridge University Press, 2010.

HUSSAIN, A.; AKHTAR, S. Review of non-destructive tests for evaluation of historic masonry and concrete structures. **Arabian Journal for Science and Engineering**, 2017, 42.3: 925-940.

IBRAHIM, M.; KRAWCZYK, R.; SCHIPPOREIT, G. CAD smart objects: potentials and limitations. **Education and Research in Computer Aided Architecture Design in Europe ECAADe**, 2003, 21: 547-552.

INZERILLO, L., *et al.* BIM and architectural heritage: towards an operational methodology for the knowledge and the management of Cultural Heritage. **Disegnarecon**, 2016, 9.16: 16-1-16.9.

IOANNIDES, M. *et al.* Digital Heritage. Progress in Cultural Heritage: Documentation, Preservation, and Protection. *In: 7th International Conference, Proceeding of EuroMed 2018*, Nicosia, Cyprus, October 29-November 3, 2018, Proceedings. Springer, 2018.

ISCARSAH, ICOMOS. **Recommendations for the analysis, conservation and structural restoration of architectural heritage**. 2003.

IVORRA, S.; PALLARÉS, F. J. Dynamic investigations on a masonry bell tower. **Engineering structures**, 2006, 28.5: 660-667.

JACOBSEN, N. J.; ANDERSEN, P.; BRINCKER, R. Using enhanced frequency domain decomposition as a robust technique to harmonic excitation in operational modal analysis. *In: Proceedings of ISMA2006: international conference on noise and vibration engineering*. Belgium Leuven, 2006. p. 18-20.

JAISHI, B., *et al.* Dynamic and seismic performance of old multi-tiered temples in Nepal. **Engineering Structures**, 2003, 25.14: 1827-1839.

KADOBAYASHI, R., *et al.* Comparison and evaluation of laser scanning and photogrammetry and their combined use for digital recording of cultural heritage. **International Archives of the Photogrammetry, Remote Sensing and Spatial Information Sciences**, 2004, 35.5: 401-406.

KAK, A. C.; SLANEY, M.; WANG, G. Principles of Computerized Tomographic Imaging. **Medical Physics**, v. 29, n. 1, p. 107-107, 2002.

KAMARDEEN, I. 8D BIM modelling tool for accident prevention through design. In: 26th annual ARCOM conference. Leeds: Association of Researchers in Construction Management, 2010. p. 281-289.

KATILI, I. A new discrete Kirchhoff-Mindlin element based on Mindlin-Reissner plate theory and assumed shear strain fields—part I: An extended DKT element for thick-plate bending analysis. **International Journal for Numerical Methods in Engineering**, 1993, 36.11: 1859-1883.

KATILI, I. A new discrete Kirchhoff-Mindlin element based on Mindlin-Reissner plate theory and assumed shear strain fields—part II: An extended DKQ element for thick-plate bending analysis. **International Journal for Numerical Methods in Engineering**, 1993, 36.11: 1885-1908.

KHADDAJ, M.; SROUR, I. Using BIM to retrofit existing buildings. **Procedia Engineering**, 2016, 145: 1526-1533.

KILAR, V.; PETROVIC, S. Seismic rehabilitation of masonry heritage structures with base-isolation and with selected contemporary strengthening measures. **Seismic Resistant Structures**, 2018, 13.

KOLCUN, A. The quality of meshes and FEM computations. **WSCG proc.** 1999 (V. Skala ed.), 100-105.

KOUROUSSIS, G.; VERLINDEN, O.; CONTI, C. Finite-dynamic model for infinite media: corrected solution of viscous boundary efficiency. **Journal of Engineering Mechanics**, 2011, 137.7: 509-511.

KUHLEMEYER, R. L.; LYSMER, J. Finite Element method accuracy for wave propagation problems. **Journal of Soil Mechanics and Foundations Div**, 1973, 99.Tech Rpt.

LABUZ, J. F.; ZANG, A. Mohr-Coulomb failure criterion. **Rock mechanics and rock engineering**, 2012, 45.6: 975-979.

LAGOMARSINO, S., *et al.* **User guide of TreMuri** (Seismic analysis program for 3D masonry buildings), Version 1.7. 34. University of Genoa, 2009.

LAGOMARSINO, S., *et al.* Classification of cultural heritage assets and seismic damage variables for the identification. **WIT Transactions on the Built Environment**, 2011, 118: 697-708.

LAGOMARSINO, S., *et al.* TREMURI program: an equivalent frame model for the nonlinear seismic analysis of masonry buildings. **Engineering structures**, 2013, 56: 1787-1799.

LAMGEO, *Laboratório de Mapeamento Geotécnico*. Geotechnical Experimental Results of Florianópolis Soils. Florianópolis, Brazil: 2018.

LAWSON, C. L. Software for C1 surface interpolation. In: Mathematical software. **Academic Press**, 1977. p. 161-194.

LERMA, C., *et al.* Pathology of building materials in historic buildings. Relationship between laboratory testing and infrared thermography. **Materiales de Construcción**, 2014, 64.313: 009.

LICHTI, D. D., *et al.* Comparison of digital photogrammetry and laser scanning. In: **Proc. International Society for Photogrammetry and Remote Sensing**. 2002. p. 39-44.

LIN, R. M.; LIM, M. K.; DU, H. Improved inverse Eigensensitivity method for structural analytical model updating. **Journal of Vibration and Acoustics**, Transactions of the ASME, 1995, 117 (2): 192-198.

LIVINGSTON, R. A. Non-destructive testing of historic structures. *In: Science and Technology in Historic Preservation*. Springer, Boston, MA, 2000. p. 97-120.

LO TURCO, M.; MATTONE, M.; RINAUDO, F. Metric survey and BIM technologies to record decay conditions. **International Archives of the Photogrammetry, Remote Sensing and Spatial Information Sciences**, 2017, 42.

LOPES, R. Tipologia de cobertura de arquitetura religiosa em Pernambuco, patologia e conservação preventiva. 2007. [In Portuguese]. Available at:  
[http://s53325a05467962c0.jimcontent.com/download/version/1302902847/module/5384826969/name/Comunicacao\\_final.pdf](http://s53325a05467962c0.jimcontent.com/download/version/1302902847/module/5384826969/name/Comunicacao_final.pdf)

LÓPEZ, F. J., *et al.* A review of heritage building information modeling (H-BIM). **Multimodal Technologies and Interaction**, 2018, 2.2: 21.

LOURENÇO, P. B. Computational strategies for masonry structures [Ph. D. thesis]. **Delft University, The Netherlands**, 1996.

LOURENÇO, P. B. Analysis and restoration of ancient masonry structures: guidelines and examples. 2004. **University of Minho, Portugal**. Available at:  
[http://repositorium.sdum.uminho.pt/bitstream/1822/3066/1/2004\\_Lourenco1.pdf](http://repositorium.sdum.uminho.pt/bitstream/1822/3066/1/2004_Lourenco1.pdf)

LOURENÇO, P. B., *et al.* Analysis of masonry structures without box behaviour. **International Journal of Architectural Heritage**, 2011, 5.4-5: 369-382.

LOURENÇO, P. B. Computations on historic masonry structures. **Progress in Structural Engineering and Materials**, 2002, 4.3: 301-319.

LOURENÇO, P. B. **The ICOMOS methodology for conservation of cultural heritage buildings: concepts, research and application to case studies**. 2014. Available at:

<https://repositorium.sdum.uminho.pt/bitstream/1822/31187/1/The%20ICOMOS%20methodology%20for%20conservation%20of%20cultural%20heritage.pdf>.

LOURENÇO, P. B.; KARANIKOLOUDIS, G.; GRECO, F. In situ testing and modelling of cultural heritage buildings in Peru. **Structural Analysis of Historical Constructions - Anamnesis, diagnosis, therapy, controls** - Van Balen and Verstryngge (Eds) © 2016 Taylor and Francis Group, London, ISBN 978-1-138-02951-4.

LUDWIG, M., *et al.* The Advantages of Parametric Modeling for the Reconstruction of Historic Buildings. **The International Archives of Photogrammetry, Remote Sensing and Spatial Information Sciences**, 2013, 40: 161-165.

LUDWIG, N., *et al.* Moisture detection in wood and plaster by IR thermography. **Infrared Physics and Technology**, 2004, 46.1-2: 161-166.

MAGALHÃES, F.; CUNHA, Á.; CAETANO, E. Vibration-based structural health monitoring of an arch bridge: from automated OMA to damage detection. **Mechanical Systems and Signal Processing**, 2012, 28: 212-228.

MAGENES, G. A method for pushover analysis in seismic assessment of masonry buildings. In: **Proceedings of the 12th world conference on earthquake engineering**. 2000. (ASTERIS; EDUCATION; MAVROULI, 2006)

MAGENES, G.; MENON, A. A review of the current status of seismic design and assessment of masonry buildings in Europe. **Journal of Structural Engineering**. SERC Chennai, 2009, 35.6: 247-256.

MAGENES, G.; PENNA, A. Existing masonry buildings: general code issues and methods of analysis and assessment. In: **Eurocode 8 perspectives from the Italian Standpoint**. 2009: 185-198.

MAIERHOFER, C., *et al.* Structural evaluation of historic walls and columns in the Altes Museum in Berlin using non-destructive testing methods. In: **Structural Analysis of Historical Constructions - 2 Volume Set: Possibilities of Numerical and Experimental Techniques- Proceedings of the IV<sup>th</sup> Int. Seminar on Structural Analysis of Historical Constructions**, 10-13 November 2004, Padova, Italy. CRC Press, 2004. p. 331.

MARQUES, R. Masonry box behaviour. **Encyclopedia of Earthquake Engineering**, 2014.

MASOTTI, L. F. C. Análise da implementação e do impacto do BIM no Brasil. Monograph (Bachelor in Civil Engineering). Federal University Of Santa Catarina. Florianópolis, 2014.

MATSUOKA, H.; NAKAI, T. Relationship among Tresca, Mises, Mohr-Coulomb and Matsuoka-Nakai failure criteria. **Soils and Foundations**, 1985, 25.4: 123-128.

MAVROULI, O., *et al.* **Damage analysis of masonry structures subjected to rockfalls. Landslides**, 2017, 14.3: 891-904.

MCCANN, D. M.; FORDE, M. C. Review of NDT methods in the assessment of concrete and masonry structures. **NDT & E International**, 2001, 34.2: 71-84.

MCKEAGUE, J. A.; STOBBE, Peter C. History of soil survey in Canada 1914-1975. **Historical series No. 11**. 1978.

MELLEY, M. E.; VERNIZZI, C.; TEDESCHI, C. The drawing for art: The Corridor Grande in Sabbioneta, from the design of ideal city of Vespasiano Gonzaga to the drawing of Galleria degli Antichi: typological models and graphic-geometric analysis of the architectural plant and the pictorial. In: **41° Convegno Internazionale dei docenti delle discipline della rappresentazione**, Perugia, Italy. 2019, 1277-1286.

MENDES, N.; LOURENÇO, P. B. Seismic Performance of Ancient Masonry Buildings: a Sensitivity Analysis. In: **Proceedings of the 4th International Conference on Computational Methods in Structural Dynamics and Earthquake Engineering (COMPDYN 2013)** 2014: 1624-1638. Available at:  
[https://repositorium.sdum.uminho.pt/bitstream/1822/27591/1/Paper%20ID%201232\\_Nuno%20Mendes.pdf](https://repositorium.sdum.uminho.pt/bitstream/1822/27591/1/Paper%20ID%201232_Nuno%20Mendes.pdf)

MENDES, N.; LOURENÇO, P. B. Sensitivity analysis of the seismic performance of existing masonry buildings. **Engineering Structures**, 2014, 80: 137-146.

MERCURI, F., *et al.* Active infrared thermography applied to the investigation of art and historic artefacts. **Journal of thermal analysis and calorimetry**, 2011, 104.2: 475.

MILANI, G.; VALENTE, M. Failure analysis of seven masonry churches severely damaged during the 2012 Emilia-Romagna (Italy) earthquake: Non-linear dynamic analyses vs conventional static approaches. **Engineering Failure Analysis**, 2015, 54: 13-56.

MESRI, G.; HAYAT, T. M. The coefficient of earth pressure at rest. **Canadian Geotechnical Journal**, 1993, 30.4: 647-666.

MIRANDA, L., *et al.* Applications of sonic tests to masonry elements: influence of joints on the propagation velocity of elastic waves. **Journal of Materials in Civil Engineering**, 2013, 25.6: 667-682.

MORGENSTERN, N. R.; EISENSTEIN, Z. Methods of estimating lateral loads and deformations. In: **Lateral Stresses in the Ground and Design of Earth-Retaining Structures**. ASCE, 1970. p. 51-102.

MOROPOULOU, A., *et al.* Non-destructive techniques as a tool for the protection of built cultural heritage. **Construction and Building Materials**, 2013, 48: 1222-1239.

MOURA, P. Reabilitação com argamassa projetada em construções históricas pedra no litoral paraibano. **PhD Thesis, Universidade Federal da Bahia - UFBA**, Brazil, 2007.

MURPHY, M. Historic Building Information Modelling (HBIM). For Recording and Documenting Classical Architecture in Dublin 1700 to 1830. **Handbook of Research on Emerging Digital Tools for Architectural Surveying, Modeling, and Representation**, April 2012.



MURPHY, M.; MCGOVERN, E.; PAVIA, S. Historic building information modelling (HBIM). **Structural Survey**, 2009.

NADAI, A. **Theory of flow and fracture of solids**. 1950.

NEU, E., *et al.* Fully automated operational modal analysis using multi-stage clustering. **Mechanical Systems and Signal Processing**, 2017, 84: 308-323.

NIETO, J. E., *et al.* Management of built heritage via HBIM Project: A case of study of flooring and tiling. **Virtual Archaeology Review**, 2016, 7.14: 1-12.

OLIVEIRA, M. Tecnologia da conservação e da restauração - materiais e estruturas: um roteiro de estudos. [2011]. 4th. ed. rev. and enl. Salvador: EDUFBA, 2011. 243 p. ISBN 978-85-232-0772-4. Available from SciELO Books <<http://books.scielo.org>>

ORENI, D., *et al.* HBIM for conservation and management of built heritage: Towards a library of vaults and wooden beam floors. *In: ISPRS Annals of photogrammetry, remote sensing and spatial information sciences*, 2013, 5: W1.

PARIVALLAL, S., *et al.* Evaluation of in-situ stress in masonry structures by flat jack technique. *In: Proc. of the National Seminar and Exhibition of Non-Destructive Evaluation*. 2011.

PASTOR, M.; BINDA, M.; HARČARIK, T. Modal assurance criterion. **Procedia Engineering**, 2012, 48: 543-548.

PAU, A.; VESTRONI, F. Vibration analysis and dynamic characterization of the Colosseum. Structural Control and Health Monitoring: **The Official Journal of the International Association for Structural Control and Monitoring and of the European Association for the Control of Structures**, 2008, 15.8: 1105-1121.

PAUWELS, P., *et al.* Architectural information modelling for virtual heritage application. *In: International conference on virtual systems and multimedia (VSMM)*. Archaeolingua, 2008. p. 18-23.

PEETERS, B.; MAECK, J.; DE ROECK, G. Vibration-based damage detection in civil engineering: excitation sources and temperature effects. **Smart Materials and Structures**, 2001, 10.3: 518.

PEETERS, B.; DE ROECK, G. Stochastic system identification for operational modal analysis: a review. **Journal of Dynamic Systems, Measurement and Control**, Transactions of the ASME, 2001, 123.4: 659-667.

PEÑA, F., *et al.* Numerical models for the seismic assessment of an old masonry tower. **Engineering Structures**, 2010, 32.5: 1466-1478.

PINTO, P. E. Eurocode 8: Background and Applications. *In: Dissemination of information for training*, Lisbon, 10-11 February 2011. Available at: [https://eurocodes.jrc.ec.europa.eu/doc/WS\\_335/S9\\_EC8-Lisbon\\_P%20PINTO.pdf](https://eurocodes.jrc.ec.europa.eu/doc/WS_335/S9_EC8-Lisbon_P%20PINTO.pdf)

PIERRON, F.; GRÉDIAC, M. The virtual fields method: extracting constitutive mechanical parameters from full-field deformation measurements. **Springer Science and Business Media**, 2012.

POCOBELLI, D. P., *et al.* BIM for heritage science: a review. **Heritage Science**, 2018, 6.1: 30.

PRADEL, D. Active pressure distribution in cohesive soils. *In: International conference on soil mechanics and foundation engineering*. 1994. p. 795-798.

PROVATIDIS, C. G.; KANARACHOS, A. E. On the use of Coons' interpolation in CAD/CAE applications. **Systems and Control: Theory and Applications**, World Scientific and Engineering Society Press, <http://www.worldses.org>, Singapore, 2000, 343-348.

QUATTRINI, R., *et al.* From TLS to HBIM. High-quality semantically aware 3D modelling of complex architecture. *In: International Archives of the Photogrammetry, Remote Sensing and Spatial Information Sciences*, Volume XL-5/W4, 3D Virtual Reconstruction and Visualization of Complex Architectures, 25-27 February 2015, Avila, Spain 2015.

RAMOS, L. F., *et al.* Monitoring historical masonry structures with operational modal analysis: two case studies. **Mechanical systems and signal processing**, 2010, 24.5: 1291-1305.

RAMOS, L. F., *et al.* Dynamic structural health monitoring of Saint Torcato church. **Mechanical Systems and Signal Processing**, 2013, 35.1-2: 1-15.

RAINIERI, C.; FABBROCINO, G. Development and validation of an automated operational modal analysis algorithm for vibration-based monitoring and tensile load estimation. **Mechanical Systems and Signal Processing**, 2015, 60: 512-534.

RELUIS. Linee guida per il rilievo, l'analisi ed il progetto di interventi di riparazione e consolidamento sismico di edifici in muratura in aggregato. v. 3, p. 105, 2010. Available at: [http://www.reluis.it/images/stories/LG\\_aggregati\\_ver1.pdf](http://www.reluis.it/images/stories/LG_aggregati_ver1.pdf)

REMONDINO, F., *et al.* State of the art in high density image matching. **The photogrammetric record**, 2014, 29.146: 144-166.

REN, W. X.; CHEN, H. B. Finite Element model updating in structural dynamics by using the response surface method. **Engineering Structures**, 2010, 32.8: 2455-2465.

ROCA, P. Considerations on the significance of history for the structural analysis of ancient constructions. **Structural analysis of historical constructions**, 2004, 4: 63-73.

ROCA, P., *et al.* Structural analysis of masonry historical constructions. Classical and advanced approaches. **Archives of Computational Methods in Engineering**, 2010, 17.3: 299-325.

ROCCO LAHR, F. A., *et al.* Poisson's ratios for wood species for structural purposes. **Advanced Materials Research**. Trans Tech Publications Ltd, 2015. p. 690-693.

RONCELLA, R.; RE, C.; FORLANI, G. Performance evaluation of a structure and motion strategy in architecture and cultural heritage. **Int. Archives of Photogrammetry, Remote Sensing and Spatial Information Sciences**, 2011, 38.5/W16: 285-292.

ROSS, Robert J., *et al.* **Wood handbook: wood as an engineering material**. USDA Forest Service, Forest Products Laboratory, General Technical Report FPL-GTR-190, 2010: 509 p. 1 v., 2010, 190.

ROSINA, E.; ROBISON, E. C. Applying infrared thermography to historic wood-framed buildings in North America. *APT Bulletin: The Journal of Preservation Technology*, 2002, 33.4: 37-44.

S.T.A. DATA. Modulo Sensibilità. In: **Teoria in Pratica**. Available: [http://www.stadata.com/3muri/documenti/3Muri\\_Modulo\\_Sensibilita.pdf](http://www.stadata.com/3muri/documenti/3Muri_Modulo_Sensibilita.pdf)

SAISI, A.; GENTILE, C.; GUIDOBALDI, M. Post-earthquake continuous dynamic monitoring of the Gabbia Tower in Mantua, Italy. **Construction and Building Materials**, 2015, 81: 101-112.

SAISI, A.; TERENCEZONI, S. Galleria degli Antichi and Palazzo Giardino at Sabbioneta: Remarks from archive research and direct survey. In: **10th International Masonry Conference, IMC 2018**. International Masonry Society, 2018. p. 907-916.

SAKAMOTO, M. Y., *et al.* Mapeamento geotécnico de áreas de risco da Bacia do Itacurubi. In: **XV Panamerican Conference on Soil Mechanics and Geotechnical Engineering**. 2015: 3073-3080.

SAKAMOTO, M.; OLIVEIRA, M. **Comparação de Dois Métodos para a Determinação dos Parâmetros de Resistência ao Cisalhamento dos Solos**. Technical Report, University of Santa Catarina. October 2015.

SANCIBRIAN, R., *et al.* Dynamic identification and condition assessment of an old masonry chimney by using modal testing. **Procedia Engineering**, 2017, 199: 3410-3415.

SCHULLER, M., *et al.* Acoustic tomography for evaluation of unreinforced masonry. **Construction and Building Materials**, 1997, 11.3: 199-204.

SALTELLI, A., *et al.* **Sensitivity analysis in practice: a guide to assessing scientific models**. New York: Wiley, 2004, p. 46.

SHAH, J. J.; MÄNTYLÄ, M. **Parametric and feature-based CAD/CAM: concepts, techniques, and applications**. John Wiley and Sons, 1995.

SIMEONE, D., *et al.* BIM and knowledge management for building heritage. In: **Acadia**. 2014. p. 681-690.

SIMÕES, A., *et al.* Flat-Jack Tests on Old Masonry Buildings. In: **15th International Conference on Experimental Mechanics**. 2012.

SIMULIA, D. S. **Abaqus/CAE user's manual**. v. 2007, 2007

SISMICA, G. **Theoretical manual of the 3DMacro software, beta version**. Gruppo Sismica, Catania, 2013.

SYRMAKEZIS, C. A.; ASTERIS, P. G. Masonry failure criterion under biaxial stress state. **Journal of Materials in Civil Engineering**, 2001, 13.1: 58-64.

SOVEJA, L.; OLTEANU, I. In Situ Assessment of Stress Strain Curve for Masonry by Flat Jack Test. **Buletinul Institutului Politehnic din Iasi. Sectia Constructii, Arhitectura**, 2016, 62.4: 53.

STANDOLI, G., *et al.* Model Updating of Historical Belfries Based on OMA Identification Techniques. **International Journal of Architectural Heritage**, 2020, 1-25.

STOBER, D., *et al.* Application of HBIM as a research tool for historical building assessment. **Civil Engineering Journal**, 2018, 4.7: 1565-1574.

STRUCTURAL VIBRATION SOLUTION, S. V. S. **ARTEMIS Modal ( Products ) Software for Operational Modal Analysis and Experimental Modal Analysis**. 2020. Available at: [https://svibs.com/?gclid=Cj0KCQjwIN32BRCCARIsADZ-J4v48VS42nIphRtbR6RbowgiEdQlGFaVSHb3TeTryt6rDWtjgc60GQYaArcAEALw\\_wcB](https://svibs.com/?gclid=Cj0KCQjwIN32BRCCARIsADZ-J4v48VS42nIphRtbR6RbowgiEdQlGFaVSHb3TeTryt6rDWtjgc60GQYaArcAEALw_wcB)

TEREZO, R. F. Avaliação das estruturas de madeira do quartel da tropa da fortaleza da ilha de Anhatomirim. GIEM, Grupo Interdisciplinar de Estudos da Madeira. Florianópolis: UFSC, 2005. Available at <<http://fortalezas.org/midias/arquivos/3167.pdf>>

TONERA, R. Fortalezas de Santa Catarina a Caminho de tornarem-se Patrimônio Mundial. Universidade Federal de Santa Catarina, Florianópolis, Brazil. 2017. <http://fortalezas.org/>

TONERA, R.; FRAGOSO, M. P. O Banco de Dados Mundial sobre Fortificações e suas contribuições para turismo como guia do desenvolvimento social. **Caderno Virtual de Turismo**. 2013.

UMAR, M. U.; HANAFI, M. H.; LATIP, N. A. Analysis of Non-Destructive Testing of Historic Building Structures. **Australian Journal of Basic and Applied Sciences**, 2015, 9.7: 326-330.

UNITED STATES. SCIENCE; EDUCATION ADMINISTRATION. **Soil taxonomy: a basic system of soil classification for making and interpreting soil surveys**. Soil Conservation Service, US Department of Agriculture, 1975.

VAIOPOULOS, A. D.; GEORGOPOULOS, A.; LOZIOS, S. G. Comparison of 3D representations depicting micro folds: overlapping imagery vs. time-of-flight laser scanner. In: **Earth Resources and Environmental Remote Sensing/GIS Applications III**. International Society for Optics and Photonics, 2012. p. 853808.

VALANIS, A.; TSAKIRI, M. Automatic target identification for laser scanners. In: **Proceedings of XX<sup>th</sup> ISPRS Congress**, Istanbul, Turkey. 2004.

- VALLE, S.; ZANZI, L. Tomography for NDT applied to masonry structures: Sonic and/or EM. **Arch Bridges**, 1998, 243.
- VAN BALEN, K.; VANDESANDE, A. Innovative built heritage models based on preventive and systemic approaches. In: **Innovative Built Heritage Models: Edited contributions to the International Conference on Innovative Built Heritage Models and Preventive Systems (CHANGES 2017)**. 2017.
- VAN LEEUWEN, J. P.; WAGTER, H. Architectural design-by-Features. In: **CAAD futures 1997**. Springer, Dordrecht, 1997. p. 97-115.
- VAN OVERSCHEE, P.; DE MOOR, B. L. Subspace identification for linear systems: Theory—Implementation—Applications. **Springer Science and Business Media**, 2012.
- VAN WAGENEN, H. W. **Building Information Modeling and Historic Buildings: How a Living Model Leads to Better Stewardship of the Past**. Master thesis, Faculties of the University of Pennsylvania, USA. 2012.
- VOLK, R.; STENGEL, J.; SCHULTMANN, F. Building Information Modelling (BIM) for existing buildings—Literature review and future needs. **Automation in construction**, 2014, 38: 109-127.
- WILSON, J. C.; LIU, T. Ambient vibration measurements on a cable-stayed bridge. **Earthquake engineering and structural dynamics**, 1991, 20.8: 723-747.
- YONG, R. N.; WARKENTIN, B. P. **Introduction to soil behavior**. Mcmillan 1966.
- YUAN, J., *et al.* Experimental Research on Influence of Granulometric Composition on Sandy soil Strength and Rheological Properties. Guangdong. **Electronic Journal of geotechnical Engineering**. 2013, 18: 4081-4091.
- ZANZI, L., *et al.* Sonic tomography of the stone pillars of a 17th-century church. **WIT Transactions on The Built Environment**, 2001, 55.
- ZENID, G. J., *et al.* Madeira: uso sustentável na construção civil. São Paulo: **Instituto de Pesquisas Tecnológicas-SVMA**, 2009. Available at: [http://www.ipt.br/download.php?filename=6-Madeiras:\\_uso\\_sustentavel\\_na\\_construcao\\_civil.pdf](http://www.ipt.br/download.php?filename=6-Madeiras:_uso_sustentavel_na_construcao_civil.pdf)
- ZIENKIEWICZ, O. C., *et al.* **The Finite Element method**. London: McGraw-hill, 1977.
- ZONNO, G., *et al.* Laboratory evaluation of a fully automatic modal identification algorithm using automatic hierarchical clustering approach. **Procedia Engineering**, 2017, 199: 882-887.
- ZONNO, G., *et al.* Automated long-term dynamic monitoring using hierarchical clustering and adaptive modal tracking: validation and applications. **Journal of Civil Structural Health Monitoring**, 2018, 8.5: 791-808.

ZONNO, G., *et al.* Environmental and ambient vibration monitoring of historical adobe buildings: applications in emblematic Andean churches. **International Journal of Architectural Heritage**, 2019, 1-17.

ZONNO, G., *et al.* Experimental analysis of the thermohygrometric effects on the dynamic behaviour of adobe systems. **Construction and Building Materials**, 2019, 208: 158-174.

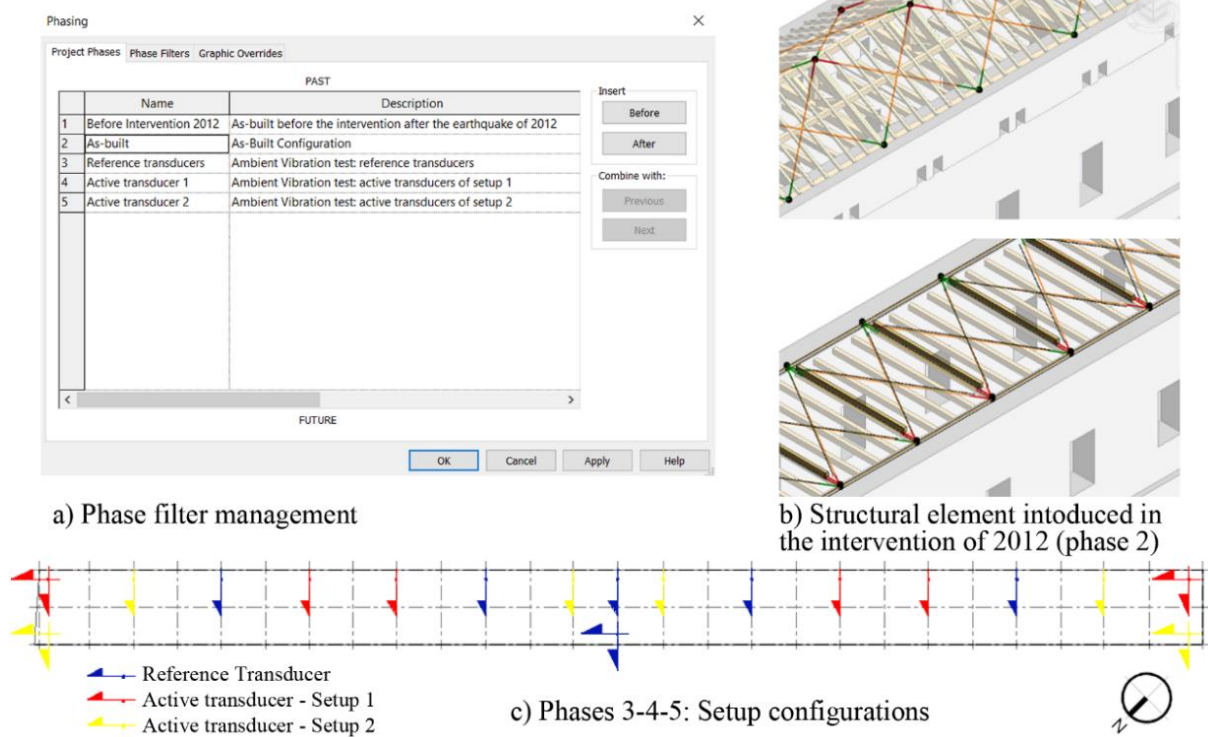
ZORDAN, T.; BRISEGHELLA, B.; LIU, T. Finite Element model updating of a tied-arch bridge using Douglas-Reid method and Rosenbrock optimization algorithm. **Journal of Traffic and Transportation Engineering** (English Edition), 2014, 1.4: 280-292.

## APPENDIX A - Increasing the level of development of the H-BIM models

The increasing the level of development (LOD) of the H-BIM model is enhanced by the data management of the heritage buildings. Such an increase is useful to further investigation on the analysed cultural heritage of *Galleria degli Antichi* and *Quartel da Tropa*. Regarding the dimensions of the BIM, the proposed methodology used the spatial (3D) and time (4D) information.

The historical research and the geometric survey allowed representing the spatial configuration of the building both in space (3D) and time (4D). The systematic use of the phase filter option in BIM software allows organizing the structural elements according to their constructive phases (Figura AP.A1.a and AP.A1.b). Furthermore, such an option is useful to represent the configuration of the setups of the experimental *in-situ* tests (AP.A1.c). In the case study of *Galleria degli Antichi*, phase filter is used to differentiate the reference transducers, from the active transducers of the first and second setups.

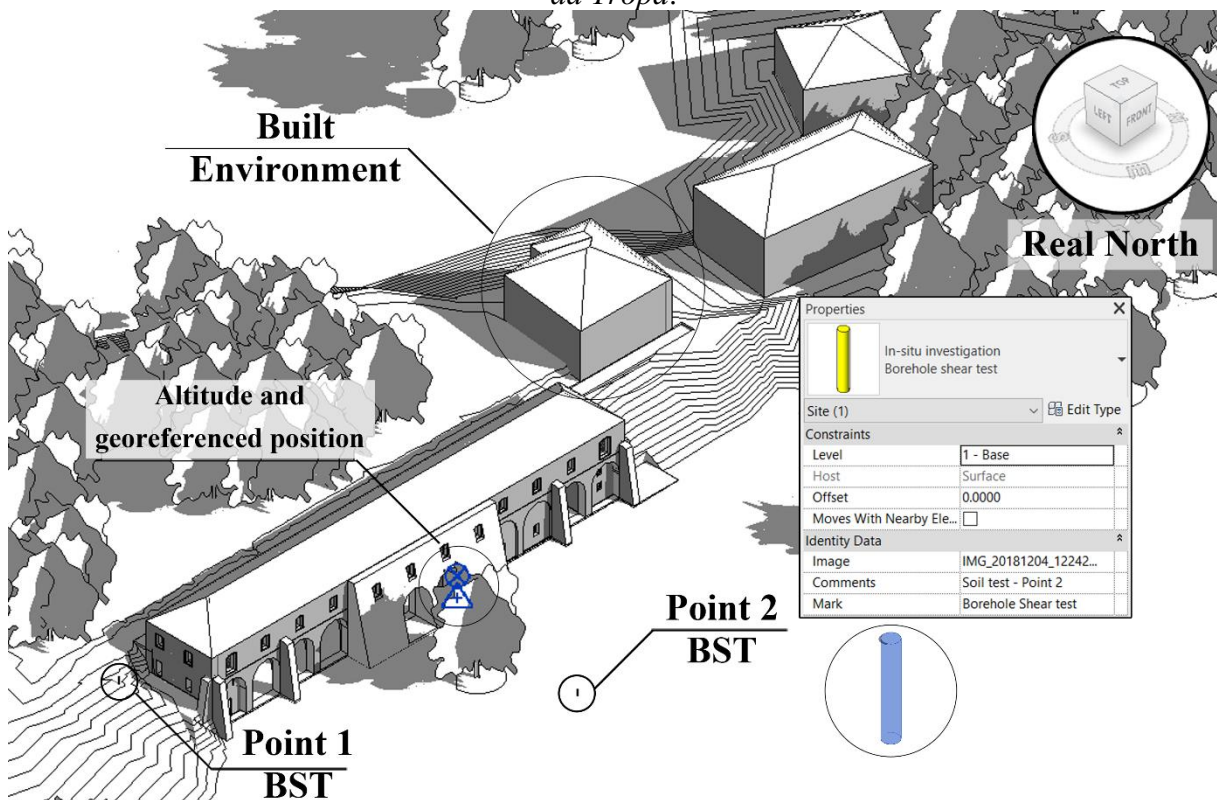
Figure AP.A1 - Management of the H-BIM data of *Galleria degli Antichi* through the phase filter (a), the definition of the structural element according to the constructive phase (b) and representation of the setups of the ambient vibration test (c).



Source: the author.

In the case study of the *Quartel da Tropa*, instead, the phase filter is used to understand the constructive phase description (see subsections 5.4.1 and 5.5.4.1). Moreover, it allows managing the information of the experimental soil tests (Appendix B) and the location of each test (Figure A2). Such systematic information management of the research data is required since from the defined level of development, LOD 200. Moreover, such a level requires that the H-BIM model be georeferenced through the definition of the altitude, the location and the real North (Figure AP.A2). Furthermore, LOD of the H-BIM models can also be increased through the modelling of the Built Environment (Figure AP.A2). Indeed, the highest LOD 500 can be achieved only when the main model is modelled into architectural and geographical environments.

Figure AP.A2 - Increase of the level of development (LOD) of the H-BIM model of *Quartel da Tropa*.



Source: the author

Such a systematic approach to the data management allows for further investigation which can explore the other dimensions of the BIM. Indeed, sustainability analysis (6D), facility management (7D) and safety assessment (8D) can be carried out after the acquisition of such information. The cost assessment could be carried out for each required intervention, improving the allocation of resources and their impact on the budget (5D).

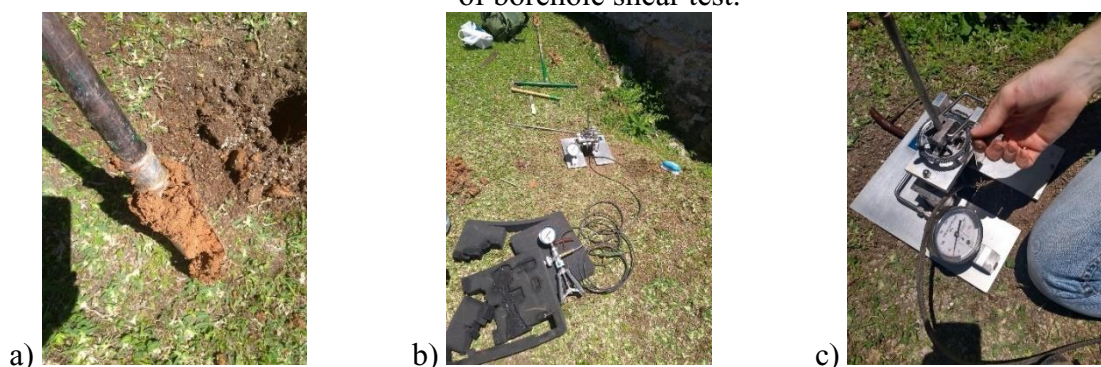


## APPENDIX B - Soil characteristic investigation

In Appendix B, the experimental test and the obtained results are shown. Experimental tests on the soil were carried out by the author together with the support of the *Laboratório de Mapeamento Geotécnico* of the Federal University of Santa Catarina (LAMGEO, 2018). Direct shear tests, granulometric analysis, and humidity tests were carried out to obtain cohesion  $C$ , friction angle  $\Phi$ , density soil  $\gamma$ .

During the soil preparation for the borehole test, specimens are acquired to the analysis of the soil in the laboratory (Figure AP.B1.a). Particle size analysis is carried out to understand the granulometric composition of the soil (Figure AP.B2). The soil type is red, yellow podzols (Figure AP.B1.a).

Figure AP.B1 - Soil preparation (a), location selection and instrument configuration (b and c) of borehole shear test.



Source: the author.



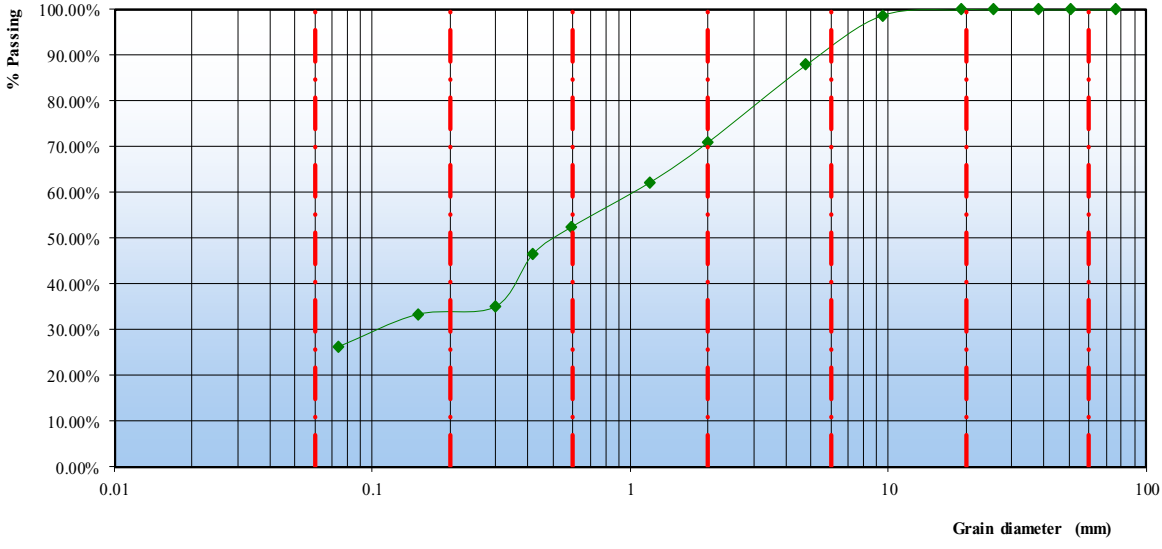
Result of the experimental test carried out in two different points are shown in Figure AP.B2. The soil is mostly characterized by Clay and Silt 26.15%, Fine sand 20.30% and Medium sand 24.46%. Coarse sand represents 16.96%, while fine and medium gravel have a low percentage (Figure AP-B2). The soil lithology is granitic rock type and it is considered as cohesive soil. For this reason, the assessment of the characteristics of cohesion and friction angle is crucial. They are obtained selecting the lower values from the two tests (Table AP-B1).

Table AP.B1 - Parameter of the selected point for the borehole shear test

	<b>Point 1</b>	<b>Point 2</b>	<b>Unit</b>
Cohesion - $C$	18.0	14.7	kN/m <sup>2</sup>
Friction Angle - $\Phi$	21.8	18.4	°

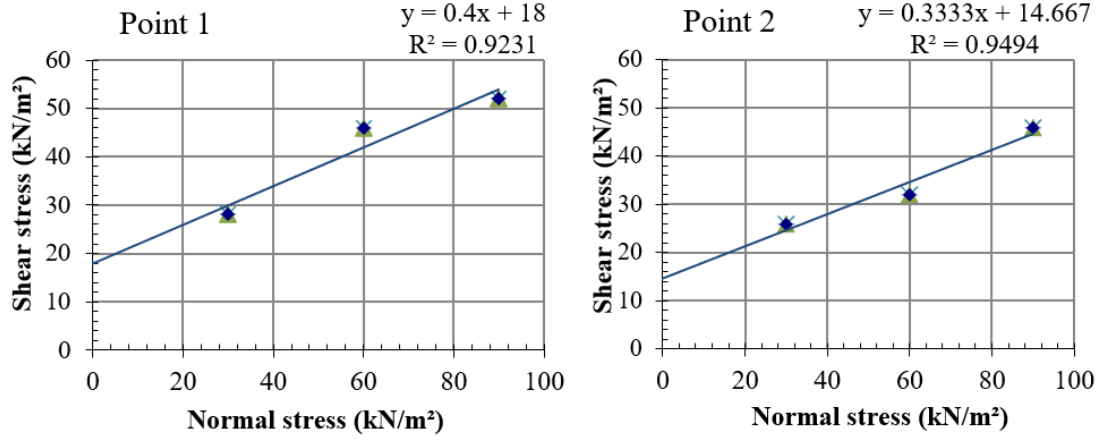
Source: LAMGEO (2018).

Figure AP.B2 - Particle size analysis report of the soil specimens.

 <b>UNIVERSIDADE FEDERAL DE SANTA CATARINA</b> DEPARTAMENTO DE GEOCIÊNCIAS / ENGENHARIA CIVIL FUNDAÇÃO DE AMPARO À PESQUISA E EXTENSÃO UNIVERSITÁRIA LABORATÓRIO DE MECÂNICA DOS SOLOS													
<b>Particle Size Analysis - NBR 07181 - 1984 - Solo - Análise Granulométrica (peneiramento simples)</b>													
Terrain:	Red-yellow podzols, lithology of granitic rock-type	Analyst: Matheus Klein Flach											
Location :	Ilha de Anhatomirim	Case Study: Quartel da Tropa											
Prof. (m):	Rafael A.R. Higashi	Resp.: Matheus Klein Flach											
		Date: #####											
<b>Sample Moisture Content</b>		<b>Determination of the dry content of the Sample</b>											
Capsule N°	15      44	Wet sample weight ( g ): 1041.58											
Capsule Weight ( g )	11.79    14.23	Retained Sample Weight in # 10 ( g ): 389.48											
Capsule + Wet soil ( g )	53.62    43.64	Passing Sample Weight at # 10, Wet ( g ): 652.1											
Capsule + Dry soil ( g )	45.70    38.03	Passing Sample Weight at # 10, Dry ( g ): 528.17											
Moisture Content	23.36%    23.57%	Total dry sample weight ( g ): 917.65											
Average Moisture Content	<b>23.46%</b>	Mh ( Fine screening ) ( g ): 120.00											
<b>Experimental data</b>													
<b>Sieve Analysis</b>	<b>Coarse fraction</b>	Sieve		Sieve weight ( g )	Sieve + Material ( g )	Retained material ( g )	PERCENTAGE						
		N°	# ( mm )				RETAINED		PASSING				
									Fine fraction	Coarse fraction	Accumulated	Fine fraction	Coarse fraction
			3"	76.2			0	0.00		0.00%	0.00%		100.00%
			2"	50.8			0	0.00		0.00%	0.00%		100.00%
			1.5"	38.1			0	0.00		0.00%	0.00%		100.00%
			1"	25.4			0	0.00		0.00%	0.00%		100.00%
			3/4"	19.1			0	0.00		0.00%	0.00%		100.00%
			3/8"	9.5			11.37	11.37		1.24%	1.24%		98.76%
			4	4.8			111.23	111.23		12.12%	12.12%		87.88%
		10	2			266.88	266.88		29.08%	29.08%		70.92%	
		<b>Fine fraction</b>	16	1.19		12.05	12.05	12.40%		12.40%	87.60%	62.12%	
			30	0.59		13.41	13.41	13.80%		26.19%	73.81%	52.34%	
			40	0.42		8.07	8.07	8.30%		34.50%	65.50%	46.45%	
			50	0.3		15.79	15.79	16.25%		50.74%	49.26%	34.93%	
	100		0.15		2.29	2.29	2.36%		53.10%	46.90%	33.26%		
	200	0.074		9.74	9.74	10.02%		63.12%	36.88%	26.15%			
	<b>Bottom</b>				0.43	0.43	0.44%		63.56%	36.44%	25.84%		
<b>Granulometric Composition</b>													
													
Clay + Silt =	26.15%	Medium sand =	24.46%	Fine gravel =	10.88%								
Fine sand =	20.30%	Coarse sand =	16.96%	Medium gravel =	1.24%								
Sousa Pinto (2000)													

Source: LAMGEO (2018).

Figure AP-B3 - Relation between normal and shear stresses in the measured points.



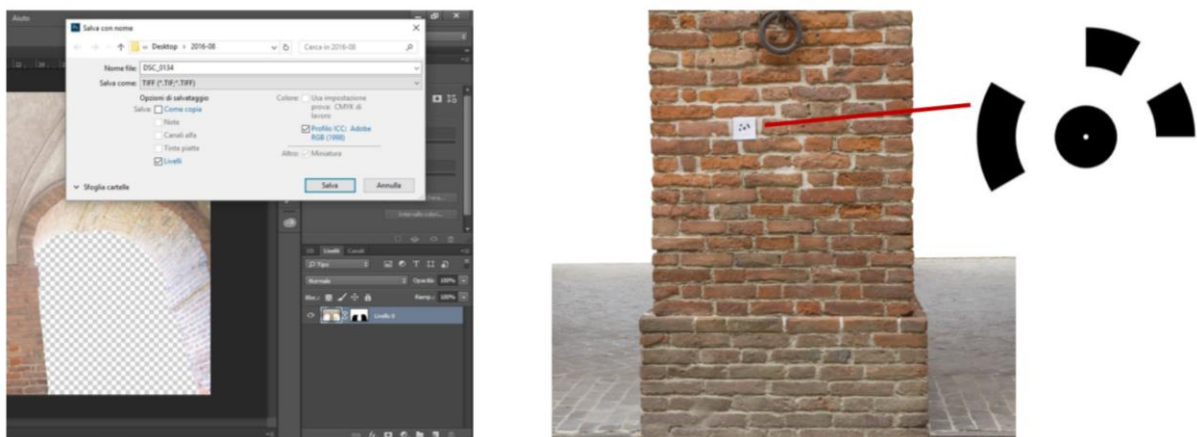
Source: LAMGEO (2018).

## ANNEXE A - Photogrammetric Survey of *Galleria degli Antichi*

The procedure of the creation of the photogrammetric survey of *Galleria degli Antichi* is here presented. In Dal Barco, Perobelli and Sartor (2016), the image data acquisition begins with the photogrammetric survey (BARAZZETTI *et al.*, 2015c; BRUMANA *et al.*, 2018a; NIETO *et al.*, 2016). It is carried out with the elaboration of RAW image files (DAL BARCO; PEROBELLI; SARTOR, 2016). Those images are acquired by a camera with the support of a tripod that assures the possibility to obtain orthogonal and diagonal high-quality images.

Markers are applied to the structure as facilitation tools for spatial identification in further phases. Markers are graphic symbols used to facilitate the software in the alignment phase and to have greater precision in the 3D model scaling phase (Figure AN.A1). Photos are taken in series - about a third away from each other files (DAL BARCO; PEROBELLI; SARTOR, 2016). Such a procedure allows for the data superposition, *i.e.* in each image, there is part of another. The RAW format files are imported into a photo-editing software where they can be modified according to the requirement of the designer, *e.g.* activating the ‘lens correction filter’, flattening the image, fixing the camera lens errors. After the process of deleting of non-interesting part of the construction, the images are exported and saved as raster images (Figure AN.A1).

Figure AN.A1 - Editing process of images and identification of markers in *Galleria degli Antichi*.



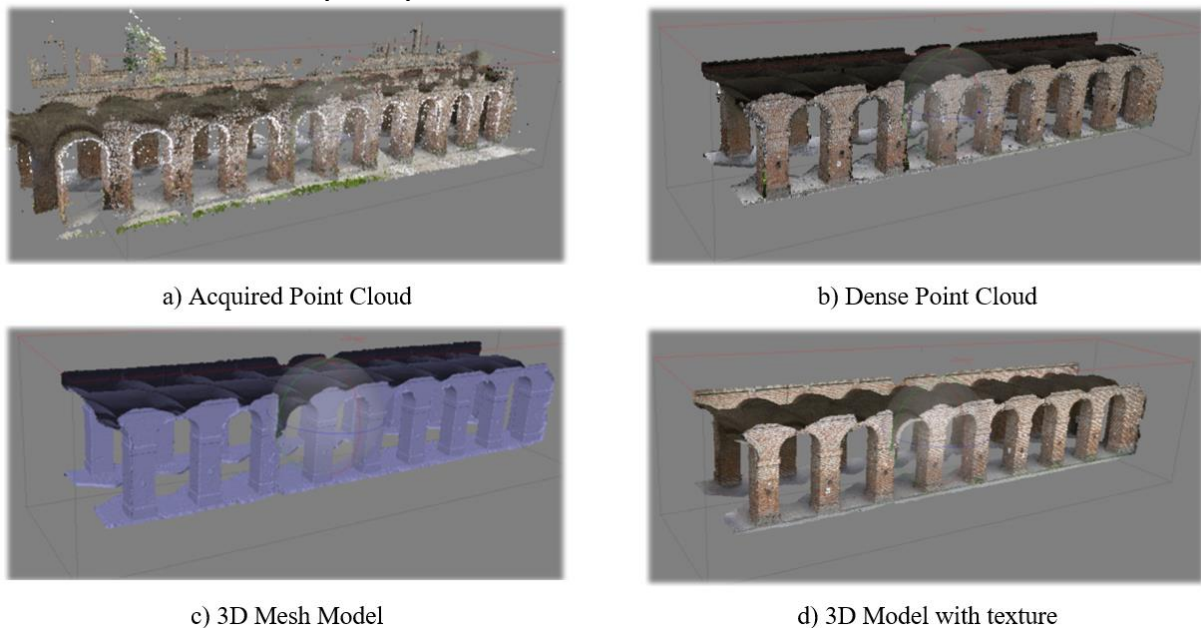
Source: Dal Barco, Perobelli, Sartor (2016).

Subsequently, an image-based 3D software performs digital image photogrammetric processing, generates orthophotos, creating 3D spatial data (DAL BARCO; PEROBELLI; SARTOR, 2016). The next step is the identification of the markers placed on the façade before

the photoshoots. After such identification, it is necessary to align the photos to allow the software to recognize the spatial layout of the rooms and to recreate the photographed object. As a result, a three-dimensional point cloud is obtained, and the required quality of the point cloud is defined (DAL BARCO; PEROBELLI; SARTOR, 2016).

Once the dense point cloud is generated, the software allows the generation of the meshes of the 3D model, where the textures are assigned, recreating the materials and colours of the construction (Figure AN.A2). The 3D model is scaled utilizing the DWG file where the spatial coordinates of the markers are recorded. Such a procedure allows identifying the markers located in heritage built and defining their spatial coordinates (DAL BARCO; PEROBELLI; SARTOR, 2016). Thus, the obtained 3D model is proportionated and scaled to the real construction dimension. The level of details of the obtained images is described by the software in terms of errors, expressed in pixels and meters (DAL BARCO; PEROBELLI; SARTOR, 2016).

Figure AN.A2 - Information acquisition process on *Galleria degli Antichi* (Italy): from the acquired point cloud to the 3d information model.



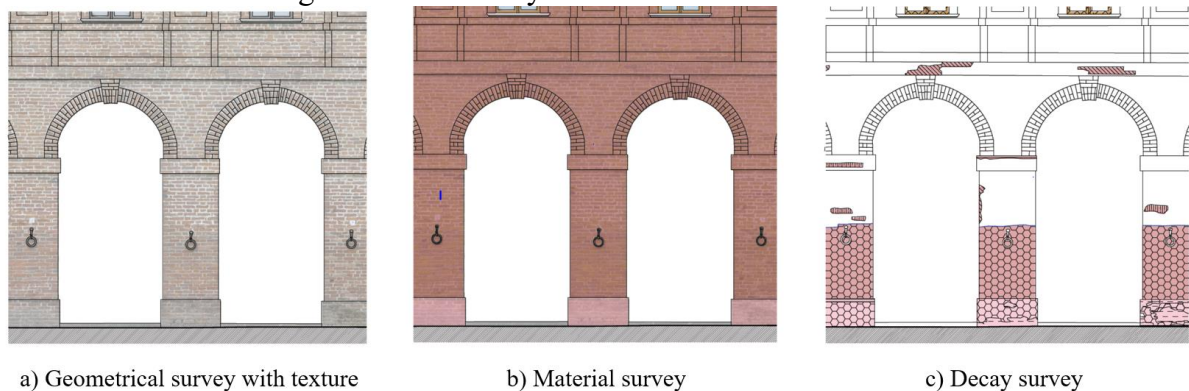
Source: Dal Barco, Perobelli, Sartor (2016).

The 3D laser scanner technology allows generating a series of laser beams, in a predetermined sequence, which is compared with the surrounding environment. The ray coming from the instrument - after hitting the surface of the object - returns to the source where it is memorized, reporting the three spatial coordinates (DAL BARCO; PEROBELLI; SARTOR,

2016). Such steps permit to obtain the so-called Point Cloud. Once such a file is imported, it is possible to proceed with the vector redesign and restitution work. The point cloud management, moreover, provides the possibility of making cut-sections in the three dimensions (x, y, z) and depending on the needs, change the slice width. In the case of obtaining the profile of a cross-section or longitudinal section, the cut will be very thin. However, in the case of a raised elevation or a more extensive section, the latter will be thicker, to incorporate a higher number of points.

The further step of the research of Dal Barco, Perobelli and Sartor (2016) is the creation of a new file, in which previous information is combined, listed and standardized in the different layers. Subsequently, it is possible to add the relative orthophotos - previously developed with the image-based 3D modelling solution software - to the vector data and to verify the agreement between the two in terms of proportions and dimensions. The completed file is used as a source of material and degradation surveys (Figure AN.A3). The orthophoto allows mapping the areas in terms of different materials and degradations (DAL BARCO; PEROBELLI; SARTOR, 2016).

Figure AN.A3 - Thematic survey of *Galleria degli Antichi* (Italy) obtained from the geometrical survey obtained from Point Cloud.



Source: Dal Barco, Perobelli, Sartor (2016).





## ANNEXE B - Evaluation of the wooden structures of *Quartel da Tropa* of the Fortress of the Island of Anhatomirim




In Annex B, the evaluation of the wooden structure of *Quartel da Tropa* developed in the research of Terezo (2005) is resumed. Such an investigation - elaborated by the Interdisciplinary Group of Studies of Madeira (GIEM) of the Federal University of Santa Catarina - was analysed for the understanding of wooden structures. The research is mainly based on the sampling of the different timber structural element to understand the different wooden species. Moreover, the humidity of the main timber element was assessed to understand the material decay. Such evaluation was developed through visual inspection and sonic test to obtain insight about the physical properties of the different evaluated samples.

### B.1. SAMPLING



For the definition of wooden species, different samples were taken from different parts of structural parts: rafters, lines, slats, brackets, bars, floor, doors, windows and jambs (TEREZO, 2005). It has been shown that the pieces have different types of species, even for the same structural types (Chart AN-B1).

Chart AN-B1 - Results of the anatomical identification of wooden pieces.

Sampling location	Brazilian popular name	Scientific name	Sample
1 <sup>st</sup> purlin between tie beams 9 and 10 – North-east	<i>Cedro</i>	<i>Cedrela fissilis</i>	
Rafter 31 – South-west	<i>Peroba</i>	<i>Aspidosperma pirycollum</i>	

Rafter 106 - Northeast	<i>Peroba</i>	<i>Aspidosperma pirycollum</i>	
Tie-beam 02 – South-west	<i>Cedro</i>	<i>Cedrela fissilis</i>	
Tie-beam 03 – South-west	<i>Licurana</i>	<i>Hieroyima alchorneoides</i>	
Tie-beam 09 – North-east	<i>Licurana</i>	<i>Hieroyima alchorneoides</i>	
Top plate beam 01 - near to tie-beam 02 – South-west	<i>Almécega</i>	<i>Protium heptaphyllum</i>	
Top plate beam 02 - near to tie-beam 09 - North	<i>Licurana</i>	<i>Hieroyima alchorneoides</i>	
Top plate beam 03 - near to tie-beam 10 – North-east	<i>Jacarandá- do-litoral</i>	<i>Platymiscium horibundum</i>	



Floor – North-east	<i>Canela preta</i>	<i>Ocotea catharinensis</i>	
Timber beam 01 – North-east	<i>Guaçatonga ou Chá de bugre</i>	<i>Carearia sylvestris</i>	
Timber beam 02 – South-west	<i>Licurana</i>	<i>Hyeronima alchorneoides</i>	
Furniture 01 – North-east	<i>Licurana</i>	<i>Hyeronima alchorneoides</i>	
Door P1 -North-west - Upper level	<i>Canela preta</i>	<i>Ocotea catharinensis</i>	
Door P5 – South-east - Upper level	<i>Imbuia</i>	<i>Ocotea porosa</i>	
Window J11 – North-west - Lower level	<i>Canela Sassafrás</i>	<i>Ocotea odorifera</i>	

Furniture - J14 – South-east	<i>Canela Preta</i>	<i>Ocotea catharinensis</i>	
Furniture - J14 – North-east	<i>Canela Preta</i>	<i>Ocotea catharinensis</i>	
Chiney lintel 01 – South-east	<i>Canela Preta</i>	<i>Ocotea catharinensis</i>	
Chimney lintel 02 – South-west	<i>Canela Preta</i>	<i>Ocotea catharinensis</i>	

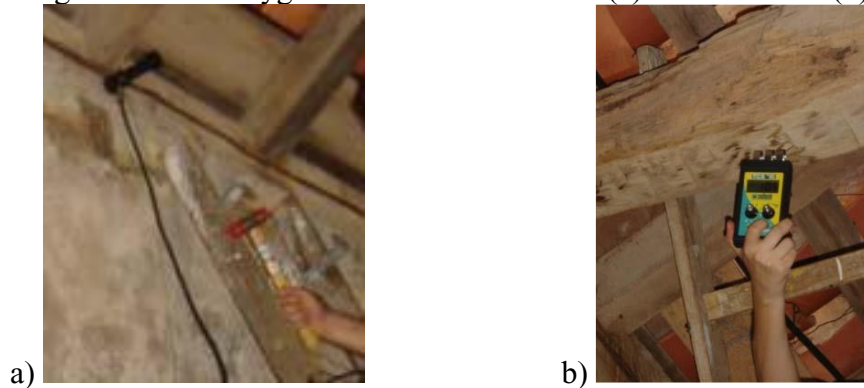
Source: Terezo (2005), modified by the author.

## B.2 HUMIDITY ASSESSMENT TESTS ON THE STRUCTURAL ELEMENTS

In the survey campaign carried out by Terezo (2005), moisture content measurements were made in several wooden pieces. In each piece, more than one measurement was performed. Two testing types of equipment were used so that the results could be compared using a resistive or inductive hygrometer (Figure AN.B1). Measurements of 20 cm by 20 cm were made in the roof tie-beams. The equipment was moved away from the wall towards the centre of the piece on the same face (Figure AN.B2). Most of the tie-beams have an average humidity of 18% (TEREZO, 2005). Regarding the rafters, measurements were made on different faces. In figures AN.B2 and AN.B3, results of the humidity test are resumed.

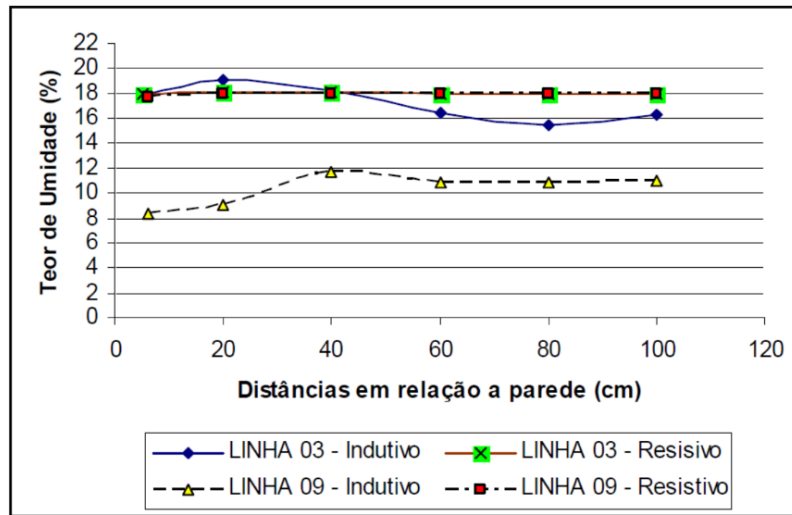
The values obtained with the inductive hygrometer were always lower. They had more variability than those measured with the resistive hygrometer (Chart AN-B2). However, this variation in the moisture content values of the inductive hygrometer is within the acceptable range for wood, which is a maximum of 18% (TEREZO, 2005).

Figure AN.B1 - Hygrometer in use: resistive (a) and inductive (b).



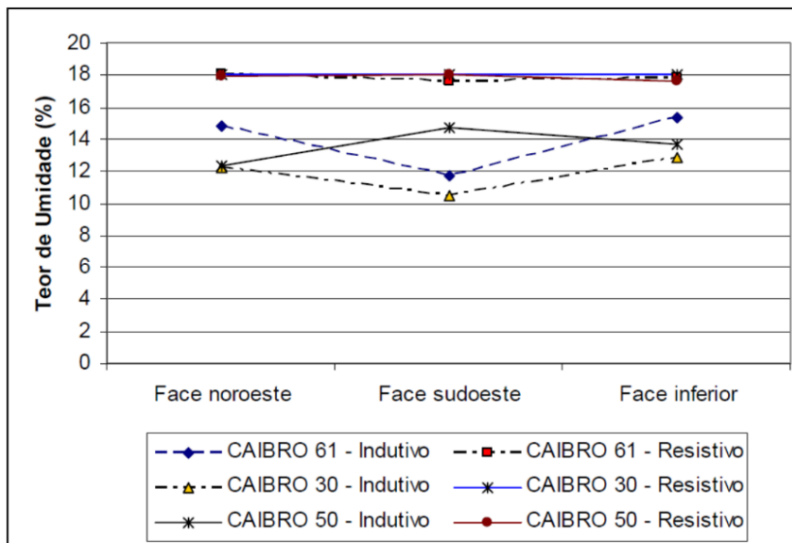
Source: Terezo (2005).

Figure AN.B2 - Moisture content of tie-beams concerning the wall support distance.



Source: Terezo (2005).

Figure AN.B3 - Moisture content of rafters on different faces.



Source: Terezo (2005).

Chart AN.B2 - Average values of moisture content and variation coefficients.

Wooden element	Average moisture content		Variation coefficient	
	Inductive	Resistive	Inductive	Resistive
Tie-beam 03	17.22	18.03	8.76	0.29
Tie-beam 09	10.27	17.95	12.80	0.68
Rafter 61	13.93	17.80	14.00	1.12
Rafter 30	11.87	18.00	10.40	0.00
Rafter 50	13.57	17.83	8.89	1.17
<b>Average</b>	<b>13.37</b>	<b>17.92</b>	<b>10.97</b>	<b>0.65</b>

Source: Terezo (2005).

### B.3 SONIC TESTS

In the survey prepared by GIEM, sonic tests were carried out, to evaluate the conservation status of the wooden pieces. Ultrasonic waves propagation velocities were measured in three types of pieces: rafters, tie-beams and top plate beams. For rafters and top plate beams, a measure of the speed of wave propagation in each piece was made. As for the tie-beams, two measurements the speed of wave propagation along the piece were made, further information could be found in the report prepared at GIEM (TEREZO, 2005). In Chart AN.B3, AN.B4 and AN.B5, the summarized results of these tests are shown, in which it is worth mentioning that the density values used in this work were obtained from the book IPT Characteristics Wood.

Chart AN.B3 - Summary of the average values of the ultrasound propagation speeds in tie-beams.

Element	Species	Density (g/cm <sup>3</sup> )	Average propagation velocity (m/s)	
			Test 01	Test 02
Tie-beam 02	<i>Cedrela fissilis</i>	0.50	2.111	3.175
Tie-beam 03	<i>Hyeronima alchorneoides</i>	0.69	2.421	4.143
Tie-beam 09	<i>Hyeronima alchorneoides</i>	0.69	3.512	3.721

Source: Terezo (2005).

Chart AN.B4 - Ultrasound propagation velocity in rafters.

Element	Time (μs)	Distance (cm)	Velocity (m/s)	Visual inspection
Rafter 61	172	80.5	4.680	Dry, good condition
Rafter 50	252	84	3.333	Wet, good condition
Rafter 30	362	81.5	2.251	Termite attack

Source: Terezo (2005).

Chart AN.B5 - Speed of propagation of ultrasound in top plate beams.

Element	Species	Density (g/cm <sup>3</sup> )	Velocity (m/s)	Location
Top plate beam 01	<i>Protium heptaphyllum</i>	0.75	2.885	South-west wall
Top plate beam 02	<i>Hyeronima alchorneoides</i>	0.69	2.432	North-east wall
Top plate beam 03	<i>Platymiscium horibundum</i>	0.89	4.315	North-east wall

Source: Terezo (2005).

The sonic results were used to validate visual inspection (TEREZO, 2005). Ultrasound propagation speeds were determined in numbered parts, according to visual inspection, and defined as: dry and in excellent condition; moist and in great condition; and degraded by termites. In such numbered parts, a change in the speed of propagation was observed. It was due to the problem diagnosed in visual inspection (TEREZO, 2005). The validation of the anatomical identification was also possible since different propagation speeds were detected for faces with the same state of conservation. This variation in speed was justified by the different species identified (TEREZO, 2005).